

# THE HYDANTOINASE PROCESS – TOWARD $\beta$ -AMINO ACIDS AND CELL- FREE REACTION SYSTEMS

Zur Erlangung des akademischen Grades eines  
DOKTORS DER NATURWISSENSCHAFTEN  
(Dr. rer. nat.)

der KIT-Fakultät für Chemie und Biowissenschaften des  
Karlsruher Institut für Technologie (KIT)

genehmigte  
DISSERTATION

von  
M. Sc. Christin Slomka

aus  
Finsterwalde

KIT-Dekan: Prof. Dr. Willem M. Klopper  
Referent: Prof. Dr. Stefan Bräse  
Korreferent: Prof. Dr. Christoph Syldatk  
Tag der mündlichen Prüfung: 22.07.2016



# ERKLÄRUNG

Hiermit erkläre ich, dass ich die vorliegende Arbeit selbstständig angefertigt und keine anderen als die darin angegebenen Quellen und Hilfsmittel benutzt sowie die wörtlich oder inhaltlich übernommenen Stellen als solche kenntlich gemacht und die Satzung des Karlsruher Institut für Technologie (KIT) zur Sicherung guter wissenschaftlicher Praxis in der gültigen Fassung beachtet habe und dass die elektrische Version der Arbeit mit der schriftlichen übereinstimmt.

Ich versichere außerdem, dass ich diese Dissertation nur in diesem und keinem anderen Promotionsverfahren eingereicht habe und, dass diesem Promotionsverfahren keine endgültig gescheiterten Promotionsverfahren vorausgegangen sind.

---

Ort, Datum

---

Unterschrift

# DANKSAGUNG

Ich möchte allen danken, die zum Gelingen dieser Arbeit beigetragen und mich währenddessen unterstützt haben.

Herrn Prof. Christoph Syldatk für die Bereitstellung des interessanten Themas, die Aufnahme in seine Arbeitsgruppe und seine stetige Bereitschaft zur wissenschaftlichen Diskussion.

Herrn Prof. Stefan Bräse für die freundliche Übernahme des Referates, eine erfolgreiche Kooperation sowie sehr hilfreiches Feedback.

Dr. Jens Rudat für die Betreuung der Doktorarbeit, gute Anregungen und tiefgehende fachliche Diskussionen.

Marc Skoupi, Theo Peschke sowie Pascal Baumann für neue Ideen und Unterstützung in neuen Projekten und in dem Zusammenhang ebenfalls danke an Prof. Christof Niemeyer sowie Prof. Jürgen Hubbuch für die Bereitstellung von Geräten.

Meinen Kollegen Marius, Ines, Judit, Julia, Florian, Alba, Michaela, Laura, Desi, Katrin, Ulrike, Pascal und Sandra für die Unterstützung und die tolle Zeit am Institut. Danke Herr Pörnbein, Jo-Hannes, Mareike, Janina, Stefan (X'Ucker), Olli, Sascha und Deepansh für die exorbitant lusitgen Stunden zusammen. Danke Super-Werner für Rettungen in der Not und Susanne und Katja für eure Hilfe zu jeder Zeit.

Ganz besonderer Dank geht an meine StudentInnen Theresa, Anna, JoKü, Daniel, Paris, Pille und Frodo für großes Interesse an den Projekten, erstaunliches Durchhaltevermögen, tatkräftige Unterstützung bei der Forschung und jede Menge Spaß.

Ich danke dem BMBF für die Förderung innerhalb des MIE-Forschungsprojektes.

Meinen Freunden für Motivation und Ablenkung, Markus für ein immer offenes Ohr und vielen Dank an meine Familie für den Rückhalt und die Kraft, die ihr mir zu jeder Zeit gebt. Danke fürs gemeinsame Durchstehen Zarah, Carmini und Darja.

## ABSTRACT

Non-canonical  $\alpha$ -amino acids are very important intermediates for pharmaceuticals, for example D-phenylglycine or substituted D-phenylglycines as constituents of penicillines and cephalosporines. Due to their structural properties,  $\beta$ -amino acids are also of great relevance for pharmaceutical products like peptidomimetics, antibiotics or biologically active secondary metabolites. The Hydantoinase Process is successfully applied in industries for the production of enantiopure  $\alpha$ -amino acids via dynamic kinetic resolution. Based on this process, a modified Hydantoinase Process was investigated for the synthesis of optically pure  $\beta$ -amino acids.

Regarding the synthesis of a novel  $\beta$ -amino acid by a modified Hydantoinase Process, in this work a new chemically synthesized substrate, 6-(4-nitrophenyl)dihydropyrimidine-2,4(1*H*,3*H*)-dione (*p*NO<sub>2</sub>PheDU), was investigated. For the qualitative as well as quantitative analysis of this substrate and the resulting *N*-carbamoyl- $\beta$ -amino acid (*N*Carb*p*NO<sub>2</sub> $\beta$ Phe), an achiral HPLC-method was established. Furthermore a chiral HPLC-method for detection of both enantiomers of the *N*-carbamoyl- $\beta$ -amino acid was developed. Consequently, alongside with the successful enzymatic hydrolysis of *p*NO<sub>2</sub>PheDU, the (*S*)-selective conversion of this novel substrate was verified conducting whole cell biotransformations with the recombinantly expressed hydantoinase from *Arthrobacter crystallopoietes* DSM 20117. These findings reveal *p*NO<sub>2</sub>PheDU as a promising substrate for the synthesis of the amino acid *para*-nitro- $\beta$ -phenylalanine (*p*NO<sub>2</sub> $\beta$ Phe). By analysis of these compounds by thin layer chromatography, it was shown that  $\alpha$ -amino acid derivatives were differently derivatized than  $\beta$ -amino acid derivatives when using ninhydrin and Ehrlich's reagent. Furthermore, derivatization of the synthesized *p*NO<sub>2</sub>- $\beta$ -derivatives differed from other  $\beta$ -derivatives without a *p*NO<sub>2</sub>-residue.

Until now, industrial applications of the Hydantoinase Process for the production of optically pure  $\alpha$ -amino acids mainly employ whole cell biocatalysts. Nevertheless, whole cell biocatalysis also bears disadvantages as intracellular degradation reactions, transport limitations as well as low substrate solubility. Therefore, this process was investigated regarding its applicability in cell-free reaction systems. For this purpose, the hydantoinase from *A. crystallopoietes* DSM 20117 was on the one hand genetically modified to receive a C-terminal His-tag and on the other hand the same hydantoinase was codon-optimized and synthesized with a C-terminal His-tag and additionally an N-terminal SBP-tag for purification and immobilization.

To improve the soluble hydantoinase expression, cultivation and induction under oxygen deficiency was investigated. Thus, markedly higher specific activities were achieved due to an improved expression. Furthermore, a successful codon-optimization was verified, since the hydantoinase without codon-optimization exhibited lower specific activities in every cultivation setup.

For further improvement of the hydantoinase expression, various cultivation and induction parameters were tested by conducting high throughput screening in a microbioreactor system (BioLector®). These results also revealed higher specific activities for the codon-optimized hydantoinase compared to the non-optimized enzyme for every investigated cultivation setup. Causing of chemical stress by the

addition of 3 % ethanol to the cultivation medium led to a further improvement of expression as well as an increased specific activity for the codon-optimized hydantoinase. Examination of the expression without induction revealed a high basic activity of the T7-promoter, but the resulting specific activities were lower than for the induced cultures. A lower pH value of the cultivation medium caused no significant improvement. Based on the high throughput screening, the cultivation at pH 7 with 3 % ethanol in the cultivation medium and induction with 1 mM IPTG emerged as the best setup for expression of soluble hydantoinase.

Additionally, the coexpression of the codon-optimized hydantoinase and five different chaperone sets to assist folding of the target enzyme was investigated. Another high throughput screening of different parameters showed, that none of the tested chaperones was able to improve soluble hydantoinase expression. This points out, that the overexpression of chaperones involves not only advantages, but probably also drawbacks, like an increased proteolytic activity or the inhibition of natural chaperone expression.

To facilitate a cell-free reaction system, the codon-optimized hydantoinase as well as the carbamoylase from *A. crystallopoietes* DSM 20117 were purified by immobilized metal ion affinity using Ni sepharose beads. The protocol was optimized and purification was conducted successfully for both enzymes.

For the immobilization of both enzymes, functionalized magnetic beads were applied, which are also able to bind the His-tag of the target molecule by metal ion affinity. After optimization of several parameters as for example the regeneration of the magnetic beads, immobilization of the hydantoinase and carbamoylase was successful. Additionally, for the immobilized enzymes much higher specific activities were achieved. Furthermore, these functionalized magnetic beads were applied for the purification of both enzymes utilizing their His-tag. This method resulted in markedly higher specific activities compared to the purification via Ni sepharose beads. Consequently, a method for direct purification and immobilization from the crude cell extract was established, that is very fast as well as simple to perform and therefore prevents the loss of enzyme activity and recovery caused by an increased number of process steps.

For the immobilized hydantoinase, the hydrolysis of phenylhydantoin, benzylhydantoin as well as hydroxymethylhydantoin was successful and the immobilized carbamoylase was able to convert *N*-carbamoylphenylglycine, *N*-carbamoylphenylalanine and *N*-carbamoylserine to the corresponding amino acids. Therefore, the requirements for the synthesis of different  $\alpha$ -amino acids by the Hydantoinase Process in cell-free reaction systems was accomplished.

## ZUSAMMENFASSUNG

Nicht-kanonische  $\alpha$ -Aminosäuren spielen unter anderem in der pharmazeutischen Industrie bei der Synthese von Antibiotika eine bedeutende Rolle. Als wichtiges Beispiel sind hierbei D-Phenylglycin oder substituierte D-Phenylglycine zu nennen, welche Bestandteile von Penicillinen und Cephalosporinen sein können.  $\beta$ -Aminosäuren sind aufgrund ihrer besonderen strukturellen Eigenschaften ebenfalls von großer Bedeutung für pharmazeutische Produkte wie Peptidmimetika, Antibiotika oder biologisch aktive Sekundärmetabolite. Der Hydantoinase-Prozess dient der Herstellung enantiomerenreiner  $\alpha$ -Aminosäuren mittels dynamisch kinetischer Resolution und wird bereits erfolgreich industriell angewendet. Basierend darauf wurde ein modifizierter Hydantoinase-Prozess zur Synthese optisch reiner  $\beta$ -Aminosäuren untersucht.

Im Hinblick auf die Synthese einer neuen  $\beta$ -Aminosäure mithilfe des modifizierten Hydantoinase-Prozesses wurde in dieser Arbeit ein neu synthetisiertes Substrat, 6-(4-nitrophenyl)dihydro-pyrimidine-2,4(1*H*,3*H*)-dione ( $pNO_2$ PheDU), untersucht. Es wurde eine achirale HPLC-Analytik zum qualitativen und quantitativen Nachweis des Substrates sowie der daraus resultierenden *N*-Carbamoyl- $\beta$ -Aminosäure, *N*Carb

$pNO_2$  $\beta$ Phe, etabliert. Des Weiteren wurde eine chirale HPLC-Analytik zum Nachweis beider Entantiomere der *N*-Carbamoyl- $\beta$ -Aminosäure entwickelt. So konnte mittels Ganzzellbiotransformationen neben der erfolgreichen enzymatischen Hydrolyse von  $pNO_2$ PheDU durch die rekombinant exprimierte Hydantoinase aus *Arthrobacter crystallopoietes* DSM 20117 auch ein (*S*)-selektiver Umsatz des neuen Substrates durch dieses Enzym nachgewiesen werden. Dies macht  $pNO_2$ PheDU zu einem vielversprechenden Substrat für die Synthese der Aminosäure *para*-nitro- $\beta$ -Phenylalanin. Bei der Analyse dieser Stoffe mittels Dünnschichtchromatographie konnte zum einen gezeigt werden, dass  $\alpha$ -Aminosäurederivate durch Ninhydrin- und Ehrlichs-Reagenz unterschiedlich derivatisiert werden als  $\beta$ -Aminosäurederivate und zum anderen, dass die synthetisierten  $pNO_2$ -Derivate wiederum anders derivatisiert werden als  $\beta$ -Aminosäuren ohne  $pNO_2$ -Rest.

In industriellen Anwendungen des Hydantoinase-Prozesses zur Herstellung optisch reiner  $\alpha$ -Aminosäuren finden bisher hauptsächlich Ganzzellkatalysatoren Einsatz. Da diese jedoch auch Nachteile wie intrazelluläre Abbaureaktionen, Transportlimitierungen und niedrige Substratlöslichkeit mit sich bringen, wurde der Prozess in dieser Arbeit bezüglich einer Einsetzbarkeit in zellfreien Reaktionssystemen untersucht. Hierfür wurde die Hydantoinase aus *A. crystallopoietes* DSM 20117 zunächst mit einem His-tag versehen und außerdem wurde eine Codon-optimierte Variante dieses Enzyms mit C-terminalen His-tag sowie einem N-terminalen SBP-tag zur Aufreinigung und Immobilisierung synthetisiert.

Um anschließend die Expression funktionaler Hydantoinase in löslicher Form zu verbessern, wurde zunächst die Kultivierung und Expression unter Hypoxie untersucht. Dies resultierte in deutlich erhöhten spezifischen Aktivitäten für die Hydantoinase aufgrund einer verbesserten Expression. Außerdem konnte eine erfolgreiche Codon-Optimierung nachgewiesen werden, da die nicht optimierte Hydantoinase in jedem Fall geringere spezifische Aktivitäten aufzeigte als die optimierte.

Zur weiteren Verbesserung der Expression der Hydantoinase wurden verschiedene Parameter zur Kultivierung und Induktion mittels High-Throughput Screening in einem Mikrobioreaktionssystem (BioLector®) untersucht. Hierbei wies die Codon-optimierte Hydantoinase ebenfalls für jede untersuchte Kultivierungsstrategie höhere spezifische Aktivitäten auf als das nicht optimierte Enzym, was auf höhere Expressionsraten zurückzuführen ist. Die Zugabe von 3 % Ethanol zum Kultivierungsmedium führte zu einer weiteren Verbesserung der Expression sowie Erhöhung der spezifischen Aktivität der Codon-optimierten Hydantoinase. Untersuchungen der Expression ohne Induktion während der Kultivierung zeigten eine sehr hohe Basalaktivität des T7-Promotors auf, die daraus resultierende spezifische Aktivität war jedoch niedriger als bei induzierten Kulturen. Eine Verringerung des pH-Wertes des Mediums ergab keine signifikante Verbesserung der Expression oder Aktivität der Hydantoinase. Aus dem High-Throughput Screening ging die Kultivierung bei pH 7 mit 3 % Ethanol und Induktion mit 1 mM IPTG als beste Variante zur Expression aktiver Hydantoinase hervor.

Zusätzlich wurde die Coexpression der codon-optimierten Hydantoinase mit fünf verschiedenen Sets von Chaperonen zur verbesserten Faltung des Zielproteins untersucht. Ein erneutes Screening zeigte, dass keines der Chaperon-Sets eine Verbesserung der Expression erzielen konnte, wodurch auch keine erhöhte spezifische Aktivität erreicht wurde. Somit wurde aufgezeigt, dass die Überexpression von Chaperonen nicht nur Vorteile, sondern eventuell auch Nachteile, wie zum Beispiel eine erhöhte Proteaseaktivität oder eine Inhibierung der Expression natürlich vorkommender Chaperone mit sich bringen kann.

Um ein zellfreies Reaktionssystem für den Hydantoinase-Prozess zu ermöglichen, wurden die Hydantoinase sowie die Carbamoylase aus *Arthrobacter crystallopoietes* DSM 20117 über den His-tag mittels Ni-Sepharose Beads aufgereinigt. Das Protokoll konnte optimiert und somit die Aufreinigung für beide Enzyme erfolgreich durchgeführt werden.

Zur Immobilisierung beider Enzyme wurden funktionalisierte Magnetbeads verwendet, die ebenfalls über Metallionenaffinität den His-tag des jeweiligen Enzyms binden können. Nach der Optimierung einiger Parameter, wie beispielsweise der Regenerierung der Magnetbeads, konnte die Immobilisierung für beide Enzyme erfolgreich durchgeführt werden. Es wurden deutlich höhere spezifische Aktivitäten für die immobilisierten Enzyme im Vergleich zu den isolierten Enzymen erzielt. Des Weiteren wurden die funktionalisierten Magnetbeads zur Aufreinigung der Carbamoylase sowie der Hydantoinase über deren His-tag verwendet. Diese Methode führte zu deutlich höheren spezifischen Aktivitäten im Vergleich zur Aufreinigung der Enzyme mittels Ni-Sepharose Beads. Somit konnte eine schnelle und einfach durchzuführende Methode zur direkten Aufreinigung und Immobilisierung der Enzyme aus dem Rohextrakt etabliert werden. Durch eine niedrige Anzahl an Prozessschritten können Verluste an Aktivität und Ausbeute der Enzyme verhindert werden.

Des Weiteren wurde für die immobilisierte Hydantoinase erfolgreich der Umsatz von Phenylhydantoin, Benzylhydantoin und Hydroxymethylhydantoin gezeigt. Mit der immobilisierten Carbamoylase konnten die Substrate *N*-Carbamoylphenylglycin, *N*-Carbamoylphenylalanin sowie *N*-Carbamoylserin ebenfalls erfolgreich zu den entsprechenden Aminosäuren umgesetzt werden. Somit wurden die



Voraussetzungen zur Synthese verschiedener  $\alpha$ -Aminosäuren durch den Einsatz des Hydantoinase-Prozesses im zellfreien Reaktionssystem geschaffen.

# TABLE OF CONTENTS

Erklärung .....	III
Danksagung.....	IV
Abstract.....	V
Zusammenfassung .....	VII
1 Introduction.....	1
1.1 Non-Canonical Amino Acids.....	1
1.1.1 Relevance of Non-canonical Amino Acids.....	1
1.1.2 Different Synthesis Strategies .....	3
1.1.2.1 Deracemization Methods Toward Enantiopure $\alpha$ -Amino Acids.....	3
1.1.2.2 Synthesis of enantiopure $\beta$ -amino acids .....	4
1.1.3 Hydantoinase Process for the Synthesis of enantiopure $\alpha$ -amino acids.....	5
1.1.4 Modified Hydantoinase Process for the Synthesis of enantiopure $\beta$ -amino acids .....	6
1.1.5 Substrates: Hydantoins and Dihydropyrimidines.....	7
1.1.5.1 Occurrence in Nature.....	7
1.1.5.2 Racemization .....	9
1.1.5.3 Chemical Synthesis via Multicomponent Reactions .....	11
1.1.6 Enzymes: Cyclic Amidohydrolases and <i>N</i> -Carbamoylamino Acid Hydrolases .....	14
1.1.6.1 Hydrolysis of Hydantoins and Dihydropyrimidines .....	14
1.1.6.2 Hydrolysis of <i>N</i> -Carbamoylamino Acids .....	16
1.2 Toward Cell-Free Reaction Systems.....	18
1.2.1 Recombinantly Expressed Enzymes .....	18
1.2.1.1 The Importance of Codon-Usage for Protein Folding.....	19
1.2.1.2 Inclusion Bodies: Drawback or Benefit? .....	20
1.2.2 Purification and Immobilization of Recombinantly Expressed Enzymes .....	20
2 Research Proposal.....	22
3 Materials and Methods .....	23
3.1 Materials .....	23
3.1.1 Strains and Plasmids.....	28
3.1.2 Media .....	29
3.1.3 Buffers and Solutions.....	30
3.1.3.1 Analytical Methods.....	30
3.1.3.2 Cultivation and Induction .....	32
3.1.3.3 Purification of Enzymes via Ni Sepharose Beads .....	32
3.1.3.4 Immobilization and Purification of Enzymes via Functionalized Magnetic Beads .....	33
3.1.3.5 Biotransformation Assays.....	34

3.2	Methods .....	34
3.2.1	Analytical Methods.....	34
3.2.1.1	Sodium Dodecyl Sulfate Polyacrylamide Gel Electrophoresis .....	34
3.2.1.2	Thin Layer Chromatography .....	35
3.2.1.3	Photometric Ehrlich´s Assay.....	36
3.2.1.4	Photometric Ninhydrin Assay .....	37
3.2.1.5	High Performance Liquid Chromatography .....	37
3.2.1.6	Nuclear Magnetic Resonance Spectroscopy .....	37
3.2.1.7	Electron Ionization Mass-Spectrometry and Fast Atom Bombardment Mass-Spectrometry .....	38
3.2.1.8	Infrared Spectroscopy.....	38
3.2.1.9	Elemental Analysis .....	38
3.2.2	A Novel Substrate for the Synthesis of $\beta$ -Amino Acids .....	39
3.2.2.1	Chemical Synthesis of $pNO_2$ PheDU.....	39
3.2.2.2	Chemical Synthesis of the corresponding <i>N</i> -Carbamoyl Derivative.....	39
3.2.3	Improvement of Soluble Hydantoinase Expression.....	40
3.2.3.1	Codon-Optimization .....	40
3.2.3.2	Expression under Oxygen Deficiency.....	40
3.2.3.3	High Throughput Screening for Expression Conditions .....	40
3.2.4	Cultivation and Induction .....	42
3.2.4.1	Hydantoinase.....	42
3.2.4.2	Carbamoylase.....	43
3.2.5	Cell Disruption .....	44
3.2.5.1	Sonication .....	44
3.2.5.2	Chemical Cell Disruption .....	44
3.2.6	Purification of Enzymes .....	45
3.2.6.1	Buffer Exchange .....	45
3.2.6.2	Ni Sepharose Beads.....	45
3.2.6.3	Functionalized Magnetic Beads (His-Tag).....	46
3.2.7	Immobilization of Enzymes .....	46
3.2.7.1	Functionalized Magnetic Beads.....	46
3.2.8	Purification of Inclusion Bodies.....	47
3.2.9	Biotransformation Assays .....	47
3.2.9.1	Whole Cells.....	47
3.2.9.2	Crude Cell Extract and Purified Enzymes .....	48
3.2.9.3	Immobilized Enzymes.....	48
3.2.9.4	Inclusion Bodies.....	49
4	Results and Discussion .....	49

4.1	Establishment of Analytical Methods.....	49
4.1.1	Thin Layer Chromatography.....	49
4.1.2	Photometric Assays.....	52
4.1.3	High Pressure Liquid Chromatography.....	53
4.2	A Novel Substrate for the Synthesis of $\beta$ -Amino Acids.....	54
4.2.1	Chemical Synthesis of $p\text{NO}_2\text{PheDU}$ .....	55
4.2.2	Chemical Synthesis of the Corresponding <i>N</i> -Carbamoyl Derivative.....	55
4.2.3	Biotransformation Assays Using $p\text{NO}_2\text{PheDU}$ as a Substrate.....	56
4.2.4	Examination of Enantioselectivity for $p\text{NO}_2\text{PheDU}$ .....	59
4.3	Toward cell-free Reaction Systems.....	61
4.3.1	Improvement of Soluble Hydantoinase Expression.....	61
4.3.1.1	Codon-Optimization.....	61
4.3.1.2	Expression under Oxygen Deficiency.....	61
4.3.1.3	High Throughput Screening for Expression Conditions.....	65
4.3.1.4	Scale-Up of Optimized Expression Conditions.....	77
4.3.2	Purification of Enzymes via Ni Sepharose Beads.....	79
4.3.2.1	Preliminary Tests.....	79
4.3.2.2	Purification of the Hydantoinase via Ni Sepharose Beads.....	84
4.3.2.3	Purification of the Carbamoylase via Ni Sepharose Beads.....	86
4.3.3	Immobilization and Purification of Enzymes via Functionalized Magnetic Beads.....	88
4.3.3.1	Preliminary Tests.....	89
4.3.3.2	Immobilization via Functionalized Magnetic Beads (His-tag).....	94
4.3.3.3	Immobilization via Functionalized Magnetic Beads (SBP-Tag).....	98
4.3.3.4	Purification via Functionalized Magnetic Beads (His-Tag).....	100
4.3.4	Comparison of Purification and Immobilization of the Hydantoinase and Carbamoylase.....	105
4.3.5	Potential Applications.....	106
4.3.6	Purification of Inclusion Bodies.....	107
5.	References.....	109
6.	List of Figures.....	116
7.	List of Tables.....	118
8.	List of Abbreviations.....	119
5.	Appendix.....	121
5.1	Formulas.....	121
5.1.1	$\text{OD}_{600}$ /Scattered Light Correlation.....	121
5.1.2	Maximum Growth Rate.....	121
5.1.1	Specific Enzyme Activities.....	121
5.1.2	Enzyme Purification.....	121
5.1	NMR-Spectra.....	122

5.1	Sequences.....	124
5.1.1	Hydantoinase from <i>A. crystallopoietes</i> DSM 20117 with C-terminal His-tag .....	124
5.1.2	Codon-optimized Hydantoinase from <i>A. crystallopoietes</i> DSM 20117 with C-terminal His-tag and N-terminal SBP-tag .....	126
	Publications and Presentations .....	1
	Publications.....	1
	Conference Publication.....	1
	Lecture .....	1
	Posters .....	2

# 1 INTRODUCTION

## 1.1 NON-CANONICAL AMINO ACIDS

### 1.1.1 RELEVANCE OF NON-CANONICAL AMINO ACIDS

Amino acids are of increasing importance, for example as intermediates for food ingredients, pharmaceuticals and agrochemicals. In compounds like this, enantiopure amino acids play an essential role for the desired interactions.<sup>[1]</sup> To give a hint about the meaning of enantiopure  $\alpha$ - and  $\beta$ -amino acids, several characteristics and applications are described below.

Proteinogenic L- $\alpha$ -amino acids act as starting materials for products in the food industry and are mainly produced by fermentation processes.<sup>[2]</sup> In contrast, non-canonical L- $\alpha$ -amino acids are of great interest, since they serve as constituents of many drugs as protease inhibitors, peptide ligands and neuronal receptor ligands. L-homophenylalanine is used in the synthesis of ramipril (Figure 1 A) and other antihypertensives.<sup>[3-5]</sup>

D- $\alpha$ -amino acids are valuable building blocks in pharmaceuticals. For example D-(phenyl or substituted phenyl)glycines are constituents of antibiotics like semisynthetic penicillins and cephalosporins (Figure 1 B). Furthermore, D- $\alpha$ -amino acids are used for the production of agrochemicals such as D-valine in fluvalinate, an insecticide. D-alanine is used in the production of the dietetic sweetening agent alitame, for also naming a valuable intermediate for food industries.<sup>[1]</sup>

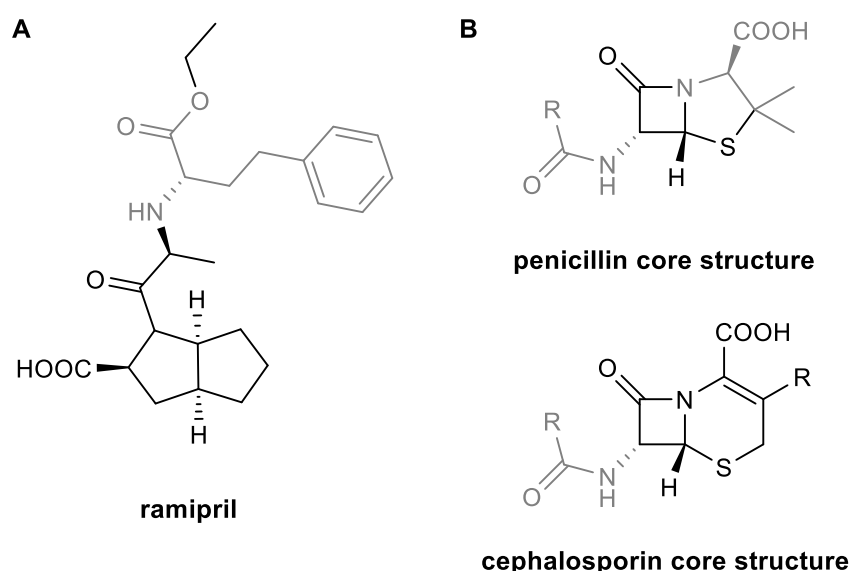


**Figure 1** Pharmaceutical products with non-canonical  $\alpha$ -amino acids as building blocks. **A** L- $\alpha$ -amino acids. **B** D- $\alpha$ -amino acids. Modified after Slomka et al.<sup>[6]</sup>

Another group of amino acids that got into focus for pharmaceutical industry lately are enantiopure  $\beta$ -amino acids. Figure 2 shows their structure compared to that of  $\alpha$ -amino acids. The amino group of  $\alpha$ -

amino acids is located at the  $\alpha$ -carbon, while  $\beta$ -amino acids show an amino group at the  $\beta$ -carbon.

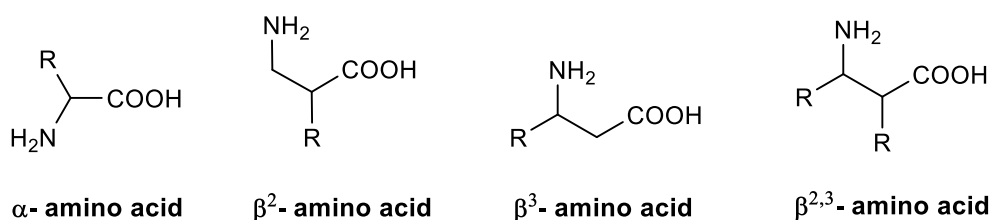


**Figure 2** Structural comparison of  $\alpha$ - and  $\beta$ -amino acids. Modified after Seebach and Gardiner<sup>[7]</sup>

Due to their special structural properties,  $\beta$ -amino acids serve as constituents of several biologically active secondary metabolites like Taxol<sup>TM</sup> (Figure 3 A), which was isolated from the pacific yew tree *Taxus brevifolia*. This antitumor agent contains a phenylisoserine moiety, a  $\beta$ -amino- $\alpha$ -hydroxy acid. Another example is the antifungal, anthelmintic and antitumor active cyclodepsipeptide Jaspamide (Figure 3 B). It contains a  $\beta$ -tyrosine moiety and occurs in the marine sponge *Japsis splendens*.<sup>[8]</sup> Further biologically active secondary metabolites containing  $\beta$ -amino acids are theopalauamide and dolastatins.<sup>[9]</sup> As building blocks for  $\beta$ -peptides, which are able to form very stable and predictable secondary structures, they are also promising in applications as peptidomimetics since canonical amino acids find limited application in this field due to rapid metabolism by proteolysis and interaction with multiple receptors.<sup>[7,10-12]</sup> Furthermore, cyclized  $\beta$ -amino acids like  $\beta$ -lactams show encouraging pharmacological properties,<sup>[13]</sup> and likewise some  $\beta$ -amino acids in their linear and free form.<sup>[14]</sup>

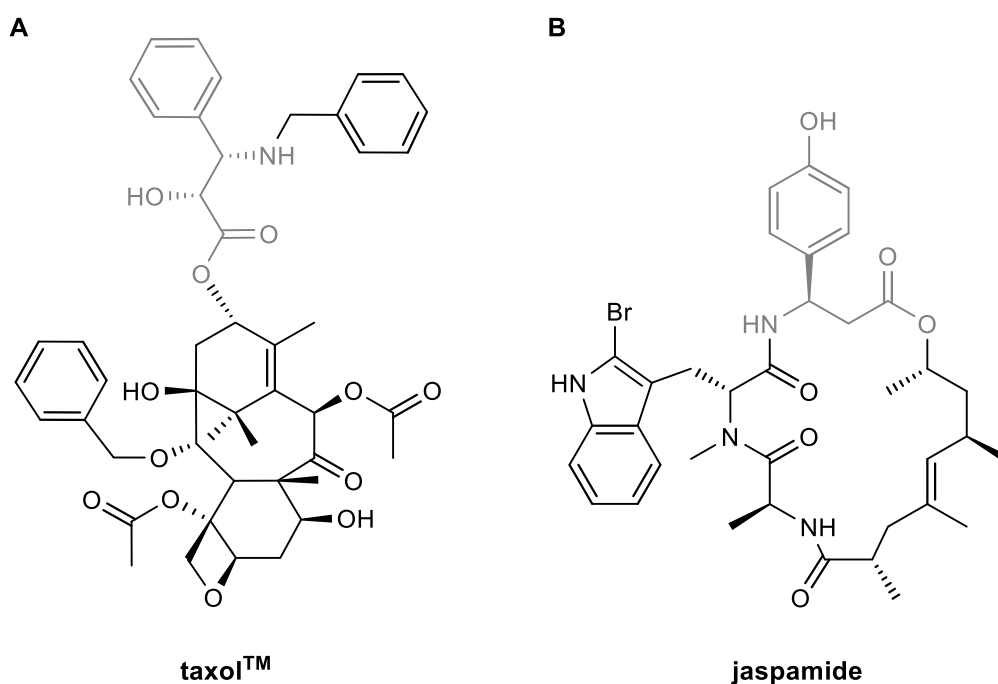


**Figure 3** Pharmaceutical products with  $\beta$ -amino acids as building blocks. Modified after Cardillo and Tomasini<sup>[15]</sup>

### 1.1.2 DIFFERENT SYNTHESIS STRATEGIES

Since enantiopure amino acids are highly valuable products, pharmaceutical as well as fine chemical companies are challenged to find new enantioselective technologies and to improve the existing processes for their synthesis. The production of most proteinogenic L- $\alpha$ -amino acids is feasible by protein hydrolysis and subsequent fractional extraction as well as by fermentation. Chemical synthesis of non-canonical amino acids is common, but without using asymmetrical starting compounds, a mixture of both enantiomers is obtained resulting in only 50 % chemical yield. Consequently additional separation steps and expensive racemization are required. From this point of view, the enzymatic synthesis of non-canonical amino acids has found broad application.<sup>[1,16]</sup> Below, various methods for the deracemization of amino acids are described, comparing chemical and biocatalytic processes.

#### 1.1.2.1 DERACEMIZATION METHODS TOWARD ENANTIOPURE $\alpha$ -AMINO ACIDS

Deracemization techniques describe processes, in which starting from a racemate, one single enantiomer is received. One possibility for deracemization of amino acids is kinetic resolution (Figure 4 A), where both enantiomers of a racemate are transformed to products at different reaction rates. In case of an efficient kinetic resolution, one of the enantiomers is converted to the desired enantiopure target molecule, while the other remains unchanged. Consequently, the yield is limited to 50 %.<sup>[12]</sup> Although kinetic resolution methods are still widespread, the fact that 50 % of the starting material has to be discarded or recycled in an additional racemization step forces the development of superior processes.<sup>[17]</sup>

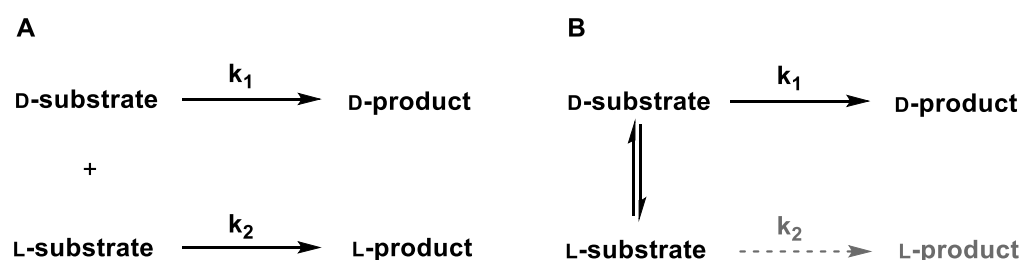


**Figure 4** Kinetic resolution (A) and dynamic kinetic resolution (B) in the synthesis of optically pure compounds.  $k_1$ : rate constant 1,  $k_2$ : rate constant 2

To overcome these limitations, the dynamic kinetic resolution of racemic mixtures was established for chemical as well as for biocatalytic processes providing optically pure products at up to 100 % of yield (Figure 4 B). Chemical methods either use chiral auxiliaries or metal complexes bearing chiral ligands like ruthenium catalysts to achieve a dynamic kinetic resolution.<sup>[18]</sup> Since chemical procedures often require drastic reaction conditions in addition to expensive catalysts, chemo-enzymatic processes or entire biocatalytic synthesis gained increasing attention. The acylase process for



example uses L-aminoacylases converting *N*-acetyl-D,L-amino acids into L-amino acids and *N*-acetyl-D-amino acids. Disadvantageous is the necessity of either extreme temperatures or pH-values or extraordinary catalysts to achieve racemization and therefore a dynamic kinetic resolution. However, Tokuyama et al. for example found *N*-acetyl amino acid racemases to handle this challenge.<sup>[19]</sup> Another enzymatic process uses L-amino acid amidases hydrolyzing amino acid amides to L-amino acids. Unsubstituted amino acid amides have to be treated with aromatic aldehydes at pH 8-11 for racemization since the resulting Schiff base can be easily racemized at a pH-value around 13.<sup>[16]</sup> A promising process for the synthesis of enantiopure  $\alpha$ -amino acids with *in situ* racemization under mild conditions is the Hydantoinase Process, which is described in more detail in Chapter 1.1.3. Starting with a hydantoinase that hydrolyses hydantoins to *N*-carbamoylamino acids, the reaction proceeds with the conversion of this intermediate by a carbamoylase to the amino acid. Depending on the residue of the hydantoins, their spontaneous racemization at basic pH is very fast or lasts several hours (see Chapter 1.1.5.2). Alternatively, dynamic kinetic resolution can be achieved by the additional application of hydantoin racemases.<sup>[20]</sup>

Also feasible is deracemization by stereo-inversion. In that case, one of the enantiomers is not enzymatically transformed while the other enantiomer is converted into a compound which can be turned into the starting compound of opposite configuration or into a racemate again. This is accomplished for example by using an amino acid oxidase and aminotransferase.<sup>[12]</sup>

### 1.1.2.2 SYNTHESIS OF ENANTIOPURE $\beta$ -AMINO ACIDS

As described above, the use of  $\beta$ -amino acids is of increasing importance for pharmaceutical industries. Thus, chemical methods for the synthesis of  $\beta$ -amino acids attracted attention over the last two decades, essentially based on classical resolution, stoichiometric use of chiral auxiliaries and homologation of  $\alpha$ -amino acids.<sup>[14,21]</sup> However, when applying in an industrial scale, these strategies show limitations as resolutions of racemic mixtures are time consuming and cause high costs.<sup>[9,21]</sup> Alternatively, various promising biocatalytical routes for the synthesis of enantiopure  $\beta$ -amino acids have been investigated and selected methods are described below. In the application of transaminases for instance, either kinetic resolution of a racemic  $\beta$ -amino acid or asymmetric synthesis starting from a prochiral  $\beta$ -keto acid is feasible.<sup>[22]</sup> The use of monooxygenases is also reported, where *N*-protected  $\beta$ -amino ketones serve as racemic substrates in a kinetic resolution resulting in an accumulation of *N*-protected  $\beta$ -amino esters. The latter are subsequently hydrolyzed to optically pure *N*-protected  $\beta$ -amino acids.<sup>[23]</sup> Another enzymatic route to enantiopure  $\beta$ -amino acids is the use of aminomutases like the phenylalanine aminomutase catalyzing the conversion of  $\alpha$ -phenylalanine to  $\beta$ -phenylalanine.<sup>[24]</sup> Most frequently, amino and ester functionalities in substrates are utilized for kinetic resolutions with hydrolytic enzymes. The best exploited enzymes for the synthesis of  $\beta$ -amino acids are lipases, for example cleaving *N*-acetylated  $\beta$ -amino acids or racemic  $\beta$ -amino acid esters.<sup>[25,26]</sup>

### 1.1.3 HYDANTOINASE PROCESS FOR THE SYNTHESIS OF ENANTIOPURE $\alpha$ -AMINO ACIDS

In 1978, the Hydantoinase Process was firstly described as a multi-enzymatic system for the production of optically pure D- $\alpha$ -amino acids.<sup>[27]</sup> The reactions and involved enzymes of this process are shown in Figure 5.

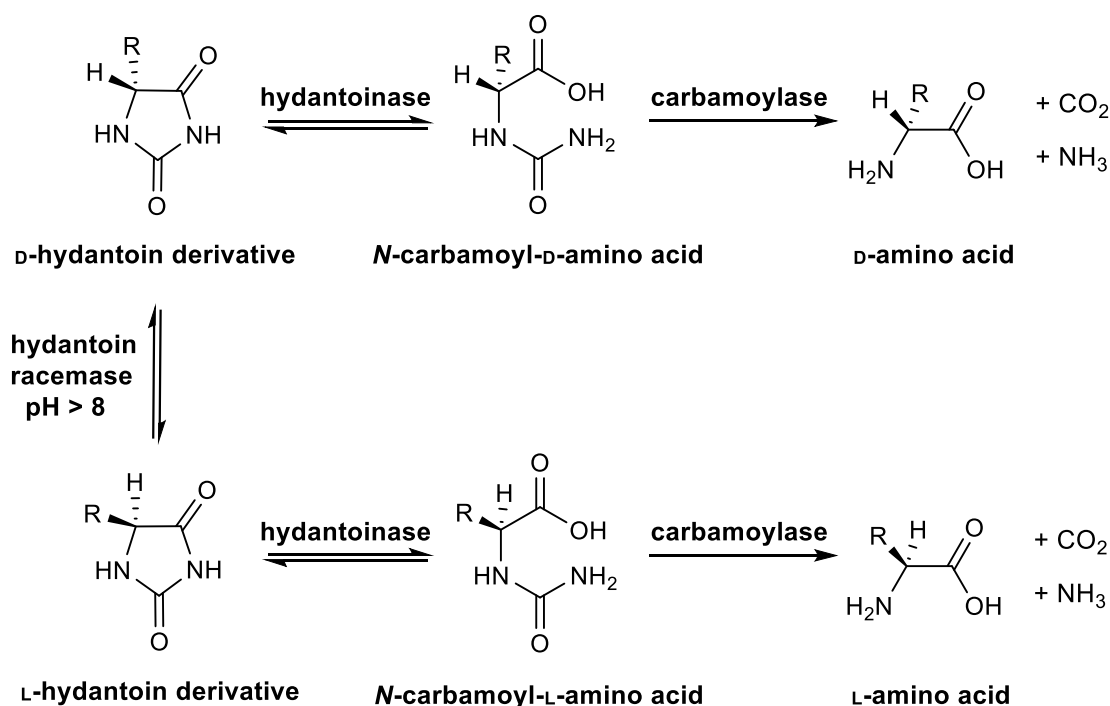


**Figure 5** Hydantoinase Process for the synthesis of optically pure  $\alpha$ -amino acids starting from racemic 5-monosubstituted hydantoins. Modified after Syldatk et al.<sup>[20]</sup>

The first step displays the hydrolysis of a D,L-5-monosubstituted hydantoin by an enantioselective hydantoinase. Simultaneously, either spontaneous racemization of the unconverted enantiomer occurs under slightly alkaline conditions or a hydantoin racemase can be applied for racemization.<sup>[28,29]</sup> (see Chapter 1.1.5.2) The resulting intermediate, an *N*-carbamoyl-D,L- $\alpha$ -amino acid is irreversibly hydrolyzed by an enantioselective *N*-carbamoylase afterwards. The combination of substrate racemization and the application of enantioselective biocatalysts results in a dynamic kinetic resolution process, allowing yield of 100 % of enantiopure  $\alpha$ -amino acid. Additionally, the wide substrate specificities of hydantoinases and carbamoylases as well as the easy synthesis of substrates from cheap compounds (see Chapter 1.1.5.3) increase the interest of the Hydantoinase Process for the industrial production of optically pure natural and non-natural amino acids. Plus, by performing enzymatic decarbamoylation, the accumulation of byproducts and waste is very low.<sup>[20]</sup> Therefore, the production of for instance D-phenylglycine and D-*p*-hydroxyphenylglycine is well-established in industries, adding up to an annual production of about 5000 tons per year.<sup>[16]</sup> To date, industrial applications of the Hydantoinase Process are focused on whole cell biocatalysis due to the simple accessibility of the biocatalyst, the reusability as well as its separation from the reaction mixture. But

since whole cell biocatalysis also bears some constraints like transport limitations for substrates and products as well as side and degradation reactions, there are several investigations toward cell-free reaction systems. Furthermore, problems like low substrate solubility and low enzyme stability could be avoided by using isolated or immobilized enzymes.<sup>[30]</sup> Therefore, this work focuses on the implementation of cell-free reaction systems based on the Hydantoinase Process by the improvement of recombinant expression of the biocatalysts as well as their purification and immobilization.

#### 1.1.4 MODIFIED HYDANTOINASE PROCESS FOR THE SYNTHESIS OF ENANTIOPURE $\beta$ -AMINO ACIDS

As mentioned above, optically pure  $\beta$ -amino acids are of increasing interest for several pharmaceutical applications. While the already discussed chemical and biocatalytical routes for their synthesis display kinetic resolutions that merely enable a maximum yield of 50 %, lately the application of a modified Hydantoinase Process was proposed (Figure 6).<sup>[31]</sup>

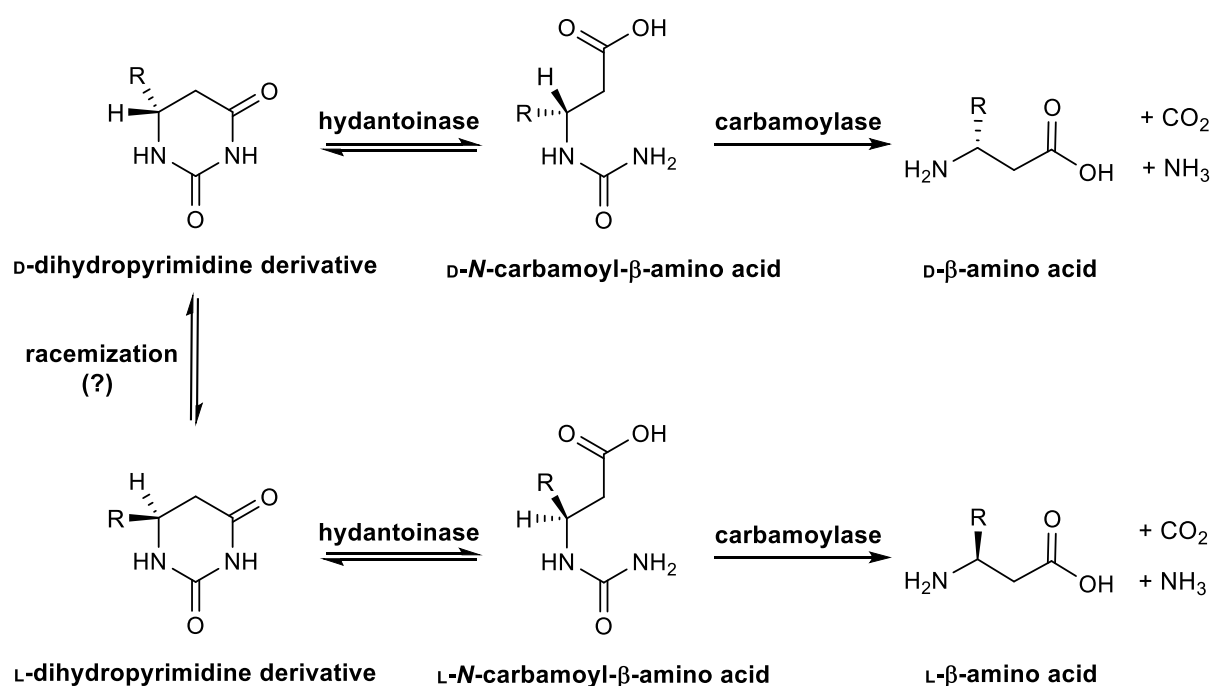


**Figure 6** Proposed modified Hydantoinase Process for the synthesis of optically pure  $\beta$ -amino acids starting from racemic 6-monosubstituted dihydrouracils<sup>[31]</sup>

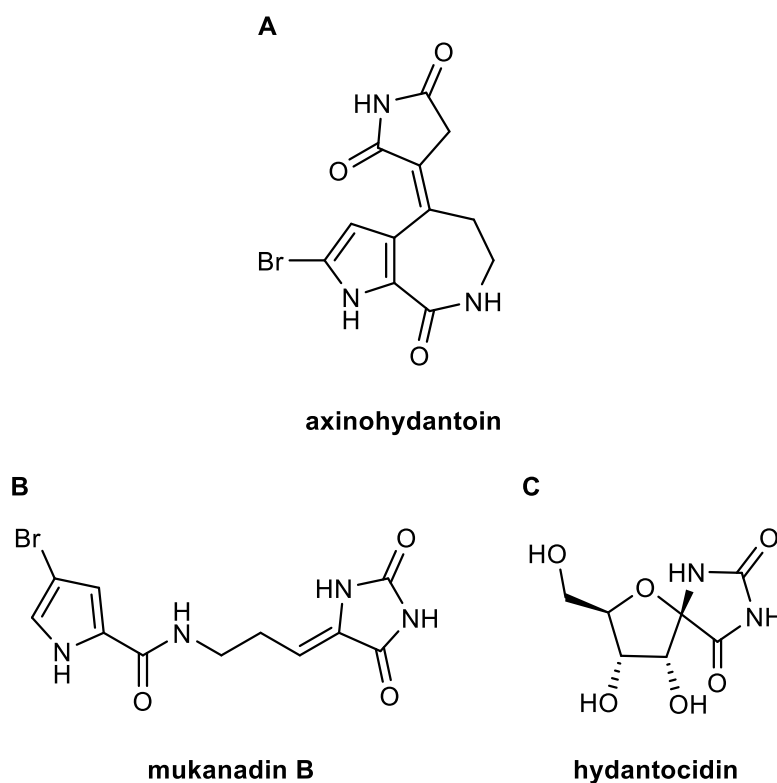
This process is based on the classical Hydantoinase Process (see Figure 5), which is well established in industrial processes for the production of enantiopure  $\alpha$ -amino acids via dynamic kinetic resolution of 5-monosubstituted hydantoins. Compared to the hydrolysis of hydantoins toward  $\alpha$ -amino acids, the hydrolysis of dihydropyrimidines to their *N*-carbamoyl derivatives as a route to  $\beta$ -amino acids has not been extensively studied yet. In 1998, May et al. showed the hydrolysis of dihydrouracil by a hydantoinase of *Arthrobacter aurescens* and later this hydantoinase was successfully employed to hydrolyze 6-phenyldihydrouracil.<sup>[32,33]</sup> Another group investigated the activity of the former

commercially available hydantoinase from *Vigna vulgaris* toward differently substituted dihydrouracils.<sup>[34]</sup> Even the second step of the modified Hydantoinase Process was realized by Martínez-Goméz et al.: The synthesis of  $\alpha$ -methyl- $\beta$ -alanine from 5-methyl-5,6-dihydrouracil was accomplished using the dihydropyrimidinase from *Sinorhizobium meliloti* CECT4114 and the  $\beta$ -ureidopropionase from *Agrobacterium tumefaciens* C58.<sup>[35]</sup> In contrast to the classical Hydantoinase Process, one of the main challenging parameters of the process development using 6-monosubstituted 5,6-dihydropyrimidines as substrates is to achieve a yield of 100 % of enantiopure product, since their spontaneous racemization is not yet known to occur and no suitable racemase is known (see Chapter 1.1.5.2).<sup>[35]</sup> Given that the viability of this route to  $\beta$ -amino acids was proven in some prior investigations<sup>[34,36]</sup>, in this work a novel substrate was investigated with regard to the biocatalytic synthesis of a new  $\beta$ -amino acid with specific properties.

## 1.1.5 SUBSTRATES: HYDANTOINS AND DIHYDROPYRIMIDINES

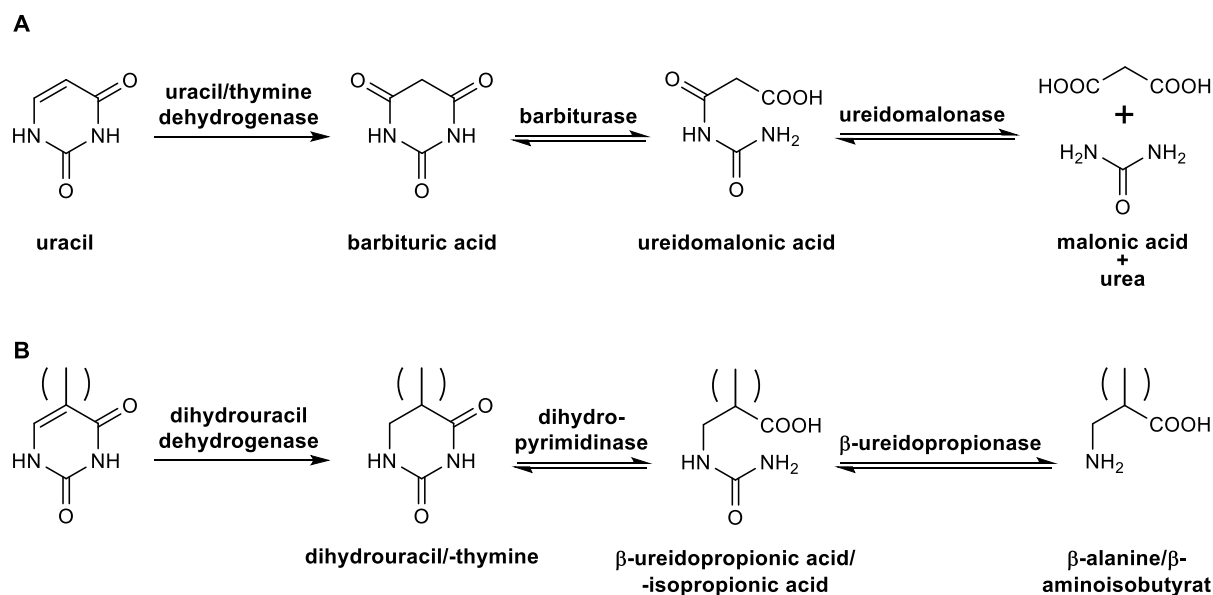
### 1.1.5.1 OCCURRENCE IN NATURE

In 1861 Adolf von Baeyer examined uric acid and in this context, by the hydrogenation of allantoin, he isolated the unsubstituted compound hydantoin for the first time and gave it its name.<sup>[37]</sup> The systematic term for hydantoin is imidazolidine-2,4-dione (IUPAC). A 5-monosubstituted hydantoin describes a cyclic ureide of an  $\alpha$ -amino acid, which is protected at the carboxy as well as at the  $\alpha$ -amino group. The urea substituted hydantoin allantoin for example is present in the urine of most mammals and in the comfrey plant *Symphyticum officinale*.<sup>[38]</sup> Other hydantoins and hydantoin derivatives occur in many marine organisms and also in bacteria. For instance, there are many alkaloids from sponges or corals containing a hydantoin moiety like axinohydantoins (Figure 7 A) from *Axinella*,<sup>[39]</sup> mukanadin B (Figure 7 B) from *Agelas* species<sup>[40]</sup> and hydantocidin (Figure 7 C), a spiro nucleoside from *Streptomyces hygrosopicus*.<sup>[41]</sup>



**Figure 7** Natural products containing hydantoins or hydantoin derivatives, modified after Meusel and Gütschow<sup>[42]</sup>

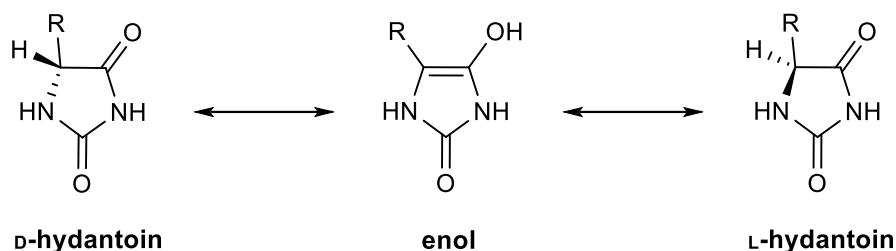
As mentioned earlier, D,L-5-monosubstituted hydantoins are used for the enzymatic synthesis of enantiomerically pure  $\alpha$ -amino acids.<sup>[43,44]</sup> Eadie et al. firstly described the hydrolysis of hydantoin to hydantoic acid (*N*-carbamoylglycine) by hydantoinases in mammals and plants in 1949.<sup>[45]</sup> Thereafter, in the 1970s the metabolism of *N*-substituted D,L-hydantoins was investigated, revealing that a dihydropyrimidinase from calf liver was able to convert D,L-5-monosubstituted hydantoins to *N*-carbamoyl-D-amino acids.<sup>[46–48]</sup> In addition to mammals and plants, microorganisms were also found to be able to hydrolyze hydantoin derivatives and even the ability of several bacteria to hydrolyze the resulting *N*-carbamoyl amino acids to D-amino acids was proven.<sup>[27,49]</sup> Several investigations of the reductive pathway of pyrimidine metabolism (see Figure 8 B) hypothesize hydantoinases are identical to dihydropyrimidinases, which catalyze the conversion of cyclic ureides. Therefore, it was assumed that some enzymes participating the pyrimidine degradation are required for D-amino acid production from D,L-5-monosubstituted hydantoins.<sup>[46,50–55]</sup> Nevertheless, it was proven that some hydantoinases converting hydantoins are not able to hydrolyze dihydrouracil and dihydrothymine, natural substrates of dihydropyrimidinases (see Chapter 1.1.6.1).<sup>[56–59]</sup> Consequently, these enzymes are not mandatorily identical and the term hydantoinases should be used for enzymes that catalyze the conversion of hydantoins and are not part of the pyrimidine degradation pathway. The term dihydropyrimidinases in contrast is suitable for enzymes of the pyrimidine metabolism that are able to hydrolyze dihydropyrimidines.<sup>[20,60]</sup> Hence, the connection between the Hydantoinase Process for the production of  $\alpha$ -amino acids and the modified Hydantoinase Process as a route to  $\beta$ -amino acids becomes apparent, since dihydropyrimidines serve as substrates for the latter.<sup>[36]</sup>



**Figure 8** Pyrimidine metabolism. **A** Oxidative pathway **B** Reductive pathway. Modified after Ogawa et al.<sup>[43]</sup>

### 1.1.5.2 RACEMIZATION

Hand in hand with the use of enantioselective enzymes, the racemization of substrates is essential to achieve a dynamic kinetic resolution in the synthesis of enantiopure amino acids (see Chapter 1.1.2.1). In this regard, the Hydantoinase Process is a promising tool given that hydantoins show a typical keto-enol tautomerism (see Figure 9).

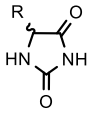
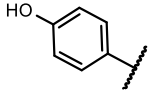
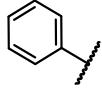
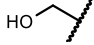
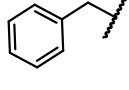
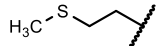
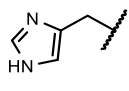
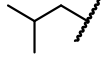
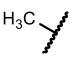
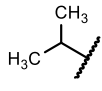
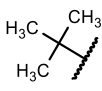


**Figure 9** Keto-enol tautomerism of 5-monosubstituted hydantoins under alkaline conditions. Modified after Engel et al.<sup>[60]</sup>

In detail, this means that under neutral conditions, the keto form is dominant, while enolization between the 4- and 5-positions may occur in alkaline environments.<sup>[61]</sup> This spontaneous racemization is perfectly suited for the complete conversion of racemic hydantoin derivatives to optically pure  $\alpha$ -amino acids. Since hydantoins cannot be D- or L- configured themselves, they are called “D” or “L” according to the configuration of their corresponding amino acid. Consequently, the same applies to the described enzymes.<sup>[62]</sup>

The electronic state of the substituent at the carbon 5 (C5) has an important impact on the ability of hydantoins to undergo racemization. Here, the release of the proton at C5 is promoted by substituents with a negative inductive effect that lower the electron density at C5 and stabilize the enolate structure. Table 1 shows the half life ( $t_{1/2, rac}$ ) for the chemical racemization of differently substituted hydantoins.

**Table 1** Racemization half-lives of differently substituted hydantoins. Conditions: 40 °C, pH 8.5, no buffer added. Modified after Bommarius et al.<sup>[16]</sup>

	Amino acid	$t_{1/2, rac}$ / h
	<i>p</i> -hydroxyphenylglycine	0.21
	phenylglycine	0.27
	serine	1.60
	phenylalanine	5.00
	methionine	5.82
	histidine	16.09
	leucine	21.42
	alanine	33.98
	valine	55.90
	tert-leucine	120.00

The shown values, differing in more than two orders of magnitude imply that hydantoins with a carboxy group on an alkyl side chain or hydantoins with arylalkylated or aryl side chains spontaneously racemize within a few minutes. In contrast, racemization may take several hours for hydantoins with alkylated side chains.<sup>[6]</sup> Therefore, depending on the used substrate, the application of a hydantoin racemase is not mandatory for the Hydantoinase Process, but supporting to get a high space-time yield.<sup>[63,64]</sup>

Hydantoin racemases (EC 5.1.99.5) are isomerases that are known to catalyze the racemization of 5-monosubstituted-D,L-hydantoins, while their natural substrate range is unknown to date. Compared to hydantoinases and *N*-carbamoylases, hydantoin racemases are rarely investigated. Nevertheless, there are some racemases that have been described in literature like for example from *Agrobacterium tumefaciens* C58, from *Sinorhizobium meliloti* CECT4114 and from *Microbacterium liquefaciens* AJ 3912.<sup>[65–67]</sup>

In contrast to the classical Hydantoinase Process, by application of the modified Hydantoinase Process toward  $\beta$ -amino acids, no dynamic kinetic resolution was achieved until now. This is caused by the fact that 6-monosubstituted 5,6-dihydropyrimidines, which serve as substrates are not yet known to chemically racemize and additionally no suitable racemase is known.<sup>[35]</sup> There are not many investigations concerning dihydropyrimidine racemization, but Argyrou *et al.* examined the interchange of protons in the C5 and revealed spontaneous racemization of 5-monosubstituted 5,6-dihydrouracils due to the acidic proton at a carbon next to a carbonyl group. In contrast, no racemization was observed for dihydroorotate (6-carboxy-dihydrouracil).<sup>[68]</sup> This was approved for further 6-monosubstituted dihydrouracil derivatives by Martínez-Gómez *et al.*<sup>[35]</sup>

### 1.1.5.3 CHEMICAL SYNTHESIS VIA MULTICOMPONENT REACTIONS

Since natural sources of hydantoins are not sufficient for the synthesis of different non-canonical  $\alpha$ -amino acids, various approaches for the synthesis of hydantoins have been examined. The most relevant methods starting from different building blocks are shown in Figure 11. One possibility is the Bucherer Bergs method, whereby *N*1- and *N*3- unsubstituted hydantoins can be formed, which is described in detail afterwards (Figure 10 a). Also feasible is the use of ureas and carbonyl compounds resulting in *N*1- and *N*3-substituted hydantoins (Figure 10 b) as well as the read-type-reaction of amino acids (esters) with inorganic iso(thio)cyanates which offers hydantoins with *N*3 as an unsubstituted position (Figure 10 c). Using alkyl- or aryl- iso(thio)cyanates leads to a substitution at the *N*3 position (Figure 10 d). Alternative substrates are amino amides that already exhibit four ring atoms which have to be completed to a hydantoin ring by an introduced C1-unit (Figure 10 e). As a last example for the synthesis of hydantoins, the reaction of  $\alpha$ -halogen amides with inorganic iso(thio)cyanates results in the formation of *N*1-unsubstituted hydantoins (Figure 10 f).<sup>[42]</sup>



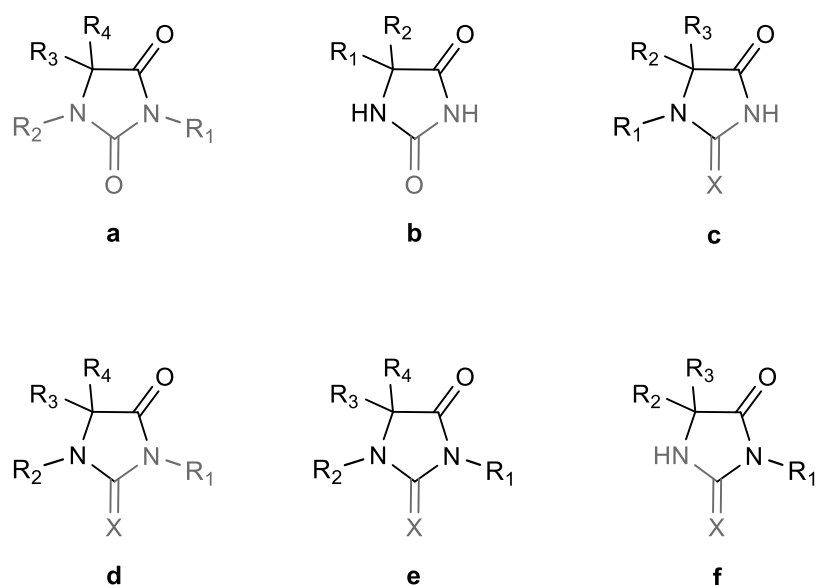


**Figure 10** Different building blocks and synthesis strategies for the synthesis of hydantoin. Modified after Meusel and Gütschow<sup>[42]</sup>

Although the Bucherer-Bergs synthesis is a very classical synthetic method for the synthesis of hydantoin, it is still commonly used due its efficiency and suitability.<sup>[69]</sup> The reaction displays the condensation of a ketone or aldehyde with cyanide, ammonia and carbon dioxide and takes place under mild conditions (see Figure 11 A). The mentioned efficiency of this four-component reaction is given by the fact that all reactants are combined in one chemical step, furnishing a product which contains substantial elements of all educts.<sup>[70]</sup> Using this methodology, only changes in the substitution of the carbonyl compound cause variations in the hydantoin structure. Therefore, this compound has to be prepared or purchased first. A method using nitriles and organometallic reagents as starting materials was conducted for this purpose, allowing the formation of the ketone in the same vessel as the Bucherer-Bergs synthesis (see Figure 11 B).<sup>[71]</sup> This strategy is suitable for the synthesis of various 5,5-disubstituted hydantoin with two points of diversity, since many nitriles are readily accessible or commercially available.

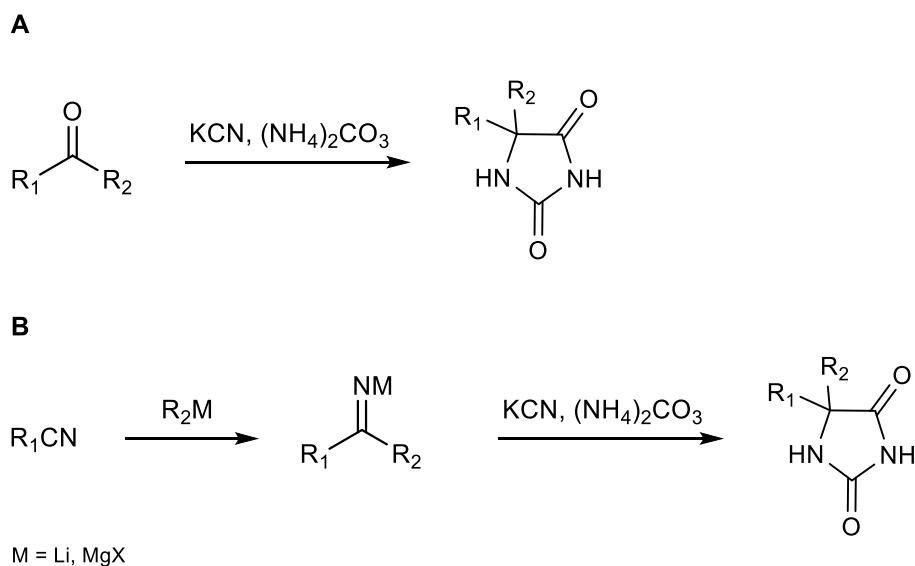


**Figure 11** **A** Bucherer-Bergs synthesis of 5-substituted hydantoin.<sup>[61]</sup> **B** Modified Bucherer-Bergs synthesis of 5-substituted hydantoin.<sup>[71]</sup>

Due to the manifold applicability of the Bucherer-Bergs synthesis, there are numerous alternative approaches for its modification. To name only two of them, for instance a microwave-assisted four-component reaction for the synthesis of 5-(4-iodophenyl)-5-phenylhydantoin was investigated, allowing the control of temperature, vessel pressure and reaction containment.<sup>[72]</sup> The second method worth mentioning is a multicomponent reaction, starting with the ring opening of a methyleneaziridine by a Grignard reagent under copper(I) iodide catalysis. Subsequently, the methylene group is alkylated and the hydantoin is formed by the Bucherer-Bergs synthesis.<sup>[73]</sup> In conclusion, this reaction enables three points of chemical diversity in the synthesis of hydantoin, by variation of the aziridine, the organometallic reagent and the electrophile.

For the synthesis of enantiomerically pure  $\beta$ -amino acids by a proposed modified Hydantoinase Process, the preparation of differently substituted dihydropyrimidines is essential. For this purpose, the Biginelli synthesis displays the most promising tool. Already in 1893, Biginelli reported about the one-pot, three-component synthesis of a dihydropyrimidine by the acid-catalyzed cyclocondensation reaction of ethyl acetoacetate, benzaldehyde and urea.<sup>[74]</sup> In the 1970s and 1980s, the interest in the synthetic potential of this heterocycle synthesis increased, since variation of the three building blocks allows a high number of multifunctionalized dihydropyrimidines.<sup>[75]</sup> One useful application of the Biginelli reaction was shown by Světlík and Veizerová, using Meldrum's acid for the synthesis of 5,6-dihydrouracils, see Figure 12.

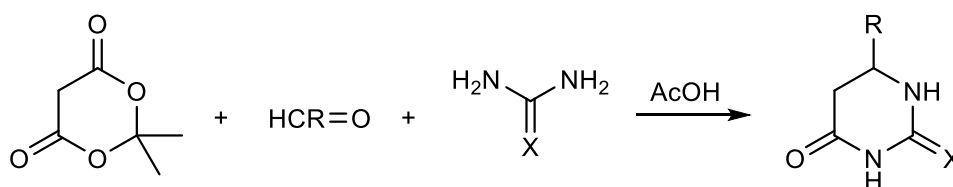


**Figure 12** Biginelli Reaction for the synthesis of differently substituted 5,6-dihydrouracils using Meldrum's Acid<sup>[76]</sup>

Alternative synthesis strategies for dihydropyrimidines are known, but since their protocols are not as simple as the one-pot, one-step procedures of Biginelli approaches, their significance is relatively low. However, the „Atwal modification“ of the Biginelli reaction is an attractive alternative: An enone is condensed with a protected urea or thiourea derivative and the resulting 1,4-dihydropyrimidine is subsequently deprotected to the desired dihydropyrimidine.<sup>[77]</sup> This method is also versatile, but requires prior synthesis of enones. Furthermore, the synthesis of dihydropyrimidines is feasible by the condensation of  $\alpha$ -tosyl-substituted (thio)ureas with the enolates of acetoacetates or 1,3-dicarbonyl compounds. The resulting hexahydropyrimidines can be directly converted into dihydropyrimidines and no isolation is necessary.<sup>[78]</sup>

### 1.1.6 ENZYMES: CYCLIC AMIDOHYDROLASES AND *N*-CARBAMOYLAMINO ACID HYDROLASES

#### 1.1.6.1 HYDROLYSIS OF HYDANTOINS AND DIHYDROPYRIMIDINES

Hydantoinases, dihydropyrimidinases, allantoinases and dihydroorotases are functionally and structurally related and represent the superfamily of cyclic amidohydrolases (EC 3.5.2).<sup>[79]</sup> Their function is to catalyze the hydrolysis of cyclic amide bonds of five- or six-membered rings occurring in the nucleotide metabolism.<sup>[6]</sup> In spite of low identities in amino acid sequences among these enzymes, investigation of primary sequences and hydropathy profiles indicated a number of conserved regions and invariant residues.<sup>[80]</sup> For example, site-directed mutagenesis of four conserved histidine residues caused a complete loss of enzyme activity as well as the loss of metal ions. Consequently, these conserved residues play a crucial role in coordination of metal ions and substrate binding of cyclic amidohydrolases.<sup>[81,82]</sup> Another fact, demonstrating the evolutionary relationship of cyclic amidohydrolases is the common triose phosphate isomerase (TIM) barrel scaffold containing two divalent metal ions. The latter are essential for the deprotonation of water molecules for the hydrophilic attack on the substrate.<sup>[79,83–86]</sup> Due to their relevance in the production of non-natural amino acids, dihydropyrimidinases and hydantoinases (EC 3.5.2.2) are highlighted below.

After the isolation of a hydantoin hydrolyzing enzyme from calf liver that has an important role in the metabolism of pyrimidines in 1956, Wallach and Grisolia called it “dihydropyrimidine hydrase”. As a result of these findings, the term hydantoinase has been used as a synonym for

dihydropyrimidinase.<sup>[87,88]</sup> Investigations of amino acid sequences showed that microbial hydantoinases and mammalian dihydropyrimidinases share 37-42 % of amino acid identity, indicating a closer relationship between these two enzymes than between allantoinases or dihydroorotases and dihydropyrimidinases.<sup>[80,89]</sup> However, further investigations revealed several hydantoinases that are able to hydrolyze hydantoins, but do not accept pyrimidines, the natural substrates of dihydropyrimidinases, as a substrate. Consequently, hydantoinases and dihydropyrimidinases are not mandatory the same enzymes.<sup>[56-59]</sup> Furthermore, hydantoinases are mostly microbial enzymes and dihydropyrimidinases are mainly found in eukaryotes.<sup>[79]</sup> Therefore, the term hydantoinases, whose natural substrates and physiological functions are still unknown, is used for hydantoin cleaving enzymes that are not involved in pyrimidine metabolism (see Figure 8). On the other hand, dihydropyrimidinases are part of the reductive pyrimidine pathway and are able to convert dihydropyrimidines, succinimides as well as hydantoins.

Similar to dihydropyrimidinases, hydantoinases exhibit hydrophobic patches to form dimers and additional hydrophobic interactions even allow the further dimerization to tetramers.<sup>[90-92]</sup> Mutational analysis showed that a dimeric hydantoinase has only 5.3 % of the specific activity of the tetrameric hydantoinase. Consequently, hydrophobic interactions as well as the dimeric interaction have a strong effect on the catalytic activity of hydantoinases.<sup>[93]</sup> As also known for dihydropyrimidinases, the dependency of hydantoinases on divalent metal ions has been reported.<sup>[94,95]</sup>

Furthermore, it has been discovered that the C-terminal region of hydantoinases is essential for the formation of the oligomeric structure.<sup>[80]</sup> For the hydantoinase from *Arthrobacter aurescens* DSM 3745 for example, it was shown that histidine residues are involved in the binding of zinc ions and therefore influence catalytic and structural properties of this enzyme.<sup>[96]</sup> The zinc ions are responsible for the activation of water; more precisely they increase its nucleophilicity for performing a nucleophilic attack on the substrate by decreasing the  $pK_a$  value.<sup>[97]</sup> Furthermore, by investigating the substrate spectra of hydantoinases, it was shown that electron density on the  $\alpha$ -position of the substrate is important for hydrolysis. Substituents like an aromatic moiety, methyl or phenyl groups influence the electron density on the  $\alpha$ -position and therefore support the ring-opening by hydantoinases. Additionally, it was shown that planar substrate structures are advantageous for the hydrolysis by hydantoinases.<sup>[98]</sup> Based on structural investigations, the specific conformation of the three chemistry gate loops (SGLs) was found to cause differences in substrate specificity as well as enantioselectivity of the enzymes.<sup>[99,100]</sup> Although the enantioselectivity of hydantoinases is often used as a characteristic for classification, it was demonstrated that the latter may differ according to the available substrate.<sup>[32,80,95]</sup> For example, May et al. showed that the hydantoinase from *Arthrobacter aurescens* DSM 3745 does not accept unsubstituted hydantoin as a substrate while hydantoin derivatives with hydrophobic substituents linked by a methylene group to the C5 of the hydantoin ring are favored. Therefore, for instance 5-phenylhydantoin is not hydrolyzed since the missing methylene group prevents interactions of the hydrophobic group of the substrate with the hydrophobic area of the enzyme. It was also discovered that there is a low enantioselectivity for substrates in which the hydrophobic group of both enantiomers can be sterically in the same position, for example 5-[2-(methylsulfanyl)ethyl]hydantoin.<sup>[32]</sup>

Investigations concerning the difference in thermostabilities of hydantoinases indicated that for instance higher numbers of aromatic residues in the interior structure increase this property. Other parameters enhancing the thermostability are high numbers of salt bridges, hydrogen-bonding interactions as well as rigid proline residues. The presence of metal ions was also found to be supportive to increase the thermostability of hydantoinases.<sup>[101]</sup>

#### 1.1.6.2 HYDROLYSIS OF *N*-CARBAMOYLAMINO ACIDS

The second step for the synthesis of non-canonical  $\alpha$ -amino acids via Hydantoinase Process is catalyzed by *N*-carbamoylases which are divided into  $\beta$ -ureidopropionases (EC 3.5.1.6), *N*-carbamoyl-D-amino acid hydrolases (EC 3.5.1.77) and *N*-carbamoyl-L-amino acid hydrolases (EC 3.5.1.87). They irreversibly hydrolyze *N*-carbamoyl- $\alpha$ -amino acids, the intermediates of this process.<sup>[43]</sup>

$\beta$ -Ureidopropionases take part in the reductive pyrimidine degradation pathway, catalyzing the hydrolysis of *N*-carbamoyl- $\beta$ -alanine to  $\beta$ -alanine as well as  $\beta$ -ureidoisobutyric acid to  $\beta$ -aminoisobutyric acid (see Figure 8). They occur in plants, yeast, bacteria, insects and slime mold.<sup>[102–105]</sup> Additionally, they have been isolated from human, calf as well as rat liver.<sup>[106–108]</sup> A wide substrate specificity was revealed for bacterial  $\beta$ -ureidopropionases, hydrolyzing several *N*-carbamoyl- $\alpha$ -,  $\beta$ - and  $\gamma$ -amino acids as well as *N*-acetyl- $\alpha$ -amino acids and *N*-formyl- $\alpha$ -amino acids.<sup>[95,104]</sup> Some L-*N*-carbamoylases accept *N*-acetyl- $\alpha$ -amino acids and *N*-formyl- $\alpha$ -amino acids as well.<sup>[109–112]</sup> The natural function of these enzymes is not yet entirely clarified, but it was supposed that eukaryotic L-*N*-carbamoylases act as detoxifying enzymes for *N*-carbamoyl-L-amino acids that have been formed by active carbamoyl groups. Another potential function is the synthesis of L-cysteine that was shown for the L-*N*-carbamoylases of the *Pseudomonas* sp. strains BS and ON-4a.<sup>[113,114]</sup> Investigations of the substrate specificity showed that L-*N*-carbamoylases from the genera *Alcaligenes*, *Bacillus* and *Pseudomonas* are able to hydrolyze aliphatic *N*-carbamoyl-L-amino acids and in contrast, enzymes from the genera *Arthrobacter* and *Flavobacterium* preferably accept aromatic *N*-carbamoyl-L-amino acids as substrates.<sup>[109–112]</sup>  $\beta$ -Ureidopropionases as well as L-*N*-carbamoylases are structurally related, as they show dependency for divalent metal ions and are both homodimers.<sup>[115,116]</sup>

Since D-*N*-carbamoylases are not able to hydrolyze  $\beta$ -ureidopropionate like  $\beta$ -ureidopropionases, a different function is assumed, but the actual natural function of D-*N*-carbamoylases stays unclear.<sup>[6]</sup> D-*N*-carbamoylases have a wide substrate specificity, as for example that from *Comamonas* sp. E222c for aromatic and aliphatic *N*-carbamoyl-D-amino acids. The D-*N*-carbamoylase from *Blastobacter* sp. A17p-4 in contrast favors *N*-carbamoyl-D-amino acids with hydrophobic groups.<sup>[117]</sup> It was reported that D-*N*-carbamoylases from *Agrobacterium* sp. exclusively accept the D-enantiomers of aliphatic and aromatic *N*-carbamoyl-D-amino acids.<sup>[58]</sup> In summary, the high stereoselectivity of these enzymes makes them a promising tool for the synthesis of enantiomerically pure  $\alpha$ -amino acids. The structure of

D-*N*-carbamoylases is different to that of  $\beta$ -ureidopropionases and L-*N*-carbamoylases. Diverse structures have been reported, like homodimers, homotetramers as well as D-*N*-carbamoylase consisting of three identical subunits.<sup>[117–119]</sup> Further structural investigations revealed the presence of cysteine residues in the active site of D-*N*-carbamoylases, indicating that they play an important role for the activity of these enzymes.<sup>[118,120]</sup> Providing this assumption, inactivation of a D-*N*-carbamoylase from *Agrobacterium* sp. by thiol reagents was observed.<sup>[49]</sup> Furthermore it was shown that the D-*N*-carbamoylase from *Agrobacterium tumefaciens* contains five cysteine residues, which are responsible for the inactivation of this enzyme under oxidizing conditions.<sup>[121]</sup> In detail, a catalytic triad consisting of glutamic acid, lysine and cysteine was found in D-*N*-carbamoylases.<sup>[122]</sup>

As already mentioned above, L-*N*-carbamoylases and D-*N*-carbamoylases have been successfully used in the Hydantoinase Process for the production of optically pure  $\alpha$ -amino acids. Transfer of the enzymes used in this process to a proposed modified Hydantoinase Process for the synthesis of  $\beta$ -amino acids was feasible for the hydantoinases/dihydropyrimidinases hydrolyzing dihydropyrimidines as well as differently substituted dihydropyrimidines.<sup>[31,32]</sup> However, the application of L-*N*-carbamoylases and D-*N*-carbamoylases for the hydrolysis of the resulting *N*-carbamoyl- $\beta$ -amino acid was not successful until now. Regarding their catalytic function in nature (see Figure 9, Reductive Pyrimidine Pathway),  $\beta$ -ureidopropionases are promising tools for the synthesis of non-natural  $\beta$ -amino acids. Martínez-Goméz et al. already managed the synthesis of  $\alpha$ -methyl- $\beta$ -alanine applying the  $\beta$ -ureidopropionase from *Agrobacterium tumefaciens* C58.<sup>[35]</sup>

## 1.2 TOWARD CELL-FREE REACTION SYSTEMS

The use of whole cell biocatalysis is widespread in industrial biocatalysis due to the easy access to the biocatalyst, low production costs and simple separation of biocatalyst and product. Nevertheless, there are also some drawbacks using whole cell biocatalysis like transport limitations of substrates as well as intermediates and products. Furthermore, uncontrollable degradative side reactions may take place inside of the cells and the substrate solubility is relatively low.<sup>[6]</sup> These are some of the reasons why cell-free reaction systems came into focus lately. By removal of the cell membrane, direct access to the complex set of chemical reactions taking place inside the cell is afforded. In detail, transport barriers are eliminated, which allows easy substrate addition as well as product extraction. Moreover, better monitoring and fine-tuning of the properties of the reaction system as well as rapid sampling is enabled. These advantages demonstrate that a decreased dependence on cells results in an increase in engineering flexibility. When working with cell-free reaction systems, there is the possibility to use either crude cell extracts or purified enzymes, depending on the amount of intracellular functions that have to be maintained. Drawbacks in using crude cell extracts are unwanted side activities that are difficult to handle and characterize. However, the application of purified enzymes is more time consuming as well as expensive and additionally, the stability of the latter is often comparatively low. It has to be taken into account that there is a major difference in enzyme concentrations between the use of whole cell biocatalysis and cell-free reaction systems, since the protein concentration in crude cell extracts is approximately 20 fold lower than in the very crowded intracellular environment. Consequently, several methods to increase concentrations as well as proximity of enzymes in cell-free systems involving multiple reactions have been investigated.<sup>[123–125]</sup>

In the synthesis of non-canonical amino acids by the Hydantoinase Process, the use of purified wild-type enzymes resulted in higher conversion yields caused by less side reactions and transport limitations. Nevertheless, the use of isolated wild-type enzymes for industrial application exhibits some drawbacks, since for instance their purification steps are very expensive and specific and they naturally occur in very low concentrations.<sup>[6]</sup> Furthermore, the inhibition of free enzymes by substrate particles in heterogeneous systems, by titrants like sodium hydroxide or due to the presence of solvents has been observed.<sup>[126–128]</sup> Concerning these facts, the application of recombinantly expressed enzymes is a promising alternative and is discussed below.

### 1.2.1 RECOMBINANTLY EXPRESSED ENZYMES

The use of recombinantly expressed enzymes provides an important tool to modulate expression levels, since the desired enzymes occur in very low concentrations in their wild-type strains which often only grow under very specific conditions with low growth rates. The application of well-established expression hosts like *Escherichia coli* eliminates these problems, allowing an

overexpression of the target molecule to obtain high concentrations.<sup>[129]</sup> This field furthermore allows enzyme engineering, for instance toward substrate specificity,<sup>[99]</sup> enantioselectivity,<sup>[130]</sup> thermostability and oxidative stability.<sup>[131,132]</sup> As mentioned above, the fact of lower enzyme concentrations in using cell-free reactions systems compared to the intracellular environment forces methods for increasing the enzyme concentrations as well as the proximity of enzymes in *in vitro* systems.<sup>[123–125]</sup> In this connection, the recombinant expression of enzymes allows the attachment of several tags to the desired enzymes for their purification and immobilization.

#### 1.2.1.1 THE IMPORTANCE OF CODON-USAGE FOR PROTEIN FOLDING

In spite of all advantages and possibilities enabled by recombinant gene expression in heterologous expression hosts, this also comes along with some challenges. The varying codon-usage from the different species when using another host than the wild-type for expression may lead to premature termination of translation, expression of non-functional or insoluble proteins or a complete lack of expression.<sup>[133,134]</sup> Consequently, the major problem in heterologous expression is the misfolding of proteins and to understand its causes, the translation step in protein expression was investigated in detail.<sup>[135]</sup> For *E. coli* and eukaryotic species, it was elucidated that a co-translational folding of proteins takes place in the ribosomal tunnel.<sup>[136,137]</sup> In this tunnel, changes in the rate of mRNA translation which depend on relative tRNA levels influence the formation of the secondary structure.<sup>[138]</sup> Specific frequencies of tRNA isoacceptor usage and abundance are directly related to proteins from different organisms. Therefore, it was suggested that the secondary structure of proteins is related to the tRNA usage frequencies.<sup>[139]</sup> Investigation of *E. coli* gene sequences as well as their corresponding protein structures proved that more frequently used codons are corresponding to highly ordered structural elements like alpha helices while less frequently used codons are related to random coils, beta-strands and structural domain boundaries.<sup>[140]</sup> It was assumed, that the reason for the latter phenomenon is that a slow translation in boundary regions between structural elements of high order enables correct folding of these elements, preventing degradation or aggregation of the protein.<sup>[135]</sup> In summary, this points out that synonymous codon substitutions have enormous consequences for the success of protein expression and should be considered for the heterologous expression of recombinant proteins. Codon-optimization of the desired gene according to the host organism, for instance, is an effective tool to improve the expression and therefore avoid misfolding and aggregation of the protein.



### 1.2.1.2 INCLUSION BODIES: DRAWBACK OR BENEFIT?

Inclusion bodies describe large protein aggregates, formed by the association of polypeptides that are unable to fold correctly inside of the cell.<sup>[141]</sup> As described in the previous chapter, they for instance are caused by wrong codon-usage. Additionally, process parameters like culture media composition, growth temperature and production rates induce the formation of inclusion bodies.<sup>[142]</sup> The use of affinity tags for purification of proteins may also interfere with the folding, depending on their location and amino acid composition.<sup>[143]</sup> Regarding biocatalysis, since inclusion bodies represent mostly inactive enzyme aggregates, they need to be avoided. In addition to changes in cultivation as well as induction conditions to slow down the expression and allow correct folding of the enzymes, the utilization of chaperones got into focus. They either can be induced by causing physical stress or coexpressed to support the correct folding of enzymes.<sup>[144,145]</sup>

On the other hand, there is also the possibility of forcing inclusion body accumulation and subsequently solubilizing and refolding them into catalytically active forms. But since protein aggregation is a higher-order reaction whereas refolding of the protein is a first-order reaction, protein aggregation is favored, resulting in poor recovery of refolded protein. Furthermore, proteins with many disulfide bonds require a very complex refolding process with optimized concentrations of oxidizing as well as reducing agents.<sup>[146,147]</sup> As a promising alternative, the use of catalytically active inclusion bodies without refolding was investigated since there are also several cases in that inclusion bodies retained a high degree of activity. This finding is very interesting, since without several purification steps, such inclusion bodies represent a simple, cost-efficient as well as stable kind of biocatalyst.<sup>[148,149]</sup>

## 1.2.2 PURIFICATION AND IMMOBILIZATION OF RECOMBINANTLY EXPRESSED ENZYMES

For working in cell-free reaction systems, especially regarding multi-stage reactions, the purification and immobilization of enzymes may be advantageous. Polypeptide fusion partners, called affinity tags, are often used to facilitate the purification of enzymes. They have to fulfill several requirements such as the applicability to various proteins, a minimal effect on structural properties and activity, a one-step absorption as well as easy removal to obtain the native protein. To name only some of the available toolbox, there is for instance the possibility to use calmodulin-binding peptides, cellulose-binding domains, maltose-binding proteins, FLAG-tags, Arg-tags, His-tags, Strep-tags und SBP-tags.<sup>[143]</sup> Since this work deals with the well-established His-tag (polyhistidine-tag) as well as the SBP-tag system, they are described more in detail.

His-tags consist of six polyhistidine residues and are therefore rather small, avoiding an influence on the tertiary structure of the enzyme. The amino acid histidine has the strongest interaction with

immobilized metal ion matrices, which is the principle of the purification via immobilized metal-affinity chromatography (IMAC). As transition metal ions,  $\text{Co}^{2+}$ ,  $\text{Ni}^{2+}$ ,  $\text{Cu}^{2+}$  and  $\text{Zn}^{2+}$  are applicable.<sup>[150]</sup> As a reliable adsorbent for IMAC, Hochuli et al. developed nitrilotriacetic acid (NTA), which forms a quadridentate chelate. Consequently, after binding, metal ions with coordination numbers of six still bear two valencies for the binding of His-tagged enzymes. After binding and washing of the matrix material, the target molecule can be eluted by adjusting the pH of the column buffer or by adding imidazole.<sup>[151]</sup> Another material that has been reported to result in higher purity of the target protein is TALON, consisting of a  $\text{Co}^{2+}$ -carboxymethylaspartate ( $\text{Co}^{2+}$ -CMA) that is coupled to a resin.<sup>[152]</sup> In spite of this improvement, there is still non-specific protein binding using IMAC.

A method that enables very specific binding is the protein purification by Strep-tag, an eight amino acid peptide. The employed matrices contain streptavidin or Strep-Tactin, a streptavidin-variant with mutations causing a higher affinity for the Strep-tag. After binding under physiological buffer conditions in the biotin binding pocket, gentle elution of the protein with biotin derivatives is conducted.<sup>[153,154]</sup> In this work, a new streptavidin-binding peptide, called SBP-tag, was applied. This tag has a length of 38 amino acids and its dissociation constant to streptavidin is 2.5 nM.<sup>[143,155]</sup> Both of the discussed methods show pros and cons, depending on the desired downstream processing. Although a His-tag provides high purification yields from cheap resins with high capacity, the purity is only moderate compared to SBP-tag purification. The latter in contrast allows very specific binding of the target molecule, but results in lower yields and causes higher costs.<sup>[156]</sup> However, if immobilization of proteins is aimed, the weak binding of a His-tag is not as suitable as the very stable and specific binding of a SBP-tag to Strep-Tactin.<sup>[157,158]</sup>

In addition to purification, the immobilization of enzymes is a suitable method for an easier handling and controllability as well as for stabilization and reutilization.<sup>[125]</sup> Concerning hydantoinases and *N*-carbamoylases, different immobilization methods have been developed using various supports like DEAE-cellulose, polyacrylamide, activated charcoal and calcium alginate.<sup>[52,159–161]</sup> Additionally, immobilization by coupling to Eupergit C and C 250 L by oxirane groups as well as by amino groups was performed successfully for both enzymes.<sup>[162–164]</sup> Nevertheless, the use of different matrices together with different surface modifications is often time-consuming and inefficient in practice, plus immobilization by covalent bond reagents may result in deactivation of the enzymes.<sup>[165]</sup> Since a metal-affinity based approach allows integrated purification and immobilization of enzymes in a simple procedure, it got into focus lately. Ho et al. applied silica-based IMAC adsorbents for the purification and immobilization of the D-hydantoinase from *Bacillus caldolyticus*.<sup>[166]</sup> Later, the simultaneous purification and immobilization of a D-hydantoinase was enabled by using an immobilized metal affinity membrane. The membrane-immobilized enzyme showed higher pH and temperature tolerances and was reusable for 15 times.<sup>[165,167]</sup>

In this work, magnetic beads that are functionalized with highly specific IMAC chemistry as well as magnetic beads carrying streptavidin have been investigated toward immobilization and purification of enzymes.

## 2 RESEARCH PROPOSAL

The increasing importance of non-canonical  $\alpha$ -amino acids as well as  $\beta$ -amino acids for the pharmaceutical industry resulted in the development of different enzymatical synthesis strategies. The Hydantoinase Process for example, which is applied in industries using whole cell biocatalysis, allows the synthesis of optically pure  $\alpha$ -amino acids via dynamic kinetic resolution and furthermore, a modified Hydantoinase Process was investigated toward the synthesis of enantiopure  $\beta$ -amino acids.

The synthesis of non-canonical  $\alpha$ - as well as  $\beta$ -amino acids exhibits great potential regarding new target molecules on the one hand and new reaction systems on the other hand. Therefore, one objective of this work was the investigation of a novel substrate for the synthesis of  $\beta$ -amino acids by a modified Hydantoinase Process. The second part of the work focused on the implementation of cell-free reaction systems for the classical Hydantoinase Process toward  $\alpha$ -amino acids.

For the first part of this work, the chemical synthesis of a novel substrate was aimed regarding the enzymatic hydrolysis by a hydantoinase for the synthesis of a novel  $\beta$ -amino acid with potentially interesting properties. Therefore, analytical methods for the qualitative and quantitative analysis of this substrate and its resulting product had to be studied, especially regarding the enantioselective conversion by the applied enzyme.

The second objective was to enable cell-free reaction systems for the Hydantoinase Process to avoid transport barriers as well as metabolic degradation of the substrate and product and additionally to allow high substrate concentrations. Therefore, the soluble expression of the hydantoinase had to be improved by testing various cultivation and expression conditions as well as by coexpression of chaperones.

Finally, purification methods for the hydantoinase and carbamoylase had to be facilitated, combined with the immobilization of both enzymes for higher stability and better handling as well as to allow the transfer of the Hydantoinase Process to cell-free systems such as microfluidic reaction systems.

### 3 MATERIALS AND METHODS

#### 3.1 MATERIALS

**Table 2** Chemicals and enzymes

Chemical	Empirical formula	Molar mass/ g/mol	Purity/ %	Supplier
( <i>R</i> )-3-amino-3-(4-nitrophenyl)-propionic acid	C <sub>9</sub> H <sub>10</sub> N <sub>2</sub> O <sub>4</sub>	210.19		Pep-Tech Corporation, Burlington (US)
1,4-dithiothreitol	C <sub>4</sub> H <sub>10</sub> O <sub>2</sub> S <sub>2</sub>	154.2	≥99	Carl Roth, Karlsruhe
1-butanol	C <sub>4</sub> H <sub>10</sub> O	74.12	≥99.5	Carl Roth, Karlsruhe
2-methoxyethanol	CH <sub>3</sub> OCH <sub>2</sub> CH <sub>2</sub> OH	76.09	99.8	Sigma Aldrich, St. Louis (US)
4-(dimethylamino)-benzaldehyde	(CH <sub>3</sub> ) <sub>2</sub> NC <sub>6</sub> H <sub>4</sub> CHO	149.19	98	Sigma Aldrich, St. Louis (US)
acetic acid	C <sub>2</sub> H <sub>4</sub> O <sub>2</sub>	60.05	99	Carl Roth, Karlsruhe
acetone	C <sub>3</sub> H <sub>6</sub> O	58.08	≥ 99.9	Carl Roth, Karlsruhe
acetonitrile	C <sub>2</sub> H <sub>3</sub> N	41.05	HPLC Grade	Carl Roth, Karlsruhe
acrylamide	C <sub>3</sub> H <sub>5</sub> NO	71.08	30	Carl Roth, Karlsruhe
ammonium formate	HCOONH <sub>4</sub>	63.06		Sigma Aldrich, St. Louis (US)
ammonium sulfate	(NH <sub>4</sub> ) <sub>2</sub> SO <sub>4</sub>	132.14	>99	Carl Roth, Karlsruhe
ammonium-peroxodisulfate	(NH <sub>4</sub> ) <sub>2</sub> S <sub>2</sub> O <sub>8</sub>	228.20	≥ 98	Carl Roth, Karlsruhe
ampicillin sodium salt	C <sub>16</sub> H <sub>19</sub> N <sub>3</sub> NaO <sub>4</sub> S	371.39	>99	Carl Roth, Karlsruhe
benzonase® nuclease (25 U/μL)				Merck Novagen, Billerica (US)
bovine serum albumin			≥ 98	Carl Roth, Karlsruhe
bromphenole blue	C <sub>19</sub> H <sub>9</sub> Br <sub>4</sub> O <sub>5</sub> SNa	691.90		Carl Roth, Karlsruhe

Chemical	Empirical formula	Molar mass/ g/mol	Purity/ %	Supplier
calcium chloride dihydrate	$\text{CaCl}_2 \cdot \text{H}_2\text{O}$	147.02	$\geq 98$	Carl Roth, Karlsruhe
chloramphenicol		323.13	$\geq 98$	Sigma Aldrich, St. Louis (US)
cobalt chloride Hexahydrate	$\text{CoCl}_2 \cdot 6\text{H}_2\text{O}$	237.93	98	Sigma Aldrich, St. Louis (US)
dipotassium hydrogen phosphate	$\text{K}_2\text{HPO}_4$	174.18	$\geq 99$	Carl Roth, Karlsruhe
ethanol	$\text{C}_2\text{H}_6\text{O}$	46.07	96	Carl Roth, Karlsruhe
glycerol	$\text{C}_3\text{H}_8\text{O}_3$	92.09	99.5	Carl Roth, Karlsruhe
glycine	$\text{C}_2\text{H}_5\text{NO}_2$	75.07	99.5	Carl Roth, Karlsruhe
guanidine hydrochloride	$\text{CH}_5\text{N}_3 \cdot \text{HCl}$	95.53	$\geq 99.7$	Carl Roth, Karlsruhe
hydrindantin hydrate	322.27	$\text{C}_{18}\text{H}_{10}\text{O}_6$	-	Sigma Aldrich, St. Louis (US)
hydrochloric acid	HCl	36.46	$\geq 32$	Merck Novagen, Billerica (US)
imidazole	$\text{C}_3\text{H}_4\text{N}_2$	68.08	$\geq 99.9$	Carl Roth, Karlsruhe
iron sulfate heptahydrate	$\text{FeSO}_4 \cdot 7 \text{H}_2\text{O}$	278.02	$\geq 99$	Carl Roth, Karlsruhe
isopropanol	$\text{C}_3\text{H}_8\text{O}$	60.1	$\geq 99.95$	Carl Roth, Karlsruhe
isopropyl- $\beta$ -D-thiogalactopyranosid	$\text{C}_9\text{H}_{18}\text{O}_5\text{S}$	238.30	$\geq 99$	Carl Roth, Karlsruhe
kanamycin	$\text{C}_{18}\text{H}_{36}\text{N}_4\text{O}_{11} \cdot \text{H}_2\text{SO}_4$	582.58		Carl Roth, Karlsruhe
L-phenylalanine	$\text{C}_6\text{H}_5\text{CH}_2\text{CH}(\text{NH}_2)\text{CO}_2\text{H}$	165.19	$\geq 98$	Sigma Aldrich, St. Louis (US)
L-phenylglycine	$\text{C}_6\text{H}_5\text{CH}(\text{NH}_2)\text{CO}_2\text{H}$	151.16	99	Sigma Aldrich, St. Louis (US)
L-serine	$\text{HOCH}_2\text{CH}(\text{NH}_2)\text{CO}_2\text{H}$	105.09	99	Sigma Aldrich, St. Louis (US)
lysozyme (40 kU/mg)				Sigma Aldrich, St. Louis (US)

Chemical	Empirical formula	Molar mass/ g/mol	Purity/ %	Supplier
magnesium sulfate heptahydrate	MgSO <sub>4</sub> · 7 H <sub>2</sub> O	246.48	≥ 99	Carl Roth, Karlsruhe
ninhydrin	C <sub>9</sub> H <sub>6</sub> O <sub>4</sub>	178.14	-	Sigma Aldrich, St. Louis (US)
potassium dihydrogen phosphate	KH <sub>2</sub> PO <sub>4</sub>	136.09	≥ 98	Carl Roth, Karlsruhe
sodium acetate trihydrate	CH <sub>3</sub> COONa · 3 H <sub>2</sub> O	136.08	≥ 99	Sigma Aldrich, St. Louis (US)
sodium chloride	NaCl	58.44	99.8	Carl Roth, Karlsruhe
sodium dodecyl sulfate, ultra pure	C <sub>12</sub> H <sub>25</sub> NaO <sub>4</sub> S	288.38	≥ 99.5	Carl Roth, Karlsruhe
tetramethylethylen-diamin	C <sub>6</sub> H <sub>16</sub> N <sub>2</sub>	116.20	≥ 99	Carl Roth, Karlsruhe
trifluoroacetic Acid	C <sub>2</sub> HF <sub>3</sub> O <sub>2</sub>	114.02	≥ 99.9	Carl Roth, Karlsruhe
tris(hydroxymethyl)-aminomethane	NH <sub>2</sub> C(CH <sub>2</sub> OH) <sub>3</sub>	121.14	≥ 99.8	Merck Novagen, Billerica (US)
tryptone				Becton Dickinson, New jersey (US)
tween® 20				Carl Roth, Karlsruhe
yeast extract				Becton Dickinson, New jersey (US)
zinc sulfate heptahydrate	ZnSO <sub>4</sub> · 7H <sub>2</sub> O	287.54	≥ 97	Carl Roth, Karlsruhe
β-phenylalanine	C <sub>6</sub> H <sub>5</sub> CH(NH <sub>2</sub> )CH <sub>2</sub> CO <sub>2</sub> H	165.19	98	Sigma Aldrich, St. Louis (US)

**Table 3** Consumption items

<b>Indication</b>	<b>Supplier</b>
Bug Buster®	Merck Novagen, Billerica (US)
Dynabeads® His-Tag Isolation and Pulldown	Life Technologies, Oslo (NOR)
Dynabeads® M-280 Streptavidin	Life Technologies, Oslo (NOR)
Imperial Protein Stain	ThermoFisher Scientific, Waltham (US)
Microbioreactor Plates, Flower-Plate®	m2p-labs, Baesweiler
Microtiter Plates, Rotilabo®-Microtest-Plates, F-Profile	Carl Roth, Karlsruhe
Ni Sepharose High Performance	GE Healthcare, Chalfont St. Giles (UK)
Page Ruler Plus	ThermoFisher Scientific, Waltham (US)
Protease Inhibitor Cocktail, Histidine-tagged Proteins	Sigma Aldrich, St. Louis (US)
Protein Quantification Kit BCA-Assay	Interchim, Montluçon (FR)
Roti®-Spin MINI, MWCO 10 kDa	Carl Roth, Karlsruhe
Slide-A-Lyzer™ MINI Dialysis Devices, MWCO 10 kDa	ThermoFisher Scientific, Waltham (US)
TLC-sheets, pre-coated ALUGRAM®SIL G, 0.20 mm silica gel	Machery-Nagel, Düren
Vivaspin® Turbo 15 Tubes, MWCO 50 kDa	Sartorius, Göttingen

**Table 4** Applied devices

<b>Device</b>	<b>Type</b>	<b>Supplier</b>
autoclave	V-150 and HX-430	Systec, Wettenberg
centrifuge	Multifuge X3 FR Rotor F21-48x1.5 Rotor 75003607	Thermo Fisher Scientific, Waltham (US)
dry freezer	Beta1-8	Christ, Osterode
elemental analyzer	vario MICRO	Elementar Analysensysteme, Hanau
HPLC	1200 series	Agilent Technologies, Santa Clare (US)
HPLC column	HyperClone ODS-C18 5 $\mu\text{m}$ , 120 $\text{\AA}$ , 50x4.6 mm	Phenomenex, Torrance (US)
HPLC column, chiral	Chiralpak QN-AX, 5 $\mu\text{m}$ , 150x46 mm, Daicel	Chiral Technologies, Illkirch- Graffenstaden (FR)
incubator	BBD 6620	Thermo Fisher Scientific, Waltham (US)
infrared spectrophotometer	FT-IR <i>Bruker</i> IFS 88	Bruker, Billerica (US)
magnetic support	DynaMag <sup>TM</sup> -2	Life Technologies, Oslo (NOR)
mass spectrophotometer	Finnigan MAT 90	Thermo Finnigan MAT GmbH, Bremen
microbioreactor	BioLector®	m2p-labs, Baesweiler
microtiter Plate Shaker	BioShake IQ	Analytik Jena, Jena
NMR- spectrophotometer	Avance 300 Avance 400	Bruker, Billerica (US)
overhead shaker	Reax 2	Heidolph, Schwabach
pH meter	InoLab® pH Level 1	WTW, Weilheim
pipettes	Research	Eppendorf, Wessling-Brensdorf
protein electrophoresis	Minigel Twin, Powerpack P25T	Biometra®, Göttingen



Device	Type	Supplier
scale	Entris 124-1S	Sartorius, Göttingen
scale	BP 3100 S	Sartorius, Göttingen
shaking incubator	Multitron	Infors HT, Bottmingen, (CH)
spectrophotometer	Ultrospec 1100 pro UV/Vis	GE Healthcare, Chalfont St. Giles (UK)
spectrophotometer	µQuant™	BioTek® Instruments, Winooski (US)
sterile bench	Lamin Air	Heto-Holten A/S, Allerød (DK)
tabletop centrifuge	Centrifuge 5415D Rotor F45-24-11	Eppendorf, Wesseling-Berzdorf
thermoshaker	Thermomixer comfort Thermomixer compact	Eppendorf, Wesseling-Berzdorf
ultrapure water system	Purelab Plus	USF Seral, Ransbach-Baumbach
ultrasonic bath	Sonorex Super RK 100	Bandelin electronic, Berlin
ultrasonic device	Model 120 Sonic Dismembrator	Thermo Fisher Scientific, Waltham (US)
ultrasonic probe	8-Tip Horn 3mm (1/8´´)	Thermo Fisher Scientific, Waltham (US)
vacuum pump	MZ2C	Vacuubrand, Wertheim

### 3.1.1 STRAINS AND PLASMIDS

**Table 5** Strains

Strain	Description	Source
<i>E. coli</i> BL21DE3	protein expression of D-Hyd	Gene bank BLT-TeBi (KIT)
<i>E. coli</i> BW3110	protein expression of D-Carb	Gene bank BLT-TeBi (KIT)
<i>E. coli</i> JM109	protein expression of D-Hyd	Gene bank BLT-TeBi (KIT)

**Table 6** Plasmids containing enzymes or chaperones

Plasmid	Resistance	Inducer	Description	Source
pDEST42	Amp	Rha	D-Hyd from <i>Arthrobacter crystallopoietes</i> DSM 20117, His-tag (C-terminus)	Marc Skoupi, (KIT, Institute for Biological Interfaces, Prof. Niemeyer)
pET28a	Kan	IPTG	codon-optimized D-Hyd from <i>Arthrobacter crystallopoietes</i> DSM 20117, His-tag (C-terminus), SBP-Tag (N-terminus)	Marc Skoupi, (KIT, Institute for Biological Interfaces, Prof. Niemeyer)
pJAVI2	Amp	Rha	D-Hyd from <i>Arthrobacter crystallopoietes</i> DSM 20117, Strep-tag (C-terminus)	Werner et al. <sup>[168]</sup>
pMW1	Amp	Rha	D-Carb from <i>Arthrobacter crystallopoietes</i> DSM 20117, His-tag (C-terminus)	Gene Bank BLT-TeBi (KIT)
pG-KJE8	Cm	L-Ara Tet	chaperones dnaK-dnaJ-grpE, groES-groEL (C1)	Takara Bio Inc.
pGro7	Cm	L-Ara	chaperones groES-groEL (C2)	Takara Bio Inc.
pKJE7	Cm	L-Ara	chaperones dnaK-dnaJ-grpE (C3)	Takara Bio Inc.
pG-Tf2	Cm	Tet	chaperones groES-groEL-tig (C4)	Takara Bio Inc.
pTf16	Cm	L-Ara	chaperone tig (C5)	Takara Bio Inc.

### 3.1.2 MEDIA

Every medium was autoclaved for 20 min at 121 °C before use and thermally unstable components were filtrated by a Rotilabo®-syringe (0.22 µm pore size, Carl Roth, Karlsruhe) filter and added afterwards.

#### Lysogeny broth medium (LB-medium)

tryptone	10 g
yeast Extract	5 g
NaCl	10 g
ddH <sub>2</sub> O	ad 1 L

All components were dissolved in  $\text{ddH}_2\text{O}$ , then the pH was adjusted to 7 and  $\text{ddH}_2\text{O}$  was added to receive a volume of 1 L. For making agar plates, the liquid LB-medium was supplied with 1.5 % agar before autoclaving.

### Terrific broth medium (TB-medium)

<u>media component</u>		<u>buffer component pH 7</u>	
Tryptone	12 g	$\text{KH}_2\text{PO}_4$	23.1 g
Yeast Extract	24 g	$\text{K}_2\text{HPO}_4$	125.4 g
Glycerol	0.4 %	$\text{ddH}_2\text{O}$	ad 100 mL
$\text{ddH}_2\text{O}$	ad 900 mL		

For TB-medium pH 6, the buffer component was adjusted to this pH before autoclaving. Then, the medium and the required buffer component were autoclaved separately and subsequently reunited to get a TB-medium with the desired pH.

## 3.1.3 BUFFERS AND SOLUTIONS

### 3.1.3.1 ANALYTICAL METHODS

#### SDS gels (2x)

	<u>stacking gel (5 %)</u>	<u>running gel (12.5 %)</u>
1.88 M TRIS/HCl (pH 8)	-	2.4 mL
0.625 M TRIS/HCl (pH 6.8)	800 $\mu\text{L}$	-
10 % w/v SDS	40 $\mu\text{L}$	120 $\mu\text{L}$
$\text{ddH}_2\text{O}$	2.5 mL	4.48 mL
acrylamide (30 %)	660 $\mu\text{L}$	5 mL
10 % w/v APS	20 $\mu\text{L}$	60 $\mu\text{L}$
TEMED	4 $\mu\text{L}$	10 $\mu\text{L}$

All components were pooled, while APS and TEMED were added as the last ones, since they start the polymerization of the gel.<sup>[169]</sup> Storage was feasible for 14 days at 4 °C.

#### SDS loading buffer

TRIS	225 mM
DTT	225 mM
bromphenole blue	0.05 % w/v
glycerol	20 % v/v
SDS	19 % v/v

The components for a 5x SDS Loading Buffer were dissolved in  $\text{d}_d\text{H}_2\text{O}$  and the pH was adjusted to 6.8.

#### SDS running buffer

TRIS	250 mM
glycine	1.92 M
SDS	1 % w/v

The components for the 10x SDS running buffer, a TGS-buffer, were dissolved in  $\text{d}_d\text{H}_2\text{O}$ .

#### TLC solvent

acetone	35 mL
1-butanol	35 mL
acetic acid	10 mL
$\text{d}_d\text{H}_2\text{O}$	20 mL

#### Ehrlich´s reagent for TLC (staining solution)

dimethylaminobenzaldehyde	0.5 g
conc. HCl	25 mL
ethanol	25 mL

The storage occurred protected from light and at -20 °C.

#### ninhydrin reagent for TLC (staining solution)

ninhydrin	0.3 g
acetone	95 mL

The storage occurred protected from light and at -20 °C.

#### Ehrlich´s reagent (photometric Ehrlich´s assay)

Dimethylaminobenzaldehyde	1 g
conc. HCl	5 mL
$\text{d}_d\text{H}_2\text{O}$	5 mL

The storage occurred protected from light and at -20 °C.

#### ninhydrin reagent (photometric ninhydrin assay)

ninhydrin	0.116 g
hydrindantin	0.116 g
2-methoxyethanol	10 mL

**acetate buffer (photometric ninhydrin assay)**

sodium acetate	35.3 g
acetic acid (96 %)	6.9 mL
$\text{ddH}_2\text{O}$	100 mL

**isopropanol solution (photometric ninhydrin assay)**

isopropanol	50 mL
$\text{ddH}_2\text{O}$	50 mL

## 3.1.3.2 CULTIVATION AND INDUCTION

**antibiotics for selection**

	<u>stock concentration</u>	<u>working concentration</u>
ampicillin	100 mg/mL	100 $\mu\text{g}/\text{mL}$
chloramphenicol	20 mg/mL	20 $\mu\text{g}/\text{mL}$
kanamycin	100 mg/mL	100 $\mu\text{g}/\text{mL}$

**inducers**

	<u>stock concentration</u>	<u>working concentration</u>
arabinose	300 mg/mL	3 mg/mL
IPTG	100 mM	1 mM
rhamnose	20 mg/mL	2 mg/mL
tetracycline	5 $\mu\text{g}/\text{mL}$	5 ng/mL

Every component was dissolved in  $\text{ddH}_2\text{O}$  whereas chloramphenicol and tetracycline were dissolved in ethanol. The solutions were filtrated by a Rotilabo®-syringe filter and stored at  $-20\text{ }^\circ\text{C}$ .

## 3.1.3.3 PURIFICATION OF ENZYMES VIA NI SEPHAROSE BEADS

**wash- and binding buffer**

<u>buffer components</u>		<u>additives (hydantoinase)</u>		<u>additives (carbamoylase)</u>
TRIS-HCl	50 mM	-		DTT 5 mM
NaCl	500 mM			
imidazole	20 mM			

**elution buffer**

<u>buffer components</u>		<u>additives (hydantoinase)</u>		<u>additives (carbamoylase)</u>	
TRIS-HCl	50 mM	ZnSO <sub>4</sub>	1 mM	DTT	5 mM
NaCl	500 mM				
imidazole	500 mM				

The buffer components were dissolved in  $\text{d}_d\text{H}_2\text{O}$ , then the pH was adjusted to 8 and  $\text{d}_d\text{H}_2\text{O}$  was added to receive a volume of 1 L. Subsequently, ZnSO<sub>4</sub> (100 mM stock) or DTT (1 M stock) solutions in  $\text{d}_d\text{H}_2\text{O}$  were added to receive the desired concentrations. The stock solutions were stored at -20 °C and DTT was additionally stored in aliquots to avoid repeated defrosting, since it is very unstable. The additive ZnSO<sub>4</sub> was not used in the wash- and binding buffer since it precipitates herein.

### 3.1.3.4 IMMOBILIZATION AND PURIFICATION OF ENZYMES VIA FUNCTIONALIZED MAGNETIC BEADS

<b>wash- and binding buffer (His-tag)</b>		<b>elution buffer (His-tag)</b>	
NaPP	50 mM	NaPP	50 mM
NaCl	300 mM	NaCl	300 mM
tween® 20	0.01 %	tween® 20	0.01 %
		imidazole	300 mM

The buffer components were dissolved in  $\text{d}_d\text{H}_2\text{O}$ , then the pH was adjusted to 8 and  $\text{d}_d\text{H}_2\text{O}$  was added to receive a volume of 1 L.

**functionalization solution (His-tag)**

For recovery of the functionalized magnetic beads, 10 mM cobalt chloride hexahydrate was dissolved in  $\text{d}_d\text{H}_2\text{O}$ .

**wash- and binding buffer (SBP-tag)**

PBS	50 mM
tween® 20	0.01 %

The buffer components were dissolved in  $\text{d}_d\text{H}_2\text{O}$ , then the pH was adjusted to 7.4 and  $\text{d}_d\text{H}_2\text{O}$  was added to receive a volume of 1 L.

### 3.1.3.5 BIOTRANSFORMATION ASSAYS

#### **catalysis buffer**

<u>buffer components</u>		<u>additives (hydantoinase)</u>		<u>additives (carbamoylase)</u>	
Tris-HCl	50 mM	ZnSO <sub>4</sub>	1 mM	DTT	5 mM

The buffer components were dissolved in  $\text{d}_2\text{O}$ , then the pH was adjusted to 8 and  $\text{d}_2\text{O}$  was added to receive a volume of 1 L. Subsequently, ZnSO<sub>4</sub> (100 mM stock) or DTT (1 M stock) solutions in  $\text{d}_2\text{O}$  were added to receive the desired concentrations. The stock solutions were stored at -20 °C and DTT was additionally stored in aliquots to avoid repeated defrosting, since it is very unstable. For whole cell biotransformation assays, no additives have been supplied to this buffer.

#### **substrate and product solutions**

The applied substrates for biotransformation assays and resulting products were dissolved in catalysis buffer to a final concentration of 10 mM. If necessary, the buffer was supplied with the required additives for the hydantoinase or carbamoylase.

<u>hydantoin (abbr.)</u>	<u>N-carbamoyl-<math>\alpha</math>-amino acid (abbr.)</u>	<u><math>\alpha</math>-amino acid (abbr.)</u>
phenylhydantoin (PheHyd)	N-carbamoylphenylglycine (NCPheGly)	Phenylglycine (PheGly)
benzylhydantoin (BnH)	N-carbamoylphenylalanine (NCPheAla)	Phenylalanine (PheAla)
hydroxymethylhydantoin (HMH)	N-carbamoylserine (NCSer)	Serine (Ser)

Since a novel synthesized dihydropyrimidine, 6-(4-nitrophenyl)dihydropyrimidine-2,4(1*H*,3*H*)-dione ( $p\text{NO}_2\text{PheDU}$ ), is poorly soluble in water, it was dissolved in DMSO to a concentration of 40 mM and subsequently it was diluted to a concentration of 4 mM by adding catalysis buffer. The corresponding N-carbamoyl- $\beta$ -amino acid (NCPNO<sub>2</sub>  $\beta$  Phe) was prepared in the same way for analytical purposes.

Every substrate and product solution was prepared freshly and the same solution was used for biotransformation assays as well as for analytics.

## 3.2 METHODS

### 3.2.1 ANALYTICAL METHODS

#### 3.2.1.1 SODIUM DODECYL SULFATE POLYACRYLAMIDE GEL ELECTROPHORESIS

For sample preparation, the insoluble part after chemical cell disruption and centrifugation was resuspended in  $\text{d}_2\text{O}$  by using twice the amount of the culture volume at the moment of harvesting. Every soluble part that had to be analyzed by sodium dodecyl sulfate polyacrylamide gel

electrophoresis (SDS-PAGE) was diluted to a protein concentration of 1 mg/mL with  $\text{d}_2\text{H}_2\text{O}$  and samples with lower protein concentrations were used without dilution. Then, 40  $\mu\text{L}$  of every prepared sample were mixed with 10  $\mu\text{L}$  of SDS-loading buffer and incubated at 99 °C and 800 rpm for 15 min. After cooling, the samples were centrifuged for 1 min at 13 000 rpm and in each case 20  $\mu\text{L}$  were loaded to the SDS-gel. Additionally, 5  $\mu\text{L}$  of the prestained protein ladder were loaded for determination of the atomic mass of the proteins. Electrophoresis was conducted at 120 V for about 1.5 h and subsequently, the SDS-gels were stained in Coomassie Brilliant Blue for at least 5 h on a platform shaker. The bleaching occurred in  $\text{d}_2\text{H}_2\text{O}$  and for about 5 h as well. After disrupting the samples of the Bio Lector® cultivations by sonication and subsequent centrifugation, the soluble parts were also diluted to a concentration of 1 mg/mL with  $\text{d}_2\text{H}_2\text{O}$ . The resulting insoluble pellets were resuspended in 300  $\mu\text{L}$   $\text{d}_2\text{H}_2\text{O}$ . The following sample preparation for SDS-PAGE was carried out as described above.

### 3.2.1.2 THIN LAYER CHROMATOGRAPHY

For separation of the samples that had been taken during biotransformation assays, in every case 5  $\mu\text{L}$  were applied with a distance of 1 cm on a silica gel thin layer chromatography plate (TLC-plate). As standards, the particular *N*-carbamoyl amino acids or amino acids were applied in the same way. After drying with a hot air gun at 50 °C, the TLC-plate was placed into a TLC-chamber that was saturated with solvent for about 20 min. When the solvent front reached 60 % of the TLC-plate, it was removed from the TLC-chamber and the solvent front was marked for determination of the retention factor ( $R_f$ ). The dried TLC-plate was then stained by dipping for several seconds into the required staining solution. In this connection, Ehrlich's reagent was used to stain primary amines of *N*-carbamoylamino acids by nucleophile addition of the amino group to the aldehyde from *p*-dimethylaminobenzaldehyde (see Figure 13 A), while ninhydrin reagent was used for staining amino acids (see Figure 13 B). For visual development, the plates were dried with a hot air gun at 140 °C.



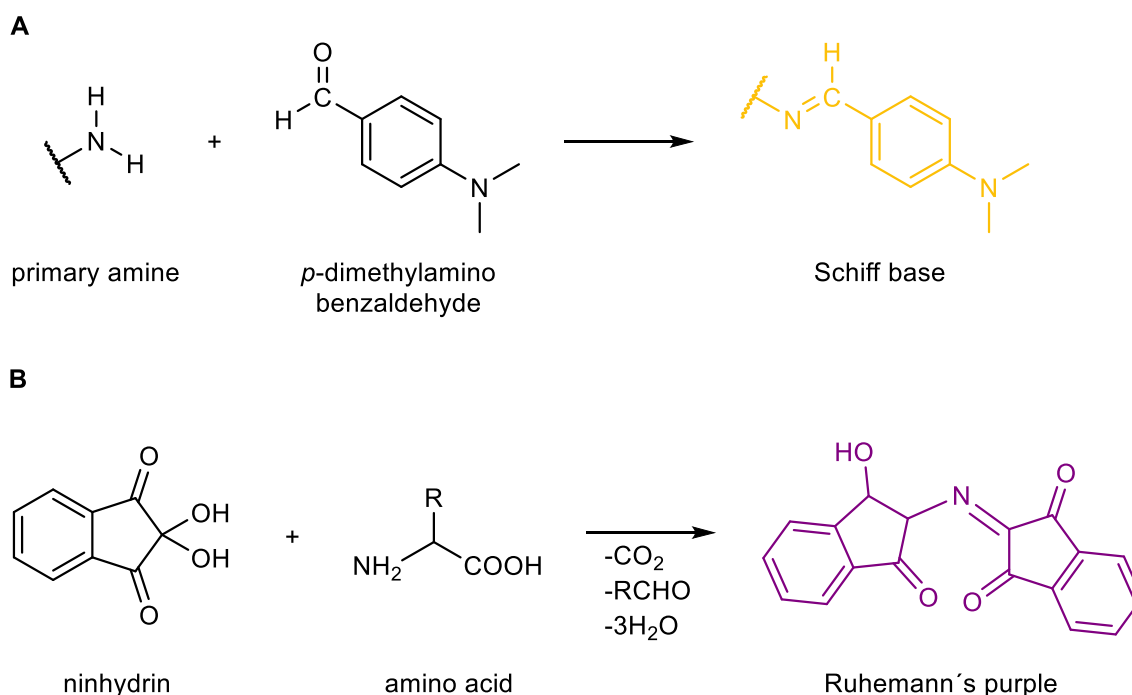


**Figure 13** **A** Reaction of Ehrlich's reagent (*p*-dimethylaminobenzaldehyde) with primary amines of *N*-carbamoylamino acids. **B** Reaction of ninhydrin with amino acids.

To improve the quality of this analytical method, it was also conducted by acidifying the samples before application on the TLC-plates in two different ways. On the one hand, acidification and precipitation of disturbing components was tested by adding 0.1 M  $\text{H}_3\text{PO}_4$  and on the other hand the addition of 1 % TFA was performed, each in a ratio of 1:1. After mixing and subsequent centrifugation for 5 min at 13 000 rpm, the supernatants were applied on TLC-plates as described above.

### 3.2.1.3 PHOTOMETRIC EHRLICH'S ASSAY

The samples for photometric assays using Ehrlich's reagent were either mixed with conc. HCl in a ratio of 1:1 or they already had been stopped using conc. HCl. After centrifugation for 5 min at 13 000 rpm, the supernatant was used for analysis. The particular *N*-carbamoylamino acids that are stained by Ehrlich's reagent were used for calibration. In triplicates, 50  $\mu\text{L}$  of every sample and standard solutions were given into a microtiter plate and subsequently 30  $\mu\text{L}$  of Ehrlich's reagent were added. After mixing for 1 min at 800 rpm, the absorption at 430 nm was quantified in a photometer.

#### 3.2.1.4 PHOTOMETRIC NINHYDRIN ASSAY

For photometric ninhydrin assay, 30  $\mu\text{L}$  acetate buffer, 30  $\mu\text{L}$  sample and 30  $\mu\text{L}$  ninhydrin reagent were added per well of a 96-well plate. After 20 min of incubation at 60  $^{\circ}\text{C}$  and 800 rpm, the plate was cooled to room temperature. Finally, 100  $\mu\text{L}$  of the isopropanol solution have been added per well and after a short mixing period, the absorption was quantified at 570 nm.

#### 3.2.1.5 HIGH PERFORMANCE LIQUID CHROMATOGRAPHY

High pressure liquid chromatography (HPLC) analysis of PheHyd, *N*C*P*heGly and PheGly as well as of BnH, *N*C*P*heAla and PheAla was conducted on an Agilent 1200 system using a HyperClone ODS-C18 column (5  $\mu\text{m}$ , 120  $\text{\AA}$ , 50  $\times$  4.6 mm, Phenomenex). An isocratic flow method with 0.8 mL/min at 22  $^{\circ}\text{C}$  was used with a mobile phase consisting of 80 % of a 0.1 %  $\text{H}_3\text{PO}_4$  solution and 20 % methanol which was degassed in an ultrasonic bath. 5  $\mu\text{L}$  of the samples were injected without dilution and measurement was carried out at a wavelength of 210 nm.

Analysis of *p*NO<sub>2</sub>PheDU and *N*C*p*NO<sub>2</sub> $\beta$ Phe was conducted on the same HPLC system and column. 5  $\mu\text{L}$  of the sample were injected without any dilution. A gradient flow method with a 0.8 mL/min flow rate was used. The initial mobile phase was composed of 5 % (v/v) acetonitrile acidified with 0.5 % (v/v) TFA and 95 % (v/v)  $\text{H}_2\text{O}$ . From 0 to 25 min, the acetonitrile ratio was increased to 10 %, afterwards from 25 to 26 min it was lowered to 5 % again. The detection wavelength was 257 nm and the column temperature 22  $^{\circ}\text{C}$ .

Chiral analysis of *N*C*p*NO<sub>2</sub> $\beta$ Phe was carried out utilizing a Chiralpak QN-AX column (5  $\mu\text{m}$ , 150  $\times$  46 mm, Diacel). An isocratic flow method with 0.3 mL/min was used; the mobile phase consisted of 98 % (v/v) methanol (0.2 % v/v ammonium formate) and 2 % (v/v) acetic acid (0.2 M, adjusted to pH 6 with ammonia). The detection wavelength was 257 nm, the column temperature was 30  $^{\circ}\text{C}$  and 5  $\mu\text{L}$  of undiluted sample were injected.

#### 3.2.1.6 NUCLEAR MAGNETIC RESONANCE SPECTROSCOPY

<sup>1</sup>H NMR (nuclear magnetic resonance spectroscopy) spectra were recorded on a BRUKER Avance 300 (300 MHz) or a BRUKER Avance 400 (400 MHz) device as solutions at room temperature. Chemical shifts are expressed in parts per million (ppm,  $\delta$ ), downfield from tetramethylsilane (TMS) and referenced to residual DMSO-d<sub>5</sub> (2.50 ppm) as internal standard. All coupling constants are absolute values and *J* values are expressed in Hertz (Hz). The spectra were analyzed according to

first order and the descriptions of signals include: s = singlet, d = doublet, dd = doublet of doublets, t = triplet, q = quartet, m = multiplet.

$^{13}\text{C}$  NMR spectra were recorded on a BRUKER Avance 300 (75 MHz) or a BRUKER Avance 400 (100 MHz) device as solutions at room temperature. Chemical shifts are expressed in parts per million (ppm,  $\delta$ ), down- field from tetramethylsilane (TMS) and referenced to DMSO- $d_6$  (39.5 ppm) as internal standard. The signal structure was analyzed by DEPT and is described as follows: + = primary or tertiary C-atom (positive signal), - = secondary C-atom (negative signal), and  $\text{C}_q$  = quaternary C-atom (no signal).

### 3.2.1.7 ELECTRON IONIZATION MASS-SPECTROMETRY AND FAST ATOM BOMBARDMENT MASS-SPECTROMETRY

Electron ionization mass spectrometry (EI-MS) and fast atom bombardment mass spectrometry (FAB-MS) was performed by using a Finnigan MAT 90 (70 eV). The molecular fragments are quoted as the relation between mass and charge ( $m/z$ ), the intensities as a percentaged value relative to the intensity of the base signal (100 %). The abbreviation  $[\text{M}]^+$  refers to the molecule ion and  $[\text{M} + \text{H}]^+$  refers to the protonated molecule ion.

### 3.2.1.8 INFRARED SPECTROSCOPY

Infrared spectroscopy (IR) data were recorded on FT-IR Bruker IFS 88 and are reported as follows: frequency of absorption ( $\text{cm}^{-1}$ ), intensity of absorption (vs = very strong, s = strong, m = medium, w = weak, vw = very weak, br = broad).

### 3.2.1.9 ELEMENTAL ANALYSIS

Elemental analysis (EA) was carried out using an ELEMENTAR vario MICRO device. The values for carbon (C), hydrogen (H), and nitrogen (N) are expressed in weight percent.

### 3.2.2 A NOVEL SUBSTRATE FOR THE SYNTHESIS OF $\beta$ -AMINO ACIDS

#### 3.2.2.1 CHEMICAL SYNTHESIS OF *p*NO<sub>2</sub>PHeDU

In Figure 14, the preparation of 6-(4-nitrophenyl)dihydropyrimidine-2,4(1H,3H)-dione after Světlík and Veizerová is illustrated.<sup>[76]</sup>

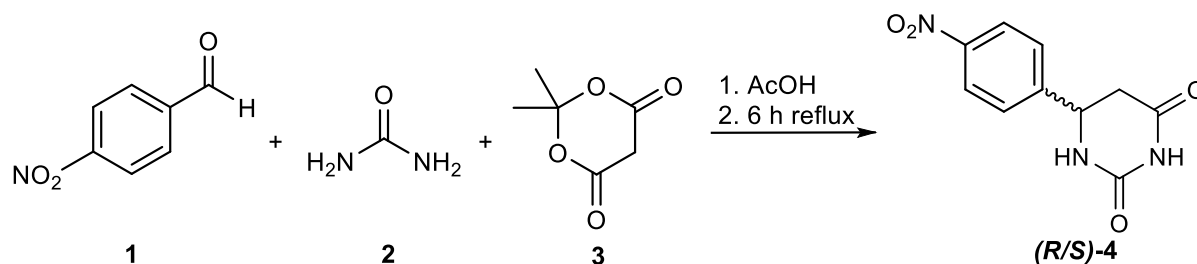


**Figure 14** Chemical synthesis of (*R/S*)-*p*NO<sub>2</sub>PheDU ((*R/S*)-4)

4-Nitrobenzaldehyde (**1**, 613 mg, 5.00 mmol, 1.00 equiv.), urea (**2**, 300 mg, 5.00 mmol, 1.00 equiv.) and Meldrum's acid (**3**, 721 mg, 5.00 mmol, 1.00 equiv.) were suspended in acetic acid (10 mL) and refluxed for 6 h. The product precipitated overnight. The solvent was removed under reduced pressure and the residue was recrystallized from EtOH to obtain *p*NO<sub>2</sub>PheDU ((*R/S*)-4).

#### 3.2.2.2 CHEMICAL SYNTHESIS OF THE CORRESPONDING *N*-CARBAMOYL DERIVATIVE

For analytical issues, the corresponding *N*-carbamoylamino acid of *p*NO<sub>2</sub>PheDU, 3-(4-Nitrophenyl)-3-ureidopropanoic acid (*NCp*NO<sub>2</sub> $\beta$ Phe, **6**), was prepared according to Posner (see Figure 15).<sup>[170]</sup>

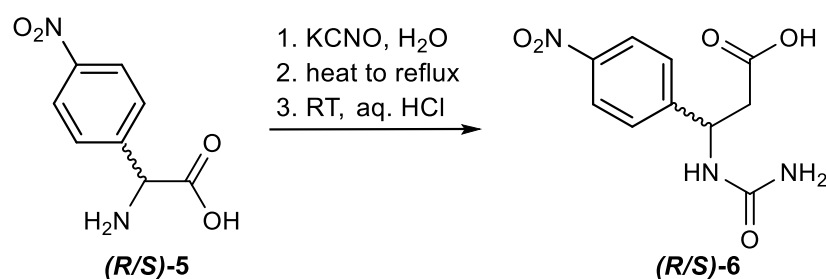


**Figure 15** Chemical synthesis of (*R/S*)-*NCp*NO<sub>2</sub> $\beta$ Phe ((*R/S*)-6)

4-Nitrophenylalanine ((*R/S*)-**5**, 488 mg, 2.38 mmol, 1.00 equiv.) was added to a solution of potassium cyanate (565 mg, 7.14 mmol, 3.00 equiv.) in H<sub>2</sub>O (8 mL). The mixture was heated to reflux for 1 h.

After cooling to room temperature, the solution was acidified with diluted aqueous HCl solution to obtain *NCpNO<sub>2</sub>βPhe ((R/S)-6)*.

### 3.2.3 IMPROVEMENT OF SOLUBLE HYDANTOINASE EXPRESSION

#### 3.2.3.1 CODON-OPTIMIZATION

The gene encoding the D-hydantoinase from *Arthrobacter crystallopoietes* DSM 20117 was optimized based on the codon bias of *E. coli* for improved soluble expression using the software of GeneArt™. Codons that are rarely used in *E. coli* were replaced by preferred ones and furthermore, GC-clusters as well as oligomeric A and T were removed. In either case, the base sequence was substituted without changing the amino acid sequence of the target enzyme.

#### 3.2.3.2 EXPRESSION UNDER OXYGEN DEFICIENCY

For the improvement of hydantoinase expression, first experiments were carried out under hypoxic conditions to decelerate expression and possibly improve the folding process of the target protein. Expression of the D-hydantoinase from *Arthrobacter crystallopoietes* DSM 20117 on the plasmid pDEST42 in *E. coli* BL21DE3 as well as for the codon-optimized version of this hydantoinase on the plasmid pET28a in *E. coli* BL21DE3 was investigated by conducting cultivations at 90, 100 and 120 rpm. Additionally, the culture volume was increased to 400 mL instead of 200 mL per 1 L baffled shaking flask.

#### 3.2.3.3 HIGH THROUGHPUT SCREENING FOR EXPRESSION CONDITIONS

Due to the poor amount of soluble hydantoinase expression, different expression conditions were screened for the D-hydantoinase from *Arthrobacter crystallopoietes* DSM 20117 on the plasmid pDEST42 in *E. coli* BL21DE3 as well as for the codon-optimized version of this hydantoinase on the plasmid pET28a in *E. coli* BL21DE3 (see Figure 16). First of all, indirect induction of chaperone expression was tested by causing chemical stress like changing the pH from 7 to 6 or addition of 3 % v/v EtOH. Furthermore, since the T7-promotor often shows basal activity, it was tested whether addition of IPTG is advantageous or rather increases the formation of inclusion bodies due to rapid expression.

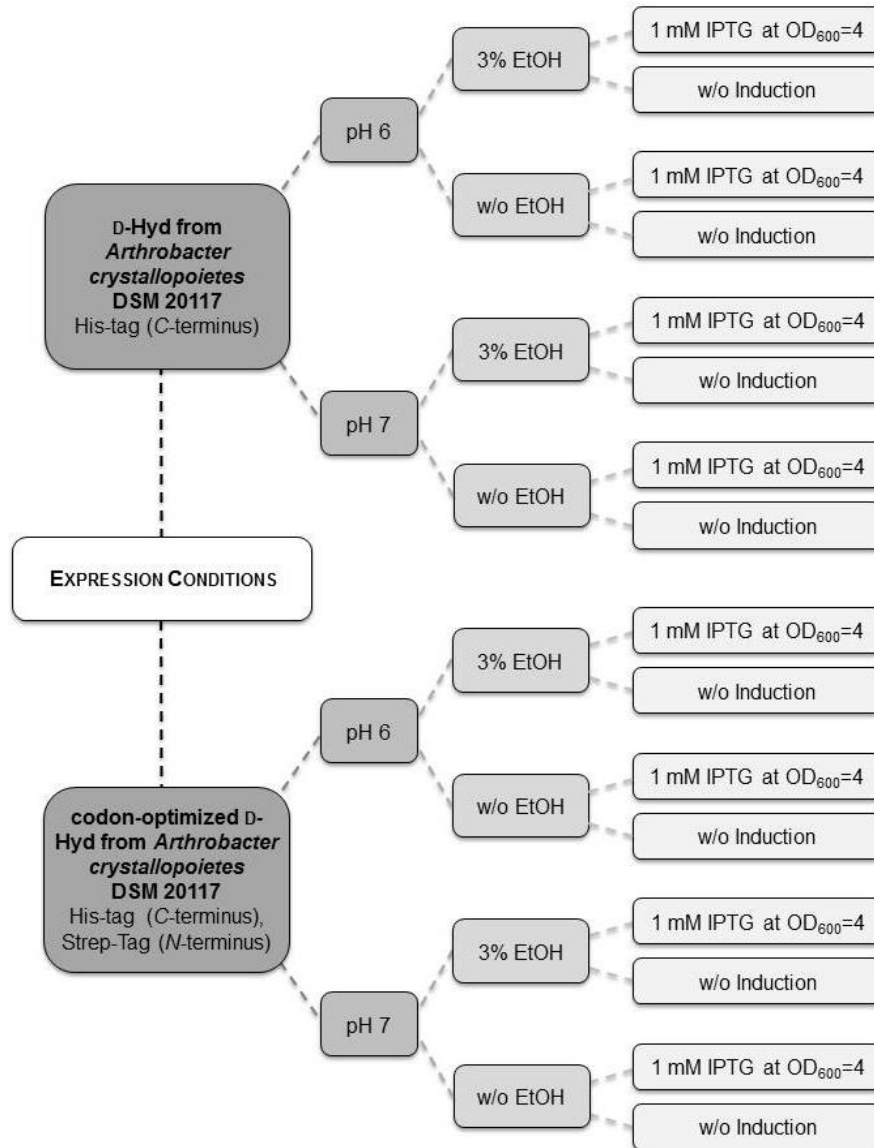


**Figure 16** Investigated conditions for the cultivation of *E. coli* BL21DE3 expressing two different recombinant hydantoinases by high throughput screening

By means of these screening experiments, it was shown that soluble expression as well as specific activity of the hydantoinase was improved by codon-optimization (see Chapters 4.3.1.2 and 4.3.1.3). Therefore, this enzyme was used for immobilization and purification approaches as well as for further improvement of hydantoinase expression by the coexpression of chaperones. Chaperone coexpression itself was conducted according to the Takara product manual (Chaperone Plasmid Set, cat. #3340) by transformation of competent cells with the particular chaperone plasmid and subsequent retransformation of competent cells containing the chaperone plasmid with the expression plasmid of the target protein.

Since prior screening experiments showed that changes in pH had no positive influence on the soluble hydantoinase expression, every experiment was conducted at pH 7. The screened expression conditions for the coexpression of chaperones are illustrated in Figure 17.

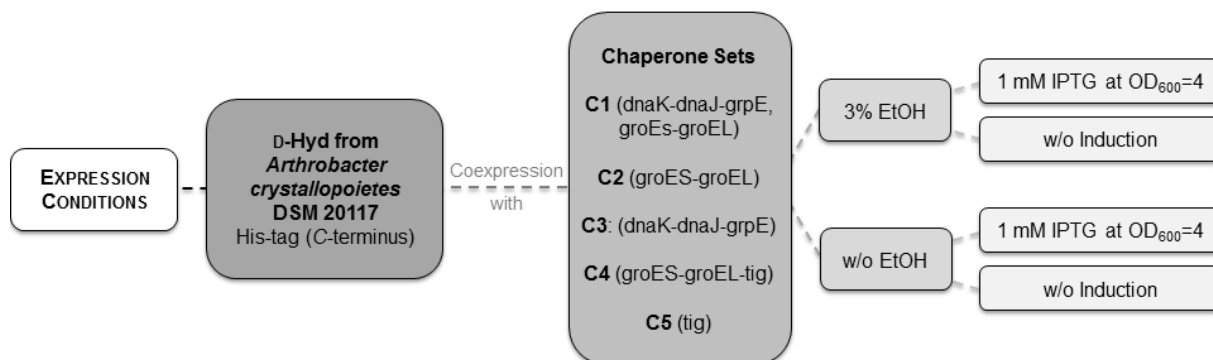


**Figure 17** Investigated conditions for the cultivation of *E. coli* BL21DE3 coexpressing a codon-optimized recombinant hydantoinase and different chaperones by high throughput screening

### 3.2.4 CULTIVATION AND INDUCTION

Different cultivation strategies were tested to optimize the expression of the carbamoylase as well as the hydantoinase. Irrespective of the used media, strain, enzyme or strategy, the precultures for cultivation were prepared similarly. They were prepared in 100 mL baffled shaking flasks by adding 20 mL medium, 10  $\mu$ L of a glycerol stock as well as the required antibiotic for selection. Cultivation of the precultures was conducted at 37 °C and 120 rpm for 18 h. The cultivation strategies of the main cultures were differing, but the harvesting was equal for every culture: After 15 min of centrifugation at 4700  $\times$ g and 4 °C, the cells were quick-frozen with liquid nitrogen and stored at 4 °C.

#### 3.2.4.1 HYDANTOINASE

*E. coli* BL21DE3 harboring the plasmid pDEST42 with the D-hydantoinase from *Arthrobacter crystallopoietes* DSM 20117 (C-terminal His-tag) as well as *E. coli* BL21DE3 harboring the plasmid pET28a with the codon-optimized D-hydantoinase from *Arthrobacter crystallopoietes* DSM 20117 (C-terminal His-tag, N-terminal SBP-tag) were cultivated in TB-medium. For inoculation, precultures were added to 200 mL medium and the particular antibiotic in 1 L baffled shaking flasks to an OD<sub>600</sub> of 0.2. The cells were cultivated at 37 °C and 120 rpm and induction was carried out at an OD<sub>600</sub> of 4. Subsequently, the cultivation was continued to an overall cultivation time of 24 h, starting from inoculation. The obtained cell pellets were used for investigations concerning purification and immobilization.

Cultivations for the high throughput screening of expression conditions were carried out under the same conditions as described above, but in 48-well Flower-Plates® and a culture volume of 1 mL. For continuous control of growth, a BioLector® was used as an incubator (parameters, see Table 7). Since this device records values for scattered light instead of the OD<sub>600</sub>, first of all an scattered light/OD<sub>600</sub>

correlation function had to be determined (see Chapter 5.1.1). The cultivations were carried out each for three times in triplicates, using two cultures of the triplicate for whole cell biotransformation assays (see Chapter 3.2.9.1) and the third culture for mechanical cell disruption by sonication and subsequent SDS-PAGE analysis as well as for determination of the cell dry weight (see Chapters 3.2.1.1 and 3.2.9.1).

**Table 7** Parameters for the BioLector® cultivation

Parameter	Adjustment
temperature	37 °C
humidity	95 %
gain of light scattering	10, 20, 30
rotation speed	600 rpm
measuring interval	10 min
cultivation time	20 h (then decrease of temperature to 10 °C)

*E. coli* JM109 containing the plasmid pJAVI2 with the D-Hyd from *Arthrobacter crystallopoietes* DSM 20117, (C-terminal Strep-tag) was cultivated in LB-medium. After inoculation by adding the preculture to an OD<sub>600</sub> of 0.1, the cultivation was conducted in 1 L baffled shaking flasks with 200 mL medium and 100 µg/mL ampicillin at 37 °C and 120 rpm. Induction was carried out at an OD<sub>600</sub> of 0.4–0.6 by adding rhamnose to a final concentration of 2 mg/mL and subsequently the cultivation was carried out at 30 °C and 120 rpm for additional 6 h. The resulting cell pellets were used for testing the conversion of a novel substrate for the synthesis of β-amino acids by whole cell biotransformations.

#### 3.2.4.2 CARBAMOYLASE

For *E. coli* BW3110 harboring the plasmid pMW1 with the D-carbamoylase from *Arthrobacter crystallopoietes* DSM 20117 (C-terminal His-tag), cultivation in LB- as well as TB-medium was tested to obtain optimal expression. 2 L baffled shaking flasks were used for 400 mL of culture volume. Inoculation was carried out by adding the preculture to obtain an OD<sub>600</sub> of 0.1 and subsequently cultivation was carried out at 37 °C and 120 rpm up to an OD<sub>600</sub> of 0.4-0.6. Then, protein expression was induced by adding rhamnose to a final concentration of 2 mg/mL and cultivation was continued at 30 °C and 120 rpm for 6 h. The obtained cell pellets were used for purification and immobilization.



### 3.2.5 CELL DISRUPTION

#### 3.2.5.1 SONICATION

In cultures from BioLector® cultivations, the cells were mechanically disrupted by sonication with an 8-tip sonication probe. For this purpose, one culture of a triplicate was centrifuged for 10 min at 12 000 rpm and the supernatant was discarded. After washing for three times with Tris-HCl buffer (50 mM, pH 8), the resulting cell pellet was resuspended in 900  $\mu\text{L}$   $\text{d}_2\text{H}_2\text{O}$ . 150  $\mu\text{L}$  of this cell suspension was transferred to a 96-well microtiter plate to perform sonication with an amplitude of 70 %. After each 20 sec of sonication, a 30 sec pause followed. This sequence was repeated for six times and the 96-well microtiter plate was cooled permanently. For separation of the crude cell extract from cell debris, the plate was centrifuged for 90 min at 4000 rpm and 4 °C. The resulting insoluble fraction was resuspended in 300  $\mu\text{L}$   $\text{d}_2\text{H}_2\text{O}$  and both the crude extract and the insoluble fraction were stored at -20 °C for further analysis.

#### 3.2.5.2 CHEMICAL CELL DISRUPTION

For every cell pellet except from BioLector® cultivations, chemical cell disruption by Bug Buster® solution in combination with lysozyme and benzonase was used. The Bug Buster® reagent represents a mixture of non-ionic as well as zwitterionic surfactants that allow perforation of the cell wall without denaturation of the target protein. Lysozyme is added to assist the disruption of the cell wall by hydrolysis of  $\beta$ -1,4-glycosidic bonds and benzonase decreases the viscosity by hydrolyzing the DNA and RNA.

After washing of the cell pellets and determination of the wet biomass, per 1 g wet biomass 1 mL Bug Buster®, 1  $\mu\text{L}$  benzonase and 25  $\mu\text{L}$  lysozyme (10 mg/mL stock) were added and the pellets were resuspended thoroughly. This suspension was incubated for 15 min at 24 °C and 1000 rpm and subsequently centrifuged for 75 min at 4 °C and 4700 rpm to separate the crude extract from cell debris and insoluble proteins. Then, 10  $\mu\text{L}$  of the protease inhibitor was added per 1 mL of crude extract which was cooled permanently and directly used for further investigations. The insoluble part resulting from cell disruption was stored at -20 °C for SDS-PAGE analysis.

### 3.2.6 PURIFICATION OF ENZYMES

#### 3.2.6.1 BUFFER EXCHANGE

The buffer exchange of samples containing imidazole after elution is crucial for the activity of enzymes. In this work, three different methods have been tested whereat the application of Slide-A-Lyzer™ MINI Dialysis Devices emerged as a suitable method (see Chapter 4.3.2.3). At first, the devices were placed in 1 L  $\text{d}_d\text{H}_2\text{O}$  for 15 min for washing out residual glycerol from the production process. Then, they were filled with a maximum of 0.5 mL of the sample, capped and placed into a vessel with 250 mL of the required catalysis buffer for 30 min under continuous stirring. The resulting samples were collected in micro test tubes and cooled at 4 °C until further use.

#### 3.2.6.2 NI SEPHAROSE BEADS

Initially, 2 mL of the Ni sepharose high performance stock solution (stored in 20 % ethanol) were taken and washed several times. For the first washing step, the Ni sepharose beads were resuspended in 5 mL  $\text{d}_d\text{H}_2\text{O}$  and subsequently centrifuged for 1 min at 4 °C and 4700 rpm. Then three more washing steps were carried out with 5 mL wash- and binding buffer supplied with additives for the particular enzyme. For every purification approach, 1 mL of this prepared bead suspension was incubated with 4 mL crude cell extract for 60 min in an overhead shaker at 4 °C. Preliminary tests showed, that in contrast to the standard protocol of GE Healthcare in that two times washing and resuspending in wash-and binding buffer are recommended, three washing steps with 1 mL wash-and binding buffer are necessary to avoid non-specific bound proteins. Furthermore, an elution gradient was applied beginning with an elution step using 2 mL of a 25 % v/v elution buffer (125 mM imidazole) and 15 min incubation in an overhead shaker at 4 °C. After 1 min centrifugation at 4700 rpm and 4 °C and collection of the supernatant, a second elution step like this was carried out with 100 % v/v elution buffer (500 mM imidazole). The supernatants of every washing- and elution step were collected and cooled for further investigations. Since imidazole may interfere with the divalent metal ions that are crucial for the activity of hydantoinases, it had to be removed. This compound is also known to interfere with other target proteins and therefore buffer exchange was conducted with every sample containing imidazole (see Chapter 3.2.6.3).

### 3.2.6.3 FUNCTIONALIZED MAGNETIC BEADS (HIS-TAG)

Another method for the purification of hydantoinase as well as carbamoylase was tested by using Dynabeads® His-tag Isolation and Pulldown. They are functionalized superparamagnetic beads, uniform and 1 µm in diameter, provided with a highly specific IMAC chemistry. In detail, cobalt is bound to a tetradentate metal chelator, whereby four of the six coordination sites of cobalt are occupied. The two remaining coordination sites are free for binding the imidazole rings of the His<sub>6</sub>-tagged enzymes. To prevent reduction of the cobalt ions, reducing agents like DTT need to be avoided. For every approach, 20 mg/mL functionalized magnetic beads were used, fractionated in 2 mL micro test tubes. Since their storage occurs in 20 % ethanol, first of all the magnetic beads were washed for four times with 0.5 mL wash- and binding buffer by using a magnetic device for removal of the supernatant. For the purification of the carbamoylase, 12 mM imidazole was added to the crude extract for avoiding non-specific binding of proteins containing histidines. This was not the case for purification of the hydantoinase, since imidazole would interfere with the zinc ions that are crucial for its activity. To the 20 mg/mL magnetic beads, 1 mL of crude extract were added and this mixture was incubated for 5 min at 25 °C and 800 rpm. Then, the supernatant was collected and cooled at 4 °C for later analysis. The loaded magnetic beads were washed for four times with 0.5 mL wash- and binding buffer. For elution of the target molecule, 0.5 mL elution buffer was added, followed by incubation at 25 °C and 800 rpm. The resulting eluate was collected by using a magnetic device and cooled at 4 °C for subsequent buffer exchange (see Chapter 3.2.6.3) to remove imidazole.

## 3.2.7 IMMOBILIZATION OF ENZYMES

### 3.2.7.1 FUNCTIONALIZED MAGNETIC BEADS

The immobilization of hydantoinase was investigated using the affinity tags His<sub>6</sub>-tag as well as SBP-tag, while the carbamoylase only possessed a His<sub>6</sub>-tag for immobilization. Immobilization of the enzymes via His<sub>6</sub>-tag applying Dynabeads® His-tag Isolation and Pulldown was carried out as described in Chapter 3.2.6.2, but without the elution step. The loaded and washed magnetic beads were resuspended in 0.5 mL of the particular catalysis buffer to perform the biotransformation assay (see Chapter 3.2.9.3).

The hydantoinase was immobilized by applying Dynabeads® M-280 Streptavidin, uniform superparamagnetic beads with a diameter of 2.8 µm. A covalently coupled streptavidin monolayer with no excess adsorbed streptavidin allows batch consistency and reproducibility without leakage. The magnetic beads were fractionated to get 0.85 mg beads for every approach. To remove the storage solution, three times washing with 0.5 mL of wash-and binding buffer was carried out using the magnetic device to remove the supernatant. Subsequently, 100 µL of crude extract was incubated for

20 min at 500 rpm and room temperature with the prepared beads. After collecting the supernatant, the loaded beads were washed for three times with 0.5 mL wash- and binding buffer and then once with 0.5 mL catalysis buffer. The beads were then resuspended in 100  $\mu$ L catalysis buffer again for the biotransformation assay (see Chapter 3.2.9.3).

### 3.2.8 PURIFICATION OF INCLUSION BODIES

For the purification of inclusion bodies after Diener et al.,<sup>[149]</sup> chemical cell disruption was carried out as described in Chapter 3.2.2.2. The insoluble fraction was washed three times using Tris-HCl buffer (50 mM, pH 8) and then stored at -80 °C until further use. After determining the wet weight of this pellet with insoluble proteins, a 10 % (w/v) suspension in  $d_2O$  was prepared and then it was frozen in liquid nitrogen and stored at -80 °C overnight. Then, the suspension was lyophilized and the dry weight was determined to analyze the protein concentration per 1 mg of the prepared inclusion bodies. Therefore, the inclusion bodies were denatured by dissolving in 6 M guanidine hydrochloride and the protein concentration was determined by measuring absorption at 280 nm as well as by using a BCA-assay with BSA in 6 M guanidine hydrochloride for calibration.

### 3.2.9 BIOTRANSFORMATION ASSAYS

#### 3.2.9.1 WHOLE CELLS

For whole cell biotransformation assays, the harvested cells were thawed on ice, washed twice with catalysis buffer and resuspended in the same buffer in a ratio of 10 mL buffer for 100 mL of harvested culture. 750  $\mu$ L from this cell suspension were added to 750  $\mu$ L of substrate solution (4 mM or 10 mM in catalysis buffer, see Chapter 3.1.3.5) to start the biotransformation reaction. Negative controls were performed on the one hand by adding catalysis buffer instead of cell suspension and on the other hand by adding catalysis buffer instead of the substrate. The assay was carried out at 40 °C for reactions applying recombinant hydantoinases and at 30 °C for assays with the wildtype strain shaking at 800 rpm. Samples were taken at selected reaction times by withdrawing 200  $\mu$ L from the reaction mixture, centrifugation at 13 000 rpm for 5 min and storage of the supernatant at -20 °C until analysis. For determination of cell dry weight (cdw), micro reaction tubes were dried overnight at 60 °C and subsequently weighed (in triplicates). After adding 1 mL culture volume to these reaction vessels and centrifugation for 5 min at 13 000 rpm, the supernatant was discarded and they were dried overnight at 60 °C again to determine the cell dry weight.

Whole cell biotransformation assays of the BioLector® cultures were performed in a smaller scale since less culture volume is obtained. Two cultures of the triplicates were united in one micro reaction

tube, centrifuged for 10 min at 12 000 rpm and the supernatant was discarded. The cell pellets were washed twice with 500  $\mu$ L catalysis buffer and then resuspended in 200  $\mu$ L of the same buffer. By adding 200  $\mu$ L of a 4 mM solution of phenylhydantoin, the reaction started and was conducted at 40 °C and 800 rpm. At selected reaction times, 20  $\mu$ L samples were taken and after centrifugation at 13 000 rpm for 5 min, the supernatant was collected and stored at -20 °C for further analysis.

### 3.2.9.2 CRUDE CELL EXTRACT AND PURIFIED ENZYMES

After chemical cell disruption, the protein concentration of crude cell extract was determined using the Protein Quantification Kit BCA-Assay and different concentrations of BSA (0-1 mg/mL) in  $d_4H_2O$  for calibration. Then the crude cell extract was diluted to the desired concentration with catalysis buffer. The samples received from enzyme purification and subsequent buffer exchange were used without prior dilution, but protein concentration was determined to calculate enzyme activities.

To start the biotransformation reaction, the prepared crude cell extract or purified enzyme was added to the substrate solution (4 mM or 10 mM in catalysis buffer, see Chapter 3.1.3.5) in a ratio of 1:1. Additionally, negative controls were conducted by adding catalysis buffer instead of crude cell extract or purified enzyme or instead of substrate, respectively. Hydantoinase activity was determined at 40 °C and 800 rpm, whereas assays employing carbamoylase or both enzymes were carried out at 30 °C and 800 rpm. At selected reaction times, 100  $\mu$ L samples were taken and treated differently, depending on the following analytical method. When HPLC-analysis was conducted, the reactions were stopped by 10 min incubation of the samples at 95 °C and subsequent centrifugation for 5 min at 13 000 rpm. The supernatant was collected and stored at -20 °C until analysis. For photometric analysis applying Ehrlich's Reagent, the samples were added to an equal amount of conc. HCl. After resuspending, the samples were centrifuged for 5 min at 13 000 rpm and the supernatant was also stored at -20 °C until analysis.

### 3.2.9.3 IMMOBILIZED ENZYMES

Magnetic beads carrying His-tagged enzymes were resuspended in 500  $\mu$ L catalysis buffer to conduct the biotransformation assay. By adding 500  $\mu$ L of the particular substrate solution (10 mM in catalysis buffer, see Chapter 3.1.3.5), the reaction was started. As described before, hydantoinase activity assays were carried out at 40 °C and 800 rpm, while assays employing carbamoylase or both enzymes were conducted at 30 °C and 800 rpm. Samples were taken at selected reaction times, by placing the micro test tubes into the magnetic device for collecting the magnetic beads and withdrawing 100  $\mu$ L. Depending on the analytical method, the samples were stopped by heat or by adding conc. HCl as described for biotransformation assays with crude cell extract or purified enzymes

(Chapter 3.2.9.2). After sampling, the reaction vessel was gently mixed to get a homogeneous suspension and the reaction was continued. When the reaction was finished, bound proteins were eluted by withdrawing the supernatant, adding 500  $\mu\text{L}$  elution buffer and incubating the suspension for 5 min at 800 rpm and 25 °C. The resulting eluate was transferred to a new micro test tube for determination of the protein concentration and for analysis by SDS-PAGE (see Chapter 3.2.1.1).

Streptavidin functionalized magnetic beads carrying SBP-tagged hydantoinases were resuspended in 100  $\mu\text{L}$  of catalysis buffer for the biotransformation. The reaction was started by adding 100  $\mu\text{L}$  of substrate solution (10 mM in catalysis buffer, see Chapter 3.1.3.5) and carried out at 40 °C and 800 rpm. Sampling was carried out as described for immobilized His-tagged enzymes, but only 20  $\mu\text{L}$  were taken, incubated for 10 min at 95 °C and centrifuged for 5 min at 13 000 rpm. The samples were stored at -20 °C until analysis by HPLC. For determination of the protein concentration and analysis by SDS-PAGE, the supernatant was taken and the loaded magnetic beads were incubated in 250  $\mu\text{L}$  1 % SDS at 95 °C for 20 min.

#### 3.2.9.4 INCLUSION BODIES

After the purification of inclusion bodies, a 5 mg/mL suspension was prepared by weighing the lyophilisate and adding catalysis buffer for the hydantoinase. For biotransformation assays, 750  $\mu\text{L}$  of this suspension were added to 750  $\mu\text{L}$  of the substrate solution in catalysis buffer (4 mM Phenylhydantoin). In another approach, a solution of 5 mg/mL purified inclusion bodies in 5 M guanidine hydrochloride was prepared and 750  $\mu\text{L}$  of this solution were added to 750  $\mu\text{L}$  substrate solution. The reaction was conducted at 40 °C and 800 rpm. Sampling was carried out as described for biotransformation assays employing crude cell extract and purified enzymes (Chapter 3.2.9.2) and analysis by HPLC was conducted.

## 4 RESULTS AND DISCUSSION

### 4.1 ESTABLISHMENT OF ANALYTICAL METHODS

#### 4.1.1 THIN LAYER CHROMATOGRAPHY

In this work, different target molecules, substrates as well as enzymes were investigated concerning the synthesis of non-canonical amino acids. Due to the resulting diversity and magnitude of biotransformation assays, a fast method for the detection of substrates as well as products was required. Since the examined Hydantoinase Process and modified Hydantoinase Process both have *N*-carbamoylamino acids as intermediates and amino acids as products, the staining reagents Ehrlich's and ninhydrin for TLC appeared applicable. At first, standards of  $\alpha$ - and  $\beta$ -amino acids and their corresponding *N*-carbamoyl derivatives were analyzed by TLC for testing the suitability of this qualitative method (see Figure 18).

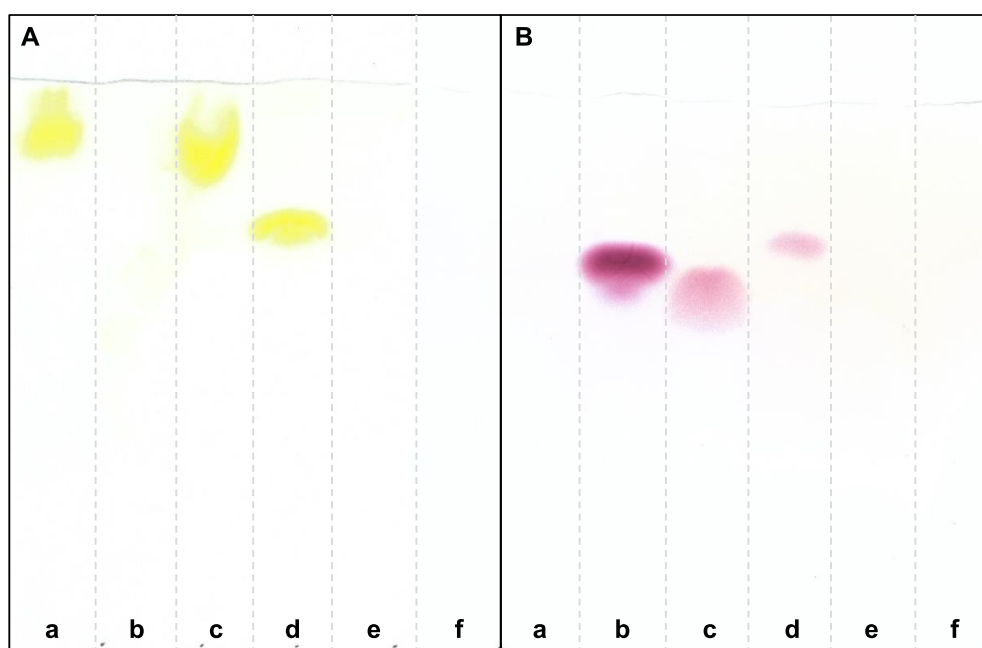


**Figure 18** Derivatization of  $\alpha$ - and  $\beta$ -amino Acids and their corresponding *N*-carbamoyl derivatives for qualitative TLC analysis **A** Ehrlich's reagent, **a** 2 mM *N*C*P*heAla **b** 2 mM PheAla **c** 2 mM *N*C*p*NO<sub>2</sub> $\beta$ Phe **d** 2 mM *p*NO<sub>2</sub> $\beta$ Phe **e** 2 mM  $\beta$ Phe **f** 2 mM *p*Cl $\beta$ Phe **B** Ninhydrin reagent, **a** 2 mM *N*C*P*heAla **b** 2 mM PheAla **c** 2 mM *N*C*p*NO<sub>2</sub> $\beta$ Phe **d** 2 mM *p*NO<sub>2</sub> $\beta$ Phe **e** 2 mM  $\beta$ Phe **f** 2 mM *p*Cl $\beta$ Phe

Figure 18 A shows the separation of  $\alpha$ - and  $\beta$ -amino acids and their corresponding *N*-carbamoyl derivatives as well as two other  $\beta$ -amino acids for comparison that were stained by Ehrlich's Reagent. Exemplarily, for the analysis of  $\alpha$ -amino acids and derivatives, *N*C*P*heAla and PheAla are shown. Lane **a** shows a single spot for *N*C*P*heAla with a retention factor of 0.92, while PheAla (lane **b**) was not stained by Ehrlich's reagent. As *p*NO<sub>2</sub>PheDU ((*R/S*)-4) was synthesized as a novel substrate for

the synthesis of  $\beta$ -amino acids, the corresponding *N*-carbamoylamino acid ((*R/S*)-**6**) as well as amino acid are shown in lane **c** and **d**. Both compounds were stained by Ehrlich's reagent and show retention factors of 0.86 and 0.74. For comparison, two further  $\beta$ -amino acids were stained by Ehrlich's reagent and no spots are visible ( $\beta$ Phe and *p*Cl $\beta$ Phe, lane **e** and **f**). By using ninhydrin as a staining reagent, only PheAla and *NCp*NO<sub>2</sub> $\beta$ Phe show visible spots with retention factors of 0.69 and 0.66 (see Figure 18 B).

Ehrlich's reagent is known to stain primary amines of *N*-carbamoylamino acids by nucleophile addition of the amino group to the aldehyde from *p*-dimethylaminobenzaldehyde (see Chapter 3.2.1.2).<sup>[48,171]</sup> Since *NC*PheAla was successfully stained by Ehrlich's reagent (lane **a**), while the corresponding amino acid PheAla showed no spot, this staining method proved to be suitable for the detection of the *N*-carbamoylamino derivatives of  $\alpha$ -amino acids. The same applies for the staining of the *N*-carbamoyl- $\beta$ -amino acid *NCp*NO<sub>2</sub> $\beta$ Phe ((*R/S*)-**6**, lane **c**). But in contrast to  $\alpha$ -amino acids it was noticeable that the corresponding  $\beta$ -amino acid, *p*NO<sub>2</sub> $\beta$ Phe ((*R/S*)-**4** lane **d**), was also stained by Ehrlich's reagent. To check whether the  $\beta$ -structure was responsible for this staining, another  $\beta$ -amino acid ( $\beta$ Phe, lane **e**) was investigated and no spot was visible which disproved this theory. Since the third tested  $\beta$ -amino acid, *p*Cl $\beta$ Phe (lane **f**), was also not stained by Ehrlich's reagent, the *p*NO<sub>2</sub>-group was suggested to have an influence on the reaction with *p*-dimethylaminobenzaldehyde.

Ninhydrin is known to derivatize amino acids and form a purple color (see Chapter 3.2.1.2),<sup>[172]</sup> which was approved for PheAla (Figure 18 B, lane **b**). As expected, the corresponding *N*-carbamoylamino acid (lane **a**) was not stained by this method, which demonstrates that this staining method is suitable for the detection of  $\alpha$ -amino acids. The amino acid *p*NO<sub>2</sub> $\beta$ Phe ((*R/S*)-**4**, lane **d**) was also stained by ninhydrin, while the other investigated  $\beta$ -amino acids,  $\beta$ Phe and *p*Cl $\beta$ Phe (lane **e** and **f**), did not show a spot after staining with ninhydrin. Primarily, the  $\beta$ -structure in general was suggested to prevent the derivatization with ninhydrin, since it was claimed that only  $\alpha$ -amino acids undergo this derivatization.<sup>[173]</sup> Another theory states that, if the ninhydrin reaction is as general as reported from McCaldin, only a fragment of the amino acid is contained in the coloured compound.<sup>[174,175]</sup> But this finding is in conflict with the results shown above, since the  $\alpha$ -amino acid PheAla as well as the  $\beta$ -amino acid *p*NO<sub>2</sub> $\beta$ Phe ((*R/S*)-**4**) were stained by ninhydrin, while the  $\beta$ -amino acids  $\beta$ Phe and *p*Cl $\beta$ Phe were not stained. Consequently, the *p*NO<sub>2</sub>-group was suggested to influence the derivatization of  $\beta$ -amino acids by ninhydrin, but since the mechanism of the ninhydrin reaction is not fully elucidated until now,<sup>[175]</sup> the actual reason can not be specified. Additionally, the *N*-carbamoyl- $\beta$ -amino acid *NCp*NO<sub>2</sub> $\beta$ Phe ((*R/S*)-**6**) was stained by ninhydrin, which is not known for *N*-carbamoyl- $\alpha$ -amino acids.

Consequently, by using the staining methods Ehrlich's and ninhydrin, *N*-carbamoyl- $\alpha$ -amino acids and  $\alpha$ -amino acids can be detected until 0.1 mM (data not shown), while the detection of  $\beta$ -amino acid derivatives turned out to be more difficult. Consequently, only  $\alpha$ -amino acid derivatives are investigated by these derivatization methods in this work. To test, whether these detection methods are suitable for samples from whole cell biocatalysis, the conversion of 2 mM *NC*PheAla by the recombinantly



expressed carbamoylase from *A. crystallopoietes* in *E. coli* BW3110 was investigated using resting cells (see Figure 19).

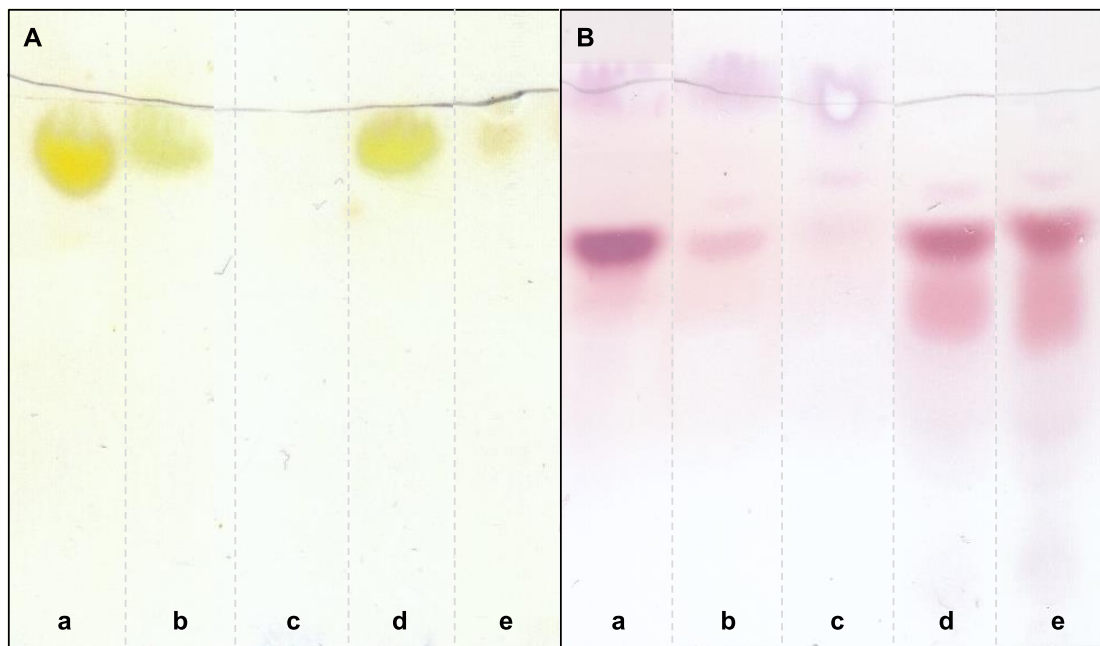


**Figure 19** Qualitative TLC analysis for the conversion of 2 mM *NCPheAla* by the carbamoylase from *A. crystallopoietes* using resting cells. **A** Ehrlich's reagent, **a** 2 mM *NCPheAla* **b** 0 h **c** 0 h ctrl (w/o *NCPheAla*) **d** 24 h **e** 24 h ctrl (w/o *NCPheAla*) **B** Ninhydrin reagent, **a** 2 mM *NCPheAla* **b** 0 h **c** 0 h ctrl (w/o *NCPheAla*) **d** 24 h **e** 24 h ctrl (w/o *NCPheAla*). The reactions were carried out at 40 °C and 800 rpm in Tris-HCl (50 mM, pH 8).

In Figure 19 A and B, the samples after running TLC and subsequent staining with Ehrlich's reagent and ninhydrin are shown, at which lane **a** represents the standard of the substrate *NCPheAla* ( $R_f=0.87$ ) the product *PheAla* ( $R_f=0.71$ ), respectively. In Figure 19 A lane **b**, the sample of 0 h whole cell biotransformation was applied and a spot with a retention factor value of 0.92 is visible, while lane **c**, which represents the 0 h sample of the control approach without the substrate *NCPhe* shows much slighter spots. Samples from the same approaches after 24 h of reaction time exhibit both spots with retention factor values of 0.93 for the sample from whole cell biotransformation (lane **d**) and of 0.85 for the sample from the control experiment (lane **e**). The results after derivatization of the resulting product *PheAla* (Figure 19 B) with ninhydrin reagent showed a slight spot after 0 h of whole cell biotransformation ( $R_f=0.73$ , lane **b**) and an even more slightly spot for the 0 h sample of the control experiment ( $R_f=0.74$ , lane **c**). After 24 h of reaction time, the sample from whole cell biotransformation (lane **d**) as well as the sample from the approach without substrate (lane **e**) showed two spots with retention factor values of 0.62 and 0.73.

The results from TLC analysis of the whole cell biotransformation with *NCPheAla* using Ehrlich's reagent showed that the substrate was detectable in the 0 h sample, but after 24 h a more intensive spot was visible, which would imply an increase in substrate concentration. Since the control experiment did not show any substrate after 0 h of reaction time, but after 24 h a spot for the substrate was detectable, it was suggested that Ehrlich's reagent also derivatizes primary amines of cell

fragments that emerge during whole cell biotransformation, causing false positive results. Consequently, the chosen analysis of *N*-carbamoylamino acids after whole cell biotransformation is not feasible. Derivatization of the resulting product by ninhydrin staining firstly appeared successful, since after 0 h of biotransformation nearly no product was detectable, while after 24 h the spot for PheAla ( $R_f=0.73$ ) was very intense. The second spot with a retention factor value of 0.62 may result from nonspecific derivatization of other amino acids that result from emerging cell fragments. But since the control experiment without substrate revealed the same spots with same intensities, it was obvious that this staining method for detection of the product was also not suitable, since non-specific derivatization of cell- or protein fragments containing free amino acid residues superposes the product spot.

Consequently, two more variations in treating the samples were tested. The addition of  $H_3PO_4$  respectively TFA should lead to denaturation of occurring cell fragments. Subsequent centrifugation and withdrawal of the supernatant was carried out to avoid nonspecific derivatization and interference with the substrate or product. The results of both methods revealed the same problems as discussed above (data not shown). The same applies for samples from biotransformations with crude cell extract and therefore another analytical method for the detection of *N*-carbamoylamino acids and amino acids had to be developed.

#### 4.1.2 PHOTOMETRIC ASSAYS

To enable rapid quantitative analysis for observation of the reaction course, photometric determination of *N*-carbamoyl- $\alpha$ -amino acids and  $\alpha$ -amino acids was tested by Ehrlich's and ninhydrin assay. Since the derivatization of *N*-carbamoyl- $\beta$ -amino acids and  $\beta$ -amino acids was ambiguous, these compounds were not analyzed photometrically, but by HPLC (see Chapter 4.1.3). As expected from the TLC analysis with Ehrlich's and ninhydrin derivatization discussed above (see Chapter 4.1.1), the calibrations of *N*CPhGly, *N*CPhAla, *N*CSer, PheGly, PheAla and Ser were carried out successful, but samples from biotransformation assays did not provide conclusive results due to the strong background signal from non-specific derivatizations of emerging cell fragments.

Nevertheless, a method to compass this drawback was tested. Every sample was treated by adding conc. HCl in a ratio of 1:1, subsequent centrifugation and withdrawal of the supernatant for photometric analysis by Ehrlich's reagent. This method resulted in reliable results for the concentrations of *N*CPhGly, *N*CPhAla and *N*CSer, since the starting substrate concentration was detectable in each case and a decrease in substrate concentration was monitored during biotransformation reactions (results see Chapters 4.3.2 and 4.3.3). Additionally, the control experiments without biocatalyst showed no decrease in substrate concentration, which verified this method once more. The possibility of a photometric assay for the detection of *N*-carbamoylamino acids during biotransformation reactions was important especially for serine derivatives, since neither

the substrate hydroxymethylhydantoin, the corresponding *N*-carbamoylamino acid nor the resulting amino acid serine was detectable by HPLC.

### 4.1.3 HIGH PRESSURE LIQUID CHROMATOGRAPHY

Due to the challenges in the derivatization of  $\beta$ -amino acid derivatives (see Chapter 4.1.1), a suitable HPLC method was necessary for the verification of the successful conversion of the novel substrate *p*NO<sub>2</sub>PheDU ((*R/S*)-4). The best separation of this substrate and the corresponding *N*-carbamoylamino acid ((*R/S*)-6) is shown in Figure 20.

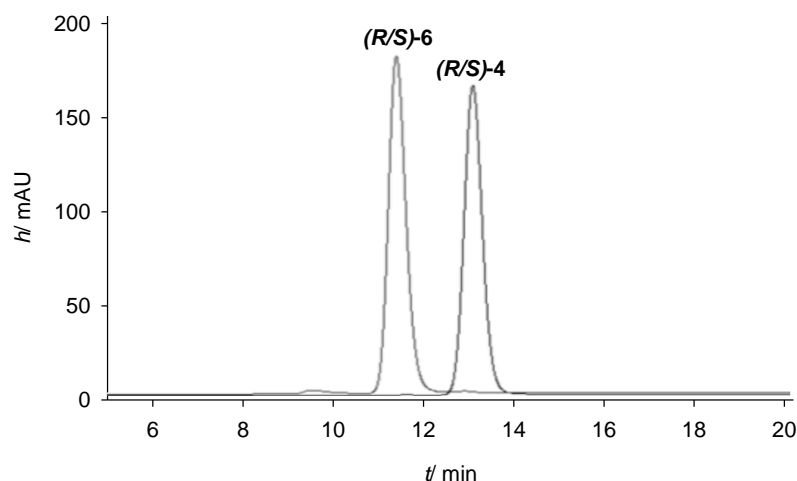


**Figure 20** Separation of 2 mM *p*NO<sub>2</sub>PheDU ((*R/S*)-4) and 2 mM *NCp*NO<sub>2</sub> $\beta$ Phe ((*R/S*)-6) by HPLC. Column: HyperClone ODS-C18, detection wavelength: 257 nm, column temperature: 22 °C, flow rate: 0.8 mL/min, initial mobile phase: 5 % (v/v) acetonitrile acidified with 0.5 % (v/v) trifluoroacetic acid and 95 % (v/v)  $\text{d}_4\text{H}_2\text{O}$ , 0–25 min: acetonitrile ratio increased to 10 % (v/v), 25–26 min: acetonitrile ratio lowered to 5 % (v/v)

Under mentioned conditions, the compounds *p*NO<sub>2</sub>PheDU ((*R/S*)-4) and *NCp*NO<sub>2</sub> $\beta$ Phe ((*R/S*)-6) were separated with retention times of 13.1 min and 11.6 min. This adequate resolution and a detection limit under 0.08 mM make this method an appropriate tool for monitoring of the reaction course during the biocatalytic conversion of *p*NO<sub>2</sub>PheDU ((*R/S*)-4). Enantioseparation of the resulting product, *NCp*NO<sub>2</sub> $\beta$ Phe ((*R/S*)-6), for investigation of the enantioselectivity of the employed hydantoinase is described in Chapter 4.2.4.

Furthermore, for investigation of different substrates for the Hydantoinase Process, analytical methods for PheHyd as well as BnH and their corresponding *N*-carbamoylamino acids and amino acids were required. For this purpose, the HPLC method from Werner et al. was slightly changed,<sup>[168]</sup> who used it to separate BnH and *NCP*heAla. In Figure 21 A, the separation of PheHyd, *NCP*heGly and PheGly is demonstrated, while Figure 21 B shows the separation of BnH, *NCP*heAla and PheAla.

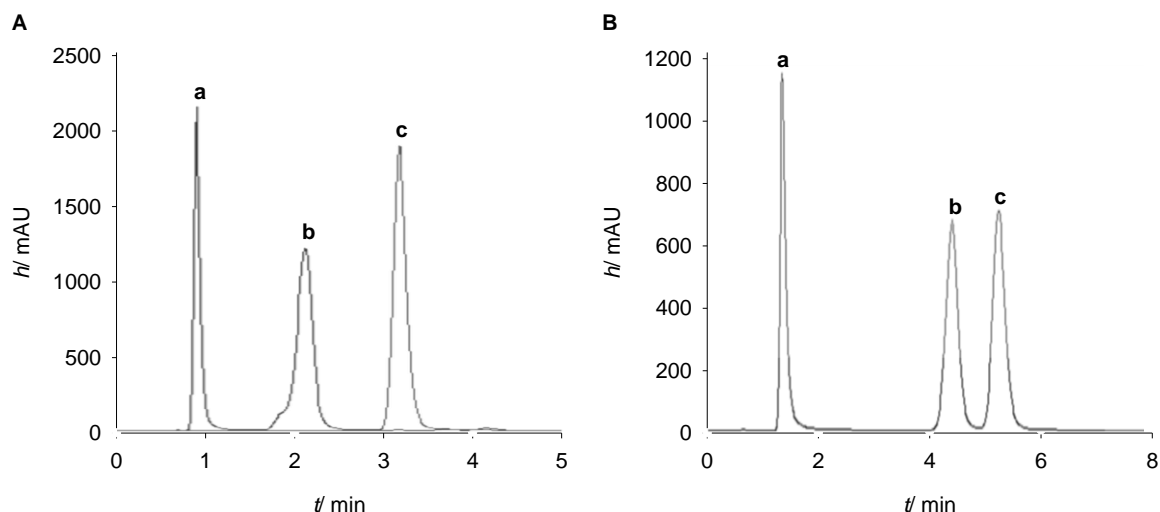


**Figure 21** **A** Separation of 5 mM PheGly (**a**), 5 mM NCPheGly (**b**) and 5 mM PheHyd (**c**). **B** Separation of 5 mM PheAla (**a**), 5 mM NCPheAla (**b**) and 5 mM BnH (**c**). Column: HyperClone ODS-C18, detection wavelength: 210 nm, column temperature: 22 °C, flow rate: 0.8 mL/min, isocratic mobile phase: 80 % of 0.1 % (v/v) H<sub>3</sub>PO<sub>4</sub> and 20 % of methanol

By means of the chosen HPLC method, the compounds PheGly (**a**), NCPheGly (**b**) and PheHyd (**c**) were detectable with retention times of 1.0 min, 2.1 min and 3.2 min by using one and the same method (Figure 21 A). The same applies to the separation of PheAla (**a**), NCPheAla (**b**) and BnH (**c**) with retention times of 1.5 min, 4.6 min and 5.4 min (Figure 21 B). Consequently, the enzyme activities for the hydantoinase as well as carbamoylase toward these substrates were determinable with the same method. Derivatives of Ser were not detectable with any of the HPLC methods tested. Therefore, the photometric Ehrlich's assay was used to determine the hydantoinase or carbamoylase activity by detection of NCSer.

## 4.2 A NOVEL SUBSTRATE FOR THE SYNTHESIS OF $\beta$ -AMINO ACIDS

As described before,  $\beta$ -amino acids attracted attention over the last two decades as they serve for example as constituents of biologically active secondary metabolites, as building blocks for  $\beta$ -peptides or as peptidomimetics. Since the viability of the modified Hydantoinase Process toward  $\beta$ -amino acids was proven in prior investigations,<sup>[31,34]</sup> a novel substrate for this process was prepared in collaboration with the working group of Prof. Stefan Bräse (Institute of Organic Chemistry, KIT). The following chapters are dealing with the synthesis and analysis of this substrate and the corresponding product as well as with its enzymatic hydrolysis.

Concerning the nomenclature, it should be noted that the two different enantiomers of  $\alpha$ -amino acids have been called D- and L- enantiomer so far, since this nomenclature is found in literature for historical reasons. But that nomenclature is not always transferable for the nomenclature of  $\beta$ -amino

acids. Consequently, in the following chapters concerning the synthesis of  $\beta$ -amino acids, the more appropriate (*R*)/(*S*)-nomenclature was used.

#### 4.2.1 CHEMICAL SYNTHESIS OF *p*NO<sub>2</sub>PheDU

After the preparation of 6-(4-nitrophenyl)dihydropyrimidine-2,4(1H,3H)-dione (see Figure 22, *p*NO<sub>2</sub>PheDU, (*R/S*)-4) according to Světlík and Veizerová (see Chapter 3.2.2.1),<sup>[76]</sup> a yellowish powder was obtained (489 mg, 2.08 mmol, 42 %). The successful synthesis was verified by different analytical procedures, the corresponding results are listed below.

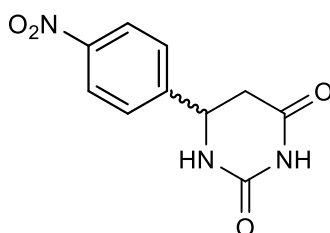


**Figure 22** 6-(4-nitrophenyl)dihydropyrimidine-2,4(1H,3H)-dione ((*R/S*)-4).

Yield: 42 % – <sup>1</sup>H NMR (400 MHz, DMSO-*d*<sub>6</sub>):  $\delta$  = 2.66 (dd, <sup>2</sup>*J* = 16.4, <sup>3</sup>*J* = 6.9 Hz, 1H, CH<sub>2</sub>), 2.91 (dd, <sup>2</sup>*J* = 16.4, <sup>3</sup>*J* = 5.9 Hz, 1H, CH<sub>2</sub>), 4.82–4.91 (m, 1H, CH), 7.62 (d, <sup>3</sup>*J* = 8.8 Hz, 2H, 2 × CH<sub>Ar</sub>), 8.12 (s, 1H, NH), 8.25 (d, <sup>3</sup>*J* = 8.8 Hz, 2H, 2 × CH<sub>Ar</sub>), 10.25 (s, 1H, NH) ppm. – <sup>13</sup>C NMR (100 MHz, DMSO-*d*<sub>6</sub>):  $\delta$  = 37.7 (–, CH<sub>2</sub>), 49.7 (+, CH), 123.8 (+, CH<sub>Ar</sub>), 127.5 (+, 2 × CH<sub>Ar</sub>), 147.0 (C<sub>q</sub>, CNO<sub>2</sub>), 148.7 (C<sub>q</sub>, 2 × C<sub>Ar</sub>), 153.7 (C<sub>q</sub>, N(CO)N), 169.3 (C<sub>q</sub>, N(CO)C) ppm. – IR (ATR):  $\tilde{\nu}$  = 3233 (vw), 3075 (w), 2846 (vw), 1702 (m), 1595 (vw), 1517 (w), 1487 (w), 1408 (w), 1342 (w), 1329 (w), 1283 (w), 1235 (w), 1212 (w), 1159 (w), 1108 (w), 1010 (vw), 991 (vw), 941 (vw), 849 (w), 764 (w), 731 (w), 691 (w), 644 (vw), 615 (w), 581 (w), 531 (w), 511 (w), 462 (vw), 441 (vw), 415 (w) cm<sup>–1</sup>. – MS (EI, 70 eV), *m/z* (%): 236 (7) [M + H]<sup>+</sup>, 235 (48) [M]<sup>+</sup>, 218 (13) [M – OH]<sup>+</sup>, 177 (32), 164 (13), 151 (42), 149 (22), 119 (13), 113 (21), 107 (100) [C<sub>6</sub>H<sub>6</sub>NO]<sup>+</sup>, 103 (17) [C<sub>4</sub>H<sub>5</sub>N<sub>2</sub>O<sub>2</sub>]<sup>+</sup>, 91 (11) [C<sub>7</sub>H<sub>7</sub>]<sup>+</sup>, 77 (43), 70 (41), 60 (22). – HRMS (EI, C<sub>10</sub>H<sub>9</sub>O<sub>4</sub>N<sub>3</sub>): calc. 235.0588; found 235.0589. – EA (C<sub>10</sub>H<sub>9</sub>O<sub>4</sub>N<sub>3</sub>) calc. C 51.07 %, H 3.86 %, N 17.87 %; found C 50.87 %, H 3.72 %, N 17.62 %.

#### 4.2.2 CHEMICAL SYNTHESIS OF THE CORRESPONDING *N*-CARBAMOYL DERIVATIVE

To enable analytical investigations, 3-(4-Nitrophenyl)-3-ureidopropanoic acid (see Figure 23, *NCp*NO<sub>2</sub> $\beta$ Phe, (*R/S*)-6), was synthesized according to Posner (see Chapter 3.2.2.2).<sup>[170]</sup> The  $\beta$ -carbamoyl amino acid *NCp*NO<sub>2</sub> $\beta$ Phe precipitated as a yellowish solid (418 mg, 1.65 mmol, 71%). Various analytical procedures were carried out to verify the successful synthesis, the results are listed below.

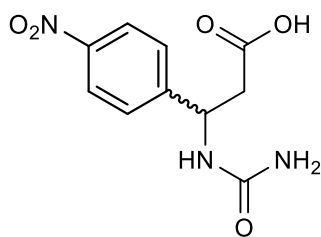


**Figure 23** 3-(4-Nitrophenyl)-3-ureidopropanoic acid ((*R/S*)-6).

Yield: 71 % –  $^1\text{H NMR}$  (400 MHz,  $\text{DMSO-d}_6$ ):  $\delta$  = 2.71 (d,  $^3J$  = 6.9 Hz, 2H,  $\text{CH}_2$ ), 5.08 (q,  $^3J$  = 7.2 Hz, 1H,  $\text{CH}$ ), 5.64 (s, 2H,  $\text{NH}_2$ ), 6.74 (d,  $^3J$  = 8.4 Hz, 1H,  $\text{NH}$ ), 7.58 (d,  $^3J$  = 8.6 Hz, 2H,  $2 \times \text{CH}_{\text{Ar}}$ ), 8.19 (d,  $^3J$  = 8.6 Hz, 2H,  $2 \times \text{CH}_{\text{Ar}}$ ) ppm. –  $^{13}\text{C NMR}$  (100 MHz,  $\text{DMSO-d}_6$ ):  $\delta$  = 40.9 (–,  $\text{CH}_2$ ), 49.9 (+,  $\text{CH}$ ), 123.4 (+,  $\text{CH}_{\text{Ar}}$ ), 127.7 (+,  $2 \times \text{CH}_{\text{Ar}}$ ), 146.3 ( $\text{C}_q$ ,  $\text{C}_{\text{Ar}}$ ), 151.8 ( $\text{C}_q$ ,  $\text{C}_{\text{Ar}}$ ), 157.8 ( $\text{C}_q$ ,  $\text{CO}$ ), 171.8 ( $\text{C}_q$ ,  $\text{CO}_2\text{H}$ ) ppm. – **IR** (ATR):  $\tilde{\nu}$  = 3390 (w), 1697 (m), 1631 (w), 1604 (w), 1506 (m), 1386 (w), 1345 (m), 1313 (m), 1210 (m), 1176 (w), 1105 (w), 1035 (w), 968 (w), 938 (w), 851 (m), 771 (vw), 751 (w), 700 (w), 649 (w), 625 (w), 555 (m), 472 (m), 448 (m)  $\text{cm}^{-1}$ . – **MS** (FAB, 3-NBA),  $m/z$  (%): 254 (23)  $[\text{M} + \text{H}]^+$ , 233 (12), 192 (100). – **HRMS** (FAB,  $(\text{M}^+ + \text{H})$ ,  $\text{C}_{10}\text{H}_{12}\text{O}_5\text{N}_3$ ): calc. 254.0771; found 254.0772.

#### 4.2.3 BIOTRANSFORMATION ASSAYS USING $p\text{NO}_2\text{PheDU}$ AS A SUBSTRATE

After synthesis and analysis of the above mentioned compounds, whole cell biotransformation reactions with *E. coli* JM109 hosting the recombinantly expressed hydantoinase (plasmid pJAVI2 with D-Hyd from *Arthrobacter crystallopoietes* DSM 20117, Strep-tag (*C*-terminus)) employing  $p\text{NO}_2\text{PheDU}$  ((*R/S*)-4) as substrate were performed. The reaction courses of substrate and product during 24 h of whole cell biotransformation are shown in Figure 24 A.

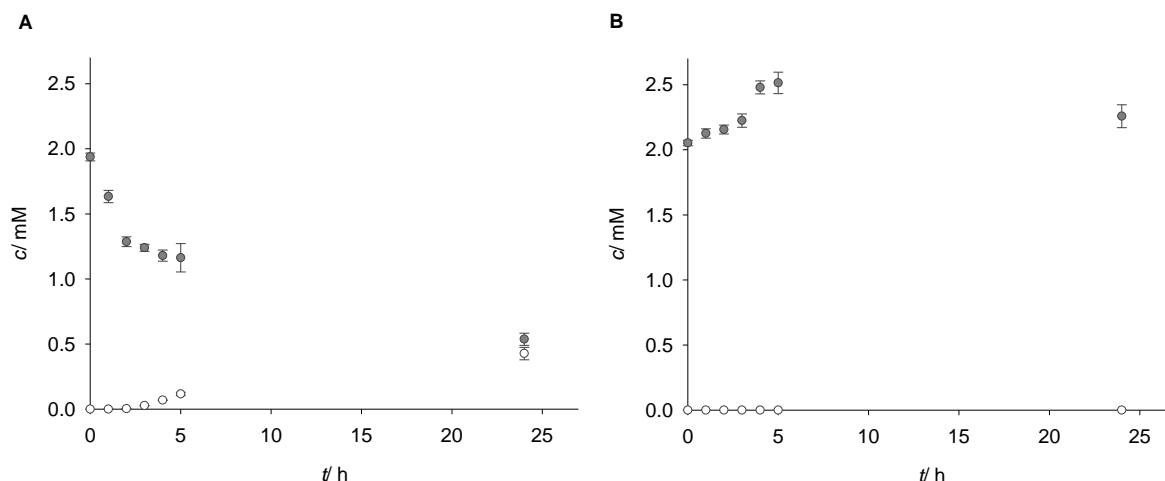


**Figure 24** Conversion of 2 mM  $p\text{NO}_2\text{PheDU}$  ((*R/S*)-4) by the hydantoinase from *A. crystallopoietes* DSM 20117 using resting cells. **A** Concentrations of  $p\text{NO}_2\text{PheDU}$  ((*R/S*)-4, filled circles) and the corresponding product ((*R/S*)-6, empty circles) during the reaction progress. **B** Concentrations of  $p\text{NO}_2\text{PheDU}$  ((*R/S*)-4, filled circles) and the corresponding product ((*R/S*)-6, empty circles) during the reaction course of control experiments without cells. Reactions and measurements were carried out in triplicates and error bars show the standard deviations of the means. The reactions were carried out at 40 °C and 800 rpm in Tris-HCl (50 mM, pH 8).

The  $p\text{NO}_2\text{PheDU}$  concentration ((*R/S*)-4) decreases from 1.94 to 1.63 mM within 1 h and finally to 0.54 mM after 24 h. The detected product concentration ((*R/S*)-6) is 0.03 mM after 3 h of reaction time and increases to a final concentration of 0.43 mM after 24 h. To exclude a possible chemical

degradation or thermal instability of the substrate, control experiments without cells were conducted (see Figure 24 B). No decrease of substrate concentration below the initial concentration of 2 mM is detected during the reaction time of 24 h and additionally, no product formation takes place during these control experiments.

Decreasing substrate concentrations during whole cell biotransformations proved the enzymatic hydrolysis of *p*NO<sub>2</sub>PheDU by the investigated hydantoinase with a specific activity of 0.326 mU/mg<sub>cdw</sub>. The observed conversion yield for the hydrolysis of the novel substrate was 72 % after 24 h. By investigating the product concentration, it was noticed that less product was formed than substrate was hydrolyzed. Nevertheless, control experiments without cells did neither show a decrease of substrate concentration nor reveal any hints of product formation and therefore prove chemical as well as thermal stability of *p*NO<sub>2</sub>PheDU ((*R/S*)-4). Consequently, the enzymatic hydrolysis of the novel substrate by the hydantoinase from *A. crystallopoietes* DSM 20117 was verified. Until now, there is no knowledge about transport limitations of the substrate as well as the emerging product and the same applies to possible adhesion of these compounds to the cell. Nevertheless, several groups reported transport limitations for the emerging intermediates through the cell membrane of *E. coli* cells after hydrolysis of various hydantoins.<sup>[176,177]</sup> Accordingly, due to the performance of whole cell experiments, emerging product was maybe not entirely detectable.

To avoid the drawback of these transport limitations, the same experiments were carried out using crude cell extract, but neither a decrease in substrate concentration nor product formation could be detected (data not shown). Since degradation by proteases was prevented by adding protease inhibitor, the applied enzyme is possibly not stable in its free form.

A limiting factor in this approach is the low solubility of the substrate. By addition of 5 % DMSO, an initial substrate concentration of 2 mM was achieved. Additionally, it was examined whether higher initial substrate concentrations with higher contents of DMSO would lead to increased enzyme activities or enzyme inactivation. The results of whole cell biotransformations as well as control experiments applying 10 mM of initial substrate concentration instead of 2 mM are shown in Figure 25.

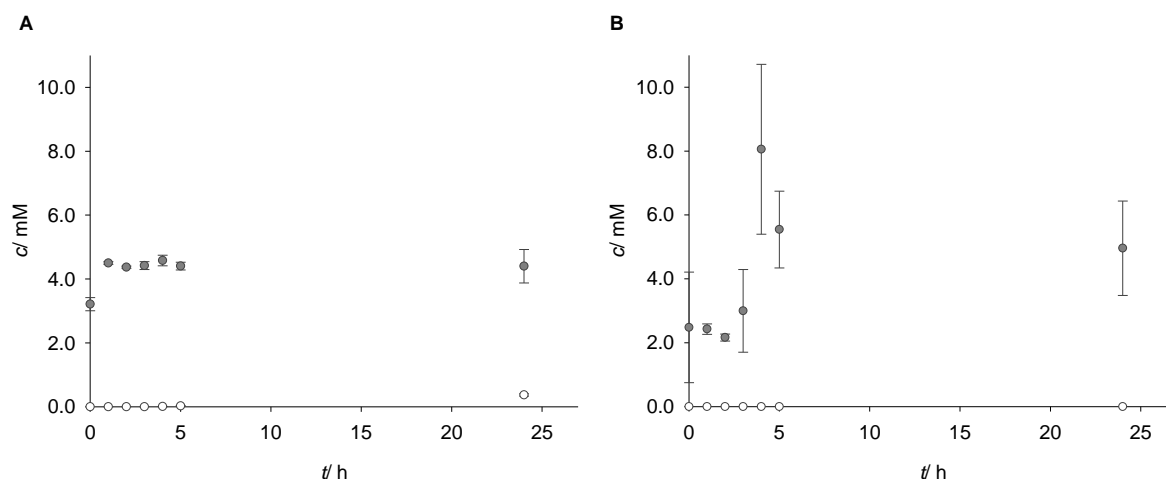


**Figure 25** Conversion of 10 mM *p*NO<sub>2</sub>PheDU ((*R/S*)-4) by the hydantoinase from *A. crystallopoietes* DSM20117 using resting cells. **A** Concentrations of *p*NO<sub>2</sub>PheDU ((*R/S*)-4, filled circles) and the corresponding product ((*R/S*)-6, empty circles) during the reaction progress. **B** Concentrations of *p*NO<sub>2</sub>PheDU ((*R/S*)-4, filled circles) and the corresponding product ((*R/S*)-6, empty circles) during the reaction course of control experiments without cells. Reactions and measurements were carried out in triplicates and error bars show the standard deviations of the means. The reactions were carried out at 40 °C and 800 rpm in Tris-HCl (50 mM, pH 8).

The determined substrate concentration is approximately 5 mM during whole cell biotransformation and no trend is recognizable, while the value after 0 h is 3.21 mM. In contrast, the concentration of the corresponding *N*-carbamoylamino acid increases up to 0.39 mM after 24 h of reaction time. Results of the control experiment without cells also show fluctuation of the substrate concentration, ranging from 2.16 mM to 8.06 mM, while no product is detectable.

Since the initial concentration could not be detected when conducting whole cell biotransformations with 10 mM *p*NO<sub>2</sub>PheDU and concentrations of the following samples fluctuated, it was assumed that the substrate was not entirely soluble and precipitated after addition of the cell suspension. Nevertheless, product formation occurred and consequently it was shown that the enzyme was not inactivated by adding a total amount of 25 % DMSO to the reaction mixture to obtain a substrate concentration of 10 mM. Control experiments showed no product formation, which additionally supports this assumption. In comparison to the whole cell biotransformations using 2 mM of initial substrate concentration slightly less product was formed. On the one hand, this could reveal that substrate saturation is already accomplished by adding 2 mM of *p*NO<sub>2</sub>PheDU and the hydantoinase loses activity during reaction progress. On the other hand, inhibition of the hydantoinase by DMSO is possible which would lead to low conversion rates although more substrate is available. Concerning these facts and the challenges concerning analytical methods as well as the solubility of the substrate is not assured, whole cell biotransformations with higher substrate concentrations are not advantageous.

To conclude, by conducting whole cell biotransformation assays with *p*NO<sub>2</sub>PheDU as a substrate, enzymatic hydrolysis by the hydantoinase from *A. crystallopoietes* DSM20117 was shown. Additionally, the stability of this novel substrate under reaction conditions was verified and it was



pointed out that the applied enzyme is not inactivated at a DMSO content of 25 %. After successful hydrolysis of  $p\text{NO}_2\text{PheDU}$ , the enantioselectivity of the hydantoinase toward this substrate was investigated regarding potential applications in pharmaceutical industries.

#### 4.2.4 EXAMINATION OF ENANTIOSELECTIVITY FOR $p\text{NO}_2\text{PheDU}$

As shown above, by performing whole cell biotransformation reactions, the hydrolysis of  $p\text{NO}_2\text{PheDU}$  (( $R/S$ )-4) via *A. crystallopoietes* DSM 20117 hydantoinase was proven. To investigate the enantioselectivity of this enzyme toward the novel substrate, HPLC analytics with chiral stationary phases were established. As apparent in Figure 26 A, the enantiomers of the product were separated with retention times of 13.2 and 14.4 min. Compared to the separation of the standard which shows both enantiomers in equal parts, the product formed after 24 h of biotransformation mostly consists of the ( $S$ )-enantiomer.

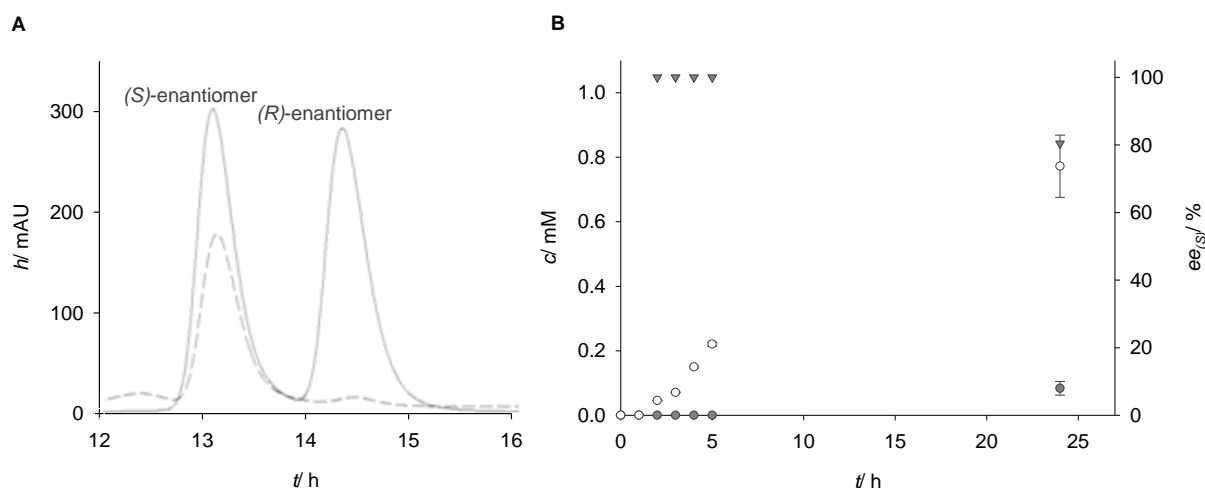


**Figure 26** Studies on the enantioselectivity of the hydantoinase from *A. crystallopoietes* DSM20117 toward  $p\text{NO}_2\text{PheDU}$  (( $R/S$ )-4). **A** Chiral separations in order to determine the enantioselectivity of the hydantoinase using  $p\text{NO}_2\text{PheDU}$  (( $R/S$ )-4) as substrate in whole cell biocatalysis with recombinant *E. coli* JM109. Separation of 2 mM  $\text{NCpNO}_2\beta\text{Phe}$  standard (( $R/S$ )-6, solid line). Separation of  $\text{NCpNO}_2\beta\text{Phe}$  (( $R/S$ )-6) after 24 h biotransformation (dashed line). **B** Concentrations of the ( $S$ )- and ( $R$ )-enantiomer (empty circles and filled circles) and enantiomeric excess (filled triangles) during the reaction progress. Reactions and measurements were carried out in triplicates and error bars show the standard deviations of the means. The reaction was carried out at 40 °C and 800 rpm in Tris-HCl (50 mM, pH 8). Column: ChiralPak QN-AX, detection wavelength: 257 nm, column temperature: 30 °C, flow rate: 0.3 mL/min, isocratic mobile phase: 98 % (v/v) methanol (0.2 % (v/v) ammonium formate and 2 % (v/v) acetic acid (0.2 M, adjusted to pH 6 with ammonia)

The reaction courses of both enantiomers show, that 0.77 mM of ( $S$ )- $\text{NCpNO}_2\beta\text{Phe}$  (( $S$ )-6) emerge after 24 h, while 0.08 mM of the ( $R$ )-enantiomer are detected (see Figure 26 B). Within the first 5 h of whole cell biotransformation an enantioselectivity of >99 % ee is achieved, while after 24 h the enantiomeric excess is 80.4 % ee.

Chiral separations of both enantiomers of the product showed that the novel substrate *p*NO<sub>2</sub>PheDU ((*R/S*)-**4**) was converted with preference to the (*S*)-enantiomer. Control experiments without cells did not reveal any product formation (data not shown), confirming the conversion of *p*NO<sub>2</sub>PheDU to the corresponding *N*-carbamoyl- $\beta$ -amino acid by the hydantoinase of *A. crystallopoietes* DSM 20117. The decrease of its enantiomeric excess for the (*S*)-enantiomer from >99 % to 80.4 % after 24 h of reaction time could be explained in two different ways. One possibility is that no substrate saturation was achieved by adding 2 mM *p*NO<sub>2</sub>PheDU to the reaction mixture. Therefore, after hydrolysis of the preferred (*S*)-*p*NO<sub>2</sub>PheDU ((*S*)-**4**), the hydantoinase maybe starts converting the (*R*)-enantiomer of the racemic substrate. Another alternative is a spontaneous racemization of the product. This has also been monitored by HPLC analytics with chiral stationary phases and no racemization was observed for (*S*)-*NCp*NO<sub>2</sub> $\beta$ Phe ((*S*)-**6**) in Tris-HCl (50 mM, pH 8) at 40 °C during 48 h. Consequently, in contrast to the hydantoins tested to date, we could show that the novel substrate *p*NO<sub>2</sub>PheDU ((*R/S*)-**4**) has been hydrolyzed with preference of the (*S*)-enantiomer, which is consistent with previous studies concerning other dihydrouracils.<sup>[31,34]</sup>

However, there is still a limiting factor for synthesis of the enantiopure  $\beta$ -amino acid with 100 % yield: the racemization of the applied substrate. As already mentioned, the racemization of dihydrouracils is challenging compared to hydantoins given that no keto-enol-tautomerism occurs. There are not many investigations concerning this topic, but Argyrou et al. examined the interchange of protons in the C5 and revealed spontaneous racemization of 5-monosubstituted 5,6-dihydrouracils due to the acidic proton at a carbon next to a carbonyl group. In contrast, for dihydroorotate (6-carboxydihydrouracil) no racemization was observed.<sup>[68]</sup> This was approved for further 6-monosubstituted dihydrouracil derivatives by Martínez- Gómez et al..<sup>[35]</sup> Due to the chosen synthesis strategy for the novel 6-monosubstituted dihydrouracil, until now we could not achieve the synthesis of enantiopure *p*NO<sub>2</sub>PheDU in terms of analyzing the racemization of this dihydrouracil. Nevertheless, the findings of this work represent a promising basis to employ the novel substrate for the synthesis of optically pure  $\beta$ -amino acids by further conversion of the resulting *N*-carbamoyl- $\beta$ -amino acid. In previous approaches, the hydrolysis of *N*-carbamoyl- $\beta$ -amino acids was performed chemically.<sup>[34]</sup> Therefore it is worthwhile to detect an appropriate carbamoylase (EC 3.5.1.77; EC 3.5.1.87) realizing this reaction to gain  $\beta$ -amino acids.  $\beta$ -Ureidopropionases (EC 3.5.1.6) may also be prospect enzymes since they catalyze the last step of the reductive pyrimidine degradation pathway, hydrolyzing *N*-carbamoyl- $\beta$ -alanine and  $\beta$ -ureidoisobutyric acid to  $\beta$ -alanine and  $\beta$ -aminoisobutyric acid.<sup>[35]</sup>

## 4.3 TOWARD CELL-FREE REACTION SYSTEMS

### 4.3.1 IMPROVEMENT OF SOLUBLE HYDANTOINASE EXPRESSION

#### 4.3.1.1 CODON-OPTIMIZATION

As already discussed before (Chapter 1.2.1.1), the expression of recombinant enzymes in another host than the wildtype is often challenging due to the differences in codon-usage.<sup>[133,134]</sup> To prevent the expression of non-functional and insoluble proteins for the expression of the recombinant D-hydantoinase from *A. crystallopoietes* DSM20117 in *E. coli* BL21DE3, this enzyme was codon-optimized and in addition to the C-terminal His-tag a N-terminal SBP-tag was added to allow purification and immobilization by two different methods. After codon-optimization, the GC-content of the protein was reduced from 54 % to 51 %. Additionally, the minimum free energy for mRNA folding was reduced from 12 192.8 kcal/mol to 11 153.8 kcal/mol, which indicates a more stable mRNA secondary structure after codon-optimization. In the following chapters, amongst others the influence of this codon-optimization on expression and enzyme activity are investigated. The D-hydantoinase from *A. crystallopoietes* DSM 20117 on plasmid pDEST42 in *E. coli* BL21DE3 with a C-terminal His-tag and a molecular weight of 52 kDa is called D-Hyd, while the codon-optimized version of this hydantoinase on plasmid pET28a in *E. coli* BL21DE3 with a C-terminal His-tag and N-terminal SBP-tag and a resulting molecular weight of 56 kDa is called D-Hyd(co) below.

Every experiment concerning the improvement of hydantoinase expression was carried out as whole cell biotransformation and samples were taken only after 0 h and 24 h due to the enormous number of different setups.

#### 4.3.1.2 EXPRESSION UNDER OXYGEN DEFICIENCY

Since enhanced solubility of recombinant proteins was reported at low temperatures and weak doses of inductor,<sup>[178–180]</sup> both parameters were investigated in this work, but no improvement in soluble hydantoinase expression was observed (data not shown). This is consistent with the findings of Baumann et al., who showed that variation of the inductor concentration had no distinctive influence on bacterial growth and protein expression. The same applied to the cultivation temperature, while the shaking speed was found to be more influencing concerning these matters.<sup>[181]</sup> On the basis of these investigations, experiments under oxygen deficiency have been carried out by using a higher culture volume (400 mL instead of 200 mL per 1 L baffled shaking flask) on the one hand and comparatively low shaking speeds (120 rpm, 100 rpm and 90 rpm) on the other hand for the expression of D-Hyd and D-Hyd(co). For comparing enzyme activities after applying these different expression conditions, whole

cell biotransformations were conducted. Figure 27 A shows the different  $OD_{600}$  values of the cultures at the time point of harvesting, while Figure 27 B indicates their specific activities for the conversion of 2 mM PheHyd.

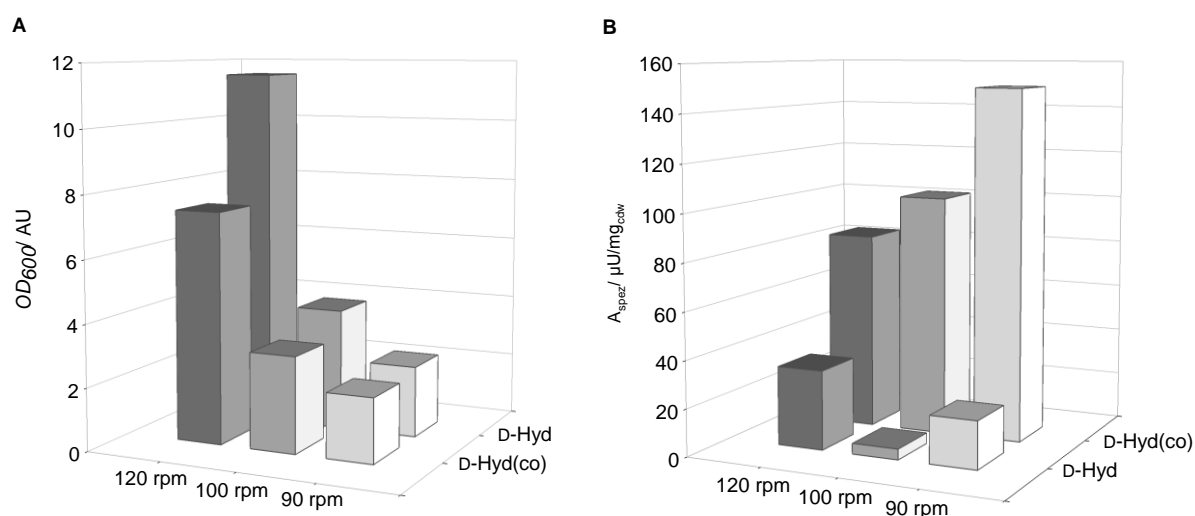


**Figure 27** Cultivation of *E. coli* BL21DE3 and expression of the recombinant hydantoinases D-Hyd and D-Hyd(co) from *A. crystallopoietes* DSM 20117 under oxygen deficiency. **A**  $OD_{600}$  values of the D-Hyd and D-Hyd(co) cultures at the moment of harvesting after cultivation at 120 rpm (dark grey), 100 rpm (grey) and 90 rpm (white). **B** Specific activities of D-Hyd and D-Hyd(co) during whole cell biotransformations with 2 mM PheHyd as substrate. The reactions were carried out at 40 °C and 800 rpm in Tris-HCl (50 mM, pH 8).

Regarding the  $OD_{600}$ -values of the differently cultured *E. coli* BL21DE2 hosting the different recombinant hydantoinases, the values of the D-Hyd cultures are generally higher than that of the D-Hyd(co) cultures and the  $OD_{600}$  values decrease with decreasing rotation speeds for both cultures (Figure 27 A). At this juncture, the culture of the D-Hyd at 120 rpm exhibits a much higher  $OD_{600}$  of 11.54 compared to that of the D-Hyd(co) with an  $OD_{600}$  of 7.37. Compared to the cultures at 120 rpm, the  $OD_{600}$  values of the D-Hyd and the D-Hyd(co) cultures decrease to 3.89 and 3.06 and the cultures at 90 rpm show  $OD_{600}$  values of 2.27 and 2.05. In contrast, the specific activities of the D-Hyd(co) cultures are much higher than that of the D-Hyd cultures (Figure 27 B). Here, the specific activity increases with decreasing rotation speed. The highest value for the D-Hyd(co) culture was determined at 90 rpm with 149.5  $\mu\text{U}/\text{mg}_{\text{cdw}}$ , while the lowest specific activity was 83.7  $\mu\text{U}/\text{mg}_{\text{cdw}}$  at 120 rpm. As mentioned before, the specific activities for the D-Hyd are much lower with values from 4.50 to 33.4  $\mu\text{U}/\text{mg}_{\text{cdw}}$  and with no noticeable tendency concerning the rotation speed.

The fact that lower rotation speeds and consequently reduced oxygen transfer rates lead to decreased growth of the cultures was expected, since *E. coli* is an aerobic microorganism. At lower rotation speeds like 100 rpm and 90 rpm, the difference is not that crucial, since the growth is already very slow. More noticeable is the fact that the growth of the D-Hyd(co) culture was much slower than that of the D-Hyd culture at 120 rpm. This implies a stronger expression of the recombinant hydantoinase after codon-optimization, given that the growth is reduced during high expression levels. The determined specific activities of the D-Hyd(co) are in each case much higher than those of the D-Hyd, which confirms this assumption. With for example 149.5  $\mu\text{U}/\text{mg}_{\text{cdw}}$  at a rotation speed of 90 rpm, the

specific activity of the D-Hyd(co) is seven times higher than the specific activity of the D-Hyd with the same expression conditions. It was observed that the specific enzyme activity of the D-Hyd(co) increases with decreasing rotation speed, which certainly results from slower growth rates as well as expression which is accompanied by correct folding of the enzyme.<sup>[142,181]</sup> Georgiou et al. reported that the time-scale for the folding of proteins may vary from milliseconds to days, depending on the amount of kinetic barriers that are included in the folding process.<sup>[182]</sup> The latter are for example caused by covalent reactions like the formation of disulfide bonds or *cis/trans* isomerizations and result in the accumulation of folded intermediates containing exposed hydrophobic surfaces that promote self-assembly. Since this self-assembly leads to the formation of inclusion bodies, it was supposed that decelerated expression of the target molecule leads to more correct folded proteins and higher specific activities.<sup>[183,184]</sup> Probably due to the differences in codon-usage or caused by the high proliferation as well as expression rates, the specific activities of the not codon-optimized D-Hyd were comparatively low for all cultivation conditions. Consequently, there was no tendency perceivable regarding the different rotation speeds during cultivation and expression.

To additionally investigate the formation of inclusion bodies and the synthesis of the hydantoinase in its native and soluble state, qualitative analysis was conducted via SDS-PAGE (Figure 28).

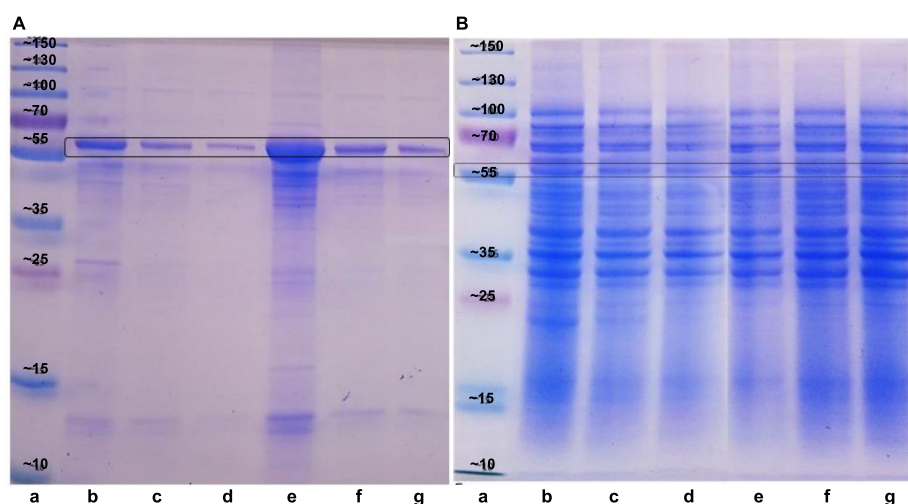


**Figure 28** SDS-PAGE of the cultures of *E. coli* BL21DE3 hosting the recombinant hydantoinases D-Hyd and D-Hyd(co) from *A. crystallopoietes* DSM 20117 after cultivation and expression under oxygen deficiency and subsequent cell disruption. **A:** Qualitative analysis of the insoluble fraction, **a** protein standard with molecular weights in kDa, **b** D-Hyd at 120 rpm, **c** D-Hyd at 100 rpm, **d** D-Hyd at 90 rpm, **e** D-Hyd(co) at 120 rpm, **f** D-Hyd(co) at 100 rpm, **g** D-Hyd(co) at 90 rpm. **B:** Qualitative analysis of the soluble fraction, **a** protein standard with molecular weights in kDa, **b** D-Hyd at 120 rpm, **c** D-Hyd at 100 rpm, **d** D-Hyd at 90 rpm, **e** D-Hyd(co) at 120 rpm, **f** D-Hyd(co) at 100 rpm, **g** D-Hyd(co) at 90 rpm.

The insoluble fractions after cultivation under hypoxic conditions, harvesting and subsequent cell disruption are shown in Figure 28 A. The molecular weight of the D-Hyd is around 52 kDa, while D-Hyd(co) has a molecular weight of around 56 kDa. Both hydantoinase cultures show a clear band in every insoluble fraction with the suitable molecular weight for the enzyme, whereat it is noticeable that the bands for the D-Hyd (lane **b-d**) are generally more slightly than the bands for the D-Hyd(co)

(lane **e-f**). Additionally, the intensities of the bands for insoluble hydantoinase decrease together with the rotation speeds for the cultured bacteria. The same applies to the amount of randomly stained proteins that remain in the insoluble fraction. Figure 28 B, illustration of the corresponding samples from the crude cell extracts, shows an identical pattern with stained proteins about the entire molecular weight range for both recombinant hydantoinase cultures with every rotation speed for the cultured bacteria. Additionally, corresponding bands for the hydantoinases are visible in every sample with molecular weights of 52 kDa respectively 56 kDa.

Since protein concentrations of the insoluble fractions were not definable by photometric assays, the pellets were diluted based on the culture volume (see Chapter 3.2.1.1). Consequently, the decreasing amount of randomly stained proteins occurring in the insoluble fraction (Figure 31 A) with decreasing rotation speed can be explained by lower  $OD_{600}$  values at the moment of harvesting (see Figure 30 A). The fact that there was more insoluble hydantoinase in the D-Hyd(co) cultures (lane **e-g**) than in the D-Hyd cultures (lane **e-g**) is remarkable, since their  $OD_{600}$  values were much lower at the moment of harvesting. This indicates that the expression of codon-optimized hydantoinase is much higher than this of the not optimized one, but a major part of this hydantoinase is misfolded. The same was observed for the D-Hyd even though the expression of this recombinant hydantoinase is generally lower than that of the D-Hyd(co). The decreasing intensity of the hydantoinase bands with decreasing shaking speed was also caused by the lower  $OD_{600}$  values. Analysis of the soluble fractions of both enzymes confirmed the assumption that most of the synthesized target protein appeared as inclusion bodies, since the bands for the D-Hyd (lane **b-d**) as well as for the D-Hyd(co) (lane **e-g**) with molecular weights of 52 kDa and 56 kDa showed no overexpression. In detail, the intensities of these hydantoinase bands are comparable to that of the randomly stained proteins or show even lower intensities.

The results from SDS-PAGE, implying that the D-Hyd(co) shows high expression rates that mostly result in inclusion bodies, stay in contrast to the determined specific activities of this enzyme (see Figure 27 B). Since the latter were found to be very high compared to the D-Hyd, it was shown that despite the major amount of inclusion bodies, a strong improvement was achieved. Therefore, it was assumed that prevention of inclusion body formation could even lead to a further improvement. As demonstrated by the above discussed experiments, the codon-optimization resulted in a much higher expression of recombinant hydantoinase. These non-physiological amounts of produced proteins promote the intermolecular association of exposed hydrophobic surfaces before completion of the protein folding, which causes precipitation of folding intermediates.<sup>[178,185]</sup> Since the direct or indirect induction of chaperones was reported to improve the expression of target molecules in their native state, the next chapter deals with the screening for different expression conditions concerning these topics.<sup>[144,182]</sup>

#### 4.3.1.3 HIGH THROUGHPUT SCREENING FOR EXPRESSION CONDITIONS

As a simple method to induce chaperones respectively heat shock proteins indirectly, cultivation and induction under physical stress was reported.<sup>[144,186]</sup> To allow the investigation of different factors, a high throughput screening was conducted using the BioLector® (m2p-labs, Baesweile). Baumann et al. also investigated various cultivation conditions including the oxygen transfer rate by varying the shaking speed as well as the inducer concentration.<sup>[181]</sup> Since these experiments showed no influence on bacterial growth and product formation after variation of IPTG concentration, but very high product concentrations were observed without induction of the T7-promoter, in this work only induction with 1 mM IPTG as well as no induction were conducted. Concerning the shaking speed, 600 rpm resulted in most product formation for every tested setup. Consequently every experiment in this work was carried out at 600 rpm only, to reduce the amount of approaches to test. The examination of two different hydantoinases, D-Hyd and D-Hyd(co) and expression at different setups (+/- EtOH, +/- IPTG, pH 6, pH 7), resulted in 16 different approaches, each as triplicates.

Since the BioLector® records scattered light values during the cultivation instead of OD<sub>600</sub> values, at first a scattered light/OD<sub>600</sub> correlation function for *E. coli* BL21DE3 had to be determined (see Chapter 5.1.1) with the aid of serial dilution. The resulting correlation function at gain 20 and 600 rpm is shown below.

$$y(\text{OD}_{600}) = 0.00794 * x(\text{scattered light}) - 1.4317$$

Based on this function, the OD<sub>600</sub> values during cultivation were calculated. Figure 29 shows the OD<sub>600</sub> values during cultivation as well as the maximum growth rates for both enzymes at every tested setup.

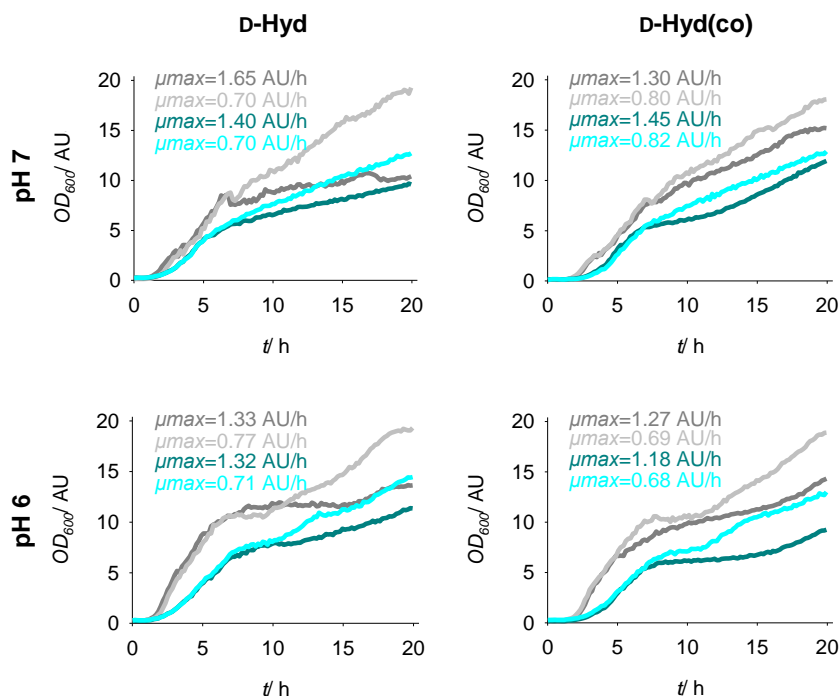


**Figure 29** High throughput screening for the cultivation conditions of *E. coli* BL21DE3 expressing the recombinant hydantoinase D-Hyd and D-Hyd(co) from *A. crystallopoietes* DSM 20117. Growth curves and maximum growth rates under different cultivation conditions. Legend: -EtOH +IPTG (dark grey), -EtOH -IPTG (grey), +EtOH +IPTG (dark cyan), +EtOH -IPTG (cyan). Cultivations were carried out in triplicates, shown are the mean values.

Regarding the  $OD_{600}$  values of the different cultures, it is noticeable that the non-induced cultures show higher  $OD_{600}$  values at the time of harvesting in every case. The same applies to the cultures without EtOH compared to that with 3 % EtOH. When comparing every cultivation setup for both hydantoinases, the D-Hyd(co) always shows higher  $OD_{600}$  values at the end of cultivation than the D-Hyd, but for the cultivation at pH 6 this observation is not distinct. Additionally, for the D-Hyd(co) the cultures at pH 6 all have lower  $OD_{600}$  values at the end of culturing, while for the D-Hyd it is contrary. The tendencies are different for the maximum growth rates, since there is no difference between induced and not induced cultures. In contrast, cultures with and without 3 % EtOH show major differences in maximum growth rates with a decrease of up to 50 % for the cultures containing EtOH. For the D-Hyd(co), a slight decrease in the maximum growth rate is observed when culturing at pH 6 instead of pH 7, while for the D-Hyd no tendency is noticeable. In general, also no tendency is perceivable concerning the maximum growth rate between the two tested hydantoinases.

The observance that non-induced cultures had higher  $OD_{600}$  values at the end of culturing in every case suggests that the proliferation is decreased after induction, since the resources are used for gene expression instead of growth. This is a fact, although the induction was conducted in a later growth phase ( $OD_{600}=4$ ) according to Baumann et al., since earlier induction would have led to faster protein expression and therefore also fast and poor folding of the target molecule.<sup>[181–183]</sup> No significant differences in maximum growth rates between induced or non-induced cultures are explainable by the late induction time at which the exponential growth phase was already finished. The addition of EtOH on the other hand had a great influence on the final  $OD_{600}$  values as well as the maximum growth



rates, since the resulting physical stress led to a decrease in proliferation. In contrast to the results of cultivation under oxygen deficiency, the  $OD_{600}$ -values for the D-Hyd(co) expressing cultures were higher as that of the D-Hyd in every case. This implies a lower specific activities for the D-Hyd(co), since earlier experiments showed that cultures with higher final  $OD_{600}$  values led to lower specific activities. However, when observing the maximum growth rates for the cultures of D-Hyd and D-Hyd(co), no significant differences or tendencies are noticeable. As it was reported that higher production yields are afforded at decreased maximum growth rates, no conclusion can be drawn by only considering the final  $OD_{600}$  values.<sup>[181]</sup> Therefore, as a next step whole cell biotransformations for determination of the specific enzyme activities were conducted.

Concerning the cultivation at different pH values, cultures of the tested hydantoinases are influenced very differently. The final  $OD_{600}$  values of the D-Hyd(co) cultures decrease with decreasing pH, while that of the D-Hyd cultures increase. The fact that for the D-Hyd(co) expressing cultures, also the maximum growth rates are lower at pH 6 suggest higher production rates of the target molecule due to more correct folding, while for the D-Hyd expressing cultures no change in maximum growth rates depending on the pH were observed.

To enable a statement, whether the recombinantly expressed hydantoinases are in their native and active form, whole cell biotransformations were carried out. The specific activities for D-Hyd as well as D-Hyd(co) after cultivation and induction at different conditions are illustrated in 3D bar plots (see Figure 30).

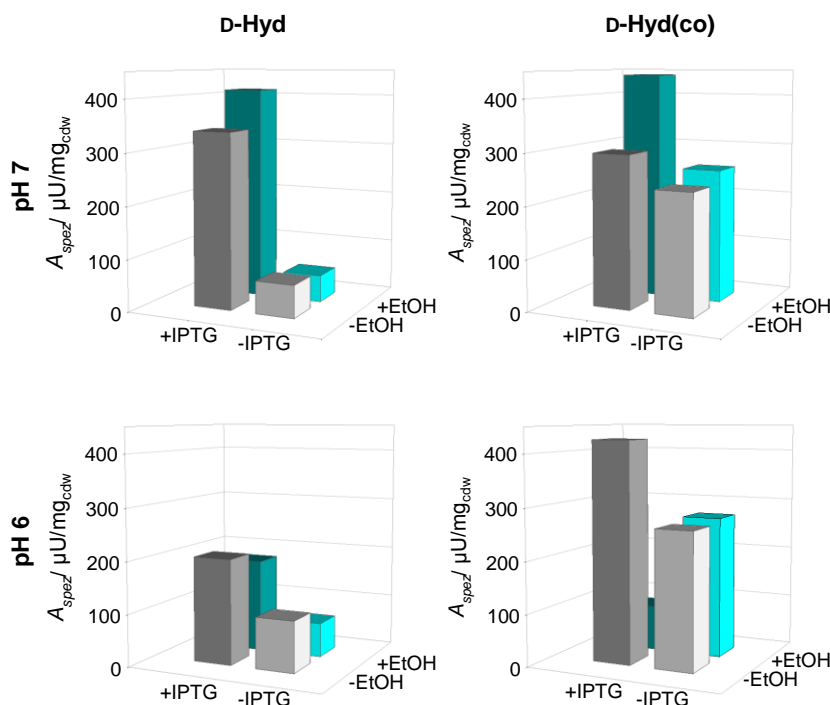


**Figure 30** High throughput screening for the cultivation conditions of *E. coli* BL21DE3 expressing the recombinant hydantoinase D-Hyd and D-Hyd(co) from *A. crystallopoietes* DSM20117. Specific activities after whole cell biotransformation with 2 mM PheHyd after cultivation and induction under different conditions. Legend: -EtOH +IPTG (dark grey), -EtOH -IPTG (grey), +EtOH +IPTG (dark cyan), +EtOH -IPTG (cyan)

The determined specific activities for the D-Hyd(co) are higher than that of the D-Hyd for every cultivation setup. The highest specific activity shows the D-Hyd(co) with 440.7  $\mu\text{U}/\text{mg}_{\text{cdw}}$  at pH 7, induction with 1 mM IPTG and 3 % EtOH, while the D-Hyd reaches with 411.1  $\mu\text{U}/\text{mg}_{\text{cdw}}$  its highest specific activity at the same cultivation setup. In contrast, the lowest specific activity for the D-Hyd(co) is determined at pH 6, induction with 1 mM IPTG and 3 % EtOH with 86.7  $\mu\text{U}/\text{mg}_{\text{cdw}}$  and for the D-Hyd at pH 7, no induction and 3 % EtOH with 51.6  $\mu\text{U}/\text{mg}_{\text{cdw}}$ . D-Hyd cultures that have not been induced show a significant decrease in specific activity for every culture conditions, while the specific activities for non-induced D-Hyd(co) cultures show only slightly decreased values compared to the induced ones. This result is not obtained for the D-Hyd(co) at pH 6 with 3 % EtOH, in which the non-induced culture show an increased specific activity. D-Hyd cultures containing EtOH exhibit decreased specific activities except for the D-Hyd at pH 7 with 1 mM IPTG. This is in contrast to the determined specific activities of the D-Hyd(co), which result in higher values when adding 3 % EtOH to the culture media, except for the cultivation setup at pH 6 with induction. When regarding the cultivations at different pH values, induced D-Hyd cultures show higher specific activities at pH 6, while non-induced cultures show higher specific activities at pH 7. For the D-Hyd(co), cultivation at pH 6 mostly results in higher specific activities than at pH 7, except for the cultivation at pH 7 with induction and 3 % EtOH that results in the highest specific activity of all investigated setups.

Since it was shown, that the specific activities for the D-Hyd(co) are in every case higher than that of the D-Hyd, it was suggested that the codon-optimization was successful and not only caused higher protein expression due to adopted codon-usage, but led also to a higher amount of native hydantoinase with an up to four times higher specific activity than the not optimized hydantoinase. This is in accordance to the results after expression under oxygen deficiency (see Chapter 4.3.1.2) and was also already reported before.<sup>[187]</sup> Cultivation without induction was also investigated for both enzymes, since the applied T7-promoter was reported to show a high basal activity caused by leaky expression of the T7-RNA-polymerase which initiates expression of the heterologous gene even at very low concentrations.<sup>[188–190]</sup> This was verified by the above discussed results, because every induced as well as non-induced culture showed activity of the particular recombinantly expressed hydantoinase.

The D-Hyd of non-induced cultures showed a significant decrease in specific activities compared to that of induced cultures, while for the D-Hyd(co) of non-induced cultures only a slight decrease specific activity was observed. This difference was also caused by codon-optimization. Due to the optimized codon bias of the D-Hyd(co) for *E. coli*, basal activity of the T7-promoter in non-induced cultures was already sufficient to produce a high amount of native target molecule. In contrast, for the non-optimized D-Hyd induction is necessary to compensate the low consistency in codon-usage of *E. coli* and *A. crystallopoietes*.

Another difference concerning the specific activities of both investigated hydantoinases was observed with the addition of 3 % EtOH to the cultivation media. The tendency of decreasing specific activity for the D-Hyd when cultured with EtOH, is due to the general low expression level for this not codon-optimized hydantoinase. Since the maximum growth rate for all D-Hyd cultures containing EtOH is significantly reduced (see Figure 32), the low expression rate without the addition of EtOH was

reduced once more resulting in low concentrations of active hydantoinase. This observation was contrary for the D-Hyd(co) cultured with 3 % EtOH in the cultivation media, which showed higher specific activities than the D-Hyd(co) that had been cultured without EtOH. According to Thomas et al., the exposure to physical stress like the addition of EtOH indirectly induces the expression of chaperones that assist in the correct folding of the target molecule.<sup>[144]</sup> Only the cultivation setup at pH 6 with induction shows a decrease in specific activity, which is probably resulting from the physical and metabolic stress at these conditions, leading to a decrease in expression of soluble D-Hyd(co).

The last investigated parameter was the cultivation and induction at different pH values, on the one hand to cause chemical stress for indirect induction of chaperones and on the other hand to maybe prevent degradation of the target protein by proteases at a lower pH value.<sup>[144,186]</sup> The fact that the specific activity of the D-Hyd cultured at the lower pH of 6 only increased for the induced cultures, while for the non-induced cultures a lower pH resulted in a decrease in specific activity of the D-Hyd, is also resulting from the generally low expression rate for the hydantoinase without codon-optimization. The latter is even lower for cultivations at pH 6 which exhibit a maximum growth rate that is reduced about 50 %, since a decreased maximum growth rate leads to a decreased expression rate. This theory was supported by the determined specific activities of the D-Hyd(co), which by trend show higher specific activities at pH 6. The exception represents the cultivation setup at pH 7 with induction and 3 % EtOH with the highest specific activity of all investigated setups. This suggests that combining both parameters causing chemical stress affected the proliferation as well as protein expression so much that potentially improved folding of the target molecule carried no weight. Additionally, it was assumed that the addition of EtOH has a greater influence on protein expression and folding than the cultivation at pH 6.

When comparing maximum growth rates and specific activities, it was shown that the theory of a more correct protein folding at lower maximum growth rates and therefore lower expression rates,<sup>[181]</sup> was only consistent for the codon-optimized hydantoinase D-Hyd(co), which generally exhibits higher expression levels. For the D-Hyd, lower maximum growth rates resulted in even more reduced expression levels and therefore decreased specific activities.

For a qualitative analysis of the investigated hydantoinases after cultivation and induction at various conditions, SDS-PAGE was conducted for every soluble and insoluble fraction after cell disruption and centrifugation (Figure 31).

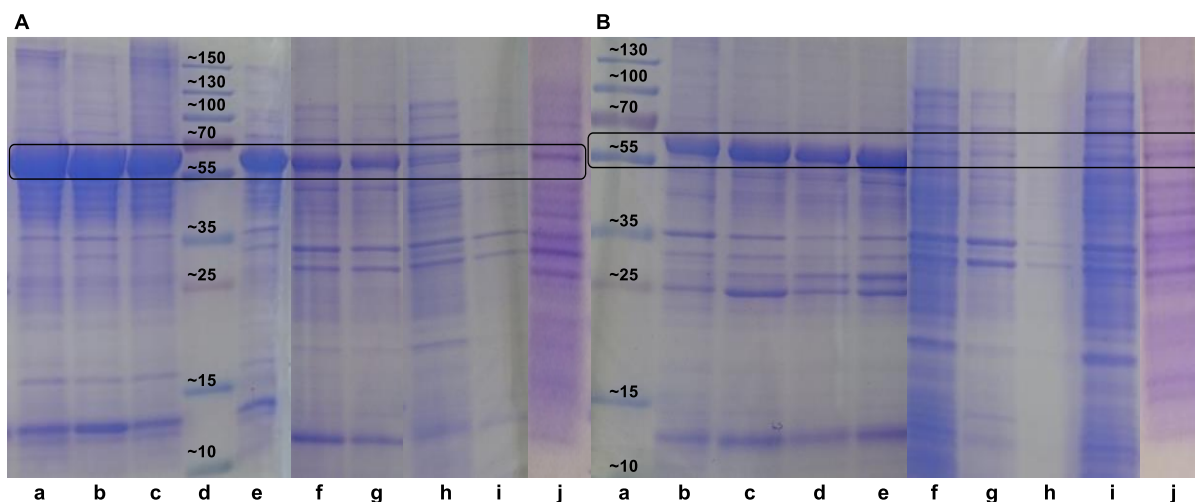


**Figure 31** SDS-PAGE of the cultures of *E. coli* BL21DE3 hosting the recombinant hydantoinases D-Hyd(co) and D-Hyd from *A. crystallopoietes* DSM 20117 after high throughput screening for cultivation conditions and subsequent cell disruption. **A** D-Hyd(co) insoluble fraction **a** +IPTG -EtOH pH 7 **b** +IPTG -EtOH pH 6 **c** +IPTG +EtOH pH 7 **d** protein standard with molecular weights in kDa, **e** +IPTG +EtOH pH 6 **f** -IPTG -EtOH pH 7 **g** -IPTG -EtOH pH 6 **h** -IPTG +EtOH pH 7 **i** -IPTG +EtOH pH 6 **j** soluble fraction **B** D-Hyd insoluble fraction **a** protein standard with molecular weights in kDa, **b** +IPTG -EtOH pH 7 **c** +IPTG -EtOH pH 6 **d** +IPTG +EtOH pH 7 **e** +IPTG +EtOH pH 6 **f** -IPTG -EtOH pH 7 **g** -IPTG -EtOH pH 6 **h** -IPTG +EtOH pH 7 **i** -IPTG +EtOH pH 6 **j** soluble fraction

In Figure 31 A, insoluble fractions of the d-Hyd(co) are shown (lane **a-i**), while Figure 31 B shows insoluble fractions of the d-Hyd (lane **a-i**). Since the soluble fractions from different cultures resulted in the same band pattern and intensity for both enzymes, lane **j** shows exemplarily the soluble fraction of the cultivation at pH 7, 1 mM IPTG and 3 % EtOH in each case. Comparing the insoluble fractions of the d-Hyd and d-Hyd(co) cultures, the latter exhibit generally bands with higher intensity at 52 kDa respectively 56 kDa for every investigated cultivation and induction setup. For the induced d-Hyd(co) cultures, the intensity of this band decreases with decreasing pH. The same cultures containing 3 % EtOH have also smaller bands for the d-Hyd(co) than the cultures without EtOH. In contrast, the induced d-Hyd cultures show no difference in intensity for the bands at 52 kDa in the insoluble fractions. The non-induced d-Hyd(co) cultures show much less intensive bands than the induced ones. By comparing the soluble fractions (band **j**) of the d-Hyd(co) with that of the d-Hyd cultures, the latter show a less intensive band for the hydantoinase in every case. The intensity of this band is generally very low for both enzymes and every cultivation setup and it does not stand out from the background pattern of randomly stained proteins.

As already discussed before, protein concentrations of the insoluble fractions were not defineable by photometric assays and therefore, the pellets were diluted according to the culture volume. Since the final  $OD_{600}$  values of the induced D-Hyd(co) cultures decrease from line **a** to line **e** from 15.18 to 9.26 (Figure 31 A), the reduced intensity of the bands at 56 kDa for the hydantoinase are not caused by a lower concentration of inclusion bodies, but by lower  $OD_{600}$  values at the time of harvesting. The same applies to the non-induced cultures expressing D-Hyd(co) (Figure 31 A, lane **f-i**), since cultures containing EtOH resulted in lower final  $OD_{600}$  values and also show bands with lower intensity than cultures without EtOH. Nevertheless, compared to the induced cultures expressing D-Hyd(co), much less inclusion bodies were detected although their final  $OD_{600}$  values were higher. This indicates that

the basal activity of the T7-promoter was sufficient for the expression of D-Hyd(co) and additionally, the decreased expression rates resulted in improved folding of the target molecule.<sup>[186]</sup> However, when comparing the specific activities of induced and non-induced cultures, the non-induced cultures mostly exhibit lower values. This points out, that the lower concentration of inclusion bodies simply results from lower expression rates of the D-Hyd(co) instead of improved protein folding.

The same conclusions apply to the SDS-PAGE of induced and non-induced D-Hyd cultures. Additionally it was observed that the intensity of the hydantoinase bands for of every insoluble fraction of the D-Hyd culture are less intensive than hydantoinase bands of the D-Hyd(co) cultures, which can result on the one hand from lower final OD<sub>600</sub> values and on the other hand from lower expression levels of the not codon-optimized enzyme. Referring to the soluble fractions of every cultivation setup, for both enzymes no differences in the pattern or intensity of the bands were noticeable, which is why for each enzyme only one setup is shown (Figure 31 A and B, lanes j). Consequently, when considering only SDS-PAGE analysis, no significant improvement in soluble hydantoinase expression was achieved by investigating different cultivation conditions. Though, it has to be considered that SDS-PAGE is mainly a qualitative analysis method. Besides, increased specific activities for several cultivation setups demonstrated an improvement in soluble hydantoinase expression. Nevertheless, two important conclusions can be drawn due to SDS-PAGE analysis: On the one hand, a more intensive hydantoinase band for D-Hyd(co) compared to the D-Hyd suggests an increased amount of native hydantoinase for the codon-optimized version, which verifies the above discussed results. On the other hand, it is noticeable that the major part of expressed hydantoinase occurs as inclusion bodies for both enzymes and every tested cultivation setup. Consequently, although the specific activity of both enzymes was improved successfully by indirect induction of chaperones or decelerated proliferation and expression rates, a further improvement of soluble expression was considered possible.

As already mentioned before, next to indirect chaperone induction, the coexpression of the target molecule and chaperones was reported to increase soluble protein expression markedly.<sup>[144,191]</sup> Therefore, the coexpression of the hydantoinase and five different chaperone sets from Takara Bio Inc. were investigated.

Since the D-Hyd(co) showed higher specific activities in every investigation discussed above, only this hydantoinase was used for further experiments. Additionally, the cultivation at pH 6 was left out, since it did not result in explicit improvement of the specific activities. Nevertheless, investigating the cultivation with or without EtOH, with or without induction and coexpression of five chaperone sets resulted in 20 cultivation setups, which were carried out each for three times in triplicates. Figure 32 shows the OD<sub>600</sub> values as well as maximum growth rates during the cultivation of *E. coli* BL21DE3 coexpressing the codon-optimized hydantoinase from *A. crystallopoietes* DSM20117 and five different chaperone sets.

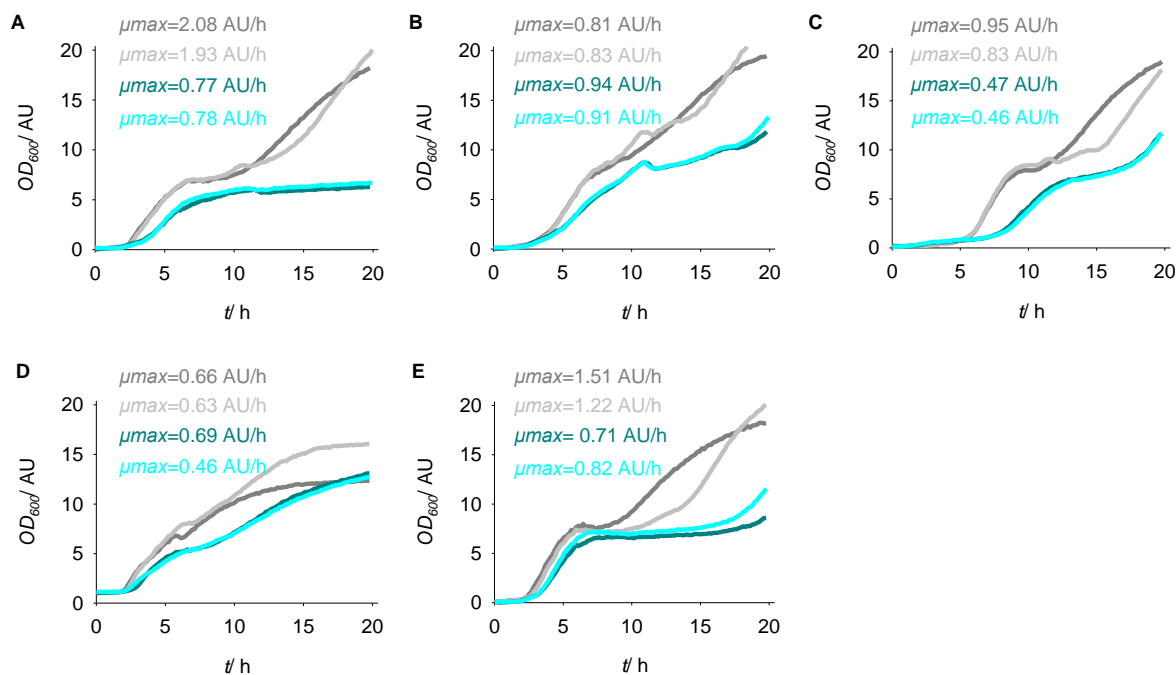


**Figure 32** High throughput screening for the cultivation of *E. coli* BL21DE3 coexpressing the recombinant hydantoinase D-Hyd(co) from *A. crystallopoietes* DSM 20117 and different chaperones. **A** Growth curves and maximum growth rates under different cultivation conditions coexpressing C1 **B** Growth curves under different cultivation conditions coexpressing C2 **C** Growth curves under different cultivation conditions coexpressing C3 **D** Growth curves under different cultivation conditions coexpressing C4. **E** Growth curves under different cultivation conditions coexpressing C5. Legend: -EtOH +IPTG (dark grey), -EtOH -IPTG (grey), +EtOH +IPTG (dark cyan), +EtOH -IPTG (cyan). Cultivations were each carried out for three times in triplicates, shown are the mean values.

When culturing *E. coli* BL21DE3 coexpressing the D-Hyd(co) and five different chaperone sets, the final OD<sub>600</sub> values of the non-induced cultures are mostly higher compared to the induced ones. Comparing cultivations with and without 3 % EtOH in the culture media, the cultures without EtOH result in much higher OD<sub>600</sub> values at the time of harvesting, except for the cultivations coexpressing the D-Hyd(co) and C4 there is no distinct tendency noticeable. In general, the coexpression of D-Hyd(co) with C2 showed the highest final OD<sub>600</sub> values for nearly every cultivation. Concerning the maximum growth rates, induced and non-induced cultures show no clear trend, but non-induced cultures either have lower maximum growth rates than the induced ones or the maximum growth rates are nearly the same. Maximum growth rates of the cultures with EtOH mostly show lower maximum growth rates than the cultures containing no EtOH in the culture medium, but for the coexpression of the D-Hyd(co) with C2 it is vice versa. Additionally it is conspicuous that the growth curves of C1, C3 and C5 exhibit partially two exponential growth phases, while the remaining two chaperone sets show only one exponential growth phase. The difference in final OD<sub>600</sub> values between induced non-induced cultures was not as clear and significant as observed for the cultivations without additional expression of chaperones. The same applies to the maximum growth rates for all investigated culture conditions. This is probably an indication for the fact that the induction of D-Hyd(co) expression was not as successful as the cultivations without chaperones, since the proliferation was not decelerated by protein expression. Additionally, the fact that there is no distinct difference between the OD<sub>600</sub> values

of cultivations coexpressing chaperones and the cultivations without chaperones supports this theory, since it was reported that coexpression of chaperones inhibits bacterial growth for some extent.<sup>[192–194]</sup> Blum et al. demonstrated that the coexpression of the target protein with the major cytosolic *E.coli* chaperone dnaK and its cochaperone dnaJ, included in C1 and C3, was bacteriocidal for cultures which were allowed to enter the stationary phase.<sup>[194]</sup> Reduced OD<sub>600</sub> values for cultivations with 3 % EtOH in the culture media result from additional physical stress and therefore also lower maximum growth rates. The fact that cultivations with coexpression of D-Hyd(co) and C2 show comparatively high final OD<sub>600</sub> values suggests that this combination will lead to low specific activities of the D-Hyd(co), since investigations without chaperones revealed the highest specific activities for comparatively low OD<sub>600</sub> values at the time of harvesting.

For investigating the availability of native D-Hyd(co) after cultivation and induction at different conditions for the coexpression of D-Hyd(co) and five different chaperone sets, whole cell biotransformations with PheHyd were conducted. The determined specific activities for every coexpression as well as cultivation setup are illustrated in Figure 33 in 3D bar plots.

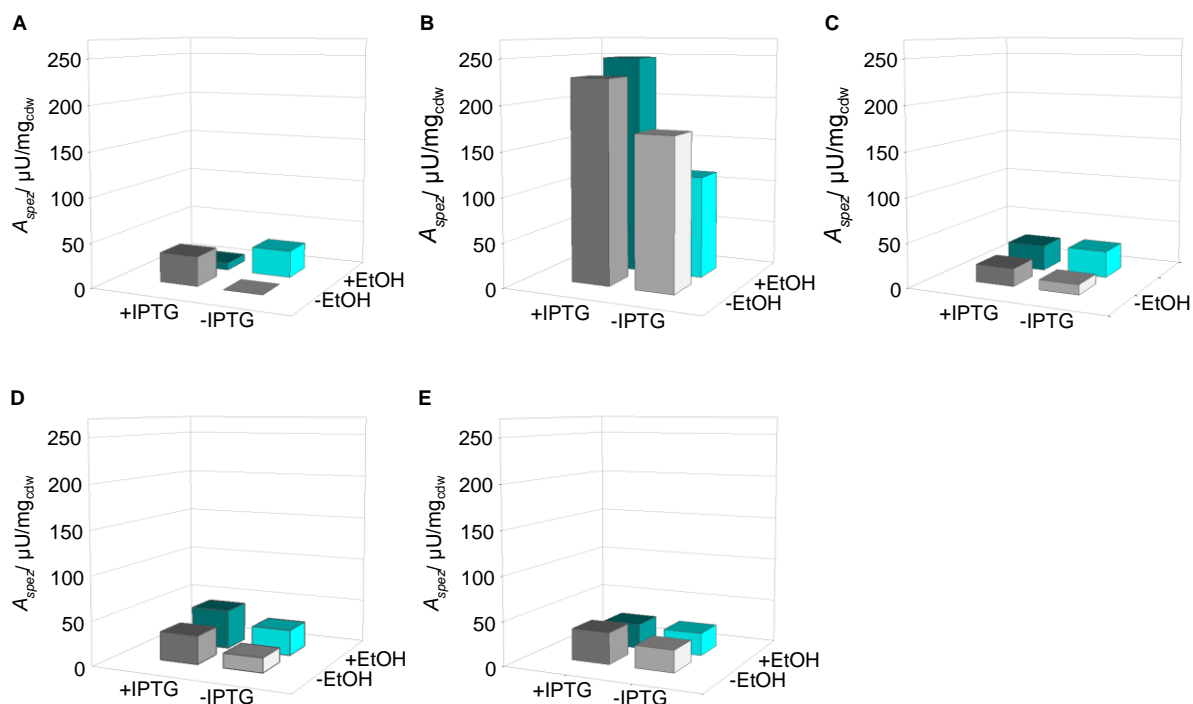


**Figure 33** High throughput screening for the cultivation of *E. coli* BL21DE3 coexpressing the recombinant hydantoinase D-Hyd(co) from *A. crystallopoietes* DSM 20117 and different chaperones. **A** C1 **B** C2 **C** C3 **D** C4 **E** C5. Specific activities after whole cell biotransformation with 2 mM PheHyd after cultivation and induction under different conditions. Reactions and measurements were carried out in triplicates, shown are the mean values. Legend: -EtOH +IPTG (dark grey), -EtOH -IPTG (grey), +EtOH +IPTG (dark cyan), +EtOH -IPTG (cyan)

Regarding the results of the activity assays, it is noticeable that coexpression of D-Hyd(co) with various chaperones generally resulted in low specific enzyme activities, ranging from 0.00  $\mu\text{U}/\text{mg}_{cdw}$  to 44.55  $\mu\text{U}/\text{mg}_{cdw}$ . Solely the coexpression of D-Hyd(co) with the chaperone set C2 (groES, groEL) is resulting in higher specific activities of from 114.58  $\mu\text{U}/\text{mg}_{cdw}$  to 248.02  $\mu\text{U}/\text{mg}_{cdw}$ . Due to the very low specific activities for coexpression of D-Hyd(co) with the chaperone sets C1, C3, C4 and C5, no

distinct tendency for specific enzyme activities was noticeable. However, for the chaperone set C2, the highest specific activity was achieved for the cultivation with induction and addition of 3 % EtOH to the culture media, while the lowest specific activity was determined for the same cultivation setup without induction.

In contrast to the cultivation and expression without chaperones, these experiments showed that cultivations with higher  $OD_{600}$  values resulted in higher specific activities, while there was no tendency observable between maximum growth rates and specific activities. This is consistent with previous investigations, which reported a negative effect of the chaperones *dnaK* and *tig* on the growth rate.<sup>[194,195]</sup> Consequently, when bacterial growth is strongly inhibited, the expression rate is decreased as well and not enough soluble hydantoinase is obtained for high specific activities. In general, only the chaperone set C2 showed adequate specific enzyme activities, while every other chaperone set resulted in very low specific activities. Though, even the chaperone set C2 with the best results concerning specific activities is only half as active as the D-Hyd(co) without coexpression of chaperones with same cultivation conditions (see Figure 30). Nevertheless, both experiments showed the same tendency concerning the best cultivation setup, which was the cultivation at pH 7 with induction and with 3 % EtOH in every case. The phenomenon of two exponential growth phases shows no distinct tendency concerning the resulting specific enzyme activity, but the cultivations with this phenomenon turned out to result in rather low specific activities for D-Hyd(co).

For qualitative analysis of hydantoinase expression, SDS-PAGE analysis was carried out after cultivating at different conditions and coexpression of the D-Hyd(co) with different chaperones. Figure 34 shows the SDS-PAGE analysis of the insoluble (A-D) as well as soluble (E-H) fractions after cell disruption and centrifugation.



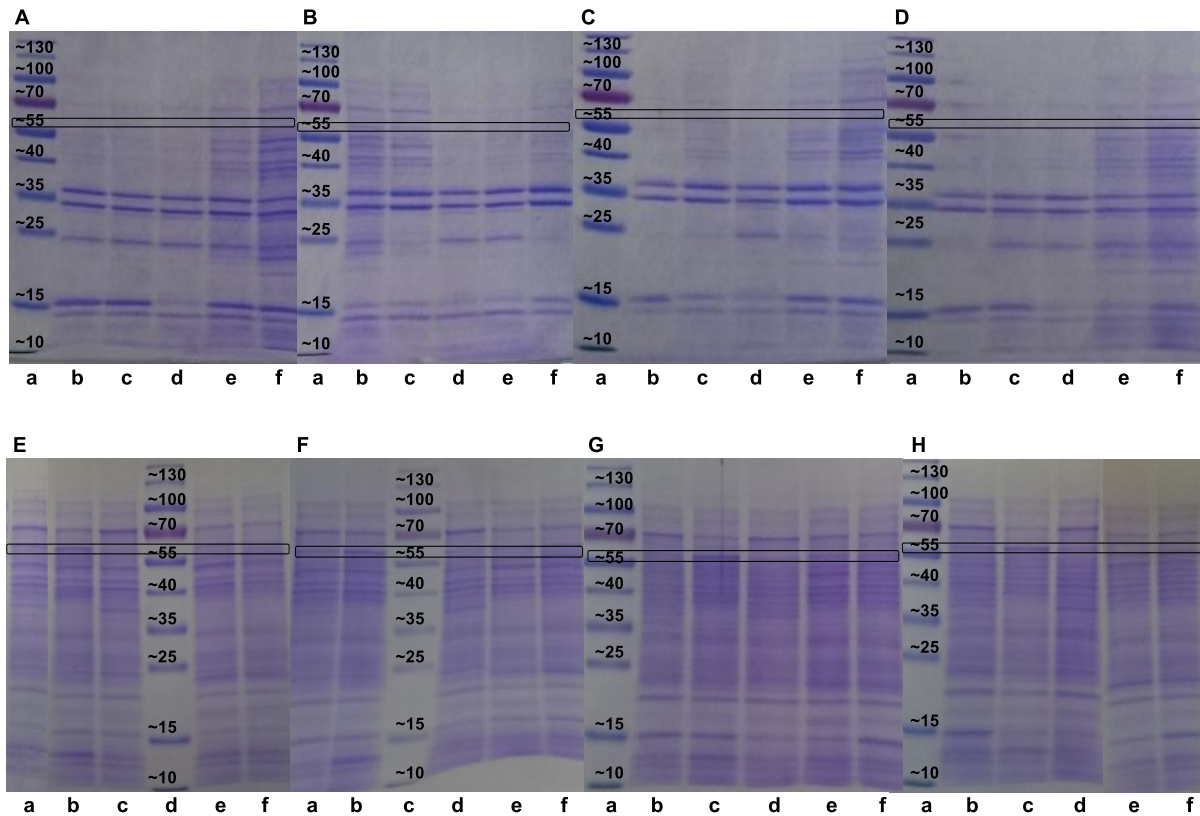


**Figure 34** SDS-PAGE of the cultures of *E. coli* BL21DE3 coexpressing the recombinant hydantoinase D-Hyd(co) from *A. crystallopoietes* DSM 20117 and different chaperones after high throughput screening for cultivation conditions and subsequent cell disruption. **A** Insoluble fraction -EtOH +IPTG **a** protein standard with molecular weights in kDa **b** C1 **c** C2 **d** C3 **e** C4 **f** C5 **B** Insoluble fraction -EtOH -IPTG **a** protein standard with molecular weights in kDa, **b** C1 **c** C2 **d** C3 **e** C4 **f** C5 **C** Insoluble fraction +EtOH +IPTG **a** protein standard with molecular weights in kDa, **b** C1 **c** C2 **d** C3 **e** C4 **f** C5 **D** Insoluble fraction +EtOH -IPTG **a** protein standard with molecular weights in kDa, **b** C1 **c** C2 **d** C3 **e** C4 **f** C5 **E** Soluble fraction -EtOH +IPTG **a** C1 **b** C2 **c** C3 **d** protein standard with molecular weights in kDa **e** C4 **f** C5 **F** Soluble fraction -EtOH -IPTG **a** C1 **b** C2 **c** protein standard with molecular weights in kDa **d** C3 **e** C4 **f** C5 **G** Soluble fraction +EtOH +IPTG **a** protein standard with molecular weights in kDa, **b** C1 **c** C2 **d** C3 **e** C4 **f** C5 **H** Soluble fraction +EtOH -IPTG **a** protein standard with molecular weights in kDa, **b** C1 **c** C2 **d** C3 **e** C4 **f** C5

While none of the investigated insoluble fractions (A-D) contains a band for the D-Hyd(co) at 56 kDa, a lot of other distinct bands with varying intensities are visible around 10 kDa, 14 kDa, 15 kDa, 24 kDa, 34 kDa and in some samples also around 70 kDa. Additionally, a randomly stained protein pattern with different intensities is present. The soluble fractions (E-H) generally show a stronger pattern of randomly stained proteins. Furthermore, every sample of the coexpression of D-Hyd(co) and C2 shows a band for the D-Hyd(co) at 56 kDa. Additionally, bands around 10 kDa, 13 kDa, 15 kDa, 20 kDa, 40 kDa, 54 kDa and 70 kDa with varying intensities, whereat their intensity is generally lower than for the insoluble fractions.

Regarding the SDS-PAGE analysis of the insoluble fractions, it is noticeable that no band for the D-Hyd(co) was detected, suggesting that no inclusion bodies were formed and the soluble expression of the enzyme was remarkably improved. However, since the soluble fractions did also not show any distinct hydantoinase band, this assumption was proved wrong. This is in accordance with the determined specific activities of the differently treated cultures, which were comparably low. The only

exception is the coexpression of the D-Hyd(co) and the chaperone set C2 that showed a band for the D-Hyd(co) in every analyzed soluble fraction. Since every culture coexpressing the D-Hyd(co) and the chaperone set C2 showed much higher specific activity than cultures coexpressing the D-Hyd(co) and other chaperone sets, this is also in accordance with previous experiments. Though, concerning the experiments without coexpressed chaperones with these results, these specific activities are comparatively low. One reason for this may be the low amount of soluble chaperones compared to the insoluble ones, which are not functional. To get a better overview, the different chaperone sets with corresponding chaperones and molecular weights are listed in Table 8. However, according to Takara Bio Inc., it has to be taken into account that individual chaperones molecular weights result in differing molecular weights in an actual gel image.

**Table 8** Applied chaperone sets, corresponding chaperones and molecular weights

<b>Term</b>	<b>Chaperones (molecular weight)</b>
C1	dnaK (~70 kDa) – dnaJ (~40 kDa) – grpE (~22 kDa) groES (~10 kDa) – groEL (~60 kDa)
C2	groES (~10 kDa) – groEL (~60 kDa)
C3	dnaK (~70 kDa) – dnaJ (~40 kDa) - grpE (~22 kDa)
C4	groES (~10 kDa) - groEL (~60 kDa) - tig (~56 kDa)
C5	tig (~56 kDa)

Despite the occurrence of insoluble chaperones, also soluble and functional chaperones were expressed. The fact that determined specific activities were very low anyway, is probably caused by negative side effects of chaperone coexpression. It was reported that the latter eventually results in undesirable side effects regarding protein yield and quality.<sup>[196]</sup> The chaperone dnaK for example is often used in coexpression approaches together with its co-chaperone dnaJ and their nucleotide exchange factor grpE, since it is amongst others involved in protein disaggregation as well as folding and refolding of misfolded proteins.<sup>[144,197]</sup> Although this system had been applied successfully in many cases and even for hydantoinases,<sup>[191]</sup> it has not been successful in every case, since often solubility was increased to the disadvantage of protein yield.<sup>[145,198]</sup> On the one hand, this was explained by the inhibition of cell growth, and on the other hand the decreased protein yield can be explained by proteolysis of the recombinant protein.<sup>[192,199]</sup> In detail, dnaK was reported to participate in the degradation of aggregation-prone but functional polypeptides by targeting them to proteases.<sup>[200,201]</sup> Additionally, the absence of dnaK resulted in a higher proteolytic resistance and therefore also higher half-life of the target molecules.<sup>[202]</sup> These findings may explain the fact that in this case, no insoluble hydantoinase as well as almost no soluble hydantoinase was detectable. Furthermore, dnaK was shown to be a negative regulator for heat shock response, which means in detail that concentrations of dnaK above physiological levels results in the down-regulation of other chaperones. This is also

consistent with the above shown results, since every sample of coexpressed C2 exhibited a distinct band at around 70 kDa for dnaK, but no comparable band for the other coexpressed chaperones.

The chaperones groEL and groES have been applied in this work as well, since they were reported to improve the solubility of proteins with remarkable success.<sup>[182,203]</sup> However, further investigations revealed no impact of these chaperones or even a decreased amount of the target molecule, since large proteins were not able to enter the cavity formed by groEL. The preferred molecular mass range of this chaperone was found to be 10-60 kDa.<sup>[204,205]</sup> Since expressed target molecule in this work has a molecular weight of 56 kDa and is therefore located in the outer threshold of the substrate range, groEL eventually did not accept the D-Hyd(co) as a substrate and consequently no improvement was achieved. Furthermore, groEL was not only reported to prevent protein aggregation, but also to play a role in enhancing proteolytic degradation.<sup>[206-208]</sup> As for dnaK, this is probably the reason for less detected inclusion bodies on the one hand and less soluble hydantoinase on the other hand.

To conclude this chapter, by codon-optimizing the recombinant hydantoinase from *A. crystallopoietes* DSM 20117 an increased expression level was obtained and moreover, the specific activities for this enzyme were improved. Further investigations of different expression conditions by high throughput screenings using the BioLector® revealed that the addition of EtOH to the culture media improves soluble hydantoinase expression by causing physical stress and indirect induction of chaperones. Cultivation and induction at pH 6 instead of pH7 had an influence on growth and expression, but did not show a distinct improvement for soluble hydantoinase expression or enzyme activities. Additionally it was shown that the basic activity of the T7-promoter is sufficient for hydantoinase expression, but experiments without induction resulted in less inclusion body formation. However, the investigated enzymes of non-induced cultures by trend showed lower specific activities than the enzymes from induced cultures. The coexpression of the codon-optimized hydantoinase and different chaperone sets did not result in further improvement of soluble expression or specific activity, potential reasons have been discussed above.

#### 4.3.1.4 SCALE-UP OF OPTIMIZED EXPRESSION CONDITIONS

An optimal cultivation and expression system is characterized by an efficient protein biosynthesis, high specific activities of the target enzyme, but also by high proliferation rates resulting in a good yield of the target molecule after short cultivation times. As discussed above, all these parameters mutually influence each other and since high proliferation and expression rates are not always of advantage for the synthesis of correctly folded proteins, a balanced compromise between all these parameters has to be found. To fulfill these requirements, a high throughput screening for optimized expression conditions was conducted. On the one hand, causing physical stress for indirect induction of chaperones was tested by cultivation under oxygen deficiency, addition of EtOH to the culture media as well as cultivation at a lower pH. Furthermore, the basic activity of the T7-promoter was

investigated and the approach of coexpressing the hydantoinase with different chaperone sets was pursued.

Since the codon-optimized D-Hyd(co) showed higher expression rates and specific activities despite higher final  $OD_{600}$  values than the D-Hyd, it was pointed out that the codon-optimization was successful in every respect. Furthermore, it was shown that cultivation under oxygen deficiency on the one hand improved soluble hydantoinase expression as well as specific activities, but on the other hand this physical stress resulted in the lowest growth rates of all investigated cultivation setups. Since this is an important factor concerning protein yield as well as cost effectiveness and the determined specific activities were still lower than other cultivation setups, the cultivation under hypoxia was out of the question for the scale-up. Other examined physical stress factors like induction, lower pH values or the addition of EtOH to the culture media did not result in equally low final  $OD_{600}$  values. Although induced cultures trended to result in lower final  $OD_{600}$  values, this drawback was mostly balanced by higher specific activities than enzymes produced from non-induced cultures. While upon lowering the pH in the culture media from 7 to 6, no distinct improvement in enzyme activities was achieved, the addition of 3 % EtOH to the culture media was advantageous for the expression of soluble D-Hyd(co). In this case, the reduction of final  $OD_{600}$  values was balanced by considerably higher specific activities, too. Consequently, for scaling up the culture volume, the cultivation setup at pH 7, induction with 1 mM IPTG and with addition of 3 % EtOH was used for the D-Hyd(co).

Since this cultivation setup was investigated for a 1 mL culture in a 48-well flowerplate at 600 rpm shaking frequency and 37 °C, it needed to be scaled up by keeping the oxygen transfer rate constant. Baumann et al. reported that 1 mL filling volume at 600 rpm in a flower plate corresponds to a  $kL_a$  value of  $88.9 \text{ h}^{-1}$ . For a 2.5 L baffled Tunair shake flask with 800 mL filling volume, they determined a incubator shaking speed of 180 rpm for equivalent oxygen uptake.<sup>[181]</sup> In this work, 1 L baffled shaking flasks were used, where a filling volume of 200 mL and a shaking speed of 120 rpm ought to result in an equivalent oxygen transfer rate.

In order to verify this, cultivation at the above mentioned conditions was conducted. The only difference was a cultivation period of 24 h instead of 20 h to achieve a higher yield and to take better advantage of the supplied nutrients. After cultivation and induction, a final  $OD_{600}$  value of 9.30 was achieved and whole cell biotransformation with 2 mM PheHyd as a substrate resulted in a specific activity of  $304.0 \text{ } \mu\text{U}/\text{mg}_{\text{cdw}}$ . The values for 1 mL culture volume in a flower plate at 600 rpm were an  $OD_{600}$  of 11.94 and a specific activity of  $440.7 \text{ } \mu\text{U}/\text{mg}_{\text{cdw}}$ . Considering the altering conditions comparing a microcultivation of 1 mL with an upscale to 200 mL culture volume, the slight decrease of final  $OD_{600}$  as well as specific activity is acceptable. Based on these experiments, this cultivation setup was used for every further investigation concerning the purification as well as immobilization of the codon-optimized hydantoinase from *A. crystallopoietes* DSM 20117.

### 4.3.2 PURIFICATION OF ENZYMES VIA NI SEPHAROSE BEADS

To date, the Hydantoinase Process is mainly conducted via whole cell biocatalysis in industries, since this is a simple and cheap method to produce biocatalysts as well as to remove them after the reaction. Nevertheless, there are also some drawbacks concerning the use of whole cell biocatalysts, as transport barriers for the substrate as well as for the product and unknown degradation processes inside the cells. Consequently, a trend toward cell-free reaction systems using isolated enzymes was noticeable lately. The next chapters handle the isolation as well as immobilization of both enzymes for the Hydantoinase Process to avoid these drawbacks.

#### 4.3.2.1 PRELIMINARY TESTS

After optimizing the cultivation and expression conditions for the target enzymes, the next important step toward cell-free reaction systems is their purification. Since many parameters need to be investigated depending on requirements of the particular enzyme, in this work instead of IMAC purification via chromatography column, batch experiments applying Ni sepharose beads were carried out. The latter allow parallel performance of different purification setups as well as simple and fast handling.

Every activity assay for investigation of the hydantoinase was carried out with 5 mM PheHyd as a substrate, while activity assays for investigation of the carbamoylase were carried out with 5 mM NCPheAla as a substrate. Furthermore, stability of the hydantoinase in crude cell extract was examined and it was shown, that the activity was reduced by 70 % after one cycle of freezing with liquid N<sub>2</sub> and storage at -20 °C overnight. Since the carbamoylase is reported to be even more instable, both enzymes were prepared freshly and used immediately.

The standard protocol from GE Healthcare for the purification of enzymes via Ni sepharose beads recommends an incubation of these beads with the crude cell extract for 30 min at 4 °C followed by two washing steps with wash- and binding buffer and a 5 min elution step with elution buffer. In this work, this method was investigated for the hydantoinase form *A. crystallopoietes* DSM 20117 and additionally a modified protocol with an 1 h incubation of crude extract with Ni sepharose beads and three washing steps instead of two. The elution was divided in two steps, whereat the first was carried out using 25 % v/v elution buffer (125 mM imidazole) and the second step was conducted using 100 % v/v elution buffer (500 mM imidazole). Additionally, the incubation time with elution buffers was increased from 5 min to 15 min. To check the suitability of these two purification protocols, firstly qualitative analysis by SDS-PAGE was conducted (Figure 35).

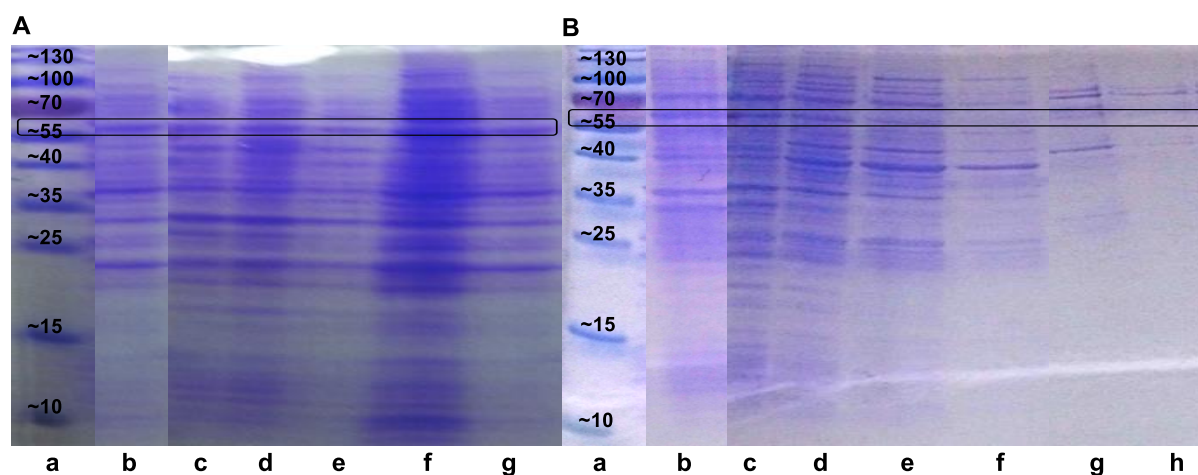


**Figure 35** SDS-PAGE analysis of every fraction after purification of the hydantoinase from *A. crystallopoietes* DSM 20117 **A** Purification using the standard protocol from GE Healthcare for Ni sepharose beads **a** protein standard with molecular weights in kDa **b** crude extract **c** wash 1 **d** wash 2 **e** wash 3 **f** eluate 1 **g** eluate 2 **B** Purification using an optimized protocol for Ni sepharose Beads **a** protein standard with molecular weights in kDa **b** crude extract **c** wash 1 **d** wash 2 **e** wash 3 **f** wash 4 **g** eluate 1 **h** eluate 2.

Figure 35 A shows SDS-PAGE analysis of the resulting fractions after conducting the recommended protocol from GE Healthcare. It is noticeable that every investigated fraction shows nearly the same band pattern, only the elution fraction (lane **f**) has bands of higher intensity. In detail, a strong background band pattern of randomly stained proteins is apparent in every fraction. Additionally, a specific band for the hydantoinase (Hyd(co)) with a molecular weight of around 56 kDa is visible with the same intensity as the randomly stained proteins. Examination of the resulting fractions from the modified protocol (Figure 35 B) again shows the same band pattern and with same intensities as revealed for the standard protocol for the crude extract (lane **b**), wash 1 (lane **c**) and wash 2 (lane **d**). In contrast to the other protocol, the fraction wash 3 (lane **e**) shows a band pattern with less intensity as well as less non-specific bands. In addition, the band at 56 kDa for the hydantoinase in wash 3 is smaller than for the same fraction of the standard protocol. Wash 4 (lane **f**) exhibits the same band pattern as wash 3, but comparatively more slightly. The same applies to the hydantoinase band at 56 kDa in this fraction. In contrast, eluate 1 (lane **g**) exhibits less non-specific stained proteins and the hydantoinase band at 56 kDa is more distinct. Eluate 2 (lane **h**) shows even less randomly stained proteins and the hydantoinase band is very slightly.

Qualitative SDS-PAGE analysis after purification of the hydantoinase according to the standard protocol revealed that the last washing step, wash 3 showed the same band patterns as the crude extract, wash 1 (crude extract after removal of the Ni sepharose beads) and wash 2. This observation and the fact that only a slight decrease in band intensities was monitored in the last washing step compared to the other washing steps suggest, that the Ni sepharose beads still bore not bound protein from the crude extract as well as non-specific bound proteins although 20 mM imidazole was added to the wash- and binding buffer to avoid the latter. Additionally, the hydantoinase band in every washing step proved that not the whole amount of the target molecule was bound by metal ion affinity. Investigation of the first elution fraction with 100 % elution buffer confirmed this assumption, since it

had the same band pattern as the other fractions, but its intensity was much higher. Therefore, many non-specifically bound proteins had been eluted together with the hydantoinase at 56 kDa and the purification was not efficient. The second elution fraction also contained many non-specific proteins and a band for the hydantoinase. These results showed that more washing steps are essential to remove non-specifically bound proteins and consequently to prevent contamination of the purified hydantoinase. Remaining hydantoinase in the washing fractions indicated that a longer incubation time of the crude extract with the Ni sepharose beads may be required. Furthermore, since the second elution fraction still showed many contamination bands as well as a clear band for the hydantoinase, presumably the elution steps were not sufficient. Therefore, a modified protocol with a longer incubation time, more washing steps and a modified elution setup was investigated. This modified protocol revealed improvements for the purification process, since the fraction wash 3 already exhibited a slighter band intensity for the hydantoinase compared to wash 2 as well as compared to the same fraction from the not modified protocol. This is probably due to the longer incubation time of the crude extract with Ni sepharose beads, allowing the target molecule to bind to the carrier more efficiently. The fraction of the last washing step, wash 4 showed even lower intensities for bands of non-specifically bound proteins as well as a very slight band for the hydantoinase, indicating that nearly every non-specifically bound protein was eluted which allows a more efficient purification. When looking at the first eluate, this assumption was verified, since this elution fraction contained much less bands for non-specific proteins than the first elution of the standard protocol. Nevertheless, the band for the hydantoinase was very small in the first and even smaller in the second eluate, which is explainable by the comparatively low concentration of soluble hydantoinase in the crude cell extract.

In addition to this qualitative analysis, a quantification of the protein content was conducted using a colorimetric assay. Determined protein concentrations of the relevant fractions are listed in Table 9.

**Table 9** Protein concentrations of selected fractions after purification of the hydantoinase from *A. crystallopoietes* DSM20117. Comparison of the standard protocol from GE Healthcare (*grey*) with a modified protocol using Ni sepharose beads (*black*)

fraction	Standard protocol			Modified protocol		
	crude extract	wash 1	eluate 1	crude extract	wash 1	eluate 1
<b>protein concentration/ mg/mL</b>	8.64	6.19	0.29	8.24	6.18	0.18

The particular protein concentrations show, that the difference between crude cell extract and wash 1 is 2.45 mg/mL when conducting the standard protocol, while the difference after conduction of the modified protocol is only 2.06 mg/mL. This is consistent with the results of SDS-PAGE analysis (Figure 35) and indicates a more effective binding of the target molecule. In addition, the lower concentration for eluate 1 of the modified protocol compared to the standard protocol demonstrated that the additional washing step results in less contamination by non-specifically bound proteins, which is also consistent with the results from SDS-PAGE analysis. Since the modified protocol reveals

major improvements as discussed above, every further purification via Ni sepharose beads was conducted with this optimized version.

Another important aspect in purification of enzymes via IMAC chemistry is the desalting step after elution of the target molecule with imidazole. This step is crucial, especially for the hydantoinase, since this is a metalloenzyme with divalent zinc ions in its catalytic center.<sup>[209]</sup> In this work, three different methods for removal of imidazole and simultaneous buffer exchange were tested. Firstly, Vivaspin® tubes (Sartorius) with a membrane of polyethersulfone and a molecular weight cut off (MWCO) of 50 000 was applied. Furthermore, Slide-A-Lyzer™ dialysis devices (Thermo Fisher Scientific) were investigated regarding the buffer exchange of elution fractions resulting from the purification of the hydantoinase. In this case, dialysis through a semipermeable cellulose membrane with a MWCO of 10 000 leads to a buffer exchange and therefore removal of undesired imidazole instead of centrifugation and filtration. The device itself is made of polypropylene. The last tested devices regarding buffer exchange were the Roti®-Spin tubes (Roth) with a membrane of modified polyethersulfone on polyethylene substrate and a MWCO of 10 000. After purification of the hydantoinase via Ni sepharose beads in a multiple approach, the resulting eluates were subjected to buffer exchange applying these three devices. Figure 36 shows the results from activity assays employing the resulting eluates and 5 mM PheHyd as a substrate as well as qualitative SDS-PAGE analysis of the different eluates.

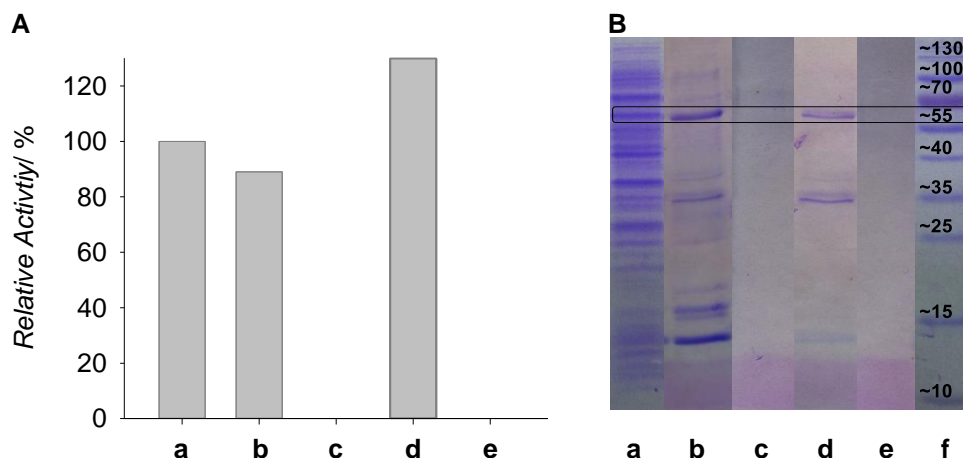


**Figure 36** Testing of different devices for buffer exchange for after purification of the hydantoinase from *A. crystallopoietes* DSM20117 for removal of imidazole. **A** Relative activities of the differently treated fractions related to the specific activity of the crude extract (substrate 5 mM PheHyd). **a** crude extract **b** untreated eluate **c** eluate after buffer exchange with Vivaspin® tube **d** eluate after buffer exchange with Slide-A-Lyzer Dialysis device **e** eluate after buffer exchange with Roti®-Spin tube **B** SDS-PAGE analysis of the differently treated fractions. **a** crude extract **b** untreated eluate **c** eluate after buffer exchange with Vivaspin® tube **d** eluate after buffer exchange with Slide-A-Lyzer Dialysis device **e** eluate after buffer exchange with Roti®-Spin tube **f** protein standard with molecular weights in kDa.

For evaluating the efficiency of the different methods regarding buffer exchange, biotransformations were carried out and Figure 36 A illustrates the resulting relative activities related to the specific activity of the crude cell extract (bar **a**, 100 %). The highest relative activity of 130 % is achieved for



buffer exchange after applying the Slyde-A-Lyzer™ dialysis devices (bar **d**). In contrast, by application of the VivaSpin® tubes (bar **c**) as well as the Roti®-Spin tubes (bar **e**) no activity is determined. The untreated eluate containing imidazole shows a relative activity of 89 % compared to the crude extract.

Qualitative analysis of the differently treated eluates (Figure 36 B) illustrates that eluates handled with VivaSpin® tubes (lane **c**) as well as the Roti®-Spin tubes (lane **e**) show no band for the purified hydantoinase around 56 kDa. Analysis of the crude extract as a positive control reveals the typical pattern for randomly stained proteins, but also a distinct band for the hydantoinase (lane **a**). For comparison, the untreated eluate was investigated which reveals much less non-specific protein bands and also a very distinct band for the hydantoinase at around 56 kDa (lane **b**). The eluate that was treated with the Slyde-A-Lyzer™ dialysis device shows a similar band pattern with fewer bands for non-specific bound proteins as well as a lower intensity for the hydantoinase band (lane **d**).

The activity assays conducted after testing of different devices for buffer exchange revealed no activity for the VivaSpin® tubes as well as for the Roti®-Spin tubes. Since the untreated eluate had a relative activity of 89 % in relation to the specific activity of the crude cell extract, a complete loss in activity during the purification process can be excluded and loss of the target molecule itself during buffer exchange is suggested. This assumption was verified by the results of the qualitative analysis by SDS-PAGE, which show no band for the hydantoinase around 56 kDa for both eluates. In contrast, after conducting the activity assay employing the eluate after buffer exchange with the Slyde-A-Lyzer™ dialysis device revealed a relative activity of 130 % relating to the crude cell extract, demonstrating a marked improvement compared to the untreated eluate. This result proves an increased activity of the hydantoinase after removal of perturbing imidazole. Results from SDS-PAGE analysis supported these findings, since in addition to a clear band for the purified hydantoinase around 56 kDa, much less non-specific bound proteins were detected. This proved on the one hand that no loss of hydantoinase occurred during buffer exchange, reflecting the results from the activity assay. On the other hand conducting dialysis improved the purity of the target molecule by removal of smaller non-specific bound proteins (MWCO 10 000). These findings suggested that materials of the VivaSpin® tubes and Roti®-Spin tubes (polyethersulfone and modified polyethersulfone on polyethylene substrate) are not suitable for purification of the hydantoinase due to adsorption and retention of this enzyme. In contrast, the polypropylene based material as well as the cellulose membrane of the dialysis devices appear not to cause adsorption of the hydantoinase. The review from Orr et al., dealing with membrane chromatography with different membrane supports, highlighted that inorganic support matrices like polyethersulfone indeed exhibit better physical properties and higher stability than organic supports like cellulose, but they tend to higher non-specific adsorption of many biomolecules.<sup>[210]</sup> Since the successfully applied Slyde-A-Lyzer dialysis devices employ cellulose membranes in contrast to the other tested devices containing polyethersulfone, this is probably the reason for the observations discussed above.

In addition to the removal of imidazole, in conducting buffer exchange via the dialysis devices, supply of the enzyme with particular required additives is enabled. Since high imidazole concentrations generally lead to a decrease in enzyme activity, this method was also applied for the carbamoylase

(data not shown). In this case, the dialysis procedure can additionally be utilized to add the required reducing agent DTT. This is important for immobilization and purification of the carbamoylase by functionalized magnetic beads, since the use of DTT is not recommended for functionality of the beads and DTT has to be added after purification.

Based on these findings, the purification of the hydantoinase as well as carbamoylase was conducted and the results are discussed below.

#### 4.3.2.2 PURIFICATION OF THE HYDANTOINASE VIA NI SEPHAROSE BEADS

Aiming at cell-free reaction systems for the synthesis of non-canonical amino acids, the first enzyme of the Hydantoinase Process, in this case the codon-optimized hydantoinase from *A. crystallopoietes* DSM 20117, was gained via cultivation and expression in *E. coli* BL21DE3 (pET28a, C-terminal His-tag, N-terminal Strep-tag, see Chapter 4.3.1). Purification was conducted applying the above mentioned modified purification protocol for Ni sepharose beads as well as buffer exchange using Slide-A-Lyzer dialysis devices. Figure 37 shows qualitative SDS-PAGE analysis of the resulting fractions after purification.

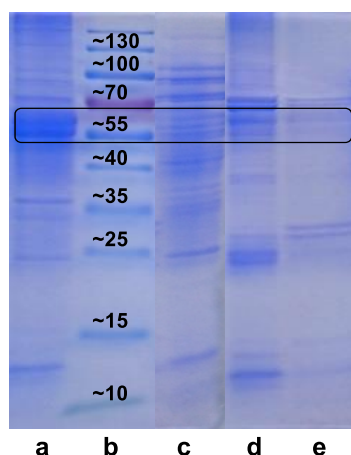


**Figure 37** SDS-PAGE analysis of the different fractions after purification of the hydantoinase from *A. crystallopoietes* DSM 20117 via Ni sepharose beads. **a** insoluble fraction **b** protein standard with molecular weights in kDa **c** crude extract **d** eluate 1 **e** eluate 2

Analysis of the different fractions reveals a band with high intensity for the hydantoinase around 56 kDa as well as bands of randomly stained proteins with lower intensities in the insoluble fraction obtained after cell disruption and centrifugation (lane **a**). The crude extract (lane **c**) exhibits the same pattern of non-specifically stained proteins, while the band for the hydantoinase shows a comparatively low intensity. In contrast to that, the first elution fraction shows fewer randomly stained proteins, but the band which is associated to the hydantoinase has a much higher intensity (lane **d**). In the second elution fraction (lane **e**), even less non-specific proteins were stained with a lower intensity compared to eluate 1, but the intensity of the hydantoinase band is also much lower.

As already stated in previous experiments, this SDS-PAGE analysis revealed a very strong expression of the codon-optimized hydantoinase, but since the corresponding band has a very low intensity in the crude cell extract compared to the insoluble fraction, the hydantoinase is mostly folded incorrect and appears as inclusion bodies. Nevertheless, the first eluate revealed a very distinct band according to the purified hydantoinase with enriched intensity compared to the crude cell extract. Additionally, individual bands with differing molecular weights indicate a contamination by non-specifically bound proteins containing histidines. Since the concentration of soluble hydantoinase is much lower compared to other proteins contained in the crude cell extract, non-specific binding is favored and addition of imidazole to the binding buffer in order to prevent the latter is not sufficient. Elution fraction 2 contains less contamination but also less hydantoinase and therefore further investigations will elucidate the success of the purification.

Biotransformation assays with 5 mM PheHyd as a substrate were conducted to determine enzyme activities as well as recovery and purification factor. The corresponding results are listed in Table 10.

**Table 10** Purification of the hydantoinase from *A. crystallopoietes* DSM 20117 via Ni sepharose beads

<b>Fraction</b>	<b>A / mU/mL</b>	<b>A<sub>vol</sub> / mU/mL</b>	<b>A<sub>tot</sub> / mU</b>	<b>C<sub>protein, tot</sub> / mg</b>	<b>A<sub>spez</sub> / mU/mg</b>	<b>Recovery / %</b>	<b>Purification fold</b>
crude extract	12.8	25.7	102.9	95.9	1.1	-	-
eluate 1	1.2	2.4	4.9	0.9	5.2	4.7	4.9
eluate 2	1.7	3.3	6.6	0.3	20.1	6.5	18.8

According to the biotransformation assay, the specific activity of the purified hydantoinase in eluate 1 is with 5.2 mU/mg five times higher than the specific activity of the crude cell extract. Eluate 2 even shows an increase in activity to 20.1 mU/mg. For eluate 1, a recovery of 4.7 % and a 4.9 fold purification are achieved, eluate 2 results in even higher values.

These results confirmed a successful purification of the hydantoinase. Although SDS-PAGE analysis of eluate 2 showed a very slight band for the hydantoinase compared to the corresponding band in eluate 1, this fraction revealed a much higher specific activity which was not caused by the lower protein concentration, since the volumetric activity of eluate 2 is higher, too. Consequently, it was shown that two elution steps allow purification with insignificant amounts of contamination. Xu et al. investigated the purification of the hydantoinase from *Burkholderia pickettii* via His-tag with a specific activity of 1.13 U/mg toward D,L-hydroxyphenylhydantoin, a recovery of 16.6 % and a 2.6 fold purification.<sup>[101]</sup> Although the specific activity of the investigated hydantoinase is comparatively low in this work, the recovery as well as purification factor is likewise when looking at both obtained elution fractions. Siemann et al. and Werner et al. investigated the purification of the same hydantoinase as in this work and every purification method was reported to result in higher specific activities.<sup>[168,211]</sup> However, the obtained recovery and purification factor are comparable to the results of this work.

Since both groups used methods like hydrophobic interaction chromatography in contrast to affinity tags and the other values are similar, the lower specific activities are suggested to result from the inserted tags. Ragnitz et al. reported a loss in activity of 90 % for the hydantoinase from *Arthrobacter aureescens* DSM3747 after purification with a TALON® column by His-tag.<sup>[212]</sup> One possibility for the comparatively low enzymatic activity of the purified hydantoinase is the negative influence of the His-tag itself, extracting the essential zinc ions from the catalytic center of this metalloenzyme. Additionally, the fact that two tags are attached to the hydantoinase may influence activity of an enzyme, since the location of affinity tags (*C*- or *N*-terminus) is sometimes crucial.<sup>[158]</sup> The purification via IMAC chemistry as well as effects of metal ions on hydantoinase purification was investigated by Ko et al., who also obtained higher specific activities for a hydantoinase, but the purification factors were much lower. The highest specific activity as well as recovery was obtained using zinc ions for immobilization, while the nickel ions applied in this work resulted in the second best values.<sup>[213]</sup>

However, a purification protocol was optimized for the purification of the hydantoinase from *A. crystallopoietes* DSM 20117, allowing a simple upscale of this method due to batch purification. Additionally, moderate enzyme activities and good recovery as well as purification factor was achieved in spite of the two containing affinity tags that potentially have a negative effect on the activity of the enzyme.

#### 4.3.2.3 PURIFICATION OF THE CARBAMOYLASE VIA NI SEPHAROSE BEADS

The same purification protocol as described in Chapters 4.3.2.1 and 4.3.2.2 was applied for the purification of the carbamoylase from *A. crystallopoietes* DSM 20117 with *C*-terminal His-tag which was received by cultivation and expression in *E. coli* BW3110. Figure 38 shows qualitative analysis of the resulting fractions after purification via Ni sepharose beads.

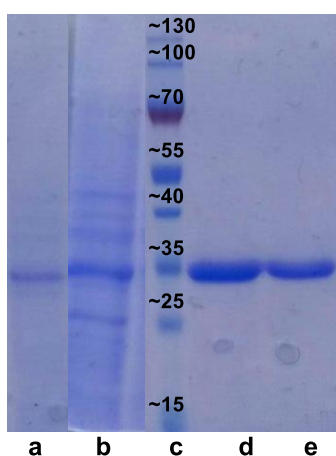


**Figure 38** SDS-PAGE analysis of the different fractions after purification of the carbamoylase from *A. crystallopoietes* DSM 20117 via Ni sepharose beads. **a** insoluble fraction **b** crude extract **c** protein standard with molecular weights in kDa **d** eluate 1 **e** eluate 2

The insoluble fraction that was obtained after cell disruption and centrifugation shows a band at around 35 kDa which corresponds to the molecular weight of the carbamoylase (lane **a**). Additionally, very slight bands for proteins of other molecular weights are visible. Analysis of the crude cell extract reveals a more intensive band for the carbamoylase as well as more randomly stained proteins (lane **b**). The elution fractions 1 and 2 (lane **d** and **e**) each show a very distinct band for the carbamoylase and no other stained proteins.

In contrast to the hydantoinase, investigation of the soluble and insoluble fraction after cell disruption revealed a low amount of carbamoylase that was folded incorrectly and precipitated as inclusion bodies, since the band for the carbamoylase was much more intensive in the crude cell extract. Additionally, the elution fractions of the carbamoylase show a high enrichment of the target molecule with no detectable contamination. This proves that the optimized purification protocol for the hydantoinase was successfully transferred to the purification of the carbamoylase. The fact that the elution fractions of the carbamoylase showed a better purification than that of the hydantoinase, results from the very high amount of soluble carbamoylase, reducing the non-specific adhesion of proteins.

For a more detailed evaluation of the purification of the carbamoylase by Ni sepharose beads, biotransformation assays using 5 mM NCPheAla as a substrate were carried out. A summary of enzyme activities, recoveries and purification factors is shown in Table 11.

**Table 11** Purification of the carbamoylase from *A. crystallopoietes* DSM 20117 via Ni sepharose beads

<b>Fraction</b>	<b>A / mU/mL</b>	<b>A<sub>vol</sub> / mU/mL</b>	<b>A<sub>tot</sub> / mU</b>	<b>c<sub>protein, tot</sub> / mg</b>	<b>A<sub>spez</sub> / mU/mg</b>	<b>Recovery / %</b>	<b>Purification fold</b>
crude extract	128.9	257.8	1031.0	61.4	16.80	-	-
eluate 1	113.8	227.6	455.3	0.8	554.9	44.2	33.0
eluate 2	59.9	119.7	239.4	0.8	300.0	23.3	17.9

The crude cell extract shows the lowest specific activity of 16.80 mU/mg, while eluate 1 has the highest specific activity of 554.9 mU/mg. Regarding recovery and purification factor, with 44.2 % and 33.0, the first elution fraction also exhibits higher values than elution 2.

It was conspicuous that the crude extract of the carbamoylase exhibited a much higher specific activity than the crude extract of the hydantoinase with 1.1 mU/mg. The purified carbamoylase exhibits less non-specifically bound proteins than the hydantoinase, which is caused by the higher concentration of soluble enzyme in the crude cell extract, since low concentrations of the target molecule promote non-specific binding. Consequently, this is a possible explanation for the much lower specific activity of the hydantoinase, although these enzymes catalyze two different reactions. Furthermore, eluate 1 of the carbamoylase purification process revealed a 33 times higher specific activity than the crude extract, which is also better compared to the purification factor from eluate 1 for the hydantoinase with a value

of 4.9. The values for specific activity, recovery and purification factor of eluate 2 were lower than for eluate 1, but still very high. Taking together both eluates, a very high recovery of 67.5 % was achieved by purification of the carbamoylase via His-tag. Purification of the L-carbamoylase from *Arthrobacter aureescens* via Streamline DEAE and MonoQ resulted in much lower values for the recovery as well as for the purification factor,<sup>[214]</sup> while Chen et al. achieved generally higher values by purification of the carbamoylase from *Agrobacterium radiobacter* via His-tag based affinity chromatography.<sup>[215]</sup> Lower specific activities of the carbamoylase may result from its oxidative sensitivity as well as thermal instability. In 1979, Olivieri et al. discovered the involvement of thiol groups in D-carbamoylase activity and Grifantini et al. confirmed these findings by stating oxidative sensitivity via sequence analysis and mutagenesis experiments.<sup>[49,121]</sup> Oxidation of cysteine thiol groups leads to inactivation of the catalytic center of carbamoylases, which can be avoided by addition of reducing agents like DTT or  $\beta$ -mercaptoethanol.<sup>[119,216]</sup> In this work, 5 mM DTT were added to every buffer solution during purification as well as during activity assays. DTT is known to be a very strong reducing agent and can be used at much lower concentrations compared to  $\beta$ -mercaptoethanol.<sup>[217]</sup> Nevertheless, since  $\beta$ -mercaptoethanol is reported to be more stable, maybe this reducing agent would result in higher activities in the purification of the carbamoylase.<sup>[218]</sup>

To overcome drawbacks like thermal instability, oxidative sensitivity as well as to enable the application of the hydantoinase as well as carbamoylase in cell-free reaction systems without major deficits in enzyme activities, the immobilization of both enzymes was investigated in the following chapter.

### 4.3.3 IMMOBILIZATION AND PURIFICATION OF ENZYMES VIA FUNCTIONALIZED MAGNETIC BEADS

Due to their thermal instability as well as oxidative and proteolytic sensitivity many efforts have been made for the immobilization of hydantoinases and carbamoylases with visible success.<sup>[162,212,219,220]</sup> Most investigations are dealing with encapsulation, covalent immobilization or non-covalent adsorption techniques. These methods exhibit not only advantages, but also drawbacks like enzyme leakage for encapsulation methods or a loss in enzyme activity upon covalent binding. Therefore, the immobilization via affinity tags displays a promising alternative. In this work, the immobilization via non-covalent adsorption by coordination bonds between immobilized metal ions and amino acids of the target molecule was investigated, which avoids the above mentioned disadvantages.

For this objective, the application of functionalized magnetic beads furthermore allows immobilization of enzymes directly from crude cell extract, avoiding time consuming purification steps that are unfavorable for the recovery as well as the activity of the target enzymes.

#### 4.3.3.1 PRELIMINARY TESTS

Since only little knowledge is noted for the immobilization of the hydantoinase and carbamoylase from *A. crystallopoietes* DSM 20117 on functionalized magnetic beads, several tests had to be conducted to allow successful immobilization. Whereas the cultivation and expression conditions for the hydantoinase were already optimized (see Chapter 4.3.1), no investigations concerning the carbamoylase were conducted until now.

The cultivation strategy that was used for hydantoinase expression (induction at  $OD_{600}=4$ , cultivation for 24 h) did not show any improvement in soluble carbamoylase expression or yield (data not shown). Therefore the cultivation method reported by Werner et al. was continued to use (induction at  $OD_{600}=0.4-0.6$ , further cultivation for 6 h) due to its much shorter cultivation time.<sup>[168]</sup> But since the use of TB-medium instead of LB-medium resulted in much higher final  $OD_{600}$  values for the hydantoinase cultures, this was also investigated for the carbamoylase regarding the immobilization by functionalized magnetic beads. Firstly, SDS-PAGE analysis was conducted for comparing the cultivation and induction in different media as well as subsequent immobilization of the carbamoylase (see Figure 39).

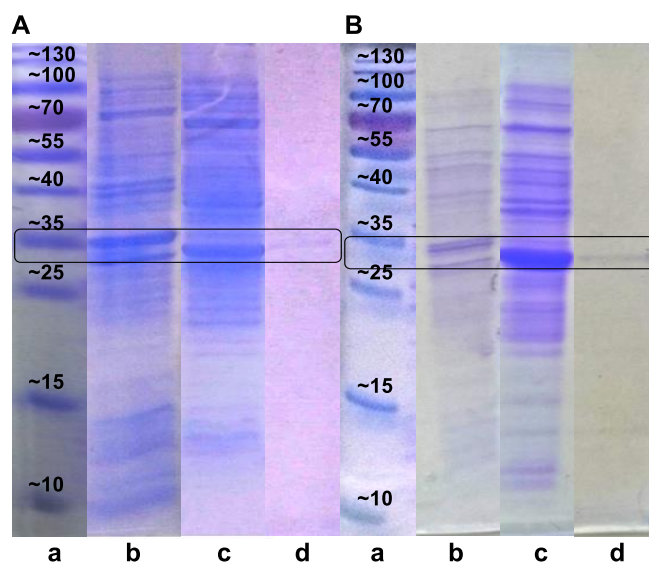


**Figure 39** SDS-PAGE analysis for comparison of two different media for the cultivation and expression of soluble carbamoylase from *A. crystallopoietes* DSM 20117 regarding immobilization on functionalized magnetic beads. **A** TB-medium **a** protein standard with molecular weights in kDa **b** insoluble fraction **b** crude extract **c** eluate after immobilization **B** LB-medium **a** protein standard with molecular weights in kDa **b** insoluble fraction **c** crude extract **d** eluate after immobilization

Figure 39 A shows the results for cultivation and expression of the carbamoylase in TB-medium. The insoluble fraction after cell disruption and centrifugation (lane **b**) exhibits a distinct band around 35 kDa for the carbamoylase as well as a lot of randomly stained proteins with differing molecular weights and a lower intensity. Analysis of the crude cell extract shows a similar band pattern with likewise intensities (lane **c**) and in the eluate after immobilization, a slight band for the carbamoylase is noticeable (lane **d**). In contrast, investigation of the cultivation and expression in LB-medium (Figure

39 B) results in a band with lower intensity for the carbamoylase as well as for other proteins (lane **b**). However, the crude cell extract exhibits a distinct band with a very high intensity for the carbamoylase around 35 kDa (lane **c**), while the eluate after immobilization shows a very slight carbamoylase band (lane **d**).

The comparison of two different culture media for the cultivation and expression of the carbamoylase revealed a better soluble carbamoylase expression employing the LB-medium than the TB-medium, since the band for the carbamoylase was much more intensive in the crude cell extract than in the insoluble fraction. This fact is explainable by a lower growth rate using LB-medium instead of TB-medium with an excess in nutrients, since lower growth rates and consequently lower expression levels were reported to improve the correct folding of recombinant proteins.<sup>[142,181]</sup> The elution fraction after immobilization in contrast showed no difference in band intensity comparing the two cultivation media.

To get more detailed information concerning enzyme activities, activity assays were conducted using 5 mM MCPhe as a substrate. Table 12 summarizes important results after cultivation and induction of *E. coli* BW3110 expressing the carbamoylase in LB-medium respectively TB-medium.

**Table 12** Comparison of two different media for the cultivation and expression of soluble carbamoylase from *A. crystallopoietes* DSM 20117 regarding immobilization on functionalized magnetic beads

	<b>Crude extract</b>	<b>Immobilized carbamoylase</b>		
	$A_{spez}/U/mg$	$A_{spez}/U/mg$	<i>Cell wet weight / g</i>	$c_{protein}/mg/mL$
<b>TB-medium</b>	0.018	1.775	3.00	21.39
<b>LB-medium</b>	0.018	2.187	2.35	30.89

The results show, that TB-medium reaches a higher yield in cell wet weight with 3.00 g, but the specific activity for immobilized carbamoylase as well as the resulting protein concentration are with 1.775 U/mg and 21.39 mg/mL both lower than the values for the cultivation and expression in LB-medium.

Since the resulting protein concentration in the crude extract for cultivation in LB-medium was with 30.89 mg/mL higher than for the TB-medium cultivation although a lower yield in cell wet weight was achieved, it was suggested that the higher protein concentration is caused by a much higher concentration of soluble carbamoylase. This is also consistent with the results from SDS-PAGE analysis (Figure 39) as well as with the achieved specific activities for the immobilized enzymes. As already discussed before, a slower growth rate probably leads to slower expression as well as more correct folding of the enzyme.<sup>[221]</sup> Consequently, a higher stability of the correctly folded and immobilized carbamoylase is supposable.

By reason of the above discussed findings, cultivation and expression of the carbamoylase from *A. crystallopoietes* DSM 20117 was conducted in LB-medium for every further investigation.



To receive an efficient investigation of enzyme immobilization via affinity tag, reproducibility has to be guaranteed as well as the leakage of the immobilized coordinating metal ion, in this case cobalt, has to be hampered. In using the Dynabeads® His-tag Isolation and Pulldown (Life Technologies), the included manual assures the reusability of the functionalized magnetic beads without regeneration of the metal ions required for immobilization. Nevertheless, during repeated use of these beads, a strong decrease in protein concentration of the eluates after immobilization was observed. For more detailed information, Figure 40 shows the decrease in protein concentration for repeated cycles of immobilization via Dynabeads® His-tag Isolation and Pulldown.

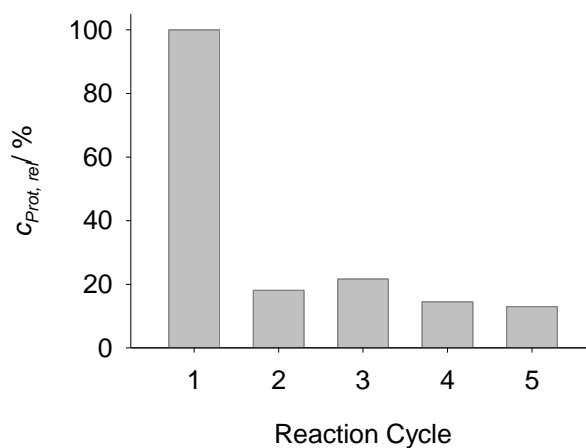


**Figure 40** Relative protein concentrations of the eluate after immobilization of the carbamoylase from *A. crystallopoietes* DSM 20117. Protein concentrations related to the first reaction cycle

The results indicate a strong decrease in protein concentration of the resulting eluates after immobilization of the carbamoylase. Whereas the protein concentration was reduced to 18 % in the second cycle compared to the first cycle, the following cycles showed similar low protein concentrations. Consequently, already after the first cycle of using the cobalt functionalized magnetic beads for immobilization under used conditions, a regeneration of the beads is necessary to maintain the quality of immobilization. It is suggested that less protein was able to bind to the beads due to leakage of the coordinating cobalt ions.

Therefore, two different methods for the regeneration of the beads were tested, which results in three different methods when comparing to the recommended way of only washing the beads for three times with elution buffer (strategy 1). Strategy 2 included also three times washing with elution buffer, but additionally subsequent functionalization with a cobaltchloride solution (see Chapter 3.2.7.1). Another method was conducted by incubating the magnetic beads with a 0.2 M EDTA solution to remove functional groups from the magnetic beads and subsequent incubation with cobalt chloride solution to obtain equal functionalized magnetic beads for every batch (strategy 3).<sup>[222]</sup> Firstly, SDS-PAGE analysis was carried out for the elution fractions after immobilization of the enzyme (Figure 41).

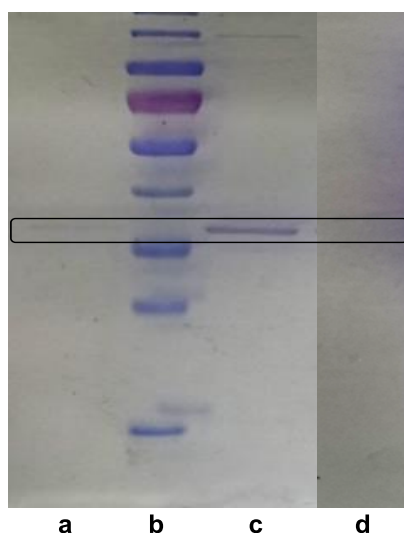


**Figure 41** SDS-PAGE analysis for comparison of different regeneration strategies for functionalized magnetic beads after immobilization of the carbamoylase from *A. crystallopoietes* DSM 20117. **a** strategy 1 **b** protein standard with molecular weights in kDa **c** strategy 2 **d** strategy 3

Lane **a** shows the eluate after regeneration with strategy 1, immobilization and elution of the enzyme after biotransformation and exhibits a very slight band around 35 kDa for the carbamoylase. By comparison, the same band corresponding to the carbamoylase in the elution fraction from strategy 2 has higher intensity (lane **c**). The elution fraction of strategy 3 shows no band for the carbamoylase (lane **d**).

Since the SDS-PAGE analysis resulted in a band with more intensity for regeneration with strategy 2 than for regeneration with strategy 1, it was suggested that strategy 2 was more successful in regenerating the cobalt ions on the surface of the magnetic beads and therefore more enzyme was able to bind than without treating with cobalt chloride solution. In contrast, the treatment with EDTA for complete removal of the metal ions and subsequent incubation with fresh cobalt chloride (strategy 3) seemed to prevent the regeneration with cobalt ions since no His-tagged enzyme was able to bind on the magnetic beads.

For further evaluation of the different regeneration methods, activity assays were conducted employing the immobilized carbamoylase and 5 mM NCPhe as substrate (Table 13).

**Table 13** Comparison of different regeneration strategies for functionalized magnetic beads after immobilization of the carbamoylase from *A. crystallopoietes* DSM 20117. Relative activity based on the recommended strategy

	Strategy 1	Strategy 2	Strategy 3
$c_{protein}/mg/mL$	0.022	0.080	0.013
<i>relative activity</i> /%	100	316	0

The results show that the highest activity for the immobilized carbamoylase is achieved by regeneration of the beads using strategy 2, which results in a relative activity of 316 % compared to the recommended strategy 1. In contrast, strategy 3 results in no determinable activity for the immobilized enzyme and also exhibits the lowest protein concentration of 0.013 mg/mL after elution of the enzyme.

The higher activity for the magnetic beads bearing the carbamoylase after regeneration with strategy 2 is consistent with the results from SDS-PAGE analysis (Figure 41). Furthermore, the determined protein concentrations correlate with the tendencies of enzyme activities. In detail, the regeneration strategy 2 that resulted in the highest enzyme activities exhibited also the highest protein concentration after elution of the carbamoylase from the beads. These findings also verify the results from SDS-PAGE analysis. The fact that no activity was determined after regeneration of the beads via strategy 3 suggests that EDTA modifies the surface of the magnetic beads in a way that prevents the immobilization of new cobalt ions and therefore also the immobilization of the enzyme via affinity tag. This was verified on the one hand with the SDS-PAGE that showed no band in this elution fraction and on the other hand, the protein concentration of the latter was very low compared to the other two regeneration methods. Consequently, a suitable method for regeneration of the functionalized magnetic beads by incubation with cobalt chloride solution was found and the other methods had been either not working efficiently or not working at all.

The last aspect that was investigated to optimize the immobilization of the His-tagged hydantoinase as well as carbamoylase was the addition of imidazole to the crude cell extract, since it has been reported to reduce non-specific binding of other proteins and therefore increase the specific activity.<sup>[215]</sup> As already discussed before, the hydantoinase is a metalloenzyme which is in conflict with the use of imidazole, since the latter is a building block of histidine and therefore it is able to coordinate with metal ions and withdrawing them from the catalytically active center. Therefore, the influence of the addition of imidazole was tested for the hydantoinase. Table 14 summarizes relative activities of different fractions resulting after immobilization of the hydantoinase on functionalized magnetic beads with imidazole added to the crude extract and without.

**Table 14** Effect of imidazole in the crude extract regarding immobilization and purification of the hydantoinase from *A. crystallopoietes* DSM 20117 via functionalized magnetic beads. Relative activities for each approach with imidazole related to each approach without imidazole

	<b>Crude extract</b> <i>relative activity/ %</i>	<b>Immobilized hydantoinase</b> <i>relative activity/ %</i>	<b>Purified hydantoinase</b> <i>relative activity/ %</i>
<b>w/o imidazole</b>	100	100	100
<b>12 mM imidazole</b>	0	154	102

The addition of 12 mM imidazole to the crude extract results in an activity of 154 % related to the activity of the immobilized hydantoinase with no addition of imidazole. The hydantoinase purified via functionalized magnetic beads shows a slight increase in activity of 2 % compared to the approach

without imidazole in the crude extract. In contrast, crude extract containing imidazole showed to activity.

The obtained results for the different fractions revealed that the presence of imidazole strongly increased the specific activity of the immobilized hydantoinase and also a very slight increase for the specific activity of the purified hydantoinase was recognized. This implies that imidazole successfully prevented non-specific binding of proteins which would result in lower activities and yields. The fact that no activity was determined for the crude extract containing imidazole suggests that imidazole is able to withdraw the required zinc ions and therefore causes inactivation of the enzyme. In contrast, the immobilized enzyme was washed with catalysis buffer containing zinc ions after immobilization, which prevented inactivation by imidazole. The same applied to the purified enzyme, which was subjected to buffer exchange after elution.

With the help of these findings and optimizations regarding the purification and immobilization of the hydantoinase as well as carbamoylase, the following experiments were conducted.

#### 4.3.3.2 IMMOBILIZATION VIA FUNCTIONALIZED MAGNETIC BEADS (HIS-TAG)

The immobilization of the hydantoinase was carried out for the codon-optimized version from *A. crystallopoietes* DSM 20117 carrying a His-tag as well as a SBP-tag expressed in *E. coli* BL21DE3 carrying the plasmid pET28a. Figure 42 shows SDS-PAGE analysis of the resulting fractions after immobilization of the hydantoinase using the optimized protcoll (see Chapter 4.3.3.1).

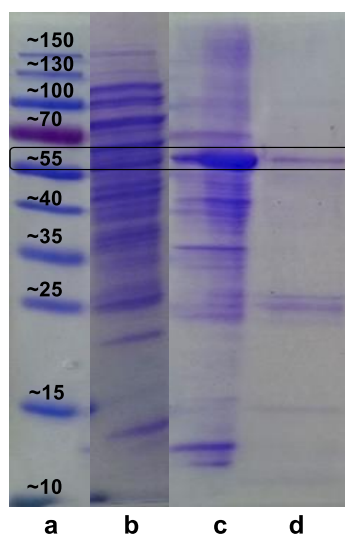


**Figure 42** SDS-PAGE analysis after immobilization of the hydantoinase from *A. crystallopoietes* DSM 20117 on functionalized magnetic beads. **a** protein standard with molecular weights in kDa **b** crude extract **c** insoluble fraction **d** eluate

Lane **b** represents the crude cell extract after expression of the hydantoinase, exhibiting a band for the hydantoinase around 56 kDa as well as many bands for randomly stained proteins of different molecular weights with the same intensity. The insoluble fraction after cell disruption and centrifugation shows a more intensive band for the hydantoinase, while the band pattern of randomly stained proteins is less intensive (lane **c**). The elution fraction after immobilization of the hydantoinase, lane **d**, reveals a band at 56 kDa according to the molecular weight of the hydantoinase and few bands for other molecular weights.

As already discussed before, the expression of the codon-optimized hydantoinase resulted mostly in the formation of inclusion bodies in the insoluble fraction after cell disruption. Nevertheless, the crude extract showed a band for soluble hydantoinase and furthermore the results proved a successful immobilization of the hydantoinase, since a distinct band is detectable after elution from the functionalized magnetic beads. Additionally, nearly no non-specifically bound proteins were detectable in this fraction. Next to the examination of resulting specific activities toward PheHyd, two more substrates were investigated: Benzylhydantoin (BnH) as well as hydroxymethylhydantoin (HMH), see Table 15.

**Table 15** Immobilization of the hydantoinase from *A. crystallopoietes* DSM 20117 via functionalized magnetic beads and hydrolysis of different substrates

	Fraction	$c_{Prot}$ / mg/mL	$A_{spez}$ / mU/mg
<b>PheHyd</b>	crude extract	5.000	0.36
	immobilized hydantoinase	0.105	70.75
<b>BnH</b>	crude extract	5.000	0.28
	immobilized hydantoinase	0.079	63.20
<b>HMH</b>	crude extract	5.000	0.76
	immobilized hydantoinase	0.079	105.47

The activity assay results in the highest specific activity for the immobilized hydantoinase converting HMH with 105.47 mU/mg, while the lowest specific activity is determined for the conversion of BnH with 63.20 mU/mg. The same tendency is observed for specific activities of the crude cell extracts, which exhibit up to 200 times lower specific activities compared to the immobilized hydantoinase.

By conducting these activity assays, it was shown that the immobilization of the hydantoinase via His-tag to functionalized magnetic beads was successful. The specific activity of the enzyme was increased by up to 200 % upon immobilization. Additionally, the obtained specific activities are much

higher than this of the purified hydantoinase with a maximal specific activity of 20.1 mU/mg (see Chapter 4.3.2.2), which is probably caused by a higher stability of the hydantoinase upon immobilization. Furthermore, the reported loss in activity due to attachment of an His-tag to this enzyme can be prevented by immobilization and therefore occupation of this tag.<sup>[212]</sup> As already discussed, the immobilization employing affinity tags displays an advantage compared to covalent immobilization methods or for example immobilization via polyglutaraldehyde particles entrapped in calcium alginate beads, since this method resulted in partially deactivation of the hydantoinase as well as induced mass transfer resistance and consequently lower reaction rates.<sup>[133]</sup>

For the synthesis of non-canonical amino acids via Hydantoinase Process in cell-free reaction systems as well as to enable the implementation of a microfluidic reaction system using immobilized enzymes on magnetic beads (see Chapter 1.2.3), the carbamoylase from *A. crystallopoietes* DSM20117 expressed in *E. coli* BW3011 carrying the plasmid pMW1 (with C-terminal His-tag) was also immobilized as described for the hydantoinase. Figure 43 illustrates the results after conducting SDS-PAGE analysis for the resulting fractions after immobilization of the carbamoylase via functionalized magnetic beads.

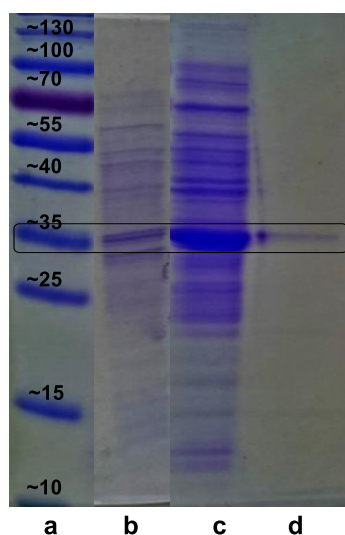


**Figure 43** SDS-PAGE analysis after immobilization of the carbamoylase from *A. crystallopoietes* DSM 20117 on functionalized magnetic beads. **a** protein standard with molecular weights in kDa **b** crude extract **c** insoluble fraction **d** eluate

Lane **b**, the insoluble fraction after cell disruption and centrifugation shows a band for the carbamoylase around 35 kDa as well as bands for other proteins. The crude extract exhibits generally the same band pattern with more intensity and the band for the carbamoylase is much stronger (lane **c**). The eluate (lane **d**) has a slight band for the carbamoylase and very little bands for other protein.

SDS-PAGE analysis showed again, that the expression of native carbamoylase was very high compared to the expression of the hydantoinase. The eluate revealed successful purification of the carbamoylase with very low impurity.

To get a more detailed insight in the quality of this immobilization process, activity assays were conducted using different substrates (Table 16).

**Table 16** Immobilization of the carbamoylase from *A. crystallopoietes* DSM 20117 via functionalized magnetic beads and hydrolysis of different substrates

	Fraction	$c_{Prot}$ / mg/mL	$A_{spez}$ / U/mg
<b>NCPheGly</b>	crude extract	5.000	0.066
	immobilized carbamoylase	0.027	11.751
<b>NCPheAla</b>	crude extract	5.000	0.099
	immobilized carbamoylase	0.026	12.906
<b>NCSer</b>	crude extract	5.000	0.084
	immobilized carbamoylase	0.027	11.751

Biotransformation assays with different substrates reveal a successful immobilization of the carbamoylase with similar specific activities, whereat the substrate *NCPheAla* was converted with the highest specific activity of 12.906 U/mg. The specific activity of the crude cell extracts range from 0.066 U/mg for the conversion of *NCPheGly* to 0.099 U/mg for the conversion of *NCPheAla*.

Immobilization of the carbamoylase resulted in very high specific activities compared to the crude cell extract with around 130 fold increased specific activities. Conversion of *NCPheAla* resulted in the highest specific activities, but the other substrates were converted in almost the same manner. The fact that the eluted carbamoylase fraction contains less impurities than the hydantoinase, suggests that the immobilization occurred more specifically for the target molecule due to the higher expression of soluble carbamoylase.<sup>[212]</sup> Consequently, the specific activities of the immobilized carbamoylase were also higher. Comparing this immobilized carbamoylase with the activities of the enzyme purified by Ni sepharose beads, the resulting specific activities were much higher, indicating a stabilization of the carbamoylase upon immobilization. Until now, immobilization of a carbamoylase via IMAC chemistry is not reported. However, immobilization of the L-carbamoylase from *Bacillus kaustophilus* on Eupergit C was investigated and a lower optimal specific activity of 2.91 U/mg was achieved.<sup>[223]</sup> Immobilization of the L-carbamoylase from *Geobacillus stearothermophilus* CECT43 on Sepabeads EC-HFA/S was reported to result in a maximum specific activity of around 14.00 U/mg by Soriano-Maldonado et al., which is comparably to our results.<sup>[224]</sup>

Recyclation of the immobilized carbamoylase was also tested, but resulted in no activity. This suggests a very fast oxidation and therefore inactivation of the carbamoylase. Since the use of DTT is

not recommended for the functionalized magnetic beads, no reducing agent was applied for preventing oxidation of the active center and therefore inactivation of this enzyme.

The investigated method for immobilization of the carbamoylase is very simple, fast and results in better or comparable specific activities of the carbamoylase although comparison with other reported results is difficult due to the varying applied methods. But this fact shows that there is much more potential in optimization of the immobilization of carbamoylases by coordination with metal ions, since there is not much found in the literature. Furthermore this method is more gentle due to the abdication of covalent binding techniques that often cause loss in enzyme activity and transport limitations that occur using encapsulation methods hold off.

A combined batch approach employing the separately immobilized hydantoinase and carbamoylase in a ratio of 1 : 1 was also conducted for testing wether the synthesis of phenylglycine, phenylalanine and serine is feasible. Biotransformation assays were carried out at 30 °C, the optimum temperature for the temperature sensitive carbamoylase. The results revealed a complete conversion of the substrates by the immobilized hydantoinase, while no conversion of the resulting intermediates by the carbamoylase was detectable (data not shown). Previous experiments demonstrated low specific activities of the hydantoinase compared to the carbamoylase and therefore it was suggested that the carbamoylase was already inactive due to oxidation until substrate was provided from the hydantoinase. Since no reducing agent was used as it was suggested to hamper binding of the target molecule to the functionalized magnetic beads, oxidation of the active center of the carbamoylase and therefore inactivation of the enzyme is assumed before hydrolysis of the hydantoin occurred. These findings result in numerous possibilities to improve this reaction system and allow the synthesis of amino acids in one step. For example, the ratio between hydantoinase and carbamoylase can be altered, using much more immobilized hydantoinase than carbamoylase. Though, the more important aspect is to prevent oxidation of the carbamoylase and therefore different kinds of reducing agents need to be tested regarding their influence on the magnetic beads. Because together with a reducing agent that is compatible with the functionalized magnetic beads, a more stable carbamoylase could result in a successful conversion of different hydantoins to amino acids in one step.

#### 4.3.3.3 IMMOBILIZATION VIA FUNCTIONALIZED MAGNETIC BEADS (SBP-TAG)

Since a more specific as well as stable affinity was reported for the application of SBP-tag compared to His-tag,<sup>[157,158]</sup> the hydantoinase from *A. crystallopoietes* DSM20117 was additionally provided with an *N*-terminal Strep-tag. Especially regarding immobilization of the hydantoinase toward applications in microfluidic reaction systems, this affinity tag should be helpful.

However, every immobilization approach for the hydantoinase on Dynabeads® M-280 Streptavidin resulted in no determinable enzyme activity for the three tested substrates PheHyd, BnH as well as



HMH. The resulting fractions after conducting immobilization via SBP-tag were investigated by qualitative SDS-PAGE analysis (see Figure 44).

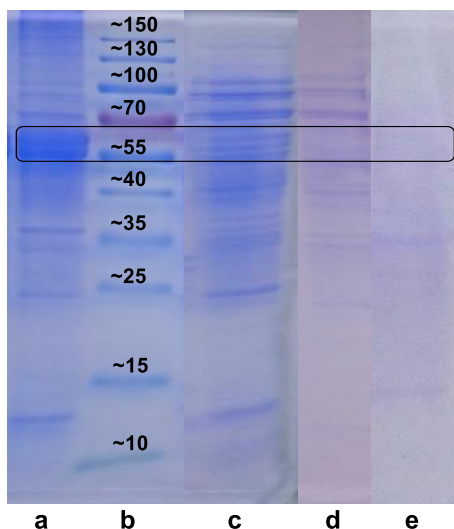


**Figure 44** SDS-PAGE analysis after immobilization of the hydantoinase from *A. crystallopoietes* DSM 20117 on functionalized magnetic beads (SBP-tag). **a** insoluble fraction **b** protein standard with molecular weights in kDa **c** crude extract **d** wash 1 **e** eluate (1 % SDS)

Lane **a**, representing the insoluble fraction after cell disruption and subsequent centrifugation shows a band for the hydantoinase around 56 kDa as well as bands for proteins with other molecular weights. The crude extract (lane **c**) exhibits a similar band pattern, but the band for the hydantoinase is more slightly. Wash 1, the supernatant resulting after incubation of the magnetic beads with the crude cell extract (lane **d**), also results in a similar band pattern but in general with less intensity. The elution fraction (lane **e**) shows very slight bands with other molecular weights than the hydantoinase and nearly no hydantoinase is detected.

For checking the expression of the hydantoinase, the insoluble fraction as well as the crude extract was investigated again and the same results were obtained as discussed before. Consequently, the missing enzyme activity did not result from absent expression of the hydantoinase. But the fact that nearly no hydantoinase was detected in the elution fraction suggests that the immobilization of the enzyme was not successful. However, determined protein concentrations for the crude extract (11.03 mg/mL) and for the elution fraction (0.23 mg/mL), proved that enzyme was present after elution of the loaded beads. Probably, no band was visible in the SDS-PAGE due to the long incubation time with 1 % SDS at 95 °C, which can lead to disaggregation of the enzyme.

Since the purification approaches in this work already showed a decreased enzyme activity for the isolated hydantoinase compared to the immobilized enzyme, it was suggested that occupation of the His-tag by immobilization employing this tag results in shielding of these histidine residues from the catalytic center of the enzyme. Consequently, the histidines of the His-tag are not able to withdraw the zinc ions that are required for an active hydantoinase. Ragnitz et al. also reported a loss in activity of up to 90 % upon purification of a hydantoinase via His-tag.<sup>[212]</sup> This would also explain the complete loss in enzyme activity upon immobilization of the hydantoinase at the *N*-terminus, which leads to an

exposure of the C-terminal His-tag and therefore promotes withdrawal of the zinc ions from the active center.

#### 4.3.3.4 PURIFICATION VIA FUNCTIONALIZED MAGNETIC BEADS (HIS-TAG)

Since a simple and gentle elution of immobilized enzymes on functionalized magnetic beads is given, the purification of both enzymes was also investigated using this method. Figure 45 shows the qualitative SDS-PAGE analysis of the resulting fractions after purification of the hydantoinase via His-tag.

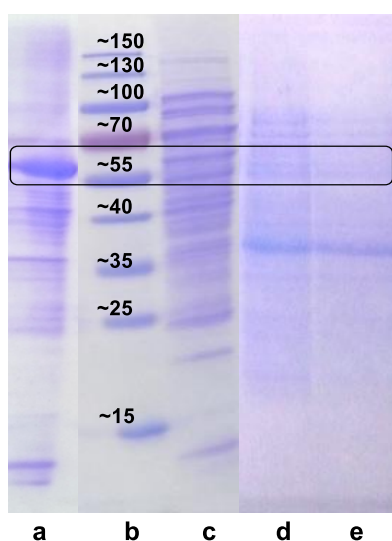


**Figure 45** SDS-PAGE analysis after purification of the hydantoinase from *A. crystallopoietes* DSM 20117 via functionalized magnetic beads. **a** insoluble fraction **b** protein standard with molecular weights in kDa **c** crude cell extract **d** wash 1 **e** eluate

Lane **a** exhibits a distinct band for the hydantoinase around 56 kDa as well as a band pattern for other stained proteins with varying molecular weights for the insoluble fraction after cell disruption. The soluble fraction (lane **b**) shows the same pattern, but the band corresponding to the hydantoinase is comparatively small. Lane **d** and **e**, respectively wash 1 and eluate, have similar band patterns of randomly stained proteins as well as a very slight band for the hydantoinase.

For the control of successful expression of the hydantoinase, the soluble as well as insoluble fraction after cell disruption were shown and they had the same properties as for the experiments discussed above. The supernatant after incubation of the functionalized magnetic beads with the crude cell extract, wash 1, showed a lot of non-bound proteins of different sizes as well as a slight band for the hydantoinase, indicating that not all the hydantoinase contained in the crude extract has bound to the beads. The fact that an even slighter band was detected for the hydantoinase in the elution fraction, while still non-specifically bound proteins were detected, indicated a contamination of the purified hydantoinase. This was not reported for previous results concerning immobilization of the

hydantoinase on functionalized magnetic beads (see Chapter 4.3.3.2), since the non-specifically bound proteins dissociated in these experiments during biotransformation assays and therefore only the hydantoinase was detectable.

To obtain a quantitative statement about the success of the hydantoinase purification via magnetic beads, activity assays were conducted employing the eluate and 5 mM PheHyd as a substrate (see Table 17).

**Table 17** Purification of the hydantoinase from *A. crystallopoietes* DSM 20117 via functionalized magnetic beads

<b>Fraction</b>	<b>A / mU/mL</b>	<b>A<sub>vol</sub> / mU/mL</b>	<b>A<sub>tot</sub> / mU</b>	<b>c<sub>protein, tot</sub> / mg</b>	<b>A<sub>spez</sub> / mU/mg</b>	<b>Recovery / %</b>	<b>Purification fold</b>
crude extract	7.7	15.5	15.5	11.97	1.3	-	-
eluate	1.8	3.7	1.8	0.04	46.4	11.9	35.9

The specific activity of the crude extract is 1.3 mU/mg, while for the eluate respectively purified hydantoinase, a specific activity of 46.4 mU/mg is determined and a recovery and purification factor of 11.9 % and 35.9 are obtained. These results revealed a successful purification of the hydantoinase by functionalized magnetic beads with a higher specific activity of the isolated hydantoinase than for the purification using Ni sepharose beads. The recovery was nearly the same when comparing both eluates of the Ni sepharose purification with the purification by magnetic beads, but the purification factor was higher with the latter method. Since the incubation times are much lower using the protocol for purification via functionalized magnetic beads, it was suggested that the hydantoinase was maybe exposed to proteolytic digestion during the incubation of the crude cell extract with the Ni sepharose beads in spite of the added protease inhibitor. Compared to the investigations of Ko et al., dealing with the purification of the hydantoinase via IMAC chemistry using different metal ions, the specific activities are relatively low, but the purification factor as well as recovery are much higher.<sup>[213]</sup> The same applies to the work of Xu et al., whereat the purification factor was lower, but the resulting specific activities were higher than in the shown results.<sup>[101]</sup> This verifies the suitability of this method for the purification of the hydantoinase regarding the obtained purification factor as well as recovery. A possible explanation for the comparatively low specific activities maybe result from the *N*-terminal SBP-tag as already discussed before (see Chapter 4.3.2.2).

The purification was also conducted for the carbamoylase using the same protocol. SDS-PAGE analysis of the different fractions is illustrated in Figure 46.

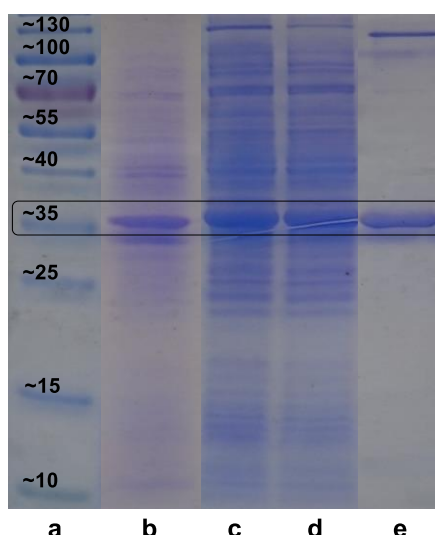


**Figure 46** SDS-PAGE analysis after purification of the carbamoylase from *A. crystallopoietes* DSM 20117 via functionalized magnetic beads. **a** protein standard with molecular weights in kDa **b** insoluble fraction **c** crude cell extract **d** wash 1 **e** eluate

The insoluble fraction (lane **b**) shows a very slight band pattern for randomly stained proteins, but a distinct band for the carbamoylase with a molecular weight of 35 kDa. The crude cell extract and wash 1 (lane **c** and **d**) of exhibits a very intensive band corresponding to the carbamoylase as well as proteins with other molecular weights with less intensity. The eluate only shows a band with a very high intensity for the carbamoylase.

These findings verify that after expression of the carbamoylase with a high yield of native enzyme in the crude cell extract, a successful purification of this enzyme without contamination bands was accomplished. Additionally, it was noticed that the supernatant after incubation of the crude cell extract with the functionalized magnetic beads still contained a band for the carbamoylase with nearly the same intensity as in the crude extract, indicating that a high amount of enzyme did not bind to the magnetic beads. Therefore, for example the incubation times or amounts of the crude cell extract with magnetic beads can still be optimized.

To evaluate this protocol, activity assays were carried out using 5 mM *NCPheAla* as a substrate and the corresponding results are summarized in Table 18.

**Table 18** Purification of the carbamoylase from *A. crystallopoietes* DSM 20117 via functionalized magnetic beads

Fraction	$A /$ mU/mL	$A_{vol} /$ mU/mL	$A_{tot} /$ mU	$c_{protein, tot} /$ mg	$A_{spez} /$ U/mg	Recovery / %	Purification fold
crude extract	76.4	152.9	152.9	15.57	0.010	-	-
eluate	49.7	99.4	49.7	0.04	1.243	32.5	126.6

The crude cell extract has a specific activity of 0.010 U/mg, while the purified carbamoylase results in a much higher specific activity of 1.243 U/mg, a recovery of 32.5 % and a 126.6 fold purification.

This determined specific activities proved a successful purification of the carbamoylase using functionalized magnetic beads with a high recovery as well as purification factor. The recovery was lower compared to the purification via Ni sepharose beads (around 68 %), while the purification factor was circa 2.5 times higher for the purification of the carbamoylase via functionalized magnetic beads. The lower recovery for this method can be explained by the large band for the carbamoylase remaining in the supernatant after incubation with the beads. The longer incubation times of the Ni sepharose protocol may cause a loss in carbamoylase activity due to oxidation as well as thermal instability.<sup>[132,219]</sup> These facts again highlight the advantages of using functionalized magnetic beads for purification as well as immobilization directly from the crude cell extract without previous purification steps. Nevertheless, magnetic beads are comparatively expensive and high batches for the purification of enzymes would cause very high costs and is therefore not profitable for industrial applications. Immobilization of enzymes by these beads displays a major benefit, since immobilized enzymes exhibited even higher activities compared to the purified enzymes using functionalized magnetic beads. This is suggested to be caused by higher oxidative as well as thermal stability of the carbamoylase after immobilization as also reported from other groups.<sup>[163,219]</sup> Pietzsch et al. purified the L-carbamoylase from *Arthrobacter aurescens* using IMAC chromatography with a specific activity of 5.9 U/mg, a yield of 55 % and a purification factor of 11.3.<sup>[225]</sup> Compared to the results shown above, the achieved specific activity and yield were slightly higher, while the purification factor was much lower. The lower recovery values in this work can be explained by the high amount of resulting carbamoylase in the supernatant after incubation with the magnetic beads. Therefore, the protocol has to be optimized regarding the incubation time or amount of applied crude cell extract. The very high purification factor is suggested to result on the one hand from higher stability of the carbamoylase in the immobilized form and on the other hand from very short incubation times when immobilizing the carbamoylase directly from the crude cell extract. Furthermore, no previous purification of the enzyme is necessary, avoiding loss of enzyme during purification steps.

For further investigation of this purification and immobilization method, the beads that were subjected to elution were subsequently treated with a 1 % SDS solution for 20 min at 95 °C (eluate 2). Table 19 shows the protein concentrations of the elution step compared to the protein concentrations after SDS treatment.

**Table 19** Comparison of protein concentrations of eluate 1 and 2 after immobilization or purification of the hydantoinase as well as carbamoylase from *A. crystallopoietes* DSM20117

	<b>Eluate 1</b> $c_{protein}/\text{mg/mL}$	<b>Eluate 2</b> $c_{protein}/\text{mg/mL}$
<b>hydantoinase</b>	0.103	0.325
<b>carbamoylase</b>	0.081	0.271

For both enzymes, the protein concentration of eluate 1 is lower than for eluate 2, while protein concentrations for the hydantoinase are generally slightly higher than for the carbamoylase. This finding showed that the elution step of this protocol was not sufficient and by treatment with 1 % SDS, every remaining attached protein was removed. Consequently, especially regarding the purification of enzymes, this protocol has to be optimized regarding the elution step to achieve a higher recovery. Additionally, for obtaining more precise information about the protein concentrations used for immobilization, an optimization is necessary.

#### 4.3.4 COMPARISON OF PURIFICATION AND IMMOBILIZATION OF THE HYDANTOINASE AND CARBAMOYLASE

To enable a better overview of the results regarding purification and immobilization, Table 20 shows the values determined in this work compared to values from literature.

**Table 20** Overview of investigated purification and immobilization methods for the enzymes from *A. crystallopoietes* DSM 20117 employing the His-tag and comparison to other works. Values for the hydantoinase (*cyan*) and carbamoylase (*grey*) determined in this work (*dark*) compared to values reported in literature (*light*). Ni sepharose purification: elution 1 + elution 2

	Via	Enzyme	$A_{spez}/$ U/mg	Recovery / %	Purification fold	Reference
<b>Ni sepharose purification</b>	Ni sepharose beads	<b>Hyd</b>	0.025	11.2	23.7	
	IMAC chromatography	<b>Hyd</b>	1.130	16.6	22.6	Xu et al. <sup>[101]</sup>
	Ni sepharose beads	<b>Carb</b>	0.855	67.5	50.9	
	IMAC chromatography	<b>Carb</b>	7.540	70.0	-	Chen et al. <sup>[215]</sup>
<b>functionalized magnetic bead purification</b>	functionalized magnetic beads	<b>Hyd</b>	0.046	11.9	35.9	
	IMAM <sup>a</sup>	<b>Hyd</b>	1.360	3.5	6.8	Ko et al. <sup>[213]</sup>
	functionalized magnetic beads	<b>Carb</b>	1.243	32.5	126.6	
	IMAC chromatography	<b>Carb</b>	5.900	55.0	11.3	Pietzsch et al. <sup>[214]</sup>
<b>immobilization</b>	functionalized magnetic beads	<b>Hyd</b>	0.071	-	-	
	IMAM <sup>a</sup>	<b>Hyd</b>	5.790	-	-	Ko et al. <sup>[165]</sup>
	functionalized magnetic beads	<b>Carb</b>	12.906	-	-	
	Eupergit C	<b>Carb</b>	2.910	-	-	Yen et al. <sup>[223]</sup>

<sup>a</sup> immobilized metal ion affinity membrane

It has to be noted that every purification approach using metal ion affinity was compared with other works using IMAC chromatography for purification instead of batch approaches, since no such approaches have been reported yet. For immobilization using metal ion affinity, the most comparable approach was the work from Ko et al. applying a immobilized metal ion affinity membrane for the immobilization of the hydantoinase.<sup>[165]</sup> Regarding immobilization of the carbamoylase, there is nothing

reported using metal ion affinity until now, therefore an approach employing Eupergit C was utilized for comparison.<sup>[223]</sup>

#### 4.3.5 POTENTIAL APPLICATIONS

The purification as well as immobilization of both enzymes achieved in this work opens a lot of possibilities in their application. Especially microfluidic reaction systems are of growing interest in the fields of biotechnology, chemical engineering as well as chemistry. They allow the use of micro- and nanoliter volumes and are therefore highly efficient and reproducible. In contrast to most of the batch reaction systems, microfluidic devices provide rapid heat exchange, mass transfer and a laminar flow for strictly controlling the reaction conditions.<sup>[226]</sup> Other benefits are the efficient control of reactant streams and retention of the biocatalyst for potential reutilization. Furthermore, a continuous flow allows simple product removal and may avoid product inhibition.<sup>[227]</sup> There are various different techniques for immobilized enzyme reactors. It is either feasible to immobilize enzymes within microchannels by particle entrapment or the immobilization of enzymes is carried out on the microchannel surface itself. Additionally, enzyme-immobilization on a membrane is feasible.<sup>[226]</sup>

By means of the findings of this work, the Hydantoinase Process could be transferable for example to the two following different kinds of microfluidic reaction systems. On the one hand, in cooperation with the working group of Prof. Franzreb, a modular 3D-printed system for the immobilization of purified enzymes on the reactor surface is intended (see Figure 47).<sup>[228]</sup>

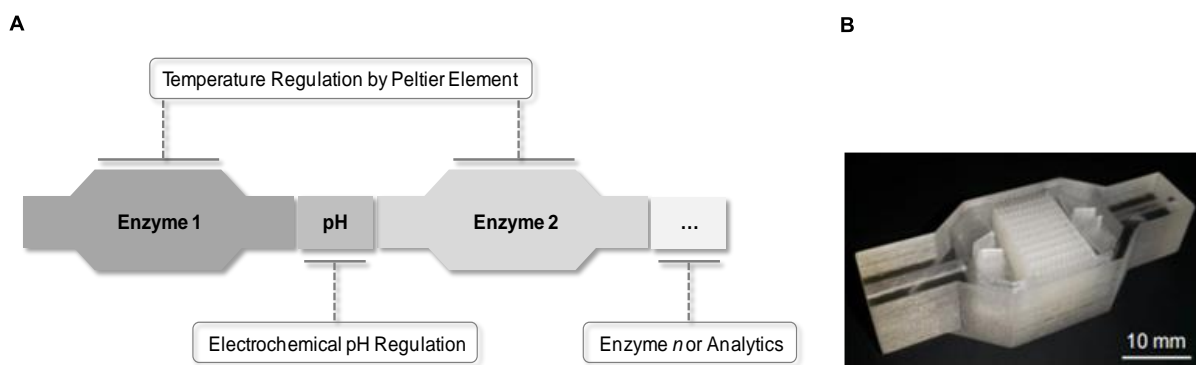


**Figure 47** Modular 3D-printed microfluidic system for immobilization of enzyme cascades. **A** Scheme of the modular setting. **B** Individual 3D-printed module. Modified after Kazenwadel et al.<sup>[228]</sup>

Another method to apply enzymes in a microfluidic reaction system is investigated by the working group of Prof. Niemeyer, applying a microchannel system with enzymes immobilized on functionalized magnetic beads (see Figure 48). Both systems allow regulation of temperature and pH and promise the realization of enzymatic enzyme cascades as for example the Hydantoinase Process.



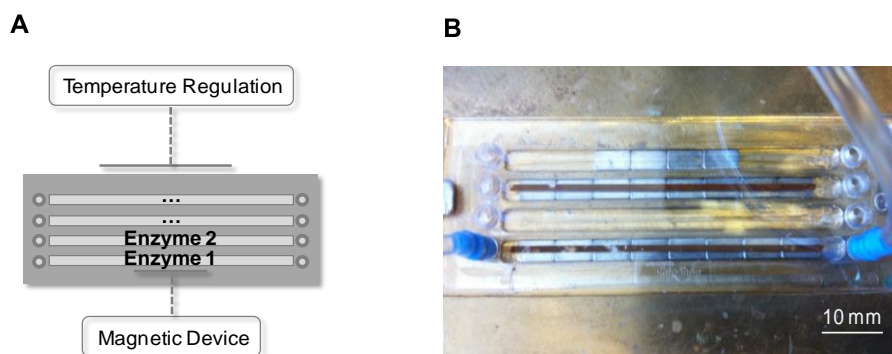


**Figure 48** Microchannel System for Reaction Cascades with Enzymes Immobilized on Magnetic Beads. **A** Scheme of the Microchannel System. **B** Photograph of the Microchannel System with Magnetic Beads.

#### 4.3.6 PURIFICATION OF INCLUSION BODIES

The drawback of insoluble expression of the hydantoinase from *A. crystallopoietes* DSM 20117 was attempted to convert into an advantage, since Diener et al. reported the application of catalytically active inclusion bodies.<sup>[149]</sup> After purification of hydantoinase inclusion bodies according to this protocol, various biotransformation assays were conducted (see Chapter 3.2.9.4). HPLC-analysis of every activity assay revealed no activity for the purified inclusion bodies toward the substrate PheHyd. Furthermore, SDS-PAGE analysis of the untreated insoluble fraction as well as the inclusion bodies was carried out (see Figure 49).

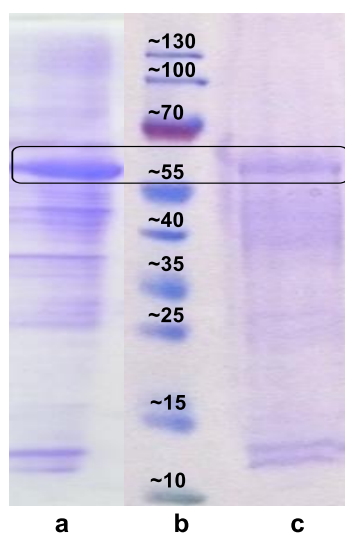


**Figure 49** SDS-PAGE Analysis before and after purification of inclusion bodies of the hydantoinase from *A. crystallopoietes* DSM 20117. **a** insoluble fraction **b** protein standard with molecular weights in kDa **c** purified inclusion bodies

The untreated insoluble fraction (lane a) shows a distinct band for the hydantoinase around 56 kDa as well as bands for other proteins as reported before. The analysis of the insoluble fraction treated

according to the protocol of Diener et al. shows a much slighter band compared to the insoluble fraction.

These results revealed that the purification of inclusion bodies using this protocol was not successful. In addition to the fact that no activity was determined for the inclusion bodies, the SDS-PAGE analysis resulted in a slighter band for the hydantoinase compared to the untreated insoluble fraction. Consequently, in this case the formation of inclusion bodies is not beneficial, since the concentration of soluble hydantoinase is reduced and the inclusion bodies themselves show no activity as reported from other groups that even force the formation of inclusion bodies.<sup>[148]</sup>

In addition to apply catalytically active inclusion bodies, the successful refolding of inclusion bodies was reported.<sup>[229]</sup> But even after considering every parameter that has to be adjusted in many refolding steps, the yield of regained native protein usually ranges between 10 and 50 %.<sup>[178]</sup> Therefore, the refolding of inclusion bodies was not investigated in this work.

## 5. REFERENCES

- [1] J. M. Clemente-Jimenez, S. Martinez-Rodriguez, F. Rodriguez-Vico, F. J. Heras-Vazquez, *Recent. Pat. Biotechnol.* **2008**, *2*, 35–46.
- [2] W. Leuchtenberger, K. Huthmacher, K. Drauz, *Appl. Microbiol. Biotechnol.* **2005**, *69*, 1–8.
- [3] J. D. J. Rozzell, B. P. Paulson, *Methods for Producing Diastereomers of Isoleucine*, **2004**.
- [4] A. L. Johnson, W. A. Price, P. C. Wong, R. F. Vavala, J. M. Stump, *J. Med. Chem.* **1985**, *28*, 1596–1602.
- [5] K. Hayashi, K. Nunami, J. Kato, N. Yoneda, M. Kubo, T. Ochiai, R. Ishida, *J. Med. Chem.* **1989**, *32*, 289–297.
- [6] C. Slomka, U. Engel, C. Sylдат, J. Rudat, in *Biocatal. Org. Synth.* (Eds.: K. Faber, W.-D. Fessner, N.J. Turner), Thieme, Stuttgart, **2014**, pp. 373–414.
- [7] D. Seebach, J. Gardiner, *Acc. Chem. Res.* **2008**, *41*, 1366–1375.
- [8] P. Crews, L. V Manes, M. Boehler, *Tetrahedron Lett.* **1986**, *27*, 2797–2800.
- [9] B. Weiner, W. Szymanski, D. B. Janssen, A. J. Minnaarda, B. L. Feringa, *Chem. Soc. Rev.* **2010**, *39*, 1656–1691.
- [10] R. P. Cheng, S. H. Gellman, W. F. DeGrado, *Chem. Rev.* **2001**, *101*, 3219–3232.
- [11] J. Frackenpohl, P. I. Arvidsson, J. V Schreiber, D. Seebach, *Chembiochem* **2001**, *2*, 445–455.
- [12] S. Servi, D. Tessaro, G. Pedrocchi-Fantoni, *Coord. Chem. Rev.* **2008**, *252*, 715–726.
- [13] P. A. Magriotis, *Angew. Chem. Int. Ed.* **2001**, *40*, 4377–4379.
- [14] E. Juaristi, in *Enantiosel. Synth. of  $\beta$ -Amino Acids* (Eds.: E. Juaristi, V.A. Soloshonok), John Wiley & Sons, Inc., New Jersey, **2005**, pp. 1–14.
- [15] G. Cardillo, C. Tomasini, *Chem. Soc. Rev.* **1996**, *25*, 117–128.
- [16] A. S. Bommarius, M. Schwarm, K. Drauz, *Ind. Biocatal.* **2001**, *55*, 50–59.
- [17] O. May, S. Verseck, A. Bommarius, K. Drauz, *Org. Process Res. Dev.* **2002**, *6*, 452–457.
- [18] H. Pellissier, *Tetrahedron* **2003**, *59*, 8291–8327.
- [19] S. Tokuyama, H. Miya, K. Hatano, T. Takahashi, *Appl. Microbiol. Biotechnol.* **1994**, *40*, 835–840.
- [20] C. Sylдат, O. May, J. Altenbuchner, R. Mattes, M. Siemann, *Appl. Microbiol. Biotechnol.* **1999**, *51*, 293–309.
- [21] M. Liu, M. P. Sibi, *Tetrahedron* **2002**, *58*, 7991–8035.
- [22] S.-M. Dold, C. Sylдат, J. Rudat, in *Green Biocatal.* (Ed.: R.N. Patel), Wiley-VCH, **2016**, p. 872.
- [23] J. Rehdorf, M. D. Mihovilovic, U. T. Bornscheuer, *Angew. Chem. Int. Ed. Engl.* **2010**, *49*, 4506–4508.
- [24] B. Wu, W. Szymanski, P. Wietzes, S. de Wildemann, G. J. Poelarends, B. L. Feringa, D. B. Janssen, *Chembiochem* **2009**, *10*, 338–344.
- [25] A. Liljeblad, L. T. Kanerva, *Tetrahedron* **2006**, *58*, 5831–5854.
- [26] G. Tasnádi, E. Forró, F. Füllöp, *Tetrahedron: Asymmetr.* **2008**, *19*, 2072–2077.
- [27] H. Yamada, S. Takahashi, Y. Kii, H. Kumagai, *J. Ferment. Technol.* **1978**, *56*, 484–491.
- [28] M. Kato, H. Kitagawa, T. Myoshi, *Microbial Racemization of Optically Active 5-Substituted Hydantions*, **1987**.
- [29] M. Pietzsch, C. Sylдат, F. Wagner, *Biotechnol. Conf.* **1990**, *4*, 259–262.
- [30] C. Mateo, J. M. Palomo, G. Fernandez-Lorente, J. M. Guisan, R. Fernandez-Lafuente, *Enzyme Microb. Technol.* **2007**, *40*, 1451–1463.
- [31] U. Engel, C. Sylдат, J. Rudat, *Appl. Microbiol. Biotechnol.* **2012**, *94*, 1221–1231.
- [32] O. May, M. Siemann, M. Pietzsch, M. Kiess, R. Mattes, C. Sylдат, *J. Biotechnol.* **1998**, *61*, 1–13.

- [33] S. Servi, C. Syldatk, O. Vielhauer, D. Tessaro, *Poster Commun. Biotrans. Delft* **2005**.
- [34] M. O'Neill, B. Hauer, N. Schneider, N. J. Turner, *ACS Catal.* **2011**, *1*, 1014–1016.
- [35] A. I. Martínez-Gómez, J. M. Clemente-Jimenez, F. Rodríguez-Vico, L. T. Kanerva, X. G. Li, F. J. Heras-Vazquez, S. Martínez-Rodríguez, *Process Biochem.* **2012**, *47*, 2090–2096.
- [36] U. Engel, C. Syldatk, J. Rudat, *AMB Express* **2012**, *2*, 33.
- [37] A. Baeyer, *Liebigs Ann. Chem.* **1861**, *117*, 178–180.
- [38] E. G. Young, H. P. Wentworth, W. W. Hawkins, *J. Pharmacol. Exp. Ther.* **1944**, *81*, 1–9.
- [39] G. R. Pettit, C. L. Herald, J. E. Leet, R. Gupta, D. E. Schaufelberger, R. B. Bates, P. J. Clewlow, D. L. Doubek, K. P. Manfredi, K. Rützler, et al., *Can. J. Chem.* **1990**, *68*, 1621–1624.
- [40] H. Uemoto, M. Tsuda, J. Kobayashi, H. Uemoto, M. Tsuda, J. Kobayashi, *J. Nat. Prod.*, *62*, 1581 (1999). **1999**, *62*, 1581.
- [41] N. Nakajima, M. Matsumoto, M. Kirihara, M. Hashimoto, T. Katoh, S. Terashima, *Tetrahedron* **1996**, *52*, 1177–1194.
- [42] M. Meusel, M. Gütschow, *Org. Prep. Proced. Int.* **2004**, *36*, 391–443.
- [43] J. Ogawa, N. Horinouchi, S. Shimizu, in *Enzym. Catal. Org. Synth.* (Eds.: K. Drauz, H. Gröger, O. May), Wiley-VCH, Weinheim, **2012**, pp. 651–674.
- [44] F. J. Las Heras-Vazquez, J. M. Clemente-Jimenez, S. Martinez-Rodriguez, F. Rodriguez-Vico, in *Mod. Biocatal.* (Eds.: W.D. Fessner, T. Anthonsen), WILEY-VCH Verlag GmbH & Co. KGaA, Weinheim, **2009**, p. 173.
- [45] G. S. Eadie, F. Bernheim, M. L. Bernheim, *J. Biol. Chem.* **1949**, *181*, 449–458.
- [46] K. H. Dudley, D. L. Bius, *Drug Metab. Dispos.* **1973**, *2*, 103–112.
- [47] K. H. Dudley, D. L. Bius, T. C. Butler, *J. Pharmacol. Exp. Ther.* **1970**, *175*, 27–37.
- [48] F. Cecere, G. Galli, F. Morisi, *FEBS Lett* **1975**, *57*, 192–194.
- [49] R. Olivieri, E. Fascetti, L. Angelini, L. Degen, *Enzym. Microb. Technol.* **1979**, *1*, 201–204.
- [50] A. Morin, W. Hummel, M.-R. Kula, *Biotechnol. Lett.* **1986**, *8*, 573–576.
- [51] G. LaPointe, S. Viau, D. LeBlanc, N. Robert, A. Morin, *Appl. Environ. Microbiol.* **1994**, *60*, 888–895.
- [52] H. Yamada, S. Shimizu, H. Shimada, Y. Tani, S. Takahashi, T. Ohashi, *Biochimie* **1980**, *62*, 395–399.
- [53] Y. Ikenaka, H. Nanba, K. Yajima, Y. Yamada, M. Takano, S. Takahashi, *Biosci. Biotechnol. Biochem.* **1999**, *63*, 91–95.
- [54] S. Runser, N. Chinski, E. Ohleyer, *Appl. Microbiol. Biotechnol.* **1990**, *33*, 382–388.
- [55] K. Yokozeki, S. Nakamori, S. Yamanaka, C. Eguchi, K. Mitsugi, F. Yoshinaga, *Agric. Biol. Chem.* **1987**, *51*, 715–719.
- [56] S. M. Runser, P. C. Meyer, *Eur. J. Biochem.* **1993**, *213*, 1315–1324.
- [57] G. J. Kim, D. E. Lee, H. S. Kim, *J. Bacteriol.* **2000**, *182*, 7021–7028.
- [58] A. Morin, *Enzym. Microb. Tech.* **1993**, *15*, 208–214.
- [59] J. H. Chung, J. H. Back, J. Lim, Y. I. Park, Y. S. Han, *Enzym. Microb. Tech.* **2002**, *30*, 867–874.
- [60] U. Engel, J. Rudat, C. Syldatk, in *Ind. Biocatal.* (Ed.: P. Grunwald), Pan Stanford Publishing Pte. Ltd., Singapore, **2014**, pp. 817–862.
- [61] E. Ware, *Chem. Rev.* **1950**, *46*, 403–470.
- [62] F. J. Las Heras-Vazquez, J. M. Clemente-Jimenez, S. Martinez-Rodriguez, F. Rodriguez-Vico, in *Mod. Biocatal. Stereoselective Environ. Friendly React.* (Eds.: W.D. Fessner, T. Anthonsen), Wiley-VCH, Weinheim, **2009**, p. 173.
- [63] R. R. Lazarus, *J. Org. Chem.* **1990**, *55*, 4755–4757.
- [64] M. Pietzsch, C. Syldatk, in *Enzym. Catal. Org. Synth. A Compr. Handb.* (Eds.: K. Drauz, H. Waldmann), Wiley-VCH, Weinheim, **2002**, pp. 761–799.
- [65] S. Martinez-Rodriguez, F. J. Las Heras-Vazquez, J. M. Clemente-Jimenez, F. Rodriguez-Vico, *Biochimie* **2004**, *86*, 77–81.
- [66] S. Martínez-Rodríguez, F. J. Las Heras-Vazquez, L. Mingorance-Cazorla, J. M. Clemente-Jimenez, F. Rodriguez-Vico, *Appl. Environ. Microbiol.* **2004**, *70*, 625–630.

- [67] S. Suzuki, N. Onishi, K. Yokozeki, *Biosci. Biotechnol. Biochem.* **2005**, *69*, 530–536.
- [68] A. Argyrou, M. W. Washabaugh, *J. Am. Chem. Soc.* **1999**, *121*, 12054–12062.
- [69] B. H., *Chem. Abstr.* **1929**, 27.
- [70] S. L. Dax, J. J. McNally, M. A. Youngman, in *Curr. Med. Chem.* (Ed.: Atta-ur-Rahman), Bentham Science Publishers, **1999**, pp. 255–270.
- [71] C. Montagne, M. Shipman, *Synlett n.d.*, 2203–2206.
- [72] E. Gallienne, G. G. Muccioli, D. M. Lambert, M. Shipman, *Tetrahedron Lett.* **2008**, *49*, 6495–6497.
- [73] C. Montagne, J. J. Shiers, M. Shipman, *Tetrahedron Lett.* **2006**, *47*, 9207–9209.
- [74] P. Biginelli, *Gazz. Chim. Ital.* **1893**.
- [75] O. Kappe, *Acc. Chem. Res.* **2000**, *33*, 879–888.
- [76] J. Světlík, L. Veizerová, *Helv. Chim. Acta* **2011**, *94*, 199–205.
- [77] K. S. Atwal, G. C. Rovnyak, B. C. O'Reilly, J. Schwartz, *J. Org. Chem.* **1989**, *54*, 5898–5907.
- [78] A. D. Shutalev, E. A. Kishko, N. V. Sivova, A. Y. Kuznetsov, *Molecules* **1998**, *3*, 100–106.
- [79] S. H. Nam, H. S. Park, H. S. Kim, *Chem. Rec.* **2005**, *5*, 298–307.
- [80] G. J. Kim, H. S. Kim, *Biochem. J.* **1998**, *330*, 295–302.
- [81] L. Holm, C. Sander, *Proteins* **1997**, *28*, 72–82.
- [82] B. H. Zimmermann, N. M. Kemling, D. R. Evans, *Biochemistry* **1995**, *34*, 7038–7046.
- [83] J. B. Thoden, G. N. Phillips Jr., T. M. Neal, F. M. Raushel, H. M. Holden, *Biochemistry* **2001**, *40*, 6989–6997.
- [84] J. Abendroth, K. Niefind, D. Schomburg, *J. Mol. Biol.* **2002**, *320*, 143–156.
- [85] Y.-H. Cheon, H.-S. Kim, K.-H. Han, J. Abendroth, K. Niefind, D. Schomburg, J. Wang, Y. Kim, *Biochemistry* **2002**, *41*, 9410–9417.
- [86] P. D. Martin, C. Purcarea, P. Zhang, A. Vaishnav, S. Sadecki, H. I. Guy-Evans, D. R. Evans, B. F. Edwards, *J. Mol. Biol.* **2005**, *348*, 535–547.
- [87] D. P. Wallach, S. Grisolia, *J. Biol. Chem.* **1956**, *226*, 277–288.
- [88] E. C. Webb, in *Enzym. Nomencl. 1992*, Academic Press, San Diego, **1992**.
- [89] N. Hamajima, K. Matsuda, S. Sakata, N. Tamaki, M. Sasaki, M. Nonaka, *Gene* **1996**, *180*, 157–163.
- [90] M. Kikugawa, M. Kaneko, S. Fujimoto-Sakata, M. Maeda, K. Kawasaki, T. Takagi, N. Tamaki, *Eur. J. Biochem.* **1994**, *219*, 393–399.
- [91] A. Morin, W. Hummel, H. Schutte, M. R. Kula, *Biotechnol. Appl. Biochem.* **1986**, *8*, 564–574.
- [92] S. Takahashi, Y. Kii, H. Kumagai, H. Yamada, *J. Ferment. Technol.* **1978**, *56*, 492–498.
- [93] J. Yoon, B. Oh, K. Kim, J. E. Park, J. Wang, H. S. Kim, Y. Kim, *Biochem. Biophys. Res. Commun.* **2003**, *310*, 651–659.
- [94] K. P. Brooks, E. A. Jones, B. D. Kim, E. G. Sander, *Arch. Biochem. Biophys.* **1983**, *226*, 469–483.
- [95] J. Ogawa, S. Shimizu, *J. Mol. Catal.* **1997**, *2*, 163–176.
- [96] O. May, M. Siemann, M. G. Siemann, C. Syldatk, *J. Mol. Catal. B Enzym.* **1998**, *4*, 211–218.
- [97] J. T. Groves, J. R. Olson, *Inorg. Chem.* **1985**, *24*, 2715–2717.
- [98] C. L. Soong, J. Ogawa, M. Honda, S. Shimizu, *Appl. Environ. Microbiol.* **1999**, *65*, 1459–1462.
- [99] Y. H. Cheon, H. S. Park, J. H. Kim, Y. Kim, H. S. Kim, *Biochemistry* **2004**, *43*, 7413–7420.
- [100] J. Abendroth, K. Niefind, O. May, M. Siemann, C. Syldatk, D. Schomburg, *Biochemistry* **2002**, *41*, 8589–8597.
- [101] Z. Xu, Y. Liu, Y. Yang, W. Jiang, E. Arnold, J. Ding, *J. Bacteriol.* **2003**, *185*, 4038–4049.
- [102] S. Lundgren, Z. Gojkovic, J. Piskur, D. Dobritsch, *J. Biol. Chem.* **2003**, *278*, 51851–51862.
- [103] T. A. Walsh, S. B. Green, I. M. Larrinua, P. R. Schmitzer, *Plant Physiol.* **2001**, *125*,

- 1001–1011.
- [104] A. I. Martinez-Gomez, S. Martinez-Rodriguez, J. Pozo-Dengra, D. Tessaro, S. Servi, J. M. Clemente-Jimenez, F. Rodriguez-Vico, F. J. Las Heras-Vazquez, *Appl. Environ. Microbiol.* **2009**, *75*, 514–520.
- [105] Z. Gojkovic, M. P. Sandrini, J. Piskur, *Genetics* **2001**, *158*, 999–1011.
- [106] K. L. Kvalnes-Krick, T. W. Traut, *J. Biol. Chem.* **1993**, *268*, 5686–5693.
- [107] P. Vreken, A. B. van Kuilenburg, N. Hamajima, R. Meinsma, H. van Lenthe, G. Gohlich-Ratmann, B. E. Assmann, R. A. Wevers, A. H. van Gennip, *Biochim. Biophys. Acta* **1999**, *1447*, 251–257.
- [108] G. Waldmann, P. F. Cook, K. D. Schnackerz, *Protein Pept. Lett.* **2005**, *12*, 69–73.
- [109] J. Ogawa, H. Miyake, S. Shimizu, *Appl. Microbiol. Biotechnol.* **1995**, *43*, 1039–1043.
- [110] N. Batisse, P. Weigel, M. Lecocq, V. Sakanyan, *Appl. Environ. Microbiol.* **1997**, *63*, 763–766.
- [111] J. Pozo-Dengra, A. I. Martinez-Gomez, S. Martinez-Rodriguez, J. M. Clemente-Jimenez, F. Rodriguez-Vico, F. J. Las Heras-Vazquez, *Biotechnol. Prog.* **2010**, *26*, 954–959.
- [112] B. Wilms, A. Wiese, C. Sylatk, R. Mattes, J. Altenbuchner, M. Pietzsch, *J. Biotechnol.* **1999**, *68*, 101–113.
- [113] T. Shiba, K. Takeda, M. Yajima, M. Tadano, *Appl. Environ. Microbiol.* **2002**, *68*, 2179–2187.
- [114] T. Ohmachi, M. Nishino, M. Kawata, N. Edo, H. Funaki, M. Narita, K. Mori, Y. Tamura, Y. Asada, *Biosci. Biotechnol. Biochem.* **2002**, *66*, 1097–1104.
- [115] T. Ohmachi, M. Narita, M. Kawata, A. Bizen, Y. Tamura, Y. Asada, *Appl. Microbiol. Biotechnol.* **2004**, *65*, 686–693.
- [116] S. Martinez-Rodriguez, A. I. Martinez-Gomez, F. Rodriguez-Vico, J. M. Clemente-Jimenez, F. J. Las Heras-Vazquez, *Appl. Microbiol. Biotechnol.* **2010**, *85*, 441–458.
- [117] J. Ogawa, M. C.-M. Chung, S. Hida, H. Yamada, S. Shimizu, *J. Biotechnol.* **1994**, *38*, 11–19.
- [118] T. Nakai, T. Hasegawa, E. Yamashita, M. Yamamoto, T. Kumasaka, T. Ueki, H. Nanba, Y. Ikenaka, S. Takahashi, M. Sato, et al., *Structure* **2000**, *8*, 729–739.
- [119] A. Louwrier, C. J. Knowles, *Enzym. Microb. Technol.* **1996**, *19*, 562–571.
- [120] W.-C. Wang, W.-H. Hsu, F.-T. Chien, C.-Y. Chen, *J. Mol. Biol.* **2001**, *306*, 251–261.
- [121] R. Grifantini, C. Pratesi, G. Galli, G. Grandi, *J. Biol. Chem.* **1996**, *271*, 9326–9331.
- [122] S. Martínez-Rodríguez, A. García-Pino, F. J. Las Heras-Vázquez, J. M. Clemente-Jiménez, F. Rodríguez-Vico, J. M. García-Ruiz, R. Loris, J. A. Gavira, *J. Bacteriol.* **2012**, *194*, 5759–5768.
- [123] C. E. Hodgman, M. C. Jewett, *Metab. Eng.* **2012**, *14*, 261–269.
- [124] A. C. Forster, G. M. Church, A. C. Forster, G. M. Church, **2007**, 1–6.
- [125] J. R. Swartz, *AIChE J.* **2011**, *58*, 5–13.
- [126] D.-C. Lee, H.-S. Kim, *Biotechnol. Bioeng.* **1998**, *60*, 729–738.
- [127] M. F. Deeb, J. M. Lee, *Biotechnol. Bioeng. Symp.* **1985**, *15*, 227–293.
- [128] D. C. Lee, J. H. Park, G. J. Kim, H. S. Kim, *Biotechnol. Bioeng.* **1999**, *64*, 272–283.
- [129] R. Chen, *Biotechnol. Adv.* **2012**, *30*, 1102–1107.
- [130] O. May, P. T. Nguyen, F. H. Arnold, *Nat. Biotechnol.* **2000**, *18*, 317–320.
- [131] K. H. Oh, S. H. Nam, H. S. Kim, *Protein Eng.* **2002**, *15*, 689–695.
- [132] K. H. Oh, S. H. Nam, H. S. Kim, *Biotechnol. Prog.* **2002**, *18*, 413–417.
- [133] C.-H. Fan, C.-K. Lee, *Biochem. Eng. J.* **2001**, *8*, 157–164.
- [134] C. Kurland, J. Gallant, *Curr. Opin. Biotechnol.* **1996**, *7*, 489–493.
- [135] E. Angov, C. J. Hillier, R. L. Kincaid, J. A. Lyon, *PLoS One* **2008**, *3*, 1–10.
- [136] G. Kramer, V. Ramachandiran, B. Hardesty, *Int. J. Biochem. Cell Biol.* **2001**, *33*, 541–553.
- [137] R. Berisio, F. Schluenzen, J. Harms, A. Bashan, T. Auerbach, D. Baram, A. Yonath, *Nat. Struct. Biol.* **2003**, *10*, 366–370.
- [138] S. Varenne, J. Buc, R. Lloubes, C. Lazdunski, *J. Mol. Biol.* **1984**, *180*, 549–576.
- [139] T. a Thanaraj, P. Argos, *Protein Sci.* **1996**, *5*, 1594–1612.
- [140] T. a Thanaraj, P. Argos, *Protein Sci.* **1996**, *5*, 1973–1983.

- [141] G. A. Bowden, A. M. Paredes, G. Georgiou, *Biotechnology. (N. Y.)* **1991**, 9, 725–730.
- [142] L. Strandberg, S. O. Enfors, *Appl. Envir. Microbiol.* **1991**, 57, 1669–1674.
- [143] K. Terpe, *Appl. Microbiol. Biotechnol.* **2003**, 60, 523–533.
- [144] J. G. Thomas, F. Baneyx, *J. Biol. Chem.* **1996**, 271, 11141–11147.
- [145] A. De Marco, E. Deuerling, A. Mogk, T. Tomoyasu, B. Bukau, *BMC Biotechnol.* **2007**, 9, 1–9.
- [146] A. Singh, V. Upadhyay, A. K. Panda, *Methods Mol. Biol.* **2015**, 1258, 283–291.
- [147] L. F. Vallejo, U. Rinas, *Microb. Cell Fact.* **2004**, 3, 11.
- [148] E. García-Fruitós, N. González-Montalbán, M. Morell, A. Vera, R. M. Ferraz, A. Arís, S. Ventura, A. Villaverde, *Microb. Cell Fact.* **2005**, 4, 27.
- [149] M. Diener, B. Kopka, M. Pohl, K. E. Jaeger, U. Krauss, *ChemCatChem* **2015**, 142–152.
- [150] J. Porath, J. Carlsson, I. Olsson, G. Belfrage, *Nature* **1975**, 258, 598–599.
- [151] E. Hochuli, W. Bannwarth, H. Dobeli, R. Gentz, D. Stuber, *Biotechnology* **1988**, 6, 1321–1325.
- [152] G. Chaga, J. Hopp, P. Nelson, C. Laboratories, E. M. Circle, P. Alto, *Biotechnol. Appl. Biochem.* **1999**, 24, 19–24.
- [153] T. G. Schmidt, a Skerra, *Protein Eng.* **1993**, 6, 109–122.
- [154] I. P. Korndörfer, A. Skerra, *Protein Sci.* **2002**, 883–893.
- [155] D. S. Wilson, A. D. Keefe, J. W. Szostak, *Proc. Natl. Acad. Sci. U. S. A.* **2001**, 98, 3750–5.
- [156] J. J. Lichty, J. L. Malecki, H. D. Agnew, D. J. Michelson-Horowitz, S. Tan, *Protein Expr. Purif.* **2005**, 41, 98–105.
- [157] S. Voss, A. Skerra, *Protein Eng.* **1997**, 10, 975–82.
- [158] A. Skerra, T. G. M. Schmidt, *Biomol. Eng.* **1999**, 16, 79–86.
- [159] D.-C. Lee, S.-G. Lee, H.-S. Kim, *Enzym. Microb. Technol.* **1996**, 18, 35–40.
- [160] P. Meyer, S. Runser, *FEMS Microbiol. Lett.* **1993**, 109, 67–74.
- [161] I. M. Foster, R. D. Dorrington, S. G. Burton, *Biotechnol. Lett.* **2003**, 25, 67–72.
- [162] M. Pietzsch, H. Oberreuter, B. Petrovska, K. Ragnitz, C. Syldatk, *Prog. Biotechnol.* **1998**, 15, 517–522.
- [163] K. Ragnitz, M. Pietzsch, C. Syldatk, *J. Biotechnol.* **2001**, 92, 179–186.
- [164] B. T. Bulawayo, R. A. Dorringtonb, S. G. Burtona, *Enzym. Microb. Tech.* **2006**, 40, 533–539.
- [165] Y. M. Ko, C. I. Chen, C. J. Shieh, Y. C. Liu, *Biochem. Eng. J.* **2012**, 61, 20–27.
- [166] L. F. Ho, S. Y. Li, S. C. Lin, W. H. Hsu, *Process Biochem.* **2004**, 39, 1573–1581.
- [167] Y. M. Ko, C. I. Chen, C. C. Lin, S. C. Kan, C. Z. Zang, C. W. Yeh, W. F. Chang, C. J. Shieh, Y. C. Liu, *Biochem. Eng. J.* **2013**, 79, 200–205.
- [168] M. Werner, F. J. Las Heras-Vazquez, C. Fritz, O. Vielhauer, M. Siemann, J. Altenbuchner, C. Syldatk, *Eng. Life Sci.* **2004**, 4, 563–572.
- [169] U. K. (1970): Laemmli, *Nature* **1970**, 227, DOI 10.1038/227680a0.
- [170] T. Posner, *Justus Liebigs Ann. Chem.* **1912**, 389, 1–120.
- [171] M. Kolšek, J. Novak, N. Perpar, *Fresenius' Zeitschrift für Anal. Chemie* **1957**, 1, 113–117.
- [172] E. W. Yemm, E. C. Cocking, R. E. Ricketts, *Analyst* **1955**, 80, 209.
- [173] C. L. A. Schmidt, Ed. , *The Chemistry of the Amino Acids and Proteins*, **1938**.
- [174] D. J. McCaldin, *Chem. Rev.* **1960**, 60, 39–51.
- [175] J. Almog, in *Adv. Fingerpr. Technol.* (Eds.: H.C. Lee, R.E. Gaensslen), **2001**, p. 181.
- [176] J. H. Park, G. J. Kim, H. S. Kim, *Biotechnol. Prog.* **2000**, 16, 564–570.
- [177] C.-H. Kao, H.-H. Lo, S.-K. Hsu, W.-H. Hsu, *J. Biotechnol.* **2008**, 134, 231–9.
- [178] M. M. Carrió, A. Villaverde, *J. Biotechnol.* **2002**, 96, 3–12.
- [179] M. Martínez-Alonso, N. González-Montalbán, E. García-Fruitós, A. Villaverde, *Microb. Cell Fact.* **2009**, 8, 4.
- [180] H. P. Sørensen, K. K. Mortensen, *Microb. Cell Fact.* **2005**, 4, 1.
- [181] P. Baumann, N. Bluthardt, S. Renner, H. Burghardt, A. Osberghaus, J. Hubbuch, *J. Biotechnol.* **2015**, 200, 27–37.
- [182] G. Georgiou, P. Valax, *Curr. Opin. Biotechnol.* **1996**, 7, 190–197.

- [183] G. Georgiou, P. Valax, M. Ostermeier, P. M. Horowitz, *Protein Sci.* **1994**, *3*, 1953–1960.
- [184] R. Wetzel, *Trends Biotechnol.* **1994**, *12*, 193–198.
- [185] J. King, C. Haase-Pettingell, A. S. Robinson, M. Speed, A. Mitraki, *FASEB J.* **1996**, *10*, 57–66.
- [186] B. Gasser, M. Saloheimo, U. Rinas, M. Dragosits, E. Rodríguez-Carmona, K. Baumann, M. Giuliani, E. Parrilli, P. Branduardi, C. Lang, et al., *Microb. Cell Fact.* **2008**, *7*, 11.
- [187] Y. Tong, S. Feng, Y. Xin, H. Yang, L. Zhang, W. Wang, W. Chen, *J. Biotechnol.* **2016**, *218*, 75–84.
- [188] N. Mertens, E. Remaut, W. Fiers, *Biotechnology* **1995**, *13*, 175–179.
- [189] J. W. Dubendorf, F. W. Studier, *J. Mol. Biol.* **1991**, *219*, 45–59.
- [190] F. W. Studier, *J. Mol. Biol.* **1991**, *219*, 37–44.
- [191] Y. Cai, P. Trodler, S. Jiang, W. Zhang, Y. Wu, Y. Lu, S. Yang, W. Jiang, *FEBS J.* **2009**, *276*, 3575–3588.
- [192] A. Kondo, J. Kohda, Y. Endo, T. Shiromizu, Y. Kurokawa, K. Nishihara, H. Yanagi, T. Yura, H. Fukuda, *J. Biosci. Bioeng.* **2000**, *90*, 600–606.
- [193] R. Levy, R. Weiss, G. Chen, B. L. Iverson, G. Georgiou, *Protein Expr. Purif.* **2001**, *23*, 338–347.
- [194] P. Blum, J. Ory, J. Bauernfeind, J. Krska, *J. Bacteriol.* **1992**, *174*, 7436–7444.
- [195] H. Mirzahoseini, M. Alibolandi, *J. Sci. I. R. Iran* **2009**, *20*, 305–310.
- [196] M. Martínez-Alonso, E. García-Fruitós, N. Ferrer-Miralles, U. Rinas, A. Villaverde, *Microb. Cell Fact.* **2010**, *9*, 64.
- [197] A. Gragerov, E. Nudler, N. Komissarova, G. A. Gaitanaris, M. E. Gottesman, V. Nikiforov, *Proc. Natl. Acad. Sci. U. S. A.* **1992**, *89*, 10341–10344.
- [198] S. G. Kim, D. H. Kweon, D. H. Lee, Y. C. Park, J. H. Seo, *Protein Expr. Purif.* **2005**, *41*, 426–432.
- [199] K. Nishihara, M. Kanemori, H. Yanagi, T. Yura, *Appl. Environ. Microbiol.* **2000**, *66*, 884–889.
- [200] S. MYu, A. L. Goldberg, *EMBO J.* **1992**, *11*, 71–77.
- [201] D. Straus, W. Walter, C. A. Gross, *Genes Dev.* **1990**, *4*, 2202–2209.
- [202] E. García-Fruitós, M. Martínez-Alonso, N. González-Montalbán, M. Valli, D. Mattanovich, A. Villaverde, *J. Mol. Biol.* **2007**, *374*, 195–205.
- [203] O. Kolaj, S. Spada, S. Robin, J. G. Wall, *Microb. Cell Fact.* **2009**, *8*, 9.
- [204] C. Sakikawa, H. Taguchi, Y. Makino, M. Yoshida, *J. Biol. Chem.* **1999**, *274*, 21251–21256.
- [205] A. Endo, Y. Kurusu, *Biosci. Biotechnol. Biochem.* **2007**, *71*, 1073–1077.
- [206] O. Kandror, M. Sherman, A. Goldberg, *J. Biol. Chem.* **1999**, *274*, 37743–37749.
- [207] O. Kandror, L. Busconi, M. Sherman, A. L. Goldberg, *J. Biol. Chem.* **1994**, *269*, 23575–23582.
- [208] D. Zahrl, A. Wagner, M. Tscherner, G. Koraimann, *J. Bacteriol.* **2007**, *189*, 5885–5894.
- [209] O. May, M. Siemann, C. Sylдатk, *Biotechnol Tech* **1998**, *12*, 309–312.
- [210] V. Orr, L. Zhong, M. Moo-Young, C. P. Chou, *Biotechnol. Adv.* **2013**, *31*, 450–65.
- [211] M. Siemann, Á. Alvarado-Marín, M. Pietzsch, C. Sylдатk, *J. Mol. Catal. B Enzym.* **1999**, *6*, 387–397.
- [212] K. Ragnitz, C. Sylдатk, M. Pietzsch, *Enzym. Microb. Tech.* **2001**, *28*, 713–720.
- [213] Y. M. Ko, C. I. Chen, H. C. Chang, H. M. Chen, C. J. Shieh, Y. J. Syu, Y. C. Liu, *J. Taiwan Inst. Chem. Eng.* **2011**, *42*, 735–740.
- [214] M. Pietzsch, A. Wiese, K. Ragnitz, B. Wilms, J. Altenbuchner, R. Mattes, C. Sylдатk, *J. Chromatogr. B* **2000**, *737*, 179–186.
- [215] H. M. Chen, C. W. Ho, J. W. Liu, K. Y. Lin, Y. T. Wang, C. H. Lu, H. L. Liu, *Biotechnol. Prog.* **2003**, *19*, 864–873.
- [216] A. Buson, A. Negro, L. Grassato, M. Tagliaro, M. Basaglia, C. Grandi, A. Fontana, M. P. Nuti, *FEMS Microbiol. Lett.* **1996**, *145*, 55–62.
- [217] W. Konigsberg, *Methods Enzymol.* **1972**, *25*, 185–8.



- [218] C. E. Bandtlow, R. Heumann, M. E. Schwab, H. Thoenen, *EMBO J.* **1987**, *6*, 891–9.
- [219] C.-J. Chiang, J.-T. Chern, J.-Y. Wang, Y.-P. Chao, *J. Agric. Food Chem.* **2008**, *56*, 6348–6354.
- [220] H. S. Nandanwar, R. M. Vohra, G. S. Hoondal, *Biotechnol. Appl. Biochem.* **2013**, *60*, 305–315.
- [221] R. R. Burgess, in *Methods Enzymol.*, Elsevier Inc., **2009**, pp. 259–282.
- [222] D. Bozhinova, B. Galunsky, G. Yueping, M. Franzreb, R. Köster, V. Kasche, *Biotechnol. Lett.* **2004**, *26*, 343–350.
- [223] M. C. Yen, W. H. Hsu, S. C. Lin, *Process Biochem.* **2010**, *45*, 667–674.
- [224] P. Soriano-Maldonado, F. J. Las Heras-Vazquez, J. M. Clemente-Jimenez, F. Rodriguez-Vico, S. Martínez-Rodríguez, *Appl. Microbiol. Biotechnol.* **2014**, *99*, 283–291.
- [225] M. Pietzsch, A. Wiese, K. Ragnitz, B. Wilms, J. Altenbuchner, R. Mattes, C. Syldatk, *J. Chromatogr. B Biomed. Sci. Appl.* **2000**, *737*, 179–186.
- [226] Y. Asanomi, H. Yamaguchi, M. Miyazaki, H. Maeda, *Molecules* **n.d.**, *16*, 6041.
- [227] F. Kazenwadel, M. Franzreb, B. E. Rapp, *Anal. Methods* **2015**, *7*, 4030–4037.
- [228] F. Kazenwadel, H. Wagner, J. Wohlgemuth, M. Franzreb, *Process. Jahrestagung und 31. DECHEMA-Jahrestagung der Biotechnol.* **2014**.
- [229] E. D. B. Clark, *Curr. Opin. Biotechnol.* **2001**, *12*, 202–207.

## 6. LIST OF FIGURES

<b>Figure 1</b> Pharmaceutical products with non-canonical $\alpha$ -amino acids as building blocks.....	1
<b>Figure 2</b> Structural comparison of $\alpha$ - and $\beta$ -amino acids .....	2
<b>Figure 3</b> Pharmaceutical products with $\beta$ -amino acids as building blocks .....	2
<b>Figure 4</b> Kinetic resolution (A) and dynamic kinetic resolution (B) in the synthesis of optically pure compounds .....	3
<b>Figure 5</b> Hydantoinase Process for the synthesis of optically pure $\alpha$ -amino acids starting from racemic 5-monosubstituted hydantoins.....	5
<b>Figure 6</b> Proposed modified Hydantoinase Process for the synthesis of optically pure $\beta$ -amino acids starting from racemic 6-monosubstituted dihydrouracils .....	6
<b>Figure 7</b> Natural products containing hydantoins or hydantoin derivatives .....	8
<b>Figure 8</b> Pyrimidine metabolism .....	9
<b>Figure 9</b> Keto-enol tautomerism of 5-monosubstituted hydantoins under alkaline conditions .....	9
<b>Figure 10</b> Different building blocks and synthesis strategies for the synthesis of hydantoins .....	12
<b>Figure 11</b> A Bucherer-Bergs synthesis of 5-substituted hydantoins. B Modified Bucherer-Bergs synthesis of 5-substituted hydantoins .....	13
<b>Figure 12</b> Biginelli Reaction for the synthesis of differently substituted 5,6-dihydrouracils using Meldrum's Acid.....	14
<b>Figure 13</b> A Reaction of Ehrlich's reagent ( <i>p</i> -dimethylaminobenzaldehyde) with primary amines of <i>N</i> -carbamoylamino acids. B Reaction of ninhydrin with amino acids.....	36
<b>Figure 14</b> Chemical synthesis of ( <i>R/S</i> )- <i>p</i> NO <sub>2</sub> PheDU (( <i>R/S</i> )-4) .....	39
<b>Figure 15</b> Chemical synthesis of ( <i>R/S</i> )- <i>NCp</i> NO <sub>2</sub> $\beta$ Phe (( <i>R/S</i> )-6) .....	39
<b>Figure 16</b> Investigated conditions for the cultivation of <i>E. coli</i> BL21DE3 expressing two different recombinant hydantoinases by high throughput screening.....	41
<b>Figure 17</b> Investigated conditions for the cultivation of <i>E. coli</i> BL21DE3 coexpressing a codon-optimized recombinant hydantoinase and different chaperones by high throughput screening .....	42
<b>Figure 18</b> Derivatization of $\alpha$ - and $\beta$ -amino Acids and their corresponding <i>N</i> -carbamoyl derivatives for qualitative TLC analysis.....	49
<b>Figure 19</b> Qualitative TLC analysis for the conversion of 2 mM <i>NCPheAla</i> by the carbamoylase from <i>A. crystallopoietes</i> using resting cells.....	51
<b>Figure 20</b> Separation of 2 mM <i>p</i> NO <sub>2</sub> PheDU (( <i>R/S</i> )-4) and 2 mM <i>NCp</i> NO <sub>2</sub> $\beta$ Phe (( <i>R/S</i> )-6) by HPLC ..	53
<b>Figure 21</b> A Separation of 5 mM <i>PheGly</i> (a), 5 mM <i>NCPheGly</i> (b) and 5 mM <i>PheGly</i> (c). B Separation of 5 mM <i>PheAla</i> (a), 5 mM <i>NCPheAla</i> (b) and 5 mM <i>PheAla</i> (c) .....	54
<b>Figure 22</b> 6-(4-nitrophenyl)dihydropyrimidine-2,4(1H,3H)-dione (( <i>R/S</i> )-4).....	55
<b>Figure 23</b> 3-(4-Nitrophenyl)-3-ureidopropanoic acid (( <i>R/S</i> )-6). .....	56
<b>Figure 24</b> Conversion of 2 mM <i>p</i> NO <sub>2</sub> PheDU (( <i>R/S</i> )-4) by the hydantoinase from <i>A. crystallopoietes</i> DSM 20117 using resting cells. ....	56
<b>Figure 25</b> Conversion of 10 mM <i>p</i> NO <sub>2</sub> PheDU (( <i>R/S</i> )-4) by the hydantoinase from <i>A. crystallopoietes</i> DSM20117 using resting cells .....	58
<b>Figure 26</b> Studies on the enantioselectivity of the hydantoinase from <i>A. crystallopoietes</i> DSM20117 toward <i>p</i> NO <sub>2</sub> PheDU (( <i>R/S</i> )-4) .....	59
<b>Figure 27</b> Cultivation of <i>E. coli</i> BL21DE3 and expression of the recombinant hydantoinases d-Hyd and d-Hyd(co) from <i>A. crystallopoietes</i> DSM 20117 under oxygen deficiency. ....	62
<b>Figure 28</b> SDS-PAGE of the cultures of <i>E. coli</i> BL21DE3 hosting the recombinant hydantoinases d-Hyd and d-Hyd(co) from <i>A. crystallopoietes</i> DSM 20117 after cultivation and expression under oxygen deficiency and subsequent cell disruption.....	63

<b>Figure 29</b> High throughput screening for the cultivation conditions of <i>E. coli</i> BL21DE3 expressing the recombinant hydantoinase d-Hyd and d-Hyd(co) from <i>A. crystallopoietes</i> DSM 20117. Growth curves and maximum growth rates under different cultivation conditions .....	66
<b>Figure 30</b> High throughput screening for the cultivation conditions of <i>E. coli</i> BL21DE3 expressing the recombinant hydantoinase d-Hyd and d-Hyd(co) from <i>A. crystallopoietes</i> DSM20117. Specific activities after whole cell biotransformation with 2 mM PheHyd after cultivation and induction under different conditions .....	67
<b>Figure 31</b> SDS-PAGE of the cultures of <i>E. coli</i> BL21DE3 hosting the recombinant hydantoinases d-Hyd(co) and d-Hyd from <i>A. crystallopoietes</i> DSM 20117 after high throughput screening for cultivation conditions and subsequent cell disruption.....	70
<b>Figure 32</b> High throughput screening for the cultivation of <i>E. coli</i> BL21DE3 coexpressing the recombinant hydantoinase d-Hyd(co) from <i>A. crystallopoietes</i> DSM 20117 and different chaperones.	72
<b>Figure 33</b> High throughput screening for the cultivation of <i>E. coli</i> BL21DE3 coexpressing the recombinant hydantoinase d-Hyd(co) from <i>A. crystallopoietes</i> DSM 20117 and different chaperones	73
<b>Figure 34</b> SDS-PAGE of the cultures of <i>E. coli</i> BL21DE3 coexpressing the recombinant hydantoinase d-Hyd(co) from <i>A. crystallopoietes</i> DSM 20117 and different chaperones after high throughput screening for cultivation conditions and subsequent cell disruption .....	75
<b>Figure 35</b> SDS-PAGE analysis of every fraction after purification of the hydantoinase from <i>A. crystallopoietes</i> DSM 20117 .....	80
<b>Figure 36</b> Testing of different devices for buffer exchange for after purification of the hydantoinase from <i>A. crystallopoietes</i> DSM20117 for removal of imidazole.....	82
<b>Figure 37</b> SDS-PAGE analysis of the different fractions after purification of the hydantoinase from <i>A. crystallopoietes</i> DSM 20117 via Ni sepharose beads .....	84
<b>Figure 38</b> SDS-PAGE analysis of the different fractions after purification of the carbamoylase from <i>A. crystallopoietes</i> DSM 20117 via Ni sepharose beads .....	86
<b>Figure 39</b> SDS-PAGE analysis for comparison of two different media for the cultivation and expression of soluble carbamoylase from <i>A. crystallopoietes</i> DSM 20117 regarding immobilization on functionalized magnetic beads .....	89
<b>Figure 40</b> Relative protein concentrations of the eluate after immobilization of the carbamoylase from <i>A. crystallopoietes</i> DSM 20117 .....	91
<b>Figure 41</b> SDS-PAGE analysis for comparison of different regeneration strategies for functionalized magnetic beads after immobilization of the carbamoylase from <i>A. crystallopoietes</i> DSM 20117 .....	92
<b>Figure 42</b> SDS-PAGE analysis after immobilization of the hydantoinase from <i>A. crystallopoietes</i> DSM 20117 on functionalized magnetic beads .....	94
<b>Figure 43</b> SDS-PAGE analysis after immobilization of the carbamoylase from <i>A. crystallopoietes</i> DSM 20117 on functionalized magnetic beads .....	96
<b>Figure 44</b> SDS-PAGE analysis after immobilization of the hydantoinase from <i>A. crystallopoietes</i> DSM 20117 on functionalized magnetic beads (SBP-tag) .....	99
<b>Figure 45</b> SDS-PAGE analysis after purification of the hydantoinase from <i>A. crystallopoietes</i> DSM 20117 via functionalized magnetic beads .....	100
<b>Figure 46</b> SDS-PAGE analysis after purification of the carbamoylase from <i>A. crystallopoietes</i> DSM 20117 via functionalized magnetic beads .....	102
<b>Figure 47</b> Modular 3D-printed microfluidic system for immobilization of enzyme cascades .....	106
<b>Figure 48</b> Microchannel System for Reaction Cascades with Enzymes Immobilized on Magnetic Beads.....	107
<b>Figure 49</b> SDS-PAGE Analysis before and after purification of inclusion bodies of the hydantoinase from <i>A. crystallopoietes</i> DSM 20117 .....	107
<b>Figure 50</b> <sup>1</sup> H NMR spectrum of compound 4, 400 MHz, DMSO-d <sub>6</sub> .....	122
<b>Figure 51</b> <sup>13</sup> C NMR spectrum of compound 4, 100 MHz, DMSO-d <sub>6</sub> .....	123
<b>Figure 52</b> <sup>1</sup> H NMR spectrum of compound 5, 400 MHz, DMSO-d <sub>6</sub> .....	123
<b>Figure 53</b> <sup>13</sup> C NMR spectrum of compound 5, 100 MHz, DMSO-d <sub>6</sub> .....	124

## 7. LIST OF TABLES

<b>Table 1</b> Racemization half-lives of differently substituted hydantoin. Conditions: 40 °C, pH 8.5, no buffer added.....	10
<b>Table 2</b> Chemicals and enzymes .....	23
<b>Table 3</b> Consumption items .....	26
<b>Table 4</b> Applied devices .....	27
<b>Table 5</b> Strains .....	28
<b>Table 6</b> Plasmids containing enzymes or chaperones .....	29
<b>Table 7</b> Parameters for the BioLector® cultivation.....	43
<b>Table 8</b> Applied chaperone sets, corresponding chaperones and molecular weights.....	76
<b>Table 9</b> Protein concentrations of selected fractions after purification of the hydantoinase from <i>A. crystallopoietes</i> DSM20117 .....	81
<b>Table 10</b> Purification of the hydantoinase from <i>A. crystallopoietes</i> DSM 20117 via Ni sepharose beads .....	85
<b>Table 11</b> Purification of the carbamoylase from <i>A. crystallopoietes</i> DSM 20117 via Ni sepharose beads .....	87
<b>Table 12</b> Comparison of two different media for the cultivation and expression of soluble carbamoylase from <i>A. crystallopoietes</i> DSM 20117 regarding immobilization on functionalized magnetic beads .....	90
<b>Table 13</b> Comparison of different regeneration strategies for functionalized magnetic beads after immobilization of the carbamoylase from <i>A. crystallopoietes</i> DSM 20117 .....	92
<b>Table 14</b> Effect of imidazole in the crude extract regarding immobilization and purification of the hydantoinase from <i>A. crystallopoietes</i> DSM 20117 via functionalized magnetic beads .....	93
<b>Table 15</b> Immobilization of the hydantoinase from <i>A. crystallopoietes</i> DSM 20117 via functionalized magnetic beads and hydrolysis of different substrates .....	95
<b>Table 16</b> Immobilization of the carbamoylase from <i>A. crystallopoietes</i> DSM 20117 via functionalized magnetic beads and hydrolysis of different substrates .....	97
<b>Table 17</b> Purification of the hydantoinase from <i>A. crystallopoietes</i> DSM 20117 via functionalized magnetic beads .....	101
<b>Table 18</b> Purification of the carbamoylase from <i>A. crystallopoietes</i> DSM 20117 via functionalized magnetic beads .....	102
<b>Table 19</b> Comparison of protein concentrations of eluate 1 and 2 after immobilization or purification of the hydantoinase as well as carbamoylase from <i>A. crystallopoietes</i> DSM20117 .....	104
<b>Table 20</b> Overview of investigated purification and immobilization methods for the enzymes from <i>A. crystallopoietes</i> DSM 20117 employing the His-tag and comparison to other works .....	105

## 8. LIST OF ABBREVIATIONS

<b>Abbreviation</b>	<b>Meaning</b>
abbr.	abbreviation
Amp	ampicillin
APS	ammoniumperoxodisulfate
Ara	arabinose
$A_{\text{spez}}$	specific enzyme activity
BCA	bichinoic acid
BnH	benzylhydantoin
BSA	bovine serum albumin
Carb	carbamoylase
cdw	cell dry weight
Cm	chloramphenicol
$d_dH_2O$	double distilled water
DMSO	Dimethylsulfoxide
DTT	dithiothreitol
FLAG-tag	polypeptide protein, sequence: DYKDDDDK
HCl	hydrochloric acid
HMH	hydroxymethylhydantoin
Hyd	hydantoinase
IMAC	immobilized metal ion affinity chromatography
IPTG	isopropyl- $\beta$ -D-thiogalactopyranosid
Kan	kanamycin
LB	lysogeny broth
NaCl	sodium chloride
NaPP	sodium phosphate buffer
NCPheAla	<i>N</i> -carbamoylphenylalanine
NCPheGly	<i>N</i> -carbamoylphenylglycine
NCSer	<i>N</i> -carbamoylserine
PBS	phosphate buffered saline
PheAla	phenylalanine
PheGly	phenylglycine
PheHyd	phenylhydantoin

<b>Abbreviation</b>	<b>Meaning</b>
Rha	rhamnose
rpm	rounds per minute
rt	room temperature
SBP-tag	streptavidin binding peptide tag
SDS	sodium dodecyl sulfate
Ser	serine
TB	terrific broth
TEMED	triethylenediamine
Tet	tetracycline
TFA	trifluoroacetic acid
TGS	buffer containing TRIS, glycerine and SDS
TLC	thin layer chromatography
TRIS	tris(hydroxymethyl)-aminomethan
v/v	volume per volume
w/o	without
w/v	weight per volume
ZnSO <sub>4</sub>	zinc sulfate

## 5. APPENDIX

### 5.1 FORMULAS

#### 5.1.1 OD<sub>600</sub>/SCATTERED LIGHT CORRELATION

$$y(\text{OD}_{600}) = m(\text{slope}) * x(\text{scattered light}) + b(\text{axis intercept})$$

#### 5.1.2 MAXIMUM GROWTH RATE

$$\mu_{\text{max}} [\text{OD}_{600}/\text{h}] = \frac{\ln(\text{OD}_{600,t2}) - \ln(\text{OD}_{600,t1})}{t_2 [\text{h}] - t_1 [\text{h}]}$$

#### 5.1.1 SPECIFIC ENZYME ACTIVITIES

$$A_{\text{spez}}(\text{protein}) [\text{U}/\text{mg}] = \frac{\text{substrate concentration } [\mu\text{mol}]}{\text{time } [\text{min}] * \text{protein content } [\text{mg}]}$$

$$A_{\text{spez}}(\text{cell dry weight}) [\text{U}/\text{mg}] = \frac{\text{substrate concentration } [\mu\text{mol}]}{\text{time } [\text{min}] * \text{cell dry weight } [\text{mg}]}$$

#### 5.1.2 ENZYME PURIFICATION

$$\text{Recovery } [\%] = \frac{\text{total activity after purification } [\text{U}]}{\text{total activity before purification } [\text{U}]} * 100$$

$$\text{Purification Fold} = \frac{\text{specific Activity after purification } [\text{U}/\text{mg}]}{\text{specific Activity before purification } [\text{U}/\text{mg}]}$$

## 5.1 NMR-SPECTRA

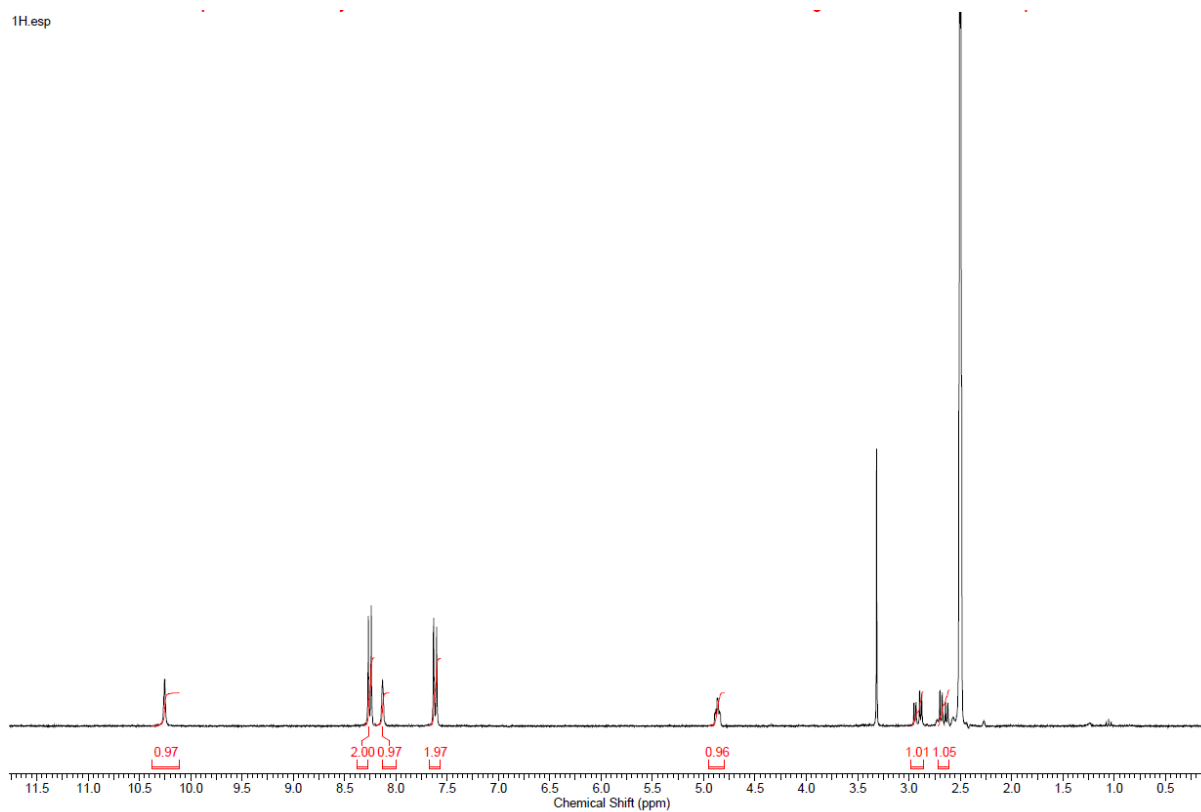


Figure 50  $^1\text{H}$  NMR spectrum of compound 4, 400 MHz,  $\text{DMSO-d}_6$



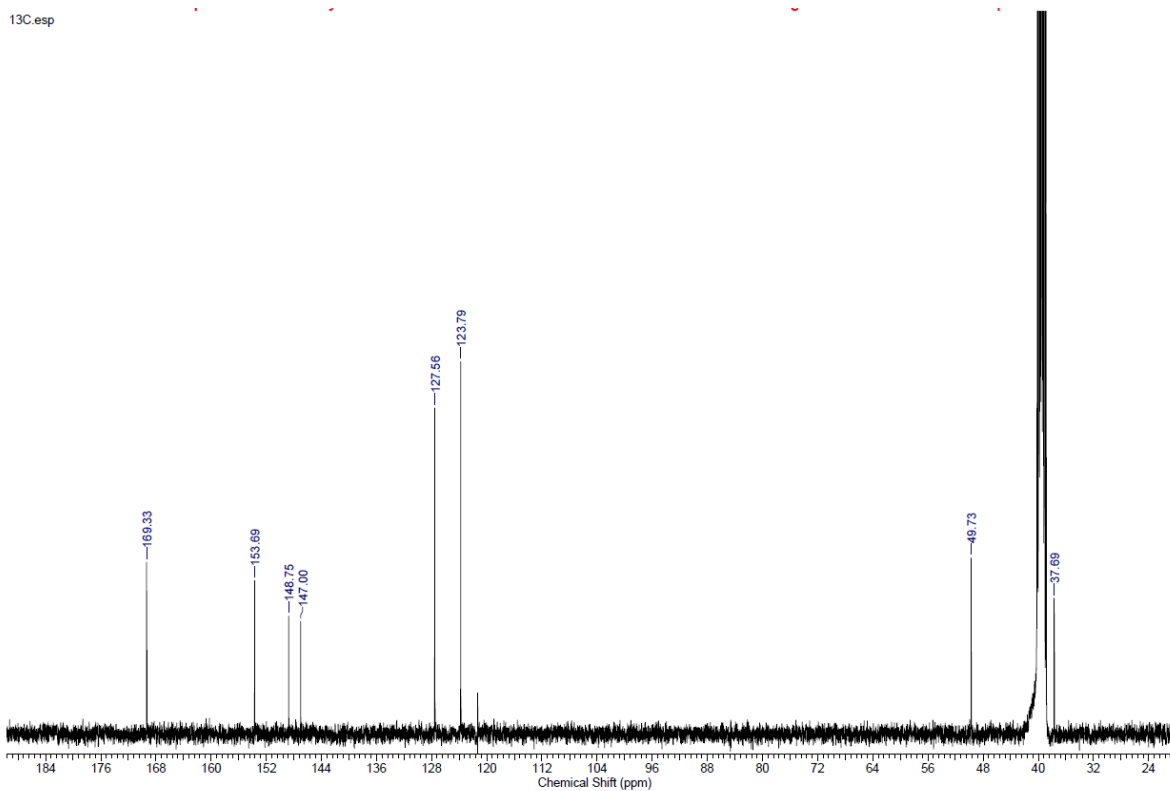


Figure 51 <sup>13</sup>C NMR spectrum of compound 4, 100 MHz, DMSO-d<sub>6</sub>

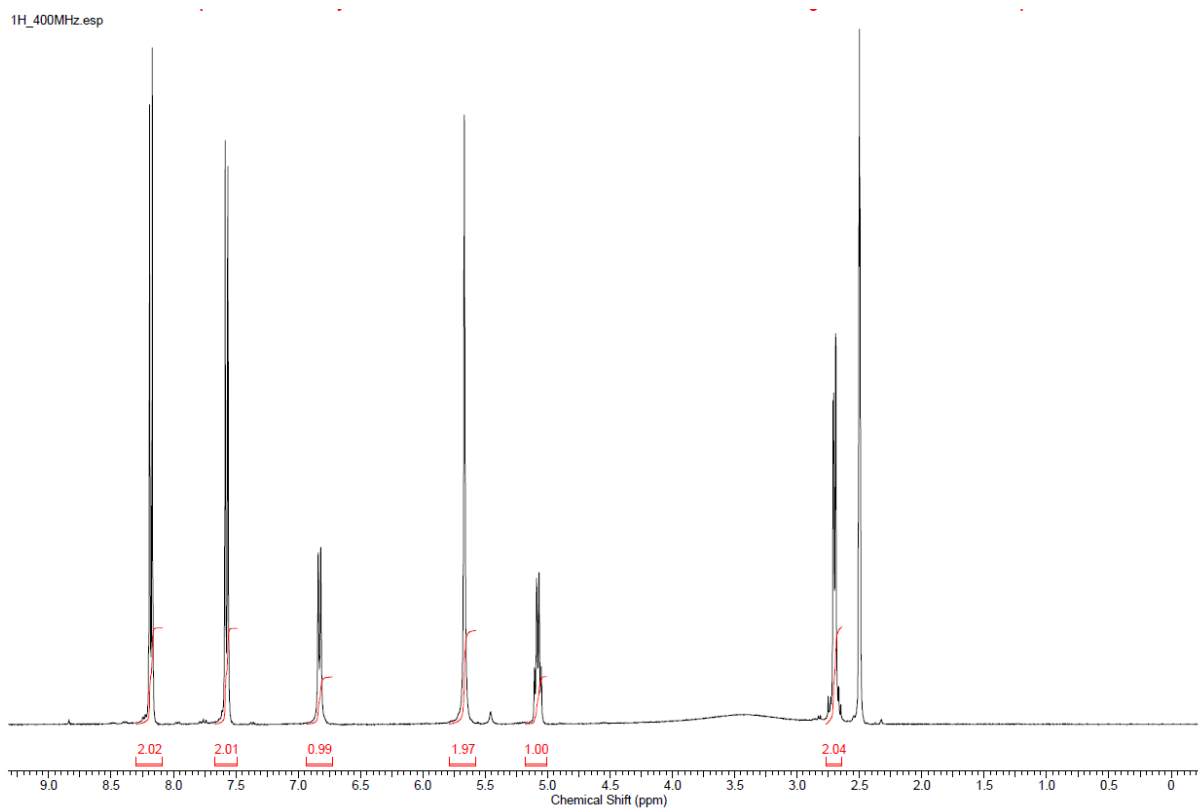
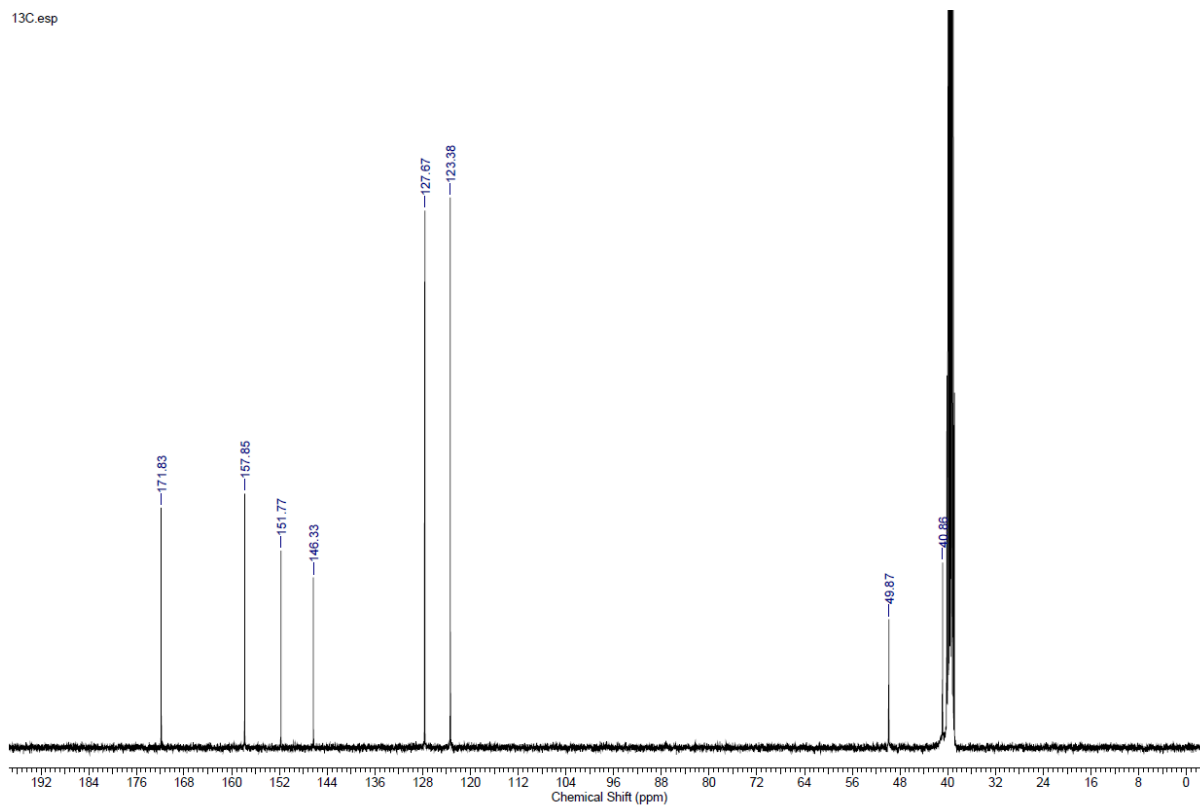


Figure 52 <sup>1</sup>H NMR spectrum of compound 5, 400 MHz, DMSO-d<sub>6</sub>



**Figure 53**  $^{13}\text{C}$  NMR spectrum of compound **5**, 100 MHz,  $\text{DMSO-d}_6$

## 5.1 SEQUENCES

### 5.1.1 HYDANTOINASE FROM *A. CRYSTALLOPOIETES* DSM 20117 WITH C-TERMINAL HIS-TAG

ATTGACTCTCTTCCGGCGCTATCATGCCATACCGGAAAGGTTTTGCGCCATTCGATGGTGTCCGGGATCTCGACGCTCTCC  
 CTTATGCGACTCCTGCATTAGGAAGCAGCCAGTAGTAGTTGAGGCCGTTGAGCACCGCCGCCGAAGGAATGGTGCATGCA  
 AGGAGATGGCGCCCAACAGTCCCCCGCCACGGGGCTGCCACCATACCCACGCCGAAACAAGCGCTCATGAGCCGAAGTGG  
 CGAGCCCGATCTTCCCATCGGTGATGTCGGCGATATAGCGCCAGCAACCGCACCTGTGGCGCCGGTGTGATGCCGGCCACGAT  
 GCGTCCGGCGTAGAGATCGAGATCTCGATCCC CGCAAATTAATACGACTCACTATAGGGGAATTGTGAGCGGATAACAATTC  
 CCCTCTAGAAATAATTTGTTTAACTTTAAGAAGGAATATCACAAGTTTGTACAAAAAGCAGGCTAAGGAGGATAGAACCAT  
 GGATGCAAAGCTACTGGTTGGCGGCACTATTGTTTCTCGACCGGCAAAATCCGAGCCGACGTGCTGATTGAAAACGGCAAAG  
 TCGCCGCTGTGGCATGCTGGACGCCGCGACGCCGGACACAGTTGAGCGGGTTGACTGCGACGGCAAATACGTCATGCCCGGC  
 GGTATCGACGTTACACCCACATCGACTCCCCCTCATGGGGACCACCACCGCCGATGATTTTGTGACGGGAACGATTGACGC  
 CGTACCGGCGGAACAACGACCATCGTCGATTTCCGACAGCAGCTCGCCGGCAAGAACCTGCTGGAATCCGACAGCGCGACC  
 AAAAAAGGCGCAGGGGAAATCCGTCATTGATTACGGCTTCCATATGTGCGTGACGAACCTCTATGACAATTTGATTTCCAT  
 ATGGCAGAACTGACACAGGACGGAATCTCCAGTTTCAAGGTCTTCATGGCCTACCGCGGAAGCCTGATGATCAACGACGGCGA  
 ACTGTTTCGACATCCTCAAGGGAGTCGGCTCCAGCGGTGCCAACTATGCGTCCACGCGAGAAACGGCGACGTCATCGACAGGA  
 TCGCCCGGACCTTACGCCAAGGAAAAACCGGGCCCGGACCCACGAGATCGCACGCCCGCCGGAATCGGAAGTCAAGCA  
 GTCAGCCGGCCATCAAGATCTCCCGATGGCCGAGGTGCCGCTGTATTTTCGTGCATCTTTCCACCCAGGGGGCCGTCGAGGA  
 AGTAGCTGCCGCGCAGATGACAGGATGGCCAATCAGCGCCGAAACGTGCACCCACTACCTGTGCTGAGCCGGGACATCTACG  
 ACCAGCCGGGATTCGAGCCGGCCAAAGCTGTCTCACACCACCGCTGCGCACACAGGAACACCAGGACGCGTTGTGGAGAGGC

ATTAACACCGGTGCGCTCAGCGTCGTCAGTTCCGACCACTGCCCTTCTGCTTTGAGGAAAAGCAGCGGATGGGGGCAGATGA  
 CTTCGGGCAGATCCCCAACGGCGGGCCGGCGTGGAGCACCGAATGCTCGTGATGTATGAGACCGGTGTCGCGGAAGGAAAA  
 TGACGATCGAGAAATTCGTCGAGGTGACTGCCGAGAACCCGGCCAAGCAATTCGATATGTACCCGAAAAAGGGAACAATTGCA  
 CCGGGCTCCGATGCAGACATCATCGTGGTCGACCCAACGGAACAACCTCATCAGTGCCGACACCCAAAAACAAACATGGA  
 CTACACGCTGTTTGAAGGCTTCAAAATCCGTTGCTCCATCGACCAGGTGTTCTCGCGTGGCGACCTGATCAGCGTCAAAGCCG  
 AATATGTCGGCACCCGCGGCCGCGGCAATTCATCAAGCGGAGCGCTTGGAGCCACCCGAGTTCGAAAAAGAAAACCTGTAT  
 TTTAGTCCACCCAGCTTTCTTGTACAAAGTGGTATCAATTCGAAGCTTGAAGGTAAGCCTATCCCTAACCTCTCCTCGG  
 TCTCGATTCTACCGTACCGGTATCATCACCATCACCATTGAGTTTGTATCCGGCTGCTAACAAAGCCCGAAAGGAAGCTGAG  
 TTGGTGTCTGCCACCGCTGAGCAATAACTAGCATAACCCTTGGGGCTCTAAACGGGTCTTGGGGGTTTTTTGCTGAAAGG  
 AGGAACTATATCCGGATATCCCGCAAGAGGCCCGGCGAGTACCGGCATAACCAAGCCTATGCCTACAGCATCCAGGGTGACGGT  
 GCCGAGGATGACGATGAGCGCATTGTTAGATTTTCATACACGGTGCCTGACTGCGTTAGCAATTTAACTGTGATAAACTACCGC  
 ATTTAAAGCTTATCGATGATAAGCTGTCAAACATGAGAAATTAATTCCTGAAGACGAAAGGGCTCGTGATACGCCTATTTTTAT  
 AGGTTAATGTATGATAATAATGGTTTCTTAGACGTGAGTGGCCTTTTTCGGGAAATGTGCGCGGAACCCCTATTTGTTTA  
 TTTTTCTAAATACATTTCAAATATGTATCCGCTCATGAGACAATAACCCTGATAAATGCTTCAATAATATTGAAAAAGGAAGAG  
 TATGAGTATTCAACATTTCCGTGTCGCCCTTATTTCCCTTTTTTTCGGCATTTTTGCCTTCTGTTTTTGTCTACCCAGAAACGC  
 TGGTGAAGTAAAAGATGCTGAAGATCAGTTGGGTGCACGAGTGGGTACATCGAACTGGATCTCAACAGCGGTAAGATCCTT  
 GAGAGTTTTTCGCCCGAAGAAGCTTTTCCAATGATGAGCACTTTTAAAGTTCTGCTATGTGGCGCGGTATTATCCCGTGTGGA  
 CGCCGGGCAAGAGCAACTCGGTGCGCCGATACACTATTCTCAGAATGACTTGGTTGAGTACTACCAGTACAGAAAAGCATC  
 TTACGGATGGCATGACAGTAAGAGAATATGAGTGTGCCATAACCATGAGTGATAACACTGCGGCCAACTTACTTCTGACA  
 ACGATCGGAGGACCGAAGGAGCTAACCGCTTTTTTGCACAACATGGGGGATCATGTAACCTGCGCTTGATCGTTGGGAACCGGA  
 GCTGAATGAAGCCATACCAAACGACGAGCGTGCACCCAGATGCCTGCAGCAATGGCAACAACGTTGCGCAAACCTATTAACCTG  
 GCGAACTACTTACTCTAGCTTCCCGCAACAATTAATAGACTGGATGGAGGCGGATAAAGTTGCAGGACCCTTCTGCGCTCG  
 GCCCTTCCGGCTGGCTGGTTTTATTGCTGATAAATCTGGAGCCGGTGGCGTGGGTCTCGCGGTATCATTGCAGCACTGGGGCC  
 AGATGGTAAGCCCTCCCGTATCGTAGTTATCTACACGACGGGGAGTCAAGCAACTATGGATGAACGAAATAGACAGATCGCTG  
 AGATAGGTGCCTCACTGATTAAGCATTTGGTAACTGTGAGACCAAGTTTACTCATATATACTTTAGATTGATTTAAACTTCAT  
 TTTTAATTTAAAGGATCTAGGTGAAGATCCTTTTTGATAATCTCATGACCAAAATCCCTAACGTGAGTTTTCGTTCCACTG  
 AGCGTCAGACCCCGTAGAAAAAGATCAAAGGATCTTCTTGGAGATCCTTTTTTCTGCGGTAATCTGCTGCTTGCAAACAAAA  
 AACACCCTGACAGCGGTGGTTTTGTTGCGGATCAAGAGCTACCAACTCTTTTTCCGAAGGTAACCTGGCTTACGAGAGCG  
 CAGATACCAAATACTGTCCTTCTAGTGTAGCCGTAGTTAGGCCACCCTTCAAGAACTCTGTAGCACCGCTACATACCTCGC  
 TCTGCTAATCCTGTTACCAGTGGCTGCTGCCAGTGGCGATAAGTCTGCTTACCAGGTTGGACTCAAGACGATAGTTACCAGG  
 ATAAGCGCAGCGGTCCGGCTGAACGGGGGTTCTGTCACACAGCCAGCTTGGAGCGAACGACCTACACCGAACTGAGATAC  
 CTACAGCGTGAAGTATGAGAAAGCGCCACGCTTCCCGAAGGGAGAAAGCGGACAGGTATCCGGTAAGCGCGAGGGTCCGAAC  
 AGGAGAGCGCACGAGGAGCTTCCAGGGGAAACGCTTGGTATCTTTATAGTCTGTCGGGTTTCGCCACCTCTGACTTGAGC  
 GTCGATTTTTGTGATGCTCGTCAGGGGGCGGAGCCTATGGAAAAACGCGCAGCAACGCGGCCTTTTTACGTTCTCGCCTTT  
 TGCTGGCCTTTTTGCTCACATGTTCTTCTGCGTTATCCCTGATTTCTGTGGATAACCGTATTACCCTTTGAGTGAGCTGA  
 TACCGCTCGCCGAGCCGAACGACCGAGCGCAGCGAGTCAAGTGAAGCGGAAAGCGGAGCGCCTGATGCGGTATTTTTCTCC  
 TTACGCATCTGTGCGGTATTTACACCCGATATATGGTGCCTCTCAGTACAATCTGCTCTGATGCCGATAGTTAAGCCAGT  
 ATACACTCCGCTATCGCTACGTGACTGGGTGATGGTGCGCCCGACACCCGCCAACACCCGCTGACGCGCCCTGACGGGCTT  
 GTCTGCTCCCGCATCCGCTTACAGACAAGCTGTGACCGTCTCCGGGAGCTGCATGTGTCAGAGTTTTACCGTCTATCACCG  
 AACCGCGGAGGACGCTGCGGTAAGCTCATCAGCGTGGTCTGGAAGCGATTACAGATGTCTGCCTGTTTATCCCGTCCAG  
 CTCGTTGAGTTTCTCCAGAAGCGTTAATGTCTGGCTTCTGATAAAGCGGGCCATGTTAAGGGCGTTTTTCTGTTTGGTCA  
 CTGATGCCTCCGTGTAAGGGGATTTCTGTTTATGGGGTAATGATAACCGATGAAACGAGAGAGGATGCTCACGATACGGGTT  
 ACTGATGATGAACATGCCCGGTTACTGGAACGTTGTGAGGGTAAACAACTGGCGGTATGGATGCGGCGGGACCAGAGAAAAAT  
 CACTCAGGGTCAATGCCAGCGCTTCGTTAATACAGATGTAGGTGTTCCACAGGGTAGCCAGCAGCATCTGCGATGCAGATCC  
 GGAACATAATGGTGCAGGGCGCTGACTTCCGCTTTCCAGACTTTACGAAACACGGAAACCGAAGACCATTCATGTTGTTGCT  
 CAGGTCGAGACGTTTTGCGAGCAGCAGTGCCTTACGTTGCTGCGGTATCGGTGATTCTGCTAACAGTAAGGCAACC  
 CCGCCAGCCTAGCCGGGCTCTAACGACAGGAGCAGATCATGCGCACCCGTGGCCAGGACCCAACGCTGCCCGAGATGCGCC  
 CGGTGCGGCTGCTGGAGATGGCGGACGCGATGGATATGTTCTGCCAAGGGTTGGTTTTGCGCATTCACAGTTCTCCGCAAGAA  
 TGATTGGCTCCAATCTTGGAGTGGTGAATCCGTTAGCGAGGTGCCGCCGGCTTCCATTCAGGTCGAGGTGGCCCGGCTCCAT  
 GCACCGCGACGCAACGCGGGGAGGCAGACAAGGTATAGGGCGGCGCTACAATCCATGCCAACCCGTTCCATGTGCTCGCCGA  
 GGCGGCATAAATCGCCGTGACGATCAGCGGTCCAGTGTGAAAGTTAGGCTGGTAAAGAGCCGCGAGCGATCCTTGAAGCTGTC  
 CCTGATGGTCTGATCTACCTGCCTGGACAGCATGGCTGCAACGCGGGCATCCCGATGCCGCGGAAAGCGAGAAAGAAATCATA  
 ATGGGGAAGGCCATCCAGCCTCGCGTCGCGAACCCAGCAAGACGTAGCCAGCGCGTCCGGCCGATGCCGGCGATAATGGC  
 CTGCTTCTCGCCGAAACGTTTTGGTGGCGGGACCAGTGCAGAAAGGCTTGAAGCGAGGGCGTGCAAGATTCCGAATACCGCAAGCG  
 ACAGGCCGATCATCGTCGCGCTCCAGCGAAAGCGGTCTCGCCGAAAATGACCCAGAGCGCTGCCGGCACCTGTCTACGAGT  
 TGCATGATAAAGAAGACAGTCATAAGTGCGGCGACGATAGTCATGCCCGCGCCACCAGGAGCTGACTGGGTTGAAGGC  
 TCTCAAGGGCATCGGTGAGATCCCGGTGCCTAATGAGTGAGCTAATTTACATTAATTGCGTTGCGCTCACTGCCCGCTTTCC  
 AGTCGGGAAACCTGCTGTCAGCTGCATTAATGAATCGGCCAACGCGCGGGGAGAGGCGGTTTTGCGTATTGGGCGCCAGGGT

GGTTTTTCTTTTACCAGTGAGACGGGCAACAGCTGATTGCCCTTACCAGCCTGGCCCTGAGAGAGTTGCAGCAAGCGGTCCA  
 CGCTGGTTTGGCCCAGCAGGCGAAAACTCTGTTTGGTGGTTAACGGCGGGATATAACATGAGCTGTCTTCGGTATCGTCG  
 TATCCCACTACCGAGATATCCGCACCAACGCGCAGCCCGGACTCGGTAATGGCGCGCATTGCGCCCAGCGCCATCTGATCGTT  
 GGCAACCAGCATCGCAGTGGGAACGATGCCCTCATTAGCATTGTCATGGTTTGTGAAAACCGGACATGGCACTCCAGTCGC  
 CTTCCTCGTTCCGCTATCGGCTGAATTTGATTGCGAGTGAGATATTTATGCCAGCCAGCCAGACGCAGACGCGCCGAGACAGAA  
 CTTAATGGGCCCCGTAACAGCGCGATTGCTGGTGACCAATGCGACCAGATGCTCCAGCCCAGTCGCGTACCGTCTTCATG  
 GGAGAAAATAATACTGTTGATGGGTGTCTGGTCAGAGACATCAAGAAAATAACGCCGGAACATTAGTGCAGGCAGCTTCCACAG  
 CAATGGCATCCTGGTCATCCAGCGGATAGTTAATGATCAGCCACTGACGCGTTGCGCGAGAAGATTGTGCACCGCCGCTTTA  
 CAGGCTTCGACGCCGCTTCGTTCTACCATCGACACCACCAGCTGGCACCAGTTGATCGGCGGAGATTTAATCGCCGCGAC  
 AATTTGCGACGGCGGTGCAGGGCCAGACTGGAGGTGGCAACGCCAATCAGCAACGACTGTTTGCCTCCAGTTGTTGTGCCA  
 CGCGGTTGGGAATGTAATTCAGCTCCGCCATCGCCGCTCCACTTTTTCCCGCTTTTCGAGAAAACGTGGCTGGCTGGTTTC  
 ACCACGCGGGAACGGTCTGATAAGAGACACCGGCATACTCTGCGACATCGTATAACGTTACTGGTTTCACATTACCACCTT  
 GA

### 5.1.2 CODON-OPTIMIZED HYDANTOINASE FROM *A. CRYSTALLOPOIETES* DSM 20117 WITH C-TERMINAL HIS-TAG AND N-TERMINAL SBP- TAG

TGGCGAATGGGACGCGCCCTGTAGCGGCGCATTAAAGCGGCGGGTGTGGTGGTTACGCGCAGCGTGACCGCTACACTTGCCA  
 GCGCCCTAGCGCCGCTCCTTTTCGCTTTCTTCCCTTCTTCTCGCCACGTTTCGCGGCTTTCCCGTCAAGCTCTAAATCGG  
 GGGTCCCTTTAGGGTTCCGATTTAGTGCTTTACGGCACCTCGACCCAAAAAACTTGATTAGGGTGATGGTTACAGTAGTGG  
 GCCATCGCCCTGATAGACGGTTTTTCGCCCTTTGACGTTGGAGTCCAGTTCTTTAATAGTGGACTCTTGTTCAAAACGGAA  
 CAACACTCAACCCTATCTCGGTCTATTCTTTTATTATAAGGGATTTTGCCGATTTCCGGCTATTGGTTAAAAAATGAGCTG  
 ATTTAACAAAAATTTAACCGAATTTAACAAAAATTTAACGCTTACAATTTAGGTGGCACTTTTCCGGGAAAATGTGCGCGGA  
 ACCCTATTTGTTTTATTTTTCTAAATACATTTCAATATGTATCCGCTCATGAATTAATTTCTTAGAAAACTCATCGAGCATCA  
 AATGAAACTGCAATTTATTCATATCAGGATTATCAATACCATATTTTTGAAAAAGCCGTTTCTGTAATGAAGGAGAAAACTCA  
 CCGAGGCAGTTCCATAGGATGGCAAGATCCTGGTATCGGTCTGCGATTCCGACTCGTCCAACATCAATACAACCTATTAATTT  
 CCCCTCGTCAAAAAAAGGTTATCAAGTGAGAAATCACCATGAGTGACGACTGAATCCGGTGAGAATGGCAAAAGTTTATGCA  
 TTTCTTTCCAGACTTGTTCAACAGGCCAGCCATTACGCTCGTCATCAAAATCACTCGCATCAACCAAACCGTTATTCATTCTG  
 GATTGCGCCTGAGCGAGACGAAATACGCGATCGCTGTTAAAAGGACAATTACAAACAGGAATCGAATGCAACCGGCGCAGGAA  
 CACTGCCAGCGCATCAACAATATTTTACCTGAATCAGGATATTTCTTAATACCTGGAATGCTGTTTTCCCGGGGATCGCAG  
 TGGTGAGTAACCATGCATCATCAGGAGTACGGATAAAATGCTTGATGGTCGGAAGAGGCATAAATTCGCTCAGCCAGTTTAGT  
 CTGACCATCTCATCTGAACATCATTGGCAACGCTACCTTTGCCATGTTTCAGAAACAACCTCTGGCGCATCGGGCTTCCATA  
 CAATCGATAGATTGTGCGACCTGATTGCCGACATTATCGCGAGCCATTTATACCCATATAAATCAGCATCCATGTTGGAAT  
 TTAATCGCGCCCTAGAGCAAGACGTTTCCCGTTGAATATGGCTCATAACACCCCTTGTATTACTGTTTTATGTAAGCAGACAGT  
 TTTATGTTTCATGACCAAAATCCCTAACGTGAGTTTTCGTTCCACTGAGCGTCAGACCCCGTAGAAAAGATCAAAGGATCTT  
 CTTGAGATCCTTTTTTCTGCGCGTAATCTGCTGCTGCAAACAAAAAAACCACCGCTACCAGCGGTGGTTTGTTCGCCGAT  
 CAAGAGCTACCAACTCTTTTTCCGAAGGTAACCTGGCTCAGCAGAGCGCAGATACCAAATACTGTCTTCTAGTGTAGCCGTA  
 GTTAGGCCACCACTTCAAGAATCTGTAGCACCCCTACATACCTCGCTCTGCTAATCCTGTTACCAGTGGCTGCTGCCAGTG  
 GCGATAAGTCGTGTCTTACCGGTTGGACTCAAGACGATAGTTACCGGATAAGGCGCAGCGGTCCGGCTGAACGGGGGTTTCG  
 TGCACACAGCCCAGCTTGGAGCGAACGACCTACACCGAATGAGATACTACAGCGTGAGCTATGAGAAAGCGCCACGCTTCC  
 CGAAGGGAGAAAGGCGACAGGTATCCGGTAAGCGGAGGGTCCGAACAGGAGAGCGCAGAGGGAGCTTCCAGGGGGAAACG  
 CCTGGTATCTTTATAGTCTGTCCGGTTTTCGCCACCTCTGACTTGAGCGTCGATTTTTGTGATGCTCGTCAGGGGGGCGGAGC  
 CTATGGAAAAACGCCAGCAACGCGGCTTTTTACGGTTCTGGCCTTTTGTGCTTTTTGCTCACATGTTCTTTCTGCGT  
 ATCCCTGATTCTGTGGATAACCGTATTACCGCTTTGAGTGAGCTGATACCGCTCGCCGAGCCGAACGACCGAGCGCAGCG  
 AGTCAGTGAGCGAGGAAGCGGAAGAGCGCCTGATGCGGTATTTCTCCTTACGCATCTGTGCGGTATTTACACCGCATATAT  
 GGTGCACTCTCAGTACAATCTGCTCTGATGCCGATAGTTAAGCCAGTATACACTCCGCTATCGCTACGTGACTGGGTTCATGG  
 CTGCGCCCCGACACCCGCCAACACCCGCTGACGCGCCCTGACGGGCTTGTCTGCTCCCGCATCCGCTTACAGACAAGCTGTG  
 ACCGCTCCGGGAGCTGCATGTGTGAGAGTTTTACCGTCTACCGAAACGCGGAGGCAGCTGCGGTAAAGCTCATCAGC  
 GTGGTCGTGAAGCGATTACAGATGCTGCTGTTTCATCCGCTCCAGCTCGTTGAGTTTCTCCAGAAGCGTTAATGTCTGGC  
 TTCTGATAAAGCGGGCCATGTTAAGGGCGGTTTTTCTGTTTGGTCACTGATGCCTCCGTGTAAGGGGGATTTCTGTTTCATG  
 GGGTAATGATAACCGATGAAACGAGAGAGGATGCTCACGATACGGTTACTGATGATGAACATGCCCGGTTACTGGAACGTTG  
 TGAGGGTAAACAACGCGGTATGGATGCGGCGGGACCAGAGAAAAATCACTCAGGGTCAATGCCAGCGCTTCGTTAATACAG  
 ATGTAGGTGTTCCACAGGGTAGCCAGCAGCATCCTGCGATGCAGATCCGGAACATAATGGTGCAGGGGCGCTGACTTCCGCGTT

TCCAGACTTTACGAAACACGGAAACCGAAGACCATTTCATGTTGTTGCTCAGGTCGCAGACGTTTTTGCAGCAGCAGTCGCTTCA  
CGTTTCGCTCGCGTATCGGTGATTTCATCTGCTAACCAGTAAGGCAACCCCGCCAGCCTAGCCGGTCTCAACGACAGGAGCA  
CGATCATGCGCACCCGTGGGGCCCGCATGCCGGCGATAATGGCCTGCTTCTCGCCGAAACGTTTTGGTGGCGGGACCAGTGACG  
AAGGCTTGAGCGAGGGCGTGCAAGATTCCGAATACCGCAAGCGACAGGCCGATCATCGTCGCGCTCCAGCGAAAGCGGTCTC  
GCCGAAAATGACCCAGAGCGCTGCCGGCACCTGTCTACGAGTTGCATGATAAAGAAGACAGTCATAAGTGCGGCGACGATAG  
TCATGCCCGCGCCACCAGGAGCTGACTGGGTGAAGGCTCTCAAGGGCATCGGTGAGATCCCGGTGCCTAATGAGTG  
AGCTAACTTACATTAATTGCGTTGCGCTCACTGCCCGCTTCCAGTCGGGAAACCTGTGTGCCAGCTGCATTAATGAATCGG  
CCAACGCGGGGAGAGGCGTTTTGCGTATTGGGCGCCAGGTGGTTTTTCTTTTACCAGTGAGACGGGCAACAGCTGATTG  
CCCTTACCGCCTGGCCCTGAGAGAGTTGCAGCAAGCGGTCCACGCTGGTTTGGCCAGCAGGCGAAAACTCTGTTTGATGGT  
GGTTAACGGCGGGATATAACATGAGCTGTCTTCGGTATCGTCGTATCCACTACCGAGATATCCGCACCAACGCGCAGCCCGG  
ACTCGGTAATGGCGCGCATTGCGCCCAGCGCCATCTGATCGTTGGCAACCAGCATCGCAGTGGAACGATGCCCTCATTCAGC  
ATTTGCATGGTTTTGTTGAAAACCGGACATGGCACTCCAGTCGCTTCCCGTTCGCTATCGGCTGAATTTGATTGCGAGTGAG  
ATATTTATGCCAGCCAGCCAGACGCGAGACGCGCCGAGACAGAACTTAATGGGCCGCTAACAGCGCGATTTGCTGGTGACCCA  
ATGCGACCAGATGCTCCACGCCCAGTCGCGTACCCTTTCATGGGAGAAAATAATACTGTTGATGGGTGCTGGTCAGAGACA  
TCAAGAAAATAACGCCGGAACATTAGTGCAGGCAGCTTCCACAGCAATGGCATCCTGGTCATCCAGCGGATAGTTAATGATCAG  
CCCCTGACGCGTTGCGCGAGAAGATTGTGCACCGCCGCTTTACAGGCTTCGACGCGGCTTCGTTCTACCATCGACACCACCA  
CGTGGCACCCAGTTGATCGGCGGAGATTTAATCGCCGCGACAATTTGCGACGGCGCGTGCAGGGCCAGACTGGAGGTGGCA  
ACGCCAATCAGCAACGACTGTTTGGCCCGCAGTTGTTGTGCCACGCGGTTGGGAATGTAATTCAGCTCCGCCATCGCCGCTTC  
CACTTTTTCCCGCTTTTTGCGAGAAACGTGGCTGGCTGGTTACCACGCGGAAACGGTCTGATAAGAGACACCGGCATACT  
CTGCGACATCGTATAACGTTACTGGTTTACATTCACCACCCTGAATTGACTCTCTTCCGGGCGCTATCATGCCATACCGCGA  
AAGTTTTGCGCCATTCGATGGTGTCCGGGATCTCGACGCTCTCCCTTATGCGACTCCTGCATTAGGAAGCAGCCAGTAGTA  
GGTTGAGGCCGTTGAGCACCGCCGCGCAAGGAATGGTGCATGCAAGGAGATGGCGCCCAACAGTCCCCGGCCACGGGGCCT  
GCCACCATACCCACGCCGAAACAAGCGCTCATGAGCCCGAAGTGGCGAGCCGATCTTCCCCATCGGTGATGTGCGCGATATA  
GGCGCCAGCAACCGCACCTGTGGCGCCGGTATGCCGGCCACGATGCGTCCGGCGTAGAGGATCGAGATCTCGATCCCGCGAA  
ATTAATACGACTCACTATAGGGGAATTGTGAGCGGATAACAATTCCTCTAGAAAGTAATTTTGTAACTTTAAGAAGGAGA  
TATACCATGGGCAGCAGCCATCATCATCATCACAGCAGCGGCGACGCAAAACTGCTGGTTGGTGGCACCATTGTTAGCAG  
CACCGGTAATAATTCGTGCAGATGTTCTGATTGAAAATGGTAAAGTTGCAGCAGTTGGTATGCTGGATGCAGCAACCCGGATA  
CCGTTGAACGTGTTGATTGTGATGGTAAATATGTTATGCCGTTGGCATTGATGTGCATACCCATATTGATAGTCCGCTGATG  
GGCACACCACCGCAGATGATTTTTGTTAGCGGTACAATTGCAGCAGCAACCGGTGGTACAACCACCATGTGGATTTTGGTCA  
GCAGTGGCAGGTAATAAATCTGCTGAAAAGCGCAGATGCCCATCATAAAAAAGCACAGGGTAAAAGCGTGATCGATTATGGTT  
TTCATATGTGCGTGACCAACCTGTATGATAAATTTGATAGTCATATGCCAGAACTGACCCAGGATGGTATTAGCAGCTTTAAA  
GTTTTTATGGCCTATCGTGGTAGCCTGATGATTAATGATGGTGAACGTTTCGATATTCGAAAGGTGTTGGTAGCAGCGGTGC  
AAAATGTGTGTTTCATGCAGAAAATGGTATGTGATTGATCGTATTGCAGCCGATCTGTATGCACAGGGCAAAACCGGTCCGG  
GTACACATGAAATTGCACGTCGCCCTGAAAGCGAAGTTGAAGCCGTTAGCCGTGCAATCAAAATTAGCCGTATGGCCGAAGTT  
CCGCTGATTTTTGTTTCATCTGAGCACCCAGGGTGCAGTTGAAGAAGTTGCCGCGACACAGATGACCGGTTGGCCGATTAGCGC  
AGAAACCTGTACCCATTATCTGAGCCTGAGCCGTGATATTTATGATCAGCCTGGTTTTGAACCGCAAAAGCAGTTCTGACCC  
CTCCGCTGCGTACCCAAGAACATCAGGATGCACTGTGGCGTGGCATTAAATACCGGTGCACTGAGCGTTGTGAGCAGCGATCAT  
TGTCGGTTTTGTTTTGAAGAAAAACAGCGTATGGGTGCCGATGATTTTCGTGAGATCCGAATGGTGGTCCGGGTGTTGAACA  
TCGTATGCTGGTTATGTATGAAACCGGTGTGGCGGAAGGTAATAATGACCATTGAAAAATTTGTTGAGGTGACCGCAGAAAAATC  
CTGCCAAACAGTTTGTATGTATCCGAAAAAAGTACGATTGCACCGGGTAGTGATGCCGATATTATGTTGTTGATCCGAAT  
GGCACCACCCTGATTAGTGCAGATACCCAGAAACAGAAATATGGATTATACCCTGTTTGAAGGCTTTAAAAATCCGCTGTAGCAT  
TGATCAGGTTTTTGTAGCCGTGGTGTGATTAGCGTTAAAGGTGAATATGTTGGCACCCGTGGTCCGTGGTGAATTTATCAAAC  
GTAGCGCTTGGAGCCATCCGAGTTTTGAAAAGGTGGTGGCGGTAGCATGGATGAAAAACCACCGGCTGGCGTGGTGGTCAT  
GTTGTTGAAGGTCTGGCAGGCGAACTGGAACAGCTGCGTGCACGCTTGGAAACATCATCCGAGGGTCAGCGTGAACCGTAACA  
AAGCCCGAAAGGAAGCTGAGTTGGCTGCTGCCACCGCTGAGCAATAACTAGCATAACCCCTTGGGGCCTCTAAACGGGTCTTG  
AGGGGTTTTTGTGAAAGGAGGAACTATATCCGGAT

# PUBLICATIONS AND PRESENTATIONS

## PUBLICATIONS

**C. Slomka, G. P. Späth, P. Lemke, M. Skoupi, C. M. Niemeyer, C. Syldatk, J. Rudat (2017)**

Toward a cell-free hydantoinase process: Screening for expression optimization and one-step purification as well as immobilization of hydantoinase and carbamoylase, *AMB Express*, 7:122, DOI: 10.1186/s13568-017-0420-3.

**C. Slomka, S. Zhong, A. Fellinger, U. Engel, C. Syldatk, S. Bräse, J. Rudat (2015)**

Chemical Synthesis and Enzymatic, Stereoselective Hydrolysis of a Functionalized Dihydropyrimidine for the Synthesis of  $\beta$ -Amino Acids. *AMB Express*, 5: 85, DOI: 10.1186/s13568-015-0174-8.

**C. Slomka, U. Engel, C. Syldatk, J. Rudat (2015)**

Hydrolysis of Hydantoins, Dihydropyrimidines and Related Compounds. In *Science of Synthesis: Biocatalysis in Organic Synthesis*, Edition: 1, Editors: K. Faber, W. D. Fessner, N. J. Turner, 373-414, DOI: 10.1055/sos-SD-214-00283.

**M. Pöhnlein, C. Slomka, O. Kukhareenko, T. Gärtner, L. O. Wiemann, V. Sieber, C. Syldatk, R. Hausmann (2014)**

Enzymatic Synthesis of Amino Sugar Fatty Acid Esters. *European Journal of Lipid Science and Technology*, 4: 423-428, DOI: 10.1002/ejlt.201300380

## CONFERENCE PUBLICATION

**C. Slomka, U. Engel, C. Syldatk, J. Rudat (2014)**

Synthesis of  $\beta$ -Amino Acids Using a Modified Hydantoinase Process as Enzymatic Reaction Cascade. *Chemie Ingenieur Technik*, 86(9):1423, DOI: 10.1002/cite.201450367

## LECTURE

**C. Slomka, U. Engel, S. Zhong, C. Syldatk, S. Bräse, J. Rudat (2015)**

Synthesis of Chiral  $\beta$ -Amino Acids Applying an Enzymatic Reaction Cascade. Transam 2.0 – Chiral Amines Through Biocatalysis, Session III: Enzyme Cascades.

## POSTERS

**C. Slomka, U. Engel, C. Syldatk, J. Rudat (2016)**

Chemoenzymatic Synthesis of Aromatic  $\beta$ -Amino Acids. Annual Conference for General and Applied Microbiology (VAAM), BTP28.

**C. Slomka, U. Engel, C. Syldatk (2015)**

Synthesis of Chiral  $\beta$ -Amino Acids Applying a Modified Hydantoinase Process. 12<sup>th</sup> Biotrans, PS-46.

**C. Slomka, U. Engel, C. Syldatk, R. Rudat (2014)**

A Modified Hydantoinase Process for the Synthesis of Enantiopure  $\beta$ -Amino Acids in an Enzymatic Reaction Cascade. Annual Conference for General and Applied Microbiology (VAAM) and German Society for Hygiene and Microbiology (DGHM), BTP01.

**C. Slomka, U. Engel, C. Syldatk, J. Rudat (2013)**

Synthesis of Non-canonical  $\beta$ -Amino Acids via Hydantoinases/Dihydropyrimidinases and Carbamoylases. Biocatalysis Using Non-conventional Media (Summer School, RWTH Aachen)